UNIVERSITAT DE BARCELONA

# IRBC-induced p53-dependent Cell Death in c-MYC-driven tumors mediated by loss of MCL1

Ana Domostegui Fernández

UNIVERSITAT DE BARCELONA

FACULTAD DE FARMÀCIA I CIENCIES DE L'ALIMENTACIÓ

# IRBC-induced p53-dependent Cell Death in c-MYC-driven tumors mediated by loss of MCL1

Doctoral Thesis submitted by Ana Domostegui Fernández

The work presented in this Thesis has been performed at the Laboratori de Metabolisme del Càncer in the Institut d'Investigació Biomèdica de Bellvitge (IDIBELL), under the direction of **Dr. Joffrey Pelletier** and **Dr. George Thomas**.

DOCTORAL PROGRAM IN BIOMEDICINE

Barcelona, 2019

**Dr. George Thomas**
Co-director

**Dr. Joffrey Pelletier**
Co-director

**Dr. Albert Tauler**
Tutor

**Ana Domostegui**
PhD Candidate


*A mis padres, en especial a ti mamá*

*A mi hermano Javier*

*Y a mi abuela*

# ACKNOWLEDGMENTS

First of all, I would like to thank my Thesis supervisor **Dr. George Thomas** for giving me the opportunity to work at his laboratory and for its guidance during the development of this Thesis. Thanks for allowing me to learn under your supervision and for helping me to develop my professional career.

Likewise, I would like to express my most sincere gratitude to my Thesis's director **Dr. Joffrey Pelletier**. Thank you for your support, your many ideas and all the help you have offered me during the development of this Thesis. I really appreciate your discussions and challenges which have allowed me to grown as a scientist. Beyond the scientific part, I would like to thank you for your understanding in many personal situations, and also for the many good moments at the lab.

I would also like to thank **Dr. Sara Kozma** for her ideas and her discussions regarding the project, and my tutor **Dr. Albert Tauler**, who has been always there to help.

I do not forget **Dr. Suresh Peddigari**, who designed and developed the Tet-inducible shRNA system in the E$\mu$-MYC cell lines and who performed some of the experiments presented in the thesis.

Thank you very much to **Dr. Joseph T. Opferman** from the St. Jude Children's Research Hospital in Memphis, who kindly provided us the vectors to generate some of the cell lines used in the study.

My most sincere gratitude to our collaborator **Dr. Rick Pearson** for allowing me to work at the Peter MacCallum Cancer Centre in Melbourne, and to all people I met there, specially to **Dr. Eric Kusnadi** and **Dr. Jian Kang**, who helped me a lot, in particular, to carry out some of the *in vivo* experiments in the E$\mu$-MYC mice. I have learnt a lot working by your side. Thanks for the amazing experience.

Quiero dar las gracias al **Dr. Elías Campos** y a su equipo, en especial a **Marta Rodríguez**, por haberme ayudado y enseñado a generar el modelo de linfoma *in vivo*.

También me gustaría agradecer a la **Dra. Cristina Muñoz** su interés en mi proyecto, sus ideas y sugerencias, y el haber estado siempre dispuesta a echar una mano. Tanto ella, como su grupo. Pero sobretodo, muchas gracias por haberme tratado siempre maravillosamente.

Por supuesto, me gustaría dar las gracias a todos y cada uno de mis compañeros de laboratorio, a los que prácticamente conozco desde que comenzó esta aventura, como la **Dra. Caroline Mauvezin**, el **Dr. Antonio Gentilella** y **Marta García**; a los que han formado parte del laboratorio, como la **Dra. Sandra Menoyo**, la **Dra. Sonia Veiga**, la **Dra. Eugènia Almacellas**, la **Dra. Cristina Mayordomo**, el **Dr. Guilherme Zweig** y el **Dr. Francisco Morón**; y a las nuevas incorporaciones, **Aina Lluch**, **Carolina Martínez** , **Flavia Iannizzotto** y la **Dra. Teresa Rubio**, que pese a llevar relativamente poco tiempo en el laboratorio, han traído muchas sonrisas y buenos momentos.

**Sandra**, muchísimas gracias por estar ahí no solo en cuanto a lo científico, sino también en lo personal. Gracias por todos tus consejos, que guardo a buen recaudo, y por el gran apoyo que me has prestado.

**Sonia**, te agradezco muchísimo todo lo que he aprendido contigo en el laboratorio, tus "truquillos" y tu ayuda en los estudios *in vivo*. Para mí eres un referente tanto como persona como en el terreno profesional.

**Eugènia**, no se puede expresar con palabras lo fácil que es trabajar contigo. Gracias por esa sonrisa y positividad con la venías cada día. También darte las gracias por todos tus consejos e ideas en relación a mi proyecto y por tu apoyo en muchos momentos. Ets molt gran com a persona i com a investigadora!

**Cris**, primero de todo agradecerte toda la gestión que hiciste para y durante mi estancia en Melbourne, que supongo que te causó algún que otro quebradero de cabeza. Pero sobretodo, gracias por tu paciencia, tus consejos y todo el apoyo que me has prestado desde el día uno.

**Fran**, gracias por saber transmitir tu calma y serenidad, por tus consejos y por estar siempre dispuesto a ayudar.

**Caroline**, gracias por tu apoyo desde que llegaste al lab, por venir con una sonrisa prácticamente cada día y por las muchas charlas en los descansos para hacer un café. Gracias por dar un punto de vista diferente a las cosas y, sobretodo, por buscar la parte positiva de las mismas. Merci beaucoup Caroline!

**Antonio**, te agradezco que finalmente te hayas dejado conocer un poco más. Eres una persona con la que discutir de cualquier experimento o paper se hace apasionante y de la que siempre hay algo nuevo por aprender.

**Marta**, has hecho que tu presencia sea vital para el laboratorio (y su funcionamiento) y te tengo que dar las gracias por ello. Pero sobretodo, no me cabe duda de que eres la persona que más me conoce del lab y con la que más buenos momentos he compartido. Gracias por haber estado siempre ahí, por nuestras miles de charlas tanto científicas como no, por haber estado siempre dispuesta a echar una mano y por los miles de momentos compartidos tanto en el lab como fuera del trabajo… y, porque no, por tener siempre una cápsula de Nespresso disponible en caso de "emergencia".

Para mi familia, no tengo más que palabras de agradecimiento. A mi padre, por que gracias a él soy la persona que soy a día de hoy; a mi abuela, por todo el cariño que me ha dado siempre y que me da cada vez que nos vemos; y a mi hermano **Javier**, por haber estado ahí en todo lo que hemos pasado a lo largo de estos años. Porque solo hay una cosa que no tiene solución, todo lo demás, siempre la tendrá.

Por último, me gustaría dar las gracias en especial a una persona que hace poco más de un año llegó a mi vida, pero que me ha demostrado que vino para quedarse. **Kiko**, a ti te tengo que agradecer todo, creo que sin duda has sido el que más me ha escuchado, el que más veces ha visto diseños preliminares de esta Tesis y la persona que me ha sabido animar y tranquilizar durante estos últimos meses. Gracias por tu paciencia infinita y por todo el cariño que me demuestras cada día. Seguro que todo aquello que esté por venir será infinitamente mejor, aunque a día de hoy no tengamos ni fecha ni destino, ya que en realidad, eso poco importa.

# ABSTRACT

# Abstract

The oncogene *MYC* is altered and its expression is deregulated in up to 70% of human cancers, including B-cell neoplasms. Earlier studies in a mouse model of E$\mu$-MYC-driven B-cell lymphomas reported that oncogenic MYC relies on aberrant rates of ribosome biogenesis (RiBi) and protein synthesis to sustain rapid growth and proliferation of B-cell lymphomas. As MYC-driven B-cell lymphomas are addicted to hyperactivation of RiBi, it has emerged as a potential clinical target. However, it is unclear whether targeting RiBi induces regression of MYC-driven tumors by decreasing translational capacity and/or by inducing the impaired ribosome biogenesis checkpoint (IRBC), leading to p53 stabilization. We set to address this question by generating an inducible system in E$\mu$-MYC-driven lymphoma cells to deplete either one of two essential 60S ribosomal proteins (RPs), RPL7a or RPL11, the latter a component of the IRBC complex. Depletion of either RP mRNA by ∼50% had an equivalent impact on RiBi, protein synthesis and cell growth, however only depletion of RPL7a led to the induction of the IRBC, p53 stabilization, and acute induction of apoptosis. Importantly, we observed that this response is driven by the selective degradation of the antiapoptotic form of MCL1, of the BCL2 family, whose overexpression is critical to sustain survival and growth of E$\mu$-MYC lymphomas. MCL1 is commonly overexpressed in many human cancers, especially in B-cell malignancies, is frequently found coamplified with MYC, and its overexpression is associated with bad prognosis, resistance to therapy and relapse. Despite the tremendous investment in the development of selective MCL1 inhibitors in the clinic, we show that nanomolar concentrations Actinomycin D (ActD), an FDA approved drug for particular cancers, specifically disrupts the synthesis of rRNA and RiBi, leading to IRBC activation, p53 stabilization and degradation of the antiapoptotic form of MCL1, and killing *Trp53*$^{+/+}$, but not *Trp53*$^{-/-}$ E$\mu$-MYC lymphoma cells. Finally, we provide preclinical data that mice bearing *Trp53*$^{+/+}$, but not *Trp53*$^{-/-}$, E$\mu$-MYC lymphomas are exquisitely protected from lymphomagenesis by ActD. Therefore, in MYC-driven tumors, the IRBC elicits p53-dependent apoptosis, which is mediated by the loss of the antiapoptotic form of MCL1.

# CONTENTS

# INDEX

# LIST OF FIGURES

## INTRODUCTION

## RESULTS

## DISCUSSION

# LIST OF TABLES

## INTRODUCTION



## MATERIALS AND METHODS

# LIST OF ABBREVIATIONS

| | |
|---|---|
| **β-TrCP** | Beta-transducin repeat-containing protein |
| **β2m** | Beta-2 microglobulin |
| **3'UTR** | 3' untranslated region |
| **4EBP1** | eIF4E binding protein 1 |
| **5-FU** | 5-fluorouracil |
| **5'TOP** | 5' terminal oligopyrimidine |
| **5'UTR** | 5' untranslated region |
| **A-site** | Aminoacyl-site |
| **aa-tRNA** | Aminoacyl-tRNA |
| **ABC-DLBCL** | Activated B-cell-like DLBCL |
| **ABCE1** | ATP-binding cassette subfamily E member 1 |
| **ActD** | Actinomycin D |
| **ALCL** | Anaplastic large cell lymphoma |
| **ALL** | Acute lymphocytic leukemia |
| **AML** | Acute myeloid leukemia |
| **AnnV** | Annexin V |
| **APAF1** | Apoptotic protease-activating factor 1 |
| **APC** | Adenomatous polyposis coli |
| **APC/C** | Anaphase-promoting complex/cyclosome |
| **ARF** | Alternative reading frame |
| **ATM** | *Ataxia-telangiectasia*-mutated kinase |
| **ATR** | *Ataxia-telangiectasia* and RAD3-related kinase |
| **B-ALL** | B-cell acute lymphoblastic lymphoma/leukemia |
| **BAD** | BCL2-antagonist of cell death |
| **BAK** | BCL2-antagonist/killer-1 |
| **BAX** | BCL2-associated X protein |
| **BC** | Breast cancer |
| **BCL2** | B-cell lymphoma 2 |
| **BCLxL** | BCL2-like protein 1 |
| **BCLW** | BCL2-like protein 2 |
| **BCR** | B-cell receptor |
| **BFL1/ A1** | BCL2-related protein A1 |

| | |
|---|---|
| **BH** | BCL2 homology |
| **BID** | BH3-interacting-domain death agonist |
| **BIK** | BCL2-interacting killer |
| **BIM** | BCL2-like protein 11 |
| **BL** | Burkitt's lymphoma |
| **BM** | Bone marrow |
| **BMF** | BCL2-modifying factor |
| **BOK** | BCL2-related ovarian killer |
| **BOP1** | Block of proliferation protein 1 |
| **BR-HLH-LZ** | Basic region helix-loop-helix leucine zipper |
| **Bst** | Belly Spot and Tail |
| **C** | Carboxy |
| **CAD** | Caspase activated DNase |
| **CARD** | Caspase recruitment domain |
| **CASP** | Caspase |
| **CASP3cv** | Cleaved caspase-3 |
| **CBP** | CREB-binding protein |
| **CC** | Cervical cancer |
| **CDC20** | Cell division cycle protein 20 homolog |
| **CDK** | Cyclin-dependent-kinase |
| **CDR** | Coding region |
| **CHK1/2** | Checkpoint kinase 1/2 |
| **Chr** | Chromosome |
| **CHX** | Cycloheximide |
| **CKI** | CDK inhibitor |
| **CKII** | Casein kinase II |
| **CLL** | Chronic lymphocytic leukemia |
| **CML** | Chronic myeloid leukemia |
| **CMML** | Chronic myelomonocytic leukemia |
| **CNS** | Central Nervous System |
| **CRC** | Colorectal cancer |
| **Cyt *c*** | Cytochrome *c* |
| **DBA** | Diamond-Blackfan anemia |
| **DBD** | DNA-binding domain |

| | |
|---|---|
| DDB2 | Damage-specific DNA-binding protein-2 |
| DDR | DNA damage response |
| DDRR | Dead receptor/extrinsic apoptotic pathway |
| del | Deletion |
| DFC | Dense fibrillar component |
| DKC | X-linked Dyskeratosis congenita |
| DLBCL | Diffuse large B-cell lymphoma |
| DMSO | Dimethyl sulfoxide |
| DNMT | DNA methyltransferase |
| dox | Doxycycline |
| DSB | Double strand break |
| dsDNA | Double-strand DNA |
| DUB | Deubiquitinase |
| DUB3 | Deubiquitinating protein 3 |
| DZ | Dark zone |
| E-box | Enhancer-box |
| E-site | Exit-site |
| E1 | Ubiquitin-activating enzyme |
| E2 | Ubiquitin-conjugating enzyme |
| E3 | Ubiquitin ligase |
| EBV | Epstein-Barr virus |
| eEF | Eukaryotic elongation factor |
| eIF | Eukaryotic initiation factor |
| EMT | Epithelial-to-mesenchymal transition |
| ER | Endoplasmic reticulum |
| ERAD | ER-associated degradation |
| eRF | Eukaryotic release factor |
| ESC | Embryonic stem cell |
| ETS | External transcribed spacer |
| EWS | Ewing's sarcoma |
| F-luc | Firefly luciferase |
| FADD | FAS-associated death domain |
| FASL | FAS ligand |
| FBP | FUSE-binding protein |

| | |
|---|---|
| FBL | Fibrillarin |
| FBW7 | F-box/WD repeat-containing protein 7 |
| FBXO4 | F-box protein 4 |
| FDA | U.S. Food and Drug Administration |
| FIR | FBP-interacting repressor |
| FL | Follicular lymphoma |
| FLT3 | Fms-like tyrosine kinase 3 |
| FOXO | Forkhead box class O |
| FOXO3A | Forkhead box protein O3 |
| FUSE | Far upstream element |
| G4 | G-quadruplex |
| GADD45α | Growth arrest and DNA-damage-inducible 45α |
| GC | Germinal center or granular component |
| GCB-DLBCL | Germinal center B-cell-like DLBCL |
| GLS2 | Liver-type glutaminase |
| GM-CSF | Granulocyte macrophage colony-stimulating factor |
| GrB | Granzyme B |
| GSK3β | Glycogen synthase kinase-3 beta |
| GTN | Gestational trophoblastic neoplasia |
| HAT | Histone acetyltransferase |
| HCC | Hepatocellular carcinoma |
| HD | High-dose |
| HDAC | Histone deacetylase |
| HECT | Homologous to the E6-AP carboxyl terminus |
| HED | Human equivalent dose |
| HIF1 | Hypoxia-inducible factor 1 |
| HRK | Harakiri |
| HSCs | Hematopoietic stem cells |
| HSPCs | Hematopoietic stem and progenitor cells |
| HPCs | Hematopoietic progenitor cells |
| IAA | Iodoacetamide |
| ICAD | CAD inhibitor |
| IDR | Intrinsically disorder regions |
| Ig | Immunoglobulin |

| | |
|---|---|
| **IGH** | Ig heavy chain |
| **IGK** | Ig kappa light chain |
| **IGL** | Ig lambda light chain |
| **IGS** | Intergenic spacer sequence |
| **IMM** | Inner mitochondrial membrane |
| **IMS** | Intermembrane space |
| **IL** | Interleukin |
| **INR** | Initiator |
| **IPO7** | Importin 7 |
| **iPSCs** | Induced pluripotent stem cells |
| **IRBC** | Impaired ribosome biogenesis checkpoint |
| **IRES** | Internal ribosome entry site |
| **ITS** | Internal transcribed spacer |
| **JNK** | c-Jun N-terminal kinase |
| **kb** | Kilobase |
| **kDa** | Kilodalton |
| **KO** | Knockout |
| **LARP1** | La-related protein 1 |
| **LDH(A)** | Lactate dehydrogenase (A) |
| **$m^7G$** | 7-methylguanosine cap |
| **MB** | MYC homology box |
| **MCL** | Mantle cell lymphoma |
| **MCL1** | Myeloid cell leukemia 1 |
| **$MCL1_{ES}$** | Extra-short MCL1 |
| **$MCL1_{L}$** | Full-length MCL1 |
| **$MCL1_{Matrix}$** | Matrix-located MCL1 |
| **$MCL1_{OM}$** | Outer mitochondrial membrane-bound MCL1 |
| **$MCL1_{S}$** | Short MCL1 |
| **MDM2** | Mouse double minute 2 |
| **MDS** | Myelodysplastic syndrome |
| **MEF** | Mouse embryonic fibroblast |
| **mESC** | Mouse embryonic stem cell |
| **Met-tRNAi** | initiating methionyl-tRNA |
| **miR** | microRNA |

| | |
|---|---|
| **MIZ1** | MYC-interacting zinc finger protein-1 |
| **MM** | Multiple myeloma |
| **MOMP** | Mitochondrial outer membrane permeabilization |
| **MPA** | Mycophenolic acid |
| **mpc** | Molecules per cell |
| **MPC** | Plasmacytoma |
| **Mr** | Relative molecular mass |
| **mRNA** | Messenger RNA |
| **mTOR** | mammalian target of rapamycin |
| **mTORC1** | mTOR complex 1 |
| **MTS** | Mitochondrial target sequence |
| **MULE** | Mcl1 ubiquitin ligase E3 |
| **MZL** | Marginal zone lymphoma |
| **N** | Amino |
| **NCL** | Nucleolin |
| **NEF** | Nucleolar export factor |
| **NES** | Nuclear export sequence |
| **NHL** | Non-Hodgkin lymphoma |
| **NLS** | Nuclear localization signal |
| **NoLS** | Nucleolar localization sequence |
| **NOR** | Nucleolar organizer region |
| **NPC** | Nuclear pore complex |
| **NPM1** | Nucleophosmin |
| **NOP56** | Nucleolar protein 56 |
| **NSCLC** | Non-small cell lung carcinoma |
| **nt** | Nucleotide |
| **NT** | Non-treated |
| **OMM** | Outer mitochondrial membrane |
| **ORF** | Open reading frame |
| **P** | Promoter |
| **p53BD** | p53-binding domain |
| **p53RE** | p53 response element |
| **P-site** | Peptidyl-site |
| **p-TEFb** | Positive transcription elongation factor b |

| | |
|---|---|
| **PABP** | Polyadenylate-binding protein |
| **PARP** | Poly (ADP-ribose) polymerase |
| **PARP1cv** | Cleaved PARP1 |
| **PBL** | Plasmablastic lymphoma |
| **PCM** | Plasma cell myeloma |
| **PCNA** | Proliferating cell antigen |
| **PCNSL** | Primary central nervous system lymphoma |
| **PDGF** | Platelet-derived growth factor |
| **PDX** | Patient-derived xenograft |
| **PEST** | Proline-glutamate-serine-threonine-rich region |
| **PFN** | Perforin |
| **PI** | Propidium iodide |
| **PIC** | Pre-initiation complex |
| **PML** | Promyelocytic leukemia protein |
| **Pol** | RNA Polymerase |
| **PP2A** | Protein phosphatase 2A |
| **PRD** | Proline-rich domain |
| **PRPS2** | Phosphoribosyl-pyrophosphatase synthetase 2 |
| **PTC** | Peptidyltransferase center |
| **PUMA** | p53-up-regulated modulator of apoptosis |
| **qRT-PCR** | Quantitative real time-PCR |
| **R/R** | Relapsed or refractory |
| **RAF** | Ribosome-associated factor |
| **rDNA** | Ribosomal DNA |
| **Ren** | Renilla |
| **RiBi** | Ribosome biogenesis |
| **RISC** | RNA-induced silencing complex |
| **RMS** | Rhabdomyosarcoma |
| **RNP** | Ribonucleoprotein particle |
| **ROS** | Reactive oxygen species |
| **RP** | Ribosomal protein |
| **RPL** | Ribosomal protein from the large subunit |
| **RPS** | Ribosomal protein from the small subunit |
| **rRNA** | Ribosomal RNA |

| | |
|---|---|
| RS | Richter's syndrome |
| S | Svedberg |
| SCF | Skp1–Cullin–F-box-protein |
| SCLC | Small-cell lung cancer |
| SDS | Schwachmann-Diamond syndrome |
| SG | Serglycine |
| SKP2 | S-phase kinase-associated protein 2 |
| SL1 | Selectively factor complex 1 |
| SLL | Small lymphocytic leukemia |
| snoRNA | Small nucleolar RNA |
| snoRNP | Small nucleolar ribonucleoprotein |
| SP1 | Specificity protein-1 |
| SSB | Single strand break |
| ssDNA | Single-strand DNA |
| Syo1 | Symportin 1 |
| T | Terminator |
| t | Translocation |
| T-ALL | T-cell acute lymphoblastic lymphoma/leukemia |
| TAD | Transcriptional activation domain |
| TAF | TATA-box-associated factor |
| tBID | Truncated BID |
| TCL | T-cell lymphoma |
| TCS | Treacher Collins syndrome |
| Tet | Tetracycline |
| TET | Tetramerization domain |
| TFIIIB | Transcription factor IIIB |
| TFIIH | Transcription factor 2H |
| TIF-IA | Transcription initiation factor IA |
| TIGAR | TP53-induced glycolysis and apoptosis regulator |
| TM | Transmembrane |
| TNBC | Triple-negative breast cancer |
| TPA | Phorbol ester |
| TRAIL | Tumor necrosis factor-related apoptosis-inducing ligand |
| tRNA | Transfer RNA |

| | |
|---|---|
| **TRRAP** | Transactivation/transformation-associated protein |
| **TS** | Tumor suppressor |
| **TSS** | Transcriptional start site |
| **Ub** | Ubiquitin |
| **UBA** | Ubiquitin-associated domain |
| **UBF** | Upstream binding factor |
| **UPS** | Ubiquitin-proteasome system |
| **USP13** | Ubiquitin-specific peptidase 13 |
| **USP9X** | Ubiquitin-specific peptidase 9X |
| **VEGF** | Vascular endothelial growth factor |
| **VOD** | Veno-occlusive disease |
| **WBCs** | White blood cells |
| **WCL** | Whole cell lysates |
| **wt** | Wild-type |
| **WT** | Wilms tumor |
| **XPO1** | Exportin |
| **ZV** | Zombie Violet |
| **ZVAD-FMK** | Z-Val-Ala-Asp-fluoromethylketone |

# INTRODUCTION

# 1. MYC and cancer

## 1.1. The 'super-transcription' factor MYC

*MYC* is one of the most extensively studied genes, which was identified over 30 years ago as the human cellular homolog of the retroviral oncogene, *v-MYC*, present in the avian Rous sarcoma virus (Bishop, 1982). The *MYC* gene belongs to the MYC transcription factor family also known as the 'super-transcription factor' family, since MYC is estimated to regulate at least a 15% of genes of the whole genome (Fernandez et al., 2003, Dang et al., 2006) and is involved in the regulation of a broad range of essential cellular processes, including cell growth, proliferation, metabolism, differentiation, (reviewed in Dang et al., 2006, Meyer and Penn, 2008, Dang, 2013), stem-cell biology (reviewed in Laurenti et al., 2009) and cell death (Hoffman and Liebermann, 2008). MYC family comprises two additional members, *MYCL* (L-MYC) and *MYCN* (N-MYC), which function in a similar manner, despite some differences in potency and expression patterns (Nesbit et al., 1999). For instance, N-MYC is highly expressed in brain tissue during embryonic development, but its expression is absent in adult tissue, whereas MYC is ubiquitous and highly expressed in rapidly proliferating cells during embryogenesis and in adult tissues with proliferative capacity (Beltran, 2014). Although MYC expression is generally low and restricted to cells with regenerative and proliferative potential, it is deregulated and/or overexpressed in ~70% human cancers (Hoffman and Liebermann, 2008).

### 1.1.1. MYC structure

At the structural level, MYC shares high homology with the other two members of the family. The amino (N)-terminus of MYC contains the **transcriptional activation domain (TAD)**, which serves as an interaction platform for proteins involved in chromatin and histone modification, and for RNA Polymerase (Pol)-II-associated proteins that drive gene transcription. The TAD is also the majorly responsible for signaling MYC ubiquitin-mediated proteasome degradation (Salghetti et al., 1999). Within the TAD domain, MYC contains two highly conserved elements that belong to the family known as **MYC homology boxes (MBs)**: MBI and II **(Fig. I-1)**. MBs are essential for transactivation of MYC target genes, control MYC protein stability and harbor critical hotspots whose mutations can contribute to oncogenic transformation. Among the MBs, MBI and MBII are the best characterized, containing many sites of interaction with chromatin modifying-complexes and conserved residues, whose phosphorylation creates phosphodegron sites for ubiquitin E3 ligases F-box/WD repeat-containing protein 7 (FBW7) (Yada et al., 2004) and S-phase kinase-associated protein 2 (SKP2) (Kim et al., 2003, von der Lehr et al., 2003). Outside the TAD, MYC contains MBIIIa, which is involved in MYC stability and transcriptional repression (Kurland and Tansey, 2008), MBIIIb, whose function is not clear and which is contained within a proline-glutamate-serine-threonine-rich (PEST) region apparently involved in MYC turnover (Gregory and Hann, 2000), and MBIV, which contains the nuclear localization signal (NLS), required for the full proapoptotic functions of MYC (Cowling et al., 2006). At the carboxy (C)-terminus, MYC possesses a basic region and a helix-loop-helix-leucine zipper (BR-HLH-LZ) motif that functions as a **DNA-binding domain (DBD)** when bound to its partner, the small BR-HLH-LZ protein MAX; and that is also a site of interaction for chromatin modifying complexes, ubiquitin E3 ligases and other MYC/MAX interactors (reviewed in Adhikary and Eilers, 2005, Meyer and Penn, 2008, Conacci-Sorrell et al., 2014).

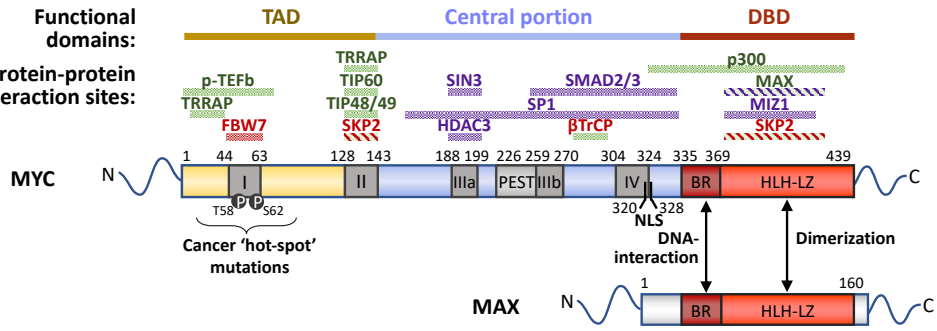


**Figure I-1. Organization of the MYC protein and binding partners.** MYC family members share structural homology. All of them contain highly conserved regions termed 'MYC homology boxes' (MBs) and two major functional domains, a N-terminal TAD and a C-terminal DBD. MBI/II, within the TAD, are essential for transcriptional activity and stability of MYC. MBI is the site of contact with p-TEFb, which stimulates Pol II transcriptional elongation, and contains two major 'hot-spot' residues recognized by FBW7, threonine (T)58 and serine (S)62. MBII is the major site of interaction for chromatin-modifying complexes including the histone acetyltransferase (HAT) components TRRAP, TIP48, TIP49 and the HAT TIP60, and it also contains a docking site for SKP2. In the central region, MBIIIa regulates stability of MYC and its repressing function via histone deacetylases (HDACs) recruitment (e.g. SIN3 and HDAC3), MBIIIb, which is contained within the PEST region, is responsible for the rapid degradation of MYC independently of ubiquitination, and MBIV is required for its proapoptotic function and contains the NLS. This region also contains a phosphodegron sequence recognized by β-TrCP and the site of contact with SP1. The C-terminus contains a BR required for binding 'E-boxes' on DNA promoters, together with MAX, and the HLH-LZ motif responsible for MYC/MAX interaction. The C-terminal region also contains the sites of contact with p300 and MIZ1, and a second interaction site for SKP2. The amino acid (aa) position of MYC domains and the interaction sites of MYC partners are indicated above MYC structure. Binding of MYC partners can promote MYC-dependent transactivation (green bars), repression (purple bars) or both (green-purple dashed bars). Interaction of E3 ligases (in red) either results in MYC destabilization (red bars) or promote its stabilization and transactivating function (green-red dashed bars). *Abbreviations:* TAD, transcriptional activation domain; DBD, DNA binding domain; p-TEFb, positive transcription elongation factor b; FBW7, F-box/WD repeat-containing protein 7; TRRAP, transactivation/ transformation-associated protein; SKP2, S-phase kinase-associated protein 2; PEST, proline-glutamate-serine-threonine-rich region; NLS, nuclear localization signal; β-TrCP, beta-transducin repeat-containing protein; SP1, specificity protein-1; MIZ1, MYC-interacting zinc finger protein-1; BR, basic region; HLH-LZ, helix-loop-helix-leucine zipper; .

### 1.1.2. Transcriptional control by MYC

MYC can both activate and repress transcription of its target genes. Activation of transcription requires the recognition of a consensus sequence 'CACGTG', known as the 'Enhancer-box' (E-box), located on the DNA promoters of MYC target genes. However, the motif is degenerate and non-canonical E-boxes can be also recognized by MYC, including CACATG, CATGTG or CACGC (Fernandez et al., 2003, Meyer and Penn, 2008, Chen et al., 2018). In order to bind either canonical or non-canonical E-box sequences MYC has to dimerize with MAX through their common BR-HLH-LZ motif. Once MYC/MAX heterodimer is bound to the DNA, MYC recruits (1) different chromatin-remodeling complexes and (2) Pol II transcriptional coactivators to the DNA promoters, promoting an open chromatin conformation and stimulating Pol II transcription, respectively, which allows transcription of MYC target genes **(Fig. I-2, left-top panel)**. Although MYC exclusively binds MAX, the later can also bind members of the MXD family through their common HLH-LZ regions, including MAD. MAD/MAX heterodimers share MYC/MAX E-boxes on the DNA promoters and counteract MYC transactivation by recruiting histone deacetylases (HDACs) through the adaptor protein SIN3, resulting in transcriptional repression **(Fig. I-2, left-bottom panel)**. Therefore, the balance between MYC and MXD family proteins determines the biological output. For example, whereas MYC/MAX promotes cell proliferation, MAD/MAX suppresses this response (Grandori et al., 2000). The accumulation of either MYC or MXD proteins, which are short-lived proteins (half-life < 1 hr) unlike MAX (6-8 hr) (Ayer and Eisenman, 1993), is largely dictated by both environmental and intracellular signals and while MYC is induced upon mitogenic signals and thus, MYC/MAX complexes predominate in proliferating cells, MAD/MAX complexes are more abundant in quiescent or differentiated cells (Grandori et al., 2000).

MYC/MAX heterodimer can alternatively act as a transrepressor complex when it is recruited by the transcription factor MYC-interacting zinc finger protein-1 (MIZ1) to the initiator (INR) element on MIZ1 target genes, or by the specificity protein-1 (SP1) to INR or SP1 elements on target genes, mostly involved in cell cycle arrest (Herkert and Eilers, 2010, Garcia-Gutierrez et al., 2019). Binding of MYC/MAX heterodimer to these elements (1) disrupts p300 interaction and (2) recruits DNA methyltransferases (DNMTs) or (3) HDACs, resulting in transcriptional repression **(Fig. I-2, right panel)**.

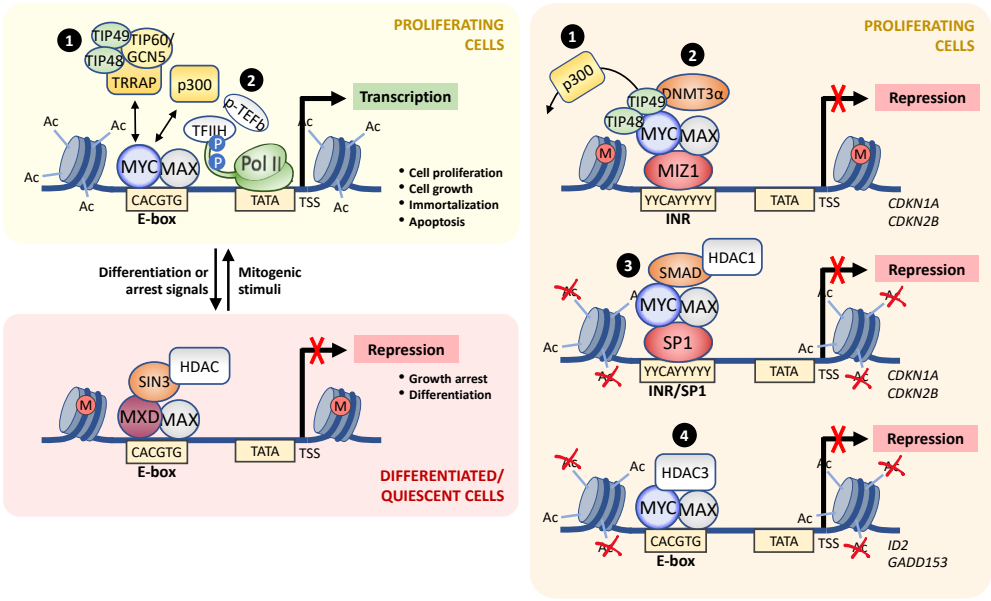


**Figure I-2. Mechanisms of gene regulation by MYC.** Different heterodimers of the MYC/MAX/MAD network, comprising MYC/MAX and alternative MXD/MAX complexes (such as MAD/MAX complexes), function as a transcriptional ON/OFF switch by binding to conserved E-boxes on DNA promoters. Left-top panel: MYC/MAX heterodimers activate transcription by (**1**) recruiting chromatin-modifying complexes which promote histone acetylation such as the HATs TIP60/GCN5 and their cofactors, including the ATPases TIP48 and TIP49, and the adaptor protein TRRAP which binds MYC via the MBII domain. Recruitment of p300 HAT does not require adaptor proteins as it directly associates with the MYC C-terminus. In addition, (**2**) MYC stimulates transcription of its target genes by recruiting several Pol II transcriptional cofactors through its TAD domain, including TFIIH and p-TEFb, responsible transcriptional initiation, Pol II pause release and elongation. Left-bottom panel: By contrast, MAX/MAD complexes repress transcription by recruiting HDACs through the adaptor protein SIN3. Right-top panel: Alternatively, MYC/MAX dimers can function as a transrepressor complex. Recruitment of MYC/MAX by MIZ1 to the INR elements of gene promoters involved in cell cycle arrest, such as *CDKN1A*, encoding $p21^{CIP1}$ (p21 herein after), and *CDKN2B*, encoding $p15^{INK4B}$, (**1**) disrupts the interaction of p300 with MIZ1, (**2**) recruits DNMT3α through TIP48 and TIP49, which methylate histones, leading to repression of MIZ1-target genes. Right-middle panel: Likewise, recruitment of MYC/MAX heterodimer by SP1-SMAD complexes to INR or SP1 elements (**3**) disrupts the SP1-SMAD complexes and recruits HDAC1 leading to the formation of a transrepressor complex. Right-bottom panel: MYC/MAX heterodimers also (**4**) directly recruits HDACs such as HDAC3 to specific MYC core promoters repressing their transcription. In addition, MYC can regulate Pol I and Pol III activity **(see Chapter 3, Section 3.3.1.)**. *Abbreviations:* TFIIH, transcription factor 2H; E-box, enhancer-box; INR, initiator element; TSS, transcriptional start site; Ac, Acetylation; M, Methylation; DNMT3α, DNA-methyltransferase 3α.

Likewise, recruitment of HDAC3 by MYC to the core promoters of its target genes represses transcription of specific growth arrest genes (e.g. *ID2* and *GADD153)* **(Fig. I-2, right panel)** (Conacci-Sorrell et al., 2014). In addition, independently of MAX, MYC directly stimulates the activity of Pol III, involved in the transcription of transfer RNA (tRNA) and the 5S ribosomal RNA (rRNA) genes, by binding the transcription factor IIIB (TFIIIB) (van Riggelen et al., 2010). By contrast, MYC stimulates Pol I activity in association with MAX **(see Section 3.3.1.)**. Therefore, MYC regulates transcription through several mechanisms, including the recruitment of HAT complexes, basal transcription factors or DNMTs, in complex with MAX, as well as by directly activating Pol III transcription in association with TFIIIB.

### 1.1.3. Regulation of MYC expression

Given the large set of genes and the many biological functions controlled by MYC (Fernandez et al., 2003), even slight changes in MYC protein levels may have a dramatic impact in cell proliferation and cell fate, so that a sophisticated regulation of both *MYC* expression and MYC activity is critical to safeguard adult tissue homeostasis, as well as to maintain proliferative potential and stemness during embryonic development (Levens, 2010). Indeed, MYC along with OCT3/4, SOX2, and KLF4 are the four essential transcription factors capable to collectively reprogram both mouse and human adult fibroblasts into pluripotent stem cells (Takahashi and Yamanaka, 2006, Takahashi et al., 2007). Likewise, during embryogenesis, high *MYC* expression ensures the proliferative potential of precursor populations until the developmental signals, such as WNT NOTCH, TGFβ and BMP are suppressed, leading to *MYC* downregulation and terminal differentiation (Levens, 2010). In adult tissues, MYC expression is finely tuned by many signal transduction pathways, driving extra- and/or intracellular signals involved in cell proliferation, growth arrest or differentiation. In general, both its messenger RNA (mRNA) and protein expression are maintained at low levels, as low as one transcript per cell, and its expression restricted to regenerating and proliferating cells, such as the epidermis and the gut. For instance, resting fibroblasts contain just 500 MYC molecules per cell (mpc), rising to 5000 mpc upon stimulation with mitogens (Waters et al., 1991).

In order to achieve an acute control of its expression, MYC regulation is exerted at every level, with the major regulation exerted at the **transcriptional level** (reviewed in Liu and Levens, 2006, Wierstra and Alves, 2008). At the transcriptional level, *MYC* mRNA is upregulated by most signal transduction pathways involved in cell proliferation and in response to mitogens, while major signaling pathways driving differentiation and anti-proliferation signals, repress *MYC* transcription. These pathways converge in downstream transcription factors, '*trans*-acting factors', which either positively or negatively regulate *MYC* transcription through binding to the canonical, non-canonical or atypical *cis* regulatory elements in the vicinity of the *MYC* promoters (reviewed in Liu and Levens, 2006, Wierstra and Alves, 2008, Levens, 2010). Binding of *trans*-acting factors is scattered through hundreds of kilobases (kb) upstream the transcriptional start site (TSS) of the major MYC promoter (P2), which accounts for ~75% of *MYC* transcripts. In addition to the many *trans*-acting factors and *cis*-elements influencing *MYC* transcription, the group of D. Leven addressed the complexity of *MYC* transcriptional regulation (see reviews from Chung and Levens, 2005, Levens, 2008). *MYC* promoter is almost always loaded, but the presence of a paused Pol II engaged 35-50 nucleotides (nt) downstream the TSS at transcriptionally inactive *MYC* genes prevents unwanted activation of the promoter and maintains *MYC* gene in a poised state, allowing a rapid upregulation of its transcription. Recruitment of TFIIH complex releases paused Pol II thus, resuming elongation and allowing basal *MYC* transcription. Full activation of *MYC* transcription, which occurs 2 hr after the binding of the early *trans*-acting factors, additionally requires the interaction of far upstream element (FUSE) binding protein (FBP) with TFIIH and the FUSE, a DNA element located 1.7 kb upstream the TSS. The dynamic supercoiling generated by the ongoing *MYC* transcription unwinds the duplex DNA of the FUSE, allowing the interaction of FBP and its binding to TFIIH drives *MYC* transcription to peak levels. In the absence of growth factor stimuli, subsequent binding of the FBP interacting repressor (FIR) to the FUSE represses *MYC* transcription by inhibiting TFIIH, which gradually promotes its dissociation from Pol II. Transcription is completely switched off when the FUSE is masked by a nucleosome, until a new cycle begins (Chung and Levens, 2005, Levens, 2008). Despite this complex regulation, *MYC* mRNA expression strongly correlates with the rate of **cell proliferation** (reviewed in Wierstra and Alves, 2008). In quiescent cells, *MYC* expression is almost

undetectable, but after exposure to specific mitogens, it is rapidly upregulated, promoting the transition of cells from G1 to S phase. *MYC* mRNA levels peak up 2 hr after mitogenic stimulation, increasing up to 10-40-fold as compared to quiescent cells, and then its expression decreases to a lower level, which is maintained during the cell cycle if mitogens are present. By contrast, mitogen deprivation, or antiproliferative or differentiation signals immediately suppresses *MYC* expression reducing its mRNA levels ~90% (Wierstra and Alves, 2008).

Following transcription, *MYC* mRNA is exported to the cytoplasm where its translation is limited by its very short half-life (~15-30 min) (Dani et al., 1984). Its rate of turnover can be further accelerated by the interaction of certain microRNAs (miR), while multiple cell growth-signaling pathways, such as the **Mammalian Target of Rapamycin Complex 1 (mTORC1)** signaling pathway enhances the efficiency of its translation (Kress et al., 2015). mTORC1-mediated phosphorylation of S6K1 kinase promotes the release of the translation eukaryotic initiation factors (eIFs), such as eIF4A, and its association with eIF4F complex facilitating the recruitment of the 43S preinitiation complex (43S PIC) to the capped 5' end of the mRNA, which is required to initiate CAP-dependent translation **(see Section 3.1.)** (Kuang et al., 2011, Csibi et al., 2014). In addition, through the inhibitory phosphorylation of the eIF4E binding protein 1 (4EBP1), mTORC1 promotes the release of eIF4E, the CAP-binding subunit of the eIF4F complex (Sonenberg, 2008), which facilitates the translation of 'eIF4E-sensitive' mRNAs. These mRNAs are characterized by long and highly structured 5' untranslated regions (5'UTRs) present in many transcripts encoding proteins involved in cell proliferation and survival as e.g. cyclins, B-cell lymphoma 2 (BCL2) family members and MYC (Larsson et al., 2012, Hinnebusch et al., 2016). However, it is controversial whether these mRNAs or a group containing short 5' terminal oligopyrimidine (5'TOP) motifs are selectively regulated by mTORC1 **(Section 3.2.3.)**.

Finally, following its synthesis, MYC protein is rapidly degraded within ~15-30 min (Hann and Eisenman, 1984). Again, major cell-growth signaling pathways regulate MYC stability through distinct post-translational modifications, including phosphorylation, acetylation and ubiquitination (Vervoorts et al., 2006, Farrell and Sears, 2014). Among them, ubiquitination is the most prominent mechanism to maintain MYC at low levels upon termination of mitogen stimulation or in response

to antiproliferative or differentiation signals (reviewed in Farrell and Sears, 2014). Thus, MYC turnover is largely controlled by the **ubiquitin-proteasome system (UPS)**, a highly specific process that requires the conjugation of ubiquitin molecules through covalent linkages on the target protein for its subsequent recognition and degradation by the 26S proteasome (Sorokin et al., 2009). This process requires the action of three different enzymes at multiple steps: (**1**) the activation of a ubiquitin molecule by a ubiquitin-activating enzyme (E1); (**2**) the transfer of the activated ubiquitin to a ubiquitin-conjugating enzyme (E2); (**3**) the recognition of the target protein by E3 ubiquitin ligase; and (**4**) the transfer of the activated ubiquitin molecule to a lysine (K) residue in the target substrate by the E2 enzyme. Successive reactions attach additional ubiquitin molecules on the K48 residue of the previous ubiquitin, leading to the formation of K48-linked polyubiquitin chains on the target protein which are then recognized by the 26S proteasome (Sorokin et al., 2009). MYC contains several elements which are recognized by a number of E3 ligases, including a degron sequence within the MBII (aa 127-158) recognized by the SKP2 (Kim et al., 2003, von der Lehr et al., 2003), a phosphodegron sequence (aa 278-283) similar to 'DpSGXXpS' recognized by β-TrCP (Popov et al., 2010), and two conserved phosphorylation sites within the MBI, T58 and S62, whose phosphorylation creates a docking site for FBW7 (Welcker et al., 2004, Yada et al., 2004) **(Fig. I-1)**. Upon mitogen stimulation activation of RAS promotes phosphorylation of S62 via MAPK/ERK kinases, while prevents T58 phosphorylation by glycogen synthase kinase-3 β (GSK3β) via PI3K/AKT pathway (reviewed in Sears, 2004, Farrell and Sears, 2014). In early G1, phosphorylation of S62 enhances MYC transcriptional activity, while later in G1, as RAS activity decreases and AKT signaling is reduced, GSK3β phosphorylates MYC at T58 and S62 is dephosphorylated by protein phosphatase 2A (PP2A). Phosphorylated T58 is recognized by FBW7 which polyubiquitinates MYC and directs it for proteasomal degradation. Likewise, SKP2 regulates G1-to-S phase transition in lymphocytes. MYC ubiquitination by SKP2 at target gene promoters first stimulates MYC transcriptional activity, promoting S-phase entry, and then directs its proteasomal-degradation (Kim et al., 2003, von der Lehr et al., 2003). During S-to-G2 phase transition, MYC ubiquitination by β-TrCP promotes its stabilization, allowing re-entry into the cell cycle after S-phase arrest (Popov et al., 2010). Thus, ubiquitination controls both MYC stability and transcriptional activity.

## 1.2. Oncogenic MYC

In contrast to normal cells, in cancer cells a number of these checkpoints involved in MYC regulation are lost, resulting in sustained and increased MYC expression. Oncogenic activation of MYC can be also achieved through direct alterations of the gene, such as retrovirus insertion, chromosomal translocation or gene amplification, activation of super enhancers within the *MYC* gene, abrogation of MYC autosuppression, and/or deregulation of upstream signaling pathways involved in MYC protein stability, such as hyperactivation of RAS oncogenic kinase or the loss of *Adenomatous Polyposis Coli* (*APC*) gene, which leads to defects in the WNT/β-catenin signaling pathway (Meyer and Penn, 2008, Murphy et al., 2008, Dang, 2012). However, as opposed to other classical oncogenes such as *RAS*, in most tumors *MYC* gene is not mutated, excepting in some blood-borne tumors, such as Burkitt's lymphoma (Bhatia et al., 1993), with deregulation of its upstream signaling pathways primarily contributing to its elevated and sustained activity (Murphy et al., 2008).

### 1.2.1 Functions regulated by MYC in tumorigenesis

Elevated MYC protein levels are frequently found in the tumor tissue in respect to surrounding normal tissue and are often associated with more advanced and aggressive tumors (Nesbit et al., 1999), indicating that MYC expression over a physiological threshold contributes to tumorigenesis (Murphy et al., 2008). For instance, MYC mpc in tumor cells is much larger than in normal cells, ranging from ~30,000 in HeLa cells (Moore et al., 1987) to almost 900,000 mpc in H2171 small-cell lung cancer (SCLC) cells (Lin et al., 2012). Such elevated numbers of MYC molecules exceeds the number of available core promoters and thus, promotes its binding to low-affinity E-box sequences. Importantly, gene-expression profiles of oncogenic MYC slightly differs from that of MYC under physiological conditions, given the promiscuous activation of E-box-driven genes, even those of low-affinity, by deregulated MYC (Fernandez et al., 2003). During the last decade, two opposing models arose to explain the mechanism of gene regulation by MYC. One supports that MYC acts as a **general 'amplifier'** of transcription, potentially interacting with all active loci in the genome, and thus, deregulated MYC expression results in global amplification rather than regulating novel genes (Lin et al., 2012, Nie et al., 2012). By

contrast, the second model argues that MYC selectively controls a **discrete set of genes**, whose products affect global transcript levels (Eilers and Eisenman, 2008, Herkert and Eilers, 2010, Dang, 2013, Sabo et al., 2014). As recently proposed by Kress et al. in a unifying model, it is likely that MYC regulates specific genes and thus, oncogenic MYC lead to the up/downregulation of a distinct set of genes, on the basis of binding affinity, many of which may be cell-type specific (Kress et al., 2015). Many efforts are still being carried out to identify critical genes regulated by oncogenic MYC that contribute to tumorigenesis, given the many genes which may be potentially regulated under these conditions. To date, most of the **'transformation-associated genes'** identified are involved in cell cycle progression and differentiation. For instance, deregulated MYC expression upregulates members of the E2F transcription factor family (e.g. *E2F1* and *E2F2*), cyclins (*cyclin D1*, *D2*, *E1* and *A2*) and cyclin-dependent-kinases, or CDKs (e.g. *CDK4* and *CDC25A*), while MYC represses transcription of cell cycle checkpoint genes (e.g. *GADD45*) and CDK inhibitors, or CKIs (e.g. *CDKN1A* and *CDKN2B*, encoding p21 and $p15^{INK4B}$, respectively), which ultimately drive unrestricted cell proliferation (reviewed in Adhikary and Eilers, 2005, Meyer and Penn, 2008). Oncogenic MYC-dependent repression of p21 not only abrogates G1-phase arrest checkpoint, but also blocks cell differentiation (van de Wetering et al., 2002). Regulation of cell cycle progression and differentiation is a common function of MYC in normal and tumor cells, but in addition, oncogenic MYC expression drives novel mechanisms that may facilitate tumor progression including deregulated cell growth, independent of growth factor signaling and nutrient availability. This is largely carried out by upregulating ribosome biogenesis (RiBi) and protein synthesis; metabolic reprogramming, inducing glycolysis and glutamine catabolism, favoring nucleotide and lipid biosynthesis, and increasing mitochondrial biogenesis, which are essential for cell growth; angiogenesis; reduction of cell adhesion; increased genomic instability and metastatic capability; and suppression of immune surveillance (reviewed in Adhikary and Eilers, 2005, Meyer and Penn, 2008, Dang, 2012, Miller et al., 2012, Dang, 2013, Casey et al., 2017). For instance, induction of glycolytic metabolism in tumor cells under hypoxic conditions is driven by deregulated MYC expression in collaboration with hypoxia inducible factor-1 (HIF1), whereas in normal conditions HIF1 suppresses *MYC* expression (Dang, 2008). Cooperation with HIF1 also induces the expression of the vascular endothelial growth

factor (VEGF), thus, inducing an angiogenic switch that is indispensable for the progression and metastasis of tumors (Kim et al., 2007). In addition, MYC deregulation promotes metastasis through the upregulation of miR9, which targets *CDH1* (encoding E-cadherin), and BMI1, which promotes epithelial-to-mesenchymal transition (EMT) and thereby metastasis, an effect not observed under physiological conditions (Dang, 2012). Examples of the essential MYC targets and its contribution to tumorigenesis are shown in **Figure I-3.** Importantly, the contribution of each specific mechanism depends on the level of MYC expression, the genetic lesion and the cell context (Yuneva et al., 2012, Dang, 2013, Gabay et al., 2014), with no a cell-type-independent core signature of MYC-responsive genes, excepting for a set of genes involved in RNA processing, RiBi and biomass accumulation, which highlights the key role of these processes in MYC tumorigenesis (Ji et al., 2011).

### 1.2.2. Intrinsic Tumor Suppressor response

It is notable that, although many targets of MYC can contribute to tumorigenesis, deregulated MYC expression alone is generally not able to induce neoplastic transformation in most normal human cells, requiring the acquisition of other genetic events (reviewed in Gabay et al., 2014). Indeed, MYC overexpression alone is not sufficient to drive cells throughout a complete cell cycle, conversely resulting in cell cycle arrest (Felsher et al., 2000), cell death (Evan et al., 1992) or cellular senescence (Grandori et al., 2003). These paradoxical outputs induced by MYC are considered as a fail-safe mechanism to restrict MYC's oncogenic potential as occurs with many others oncogenes, such as E1A, E2F1 or RAS (Gabay et al., 2014). The distinct mechanisms executed by normal cells to prevent malignant transformation upon oncogene activation are globally referred as the intrinsic tumor suppressor (TS) response (Lowe et al., 2004). Therefore, the cooperation of additional genetic events that abrogate these TS checkpoint mechanisms with MYC deregulation is essential to induce proliferation and to promote malignant transformation (Gabay et al., 2014). The ability of MYC to execute its proliferative program or distinct TS responses is cell type, cell context and level dependent (Murphy et al., 2008, Gabay et al., 2014). For instance, strong activation of MYC is frequently associated with DNA damage and cell death response, whereas more restrained activation usually involves proliferation arrest and senescence.

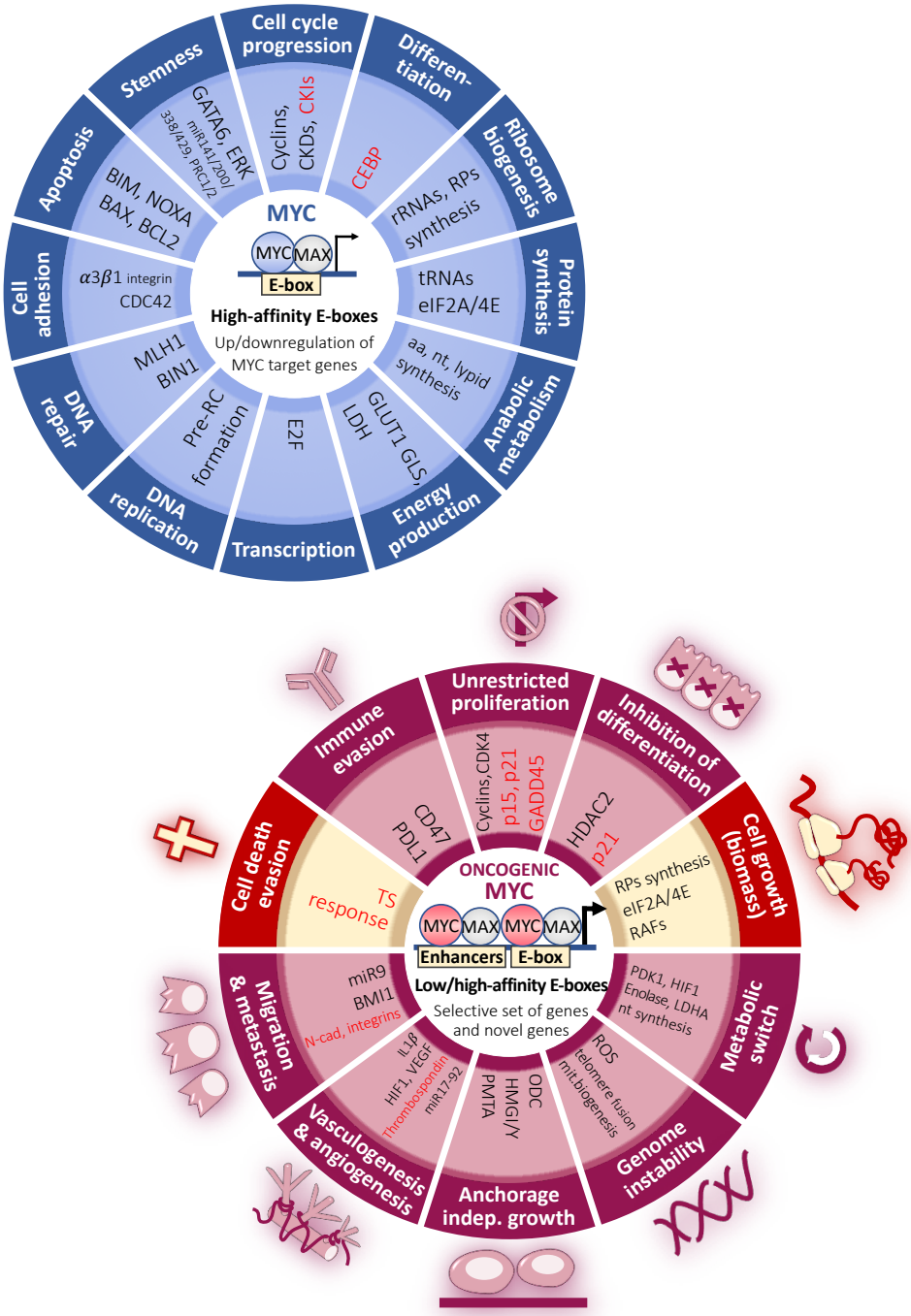


**Figure I-3. Physiological and oncogenic functions regulated by MYC.** (See next page)

**Figure I-3. (continued)** Top circle: well-characterized MYC targets (light blue) or cellular functions (dark circle) regulated by MYC expression under physiological conditions. Bottom circle: oncogenic MYC regulation of essential genes (light red) and cellular outputs (dark red) contributing to tumorigenesis, some are well-known hallmarks of cancer. Targets upregulated by MYC are displayed in black, while targets repressed by MYC in red. Upregulation of ribosomal proteins (RPs), eukaryotic initiation factors (eIFs) and ribosome-associated factors (RAFs), which leads to biomass accumulation and cell growth, as well as deregulation of tumor suppressor (TS) response, which promotes cell death evasion, are highlighted in yellow due to their key roles in promoting MYC-driven tumorigenesis. *Abbreviations:* CEBP, CCAAT/Enhancer-binding protein; GLUT1, glucose transporter 1; GLS, glutamine synthase; LDH, lactate dehydrogenase; pre-RC, pre-replication complex; MLH1, MutL homolog 1; BIN1, bridging integrator 1; CDC42, cell division control protein 42 homolog; PRC1/2, polycomb repressive complex 1/2; GADD45, growth arrest and DNA damage-inducible 45; HDAC2, histone deacetylase 2; PDK1, pyruvate dehydrogenase kinase isoform 1; ROS, reactive oxygen species; mit., mitochondrial; ODC, ornithine decarboxylase; HMGI/Y, high mobility group proteins I and Y; PMTA, prothymosin-α; IL1β, interleukin 1β; CD47, cluster of differentiation 47; PD-L1, programmed dead ligand 1.

TS responses are also oncogene-dependent. For instance, oncogenic MYC signaling largely engages components of the apoptotic pathway, promoting cell death instead, whereas oncogenic RAS expression usually drives senescence (Lowe et al., 2004). Of note, apoptosis-induced upon MYC overexpression has been extensively studied in cells or transgenic mouse models in which *MYC* was expressed from an ectopic promoter in the presence of limited survival signals or under cellular stresses. Therefore it is still controversial whether apoptosis limits tumorigenesis in solid tumors, in which *MYC* is frequently expressed from its own promoter, or whether tumor regression is a consequence of limited survival signals and/or the distinct stress stimuli that might downregulate MYC promoter (Adhikary and Eilers, 2005).

The classical intrinsic TS pathway implicated in oncogenic MYC-induced cell death is the ARF-MDM2-p53 TS pathway through the intrinsic apoptotic cell death pathway **(Fig. I-4)** (reviewed in Meyer et al., 2006, Campaner and Amati, 2012). However, it is not the only TS pathway elicited upon deregulated MYC expression, since oncogenic MYC also induces apoptosis through the *ataxia-telangiectasia*-mutated kinase (ATM)-p53 DNA damage response (DDR) pathway, in response to DNA damage (Pusapati et al., 2006), and through a ribosomal stress pathway which involves components of the ribosome **(see also Section 1.3.5. and Chapter 3)**.

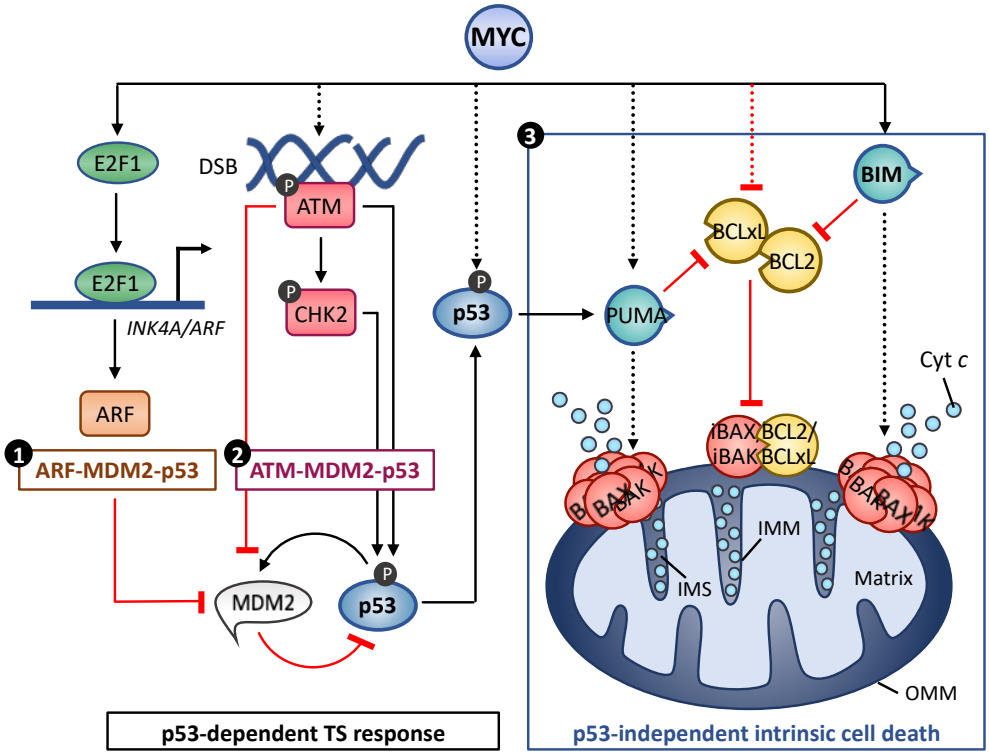


**Figure I-4. Major intrinsic tumor suppressor pathways involved in MYC-induced apoptosis.** (1) MYC induces expression of ARF presumably through E2F1 which induces the expression of the *INK4A/ARF* locus (encoding ARF), thus leading to the activation of the ARF-MDM2-p53 TS response. (2) MYC-induced DNA damage also leads to the stabilization and activation of p53 through the ATM-CHK2 kinases which are activated in response to DNA double-strand breaks (DSBs). (3) In addition, MYC overexpression alters the balance of BCL2 family members towards the apoptotic threshold in both a p53-dependent and -independent manner, the latter through the direct upregulation of BIM and BAX, and the indirect repression of BCL2 and BCLxL, which promotes BAX/BAK activation and oligomerization, leading to MOMP and cytochrome (cyt) *c* release, which irreversibly commits the cell to death. Dashed lines indicate indirect activation. *Abbreviations:* MDM2, mouse double minute 2; ATM, *ataxia-telangiectasia*-mutated kinase; CHK2, checkpoint kinase 2; IMS, intermembrane space; IMM, inner mitochondrial membrane; OMM, outer mitochondrial membrane.

These TS mechanisms are mostly executed in a p53-dependent manner, but the intrinsic cell death (or apoptotic) pathway can be induced by MYC in both p53-dependent and p53-independent systems (reviewed in Meyer et al., 2006). In a p53-independent manner, MYC overexpression most likely induces the intrinsic apoptotic pathway by altering the balance among the distinct pro- and antiapoptotic members

of the BLC2 family of proteins, the key modulators of this response, driving the cell to the apoptotic threshold, which leads to mitochondrial outer membrane permeabilization (MOMP) and finally, to cell death **(See also Chapter 2)**. As reviewed by Meyer et al., MYC can sensitize the cell to undergo apoptosis by inducing or repressing certain members of the BCL2 family. For instance, in an indirect manner, MYC suppresses antiapoptotic BCL2 and BCL2-like protein 1 (BCLxL) (Meyer et al., 2006), while directly upregulates proapoptotic BCL2-interacting mediator of cell death (BIM) (Lee et al., 2013). Another BCL2 member, the proapoptotic effector BCL2-associated X protein (BAX) is also directly upregulated by MYC (Mitchell et al., 2000). Induction of BAX is required to elicit apoptosis both in MYC tumorigenic and MYC physiological setting, contrary to the other proapoptotic effectors of the family, such as BCL2-antagonist/killer-1 (BAK) (Dansen et al., 2006). Likewise, release of cytochrome (cyt) *c* from the mitochondria is also essential to drive cell death (Juin et al., 1999), and its release can be elicited in a p53-independent manner (Morrish et al., 2003). Importantly, some these mechanisms may be entirely p53-independent, since the loss of BAX or BIM, or the forced expression of BCLxL in a MYC-driven lymphoma mouse model does not inactivate the ARF-MDM2-p53 TS pathway (Eischen et al., 2001a, Eischen et al., 2001b, Egle et al., 2004). Likewise, MYC point mutants fail to induce apoptosis through BIM, but are still able to induce the ARF-MDM2-p53 TS pathway (Hemann et al., 2005). By contrast, in response to DNA damage, MYC induces another proapoptotic member of the BCL2 family, p53-up-regulated modulator of apoptosis (PUMA) in a p53-dependent manner (Jeffers et al., 2003). Following its induction by MYC, PUMA promotes cell death by releasing p53 from its complex with BCLxL at the mitochondria, presumably allowing p53 to directly activate BAX and induce MOMP (Chipuk et al., 2005). Additional mechanisms, such as the dead receptor (DDRR) or extrinsic apoptotic pathway, and several components of the protein translation machinery seem to be also involved in MYC-induced cell death response (reviewed in Meyer et al., 2006). However, these mechanisms are not central to this thesis, as is the p53-dependent TS responses **(see Section 1.3.5.)**.

## 1.3. MYC and p53

p53 is a master tumor suppressor, widely known as the "guardian of the genome" (Lane, 1992), that senses and integrates cell damage signals, including distinct types of DNA damage, oxidative stress, nutrient deprivation, impaired RiBi, and the activation of some oncogenes (Riley et al., 2008). These stress signals are driven through different mediators converging on p53 or on its negative regulators MDM2 and MDM4, thereby allowing its stabilization and activation. Activation of p53 leads to the execution of a wide variety of downstream transcriptional programs, some of which drive important TS pathways such as DNA repair, transient cell cycle arrest, cellular senescence and/or apoptosis **(Fig. I-5)**. What determines the specific cellular output is not well understood, though it seems to strongly depend on cell-type and cell-context, the initial stimuli, and p53 cellular levels, as well as its post-translational modification state and on the cofactors or partners present at specific promoters (reviewed in Vousden and Prives, 2009, Hafner et al., 2019). In addition to the classical p53-dependent TS mechanisms, p53 regulates additional processes that may contribute to tumor suppression including cell metabolism, stem cell function, invasion and metastasis, and cell-cell communication within the tumor microenvironment (Bieging et al., 2014). Consistent with its major role in tumor suppression, more than 50% of all sporadic human cancers harbor inactivating mutations of p53, primarily located within its DBD **(Fig. I-6)**. Furthermore, some p53 mutations even in heterozygosis setting, predispose to cancer, as observed in Li-Fraumeni syndrome patients, who bear a mutant *TP53* allele, encoding p53, and display high susceptibility to cancer (Bieging et al., 2014).

### 1.3.1. p53 as a transcription factor

The major function of p53 is that of a transcription factor, but it also has transcriptional-independent functions, playing a direct role in DNA repair and DNA recombination, by binding to proteins involved in genome stability and chromatin modification (Helton and Chen, 2007). In this manner it can promote apoptosis by directly interacting with several BCL2 family members in the cytoplasm (reviewed in Green and Kroemer, 2009, Speidel, 2010). As with many other transcription factors, p53 possesses discrete domains responsible for binding to specific sequences on

DNA, for transcriptional activation and for oligomerization **(Fig. I-6)**. Indeed, its N-terminal region contains **two TADs (TAD1/2)**, **a proline-rich domain (PRD)**, and **the DBD**, while its C-terminus is a basic region which contains **the tetramerization (TET)** domain (Bieging et al., 2014). Through this domain p53 monomers interact to form tetramers, which is also critical for transcriptional activation as p53 functions as a tetramer (dimer of dimers) to recognize and bind specific **p53 response elements (p53REs)** in the promoter regions of a number of p53-target genes on the DNA (Bieging et al., 2014). A recent study has shown that p53 monomers or dimers are also able to activate genes involved in cell cycle arrest, but not in cell death, suggesting that tetramerization is essential for p53-dependent apoptotic response (Fischer et al., 2016). Similarly, in response to DNA damage p53 tetramerizes and activates gene expression, before it achieves substantial protein accumulation, thus initial p53 response is driven by tetramerization rather than by an increase in p53 levels (Gaglia et al., 2013). In addition to its oligomerization status, the ability of p53 to bind to p53REs and to transactivate its target genes depends on its post-translational modification state, e.g. acetylation by p300 and CREB-binding protein (CBP) facilitates p53-binding to the p53REs (Grossman, 2001). Likewise, the organization, arrangement and location of the p53REs within the target genes result in distinct binding affinities for p53, which is also important for the biological response (Menendez et al., 2009). For instance, *p21* gene (*CDKN1A*), has one high-affinity and several low-affinity p53REs within its promoter region. In general terms, it is considered that high-affinity-binding sites dictate cell cycle arrest responses, whereas transactivation of low-affinity p53REs drives apoptotic responses (Menendez et al., 2009). In addition, the two p53 TADs act in an autonomous manner, promoting the transactivation of distinct target genes and exerting different biological responses. TAD1 plays a predominant role in transactivation over TAD2 and is required for transcription of genes involved in DNA-damage-induced G1 arrest (e.g. *p21*) and apoptosis (e.g. *PUMA*, *NOXA*). On the other hand, senescence program in response to oncogenic stress can be driven by either TAD (Sullivan et al., 2018).

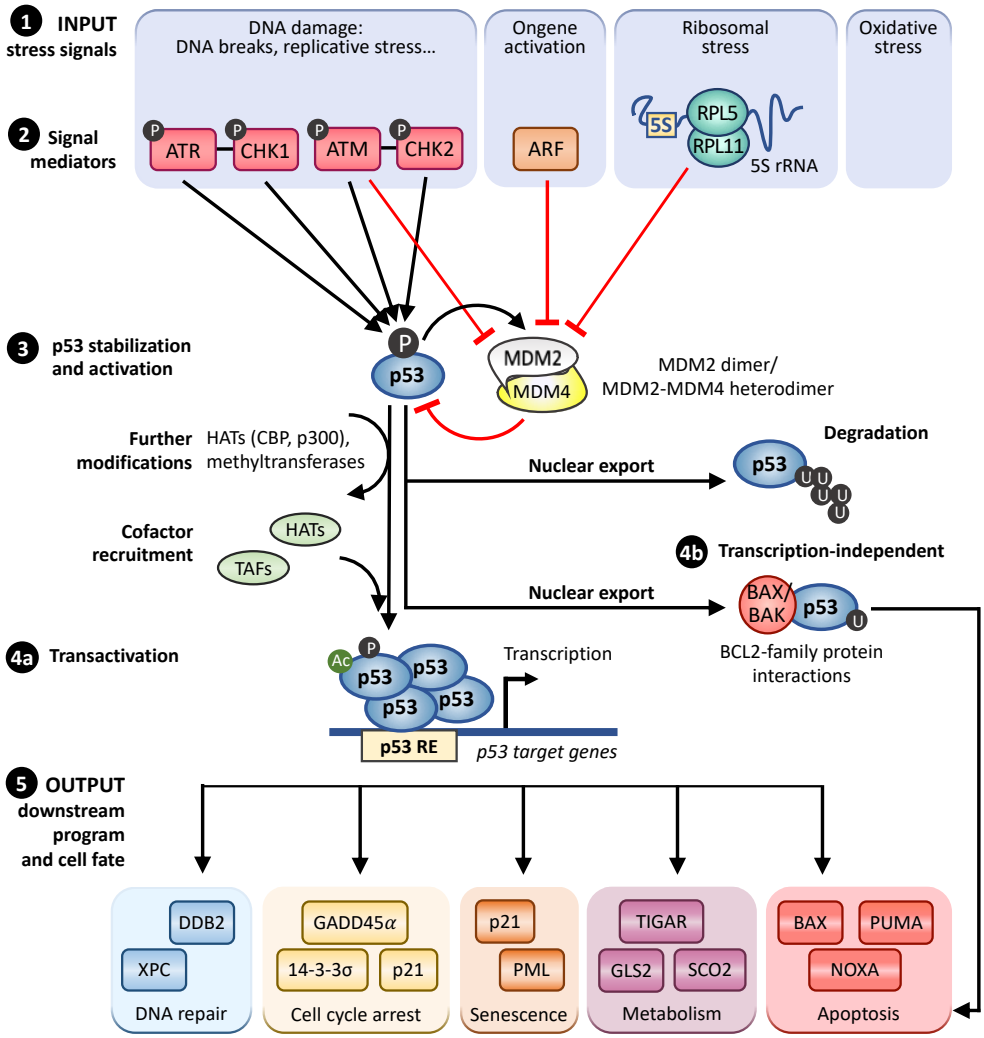


**Figure I-5. Overview of p53 activation, regulation and p53-mediated downstream pathways involved in tumor suppression.** (1) Extra- or intracellular stress signals (2) are driven by distinct signal mediators to converge the stress stimuli in (3) the activation and stabilization of p53, either by phosphorylating the protein at several residues or by inhibiting their major E3 ligases MDM2 and/or MDM4. Once activated, modifier proteins, such as HATs or methyltransferases, further stabilize p53 and increase its binding to the DNA. (4a) On its active state, p53 binds to p53REs on the vicinity of p53 target genes and recruits cofactors such as HATs or TATA-box-associated factors (TAFs), ultimately inducing transcription of its target genes. (4b) p53 can also induce apoptosis in a transcription-independent manner by directly engaging certain BCL2 family members in the cytoplasm (5) In a transcription-dependent manner, p53 activates downstream programs important in tumor suppression such as DNA repair, proliferation arrest, senescence and apoptosis. (See next page)

**Figure I-5. (continued)** Adapted from Riley et al. (2008). *Abbreviations:* ATR, *Ataxia-telangiectasia* and RAD3-related kinase; CHK1, checkpoint kinase 1; CBP, CREB-binding protein; DDB2, damage-specific DNA-binding protein-2; GADD45α, growth arrest and DNA-damage-inducible 45α; PML, promyelocytic leukemia protein; TIGAR, TP53-induced glycolysis and apoptosis regulator; GLS2, liver-type glutaminase.

### 1.3.2. p53 Tumor Suppressor response

Although how p53 differentially regulates its target genes to drive a specific biological response is not clear, which p53 target genes are responsible for the cellular outcome is better understood. For instance, p53 is known to promote cell cycle arrest through the transactivation of three critical genes: *p21* gene, *GADD45A* (encoding growth arrest and DNA-damage-inducible 45α, GADD45α) and *SFN* (encoding 14-3-3σ) (Benchimol, 2001). Critically, transcription is not the only mechanism exerted by p53 to suppress tumorigenesis, as p53 can induce apoptosis in both a transcriptional-dependent and independent manner (Green and Kroemer, 2009, Speidel, 2010). First, p53 induces the transactivation of several proapoptotic mediators involved in the intrinsic, as *BAX*, *PUMA* and *NOXA*, and extrinsic apoptotic pathways, including the DDRR *CD95/FAS* and *DR5*. However, none of these proapoptotic p53 target genes alone can explain the full apoptotic capacity of p53 and depending on the context or the cell type, some are dispensable for apoptosis, which suggests that p53-mediated apoptosis is a result of multiple proapoptotic signals (Benchimol, 2001, Schuler and Green, 2001). On the other hand, p53 can trigger apoptosis in a transcription-independent manner through the direct interaction with several BCL2 family members **(Fig. I-5)**. In response to a stress signal p53, which shuttles from the nucleus to the cytoplasm, can accumulate in the cytosol close to mitochondria, where it can interact with BCL2, BCLxL, BAX and/or BAK (reviewed in Green and Kroemer, 2009, Speidel, 2010). The binding of BAX is thought to be a 'hit-run' interaction, but sufficient to promote its activation, whereas the interaction with BAK through its central DBD domain is more stable. However, the DBD domain is also the docking site for antiapoptotic BCL2 and BCLxL, which bind p53 with stronger affinity. This suggests that p53 may first interact with antiapoptotic BCL2 proteins, sensitizing cells to apoptosis, and then with BAX and BAK, promoting its oligomerization and activation at the outer mitochondrial membrane (OMM), which results in MOMP and cell death. Given that p53 accumulates preferentially in

the nucleus, p53 needs to reach the cytosol over a certain threshold to induce non-transcriptional apoptosis. It has been proposed that accumulation of cytosolic p53 can result from specific post-translational modifications that regulate its localization or from the interaction with nuclear export factors (reviewed Speidel, 2010). For instance, monoubiquitination of p53 appears to promote its cytosolic accumulation and the induction of non-transcriptional apoptosis (Marchenko et al., 2007). It should be noted that the relevance of non-transcriptional apoptosis versus transcriptional apoptosis is still debated some evidence for crosstalk and interdependence between both pathways. For example, sequestration of cytoplasmic p53 by BCLxL is abrogated by PUMA, whose expression, in turn, is induced by nuclear p53 (Chipuk et al., 2005), reflecting the complexity of the regulation of p53-mediated cell death.

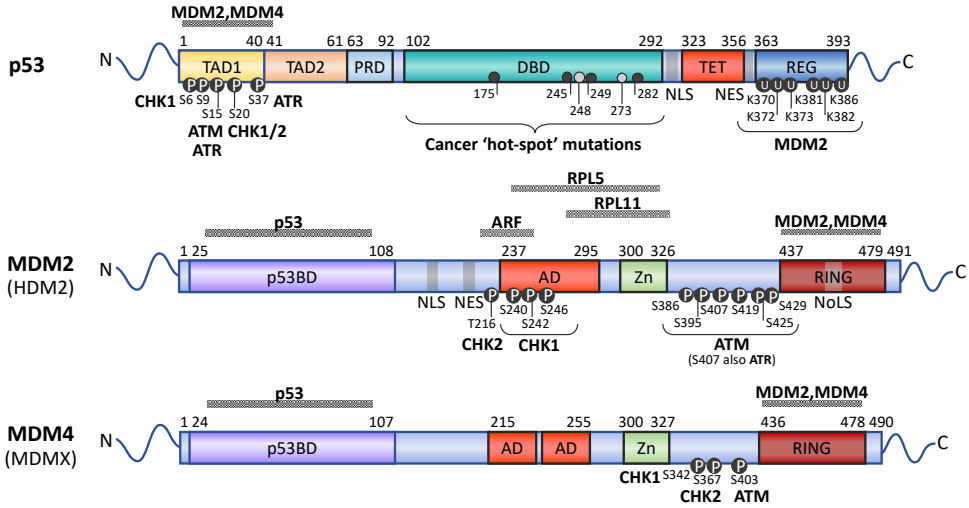


**Figure I-6. Functional domains of p53 and its two negative regulators, MDM2 and MDM4.** p53 protein contains two TADs (TAD1/2) and a PRD at its N-terminus, a central DBD, and a TET domain and a regulatory (REG) region rich in basic residues at its C-terminus. It also possesses a NLS and a nuclear export sequence (NES). *TP53* inactivating mutations typically occur within the DBD, with the six most common 'hot-spot' mutations displayed in the figure. Mutations of these residues disrupt the DNA interaction and the transactivation function of p53. MDM2 and MDM4 contain a N-terminal p53-binding domain (p53BD), a central acidic domain (AD) and a C-terminal RING-finger domain. MDM2 possesses a NLS, a NES, a cryptic nucleolar localization sequence (NoLS) and E3 ligase activity within its RING-finger domain all of which lack on MDM4. Major residues phosphorylated in response to DNA damage and the correspondent kinase, and the residues where p53 is ubiquitinated by MDM2, are displayed below each protein structure. Protein interaction domains discussed along the text are shown above each protein structure. Adapted from Bieging et al. (2014), Cheng and Chen (2010) and Meek and Anderson (2009).

### 1.3.3. p53-MDM2-MDM4 axis

Likewise, the upstream events that converge on p53 activation are best characterized for the response to acute DNA damage signals, through ATM, and to hyperproliferative signals, through the ARF-MDM2-p53 axis (Bieging et al., 2014), which are two of the major mechanisms of cell death induced by MYC overexpression **(Fig. I-4)**. Interestingly, the activation of these p53-dependent TS pathways frequently relies in the inhibition of the p53 **negative regulators MDM2 and MDM4** (also known as MDMX). Both MDM2 and MDM4 possess a **p53-binding domain (p53BD)** through which they can bind and sterically block the TAD of p53 **(Fig. I-6)**, inhibiting p53 transactivation (Oliner et al., 1993, Danovi et al., 2004). At its C-terminal domain, MDM2 and MDMX possess a **RING-finger domain** through which they can form homo- or heterodimers, preferentially MDM2-MDM2 homodimers or MDM2-MDMX heterodimers (Wu et al., 1993). Additionally, the MDM2 RING domain possesses **E3 ligase activity** and thus, can target p53 for degradation. Under physiological conditions, MDM2 homodimers preferentially monoubiquitinate p53, which promotes its nuclear export. Effective E3 ligase activity is achieved upon heterodimerization with MDM4, which does not have E3 ligase activity (Wu et al., 1993). Thus, cooperation between MDM2 and MDM4 prevents p53 transactivation in the nucleus, and promotes p53 nuclear export and subsequent proteasome-mediated degradation via mono- and polyubiquitination, respectively. In addition, MDM2-MDM4 heterodimerization blocks MDM2 auto-ubiquitination and degradation, which ensures its inhibitory activity towards p53 in basal conditions (Wu et al., 1993). Importantly, MDM2 is a direct target of p53, constituting a negative-feedback loop in which p53 promotes its own degradation **(Fig. I-6)** (Levine and Oren, 2009). This MDM2-p53 feedback loop ensures that upon non-stressed conditions, p53 expression is kept at low basal levels, but upon a stress signal, several mechanisms rapidly disrupt the interaction between MDM2 or MDM4 with p53, allowing the rapid activation of p53. Once the stress signal or its consequences are alleviated, this negative feedback loop ensures the restoration of p53 expression to its basal levels (reviewed in Wu et al., 1993, Levine and Oren, 2009).

### 1.3.4. Genotoxic stress: DNA damage response

As stated above a well characterized cellular insult that elicits p53 activation is DNA damage. DSBs on the DNA trigger activation of ATM kinase, whereas single strand breaks (SSBs), leads to a stalling or collapse DNA replication forks and the recruitment of the *ataxia-telangiectasia* and RAD3-related (ATR) protein kinase. Both ATR and ATM kinases act through the phosphorylation of multiple substrates, including the checkpoint kinases (CHK) CHK1 and CHK2, respectively. Both ATR/ATM kinases together with CHK1/CHK2 kinases coordinately phosphorylate p53 at several sites of its N-terminal region (Blackford and Jackson, 2017). For instance, p53 phosphorylation at S15 by ATM and at S20 by CHK2 **(Fig. I-6)** promote its stabilization by disrupting its interaction with MDM2 and MDM4, allowing it to interact with transcriptional cofactors, required for transactivation (Bieging et al., 2014). In parallel, ATM and ATR phosphorylate MDM4 and MDM2 **(Fig. I-6)** (Cheng and Chen, 2010). Phosphorylation of MDM4 led to increased binding, ubiquitination, and degradation by MDM2, while phosphorylation of MDM2 inhibits its ability to polyubiquitinate p53 for proteasomal degradation (Cheng and Chen, 2010). However, phosphorylation of MDM2 by ATM does not impair its ability to polyubiquitinate itself (Riley et al., 2008), further contributing to augment p53 cell levels in response to DNA damage (Cheng and Chen, 2010, Blackford and Jackson, 2017). Therefore, ATM-mediated phosphorylation of both p53 and its negative regulators MDM2 and MDM4, are required for the activation of p53 and the transactivation of its target genes.

Phosphorylation of p53 by of ATM/ATR blocks cell proliferation by upregulating *p21* gene, which triggers G1 arrest, blocking S-phase entry and allowing cells to repair the damaged DNA, thereby preventing DNA replication with a damaged template and thus, limiting the propagation of potentially oncogenic mutations (Bieging et al., 2014). Similarly, transactivation of *GADD45A* or *SFN* induces cell cycle arrest, but at the G2-to-M phase transition (Wang et al., 1999). If the amount and type of DNA lesion is excessive or cannot be repaired, cells will not resume cell cycle progression and apoptosis will be evoked (reviewed Shiloh, 2003, Roos and Kaina, 2006). Therefore, low levels of DSBs induce activation of a minor fraction of p53, sufficient to drive *p21* transcription and cell cycle arrest, whereas high levels of DSBs result in

an accumulation of p53 above a threshold sufficient to activate proapoptotic genes such as *BAX*, *PUMA* and *CD95/FAS* receptor. Hence, the levels of ATM-ATR-p53 activation are important for triggering apoptosis in response to DNA damage.

As explained in **Section 1.2.2.**, MYC overexpression also elicits ATM-MDM2-p53 DDR as a mechanism of tumor suppression (Pusapati et al., 2006). Oncogenic MYC expression induces DNA damage and the formation of DSBs on the DNA due to an increased production of reactive oxygen species (ROS) and replicative stress (Vafa et al., 2002). Replicative stress, characterized by increased numbers of stalled and collapsed replication forks (Dominguez-Sola et al., 2007, Srinivasan et al., 2013), is induced due to the hyperactivation of DNA replication by oncogenic MYC, which generates genomic instability and accounts for early DNA damage. Thus, MYC-induced replicative stress triggers DDR, which leads to cell death, as a mechanism that limits tumorigenesis at early stages (reviewed in Campaner and Amati, 2012). Interestingly, oncogenic MYC-induced DDR elicits cell death and not cell cycle arrest. The work by Seoane et al. attributed this effect to the ability of MYC to repress p21 expression through the recruitment by MIZ1 to the *CDKN1A* promoter **(Fig. I-2)**. They demonstrated that deregulated MYC expression overrides p21-mediated DDR-induced cell cycle arrest and enables p53-transactivation of proapoptotic factors through the ATM-MDM2-p53 pathway, resulting in cell death, with MYC levels being critical in promoting either a cytostatic or an apoptotic response to DNA damage (Seoane et al., 2002).

### 1.3.5. Oncogenic stress: ARF-MDM2-p53 pathway

Another important p53-dependent TS pathway, discovered over 20 years ago by Sherr and co-workers, is the **ARF-MDM2-p53 pathway** (Quelle et al., 1995). Like the DDR induced by oncogenes, this pathway, which is induced by oncogenic stress or hyperproliferative signals, leads to the disruption of MDM2-p53 interaction and the subsequent stabilization and activation of p53 (reviewed in Meyer et al., 2006). Hyperproliferative signals, such as deregulated MYC or E2F1 expression, or oncogenic RAS activation induce the expression of ARF ($p14^{ARF}$ in humans and $p19^{ARF}$ in mice) tumor suppressor through a mechanism that is not well understood. ARF is a nucleolar protein encoded on chromosome (Chr) 9p21 at an alternative reading

frame (ARF) within the *INK4B-ARF-INK4A* locus (Quelle et al., 1995). The locus, which is among the most frequently deleted sites in human cancer, contains two additional tumor suppressors of the INK4 family, $p16^{INK4A}$ and $p15^{INK4B}$, which bind and inhibit CDK4 and CDK6, involved in G1-to-S-cell cycle transition. By contrast, ARF is not a CKI but an inhibitor of MDM2. ARF either functions by binding and inhibiting MDM2 ubiquitin ligase activity towards p53, through a conserved minimal region at its N-terminus, or by sequestering MDM2 in the nucleolus, thereby preventing its binding to p53 (reviewed in Sharpless, 2005, Gil and Peters, 2006). The mechanism by which MYC induces ARF expression remains unclear, as ARF does not seem to be a direct target of MYC (Cleveland and Sherr, 2004). It has been proposed that MYC induces ARF expression through E2F1, a direct target of MYC (Leone et al., 1997, Sears et al., 1997). E2F1 directly induces ARF expression by displacing a repressor complex comprised by another E2F family member, E2F3b-repressor complex, located on the *ARF* promoter (Aslanian et al., 2004). Whether MYC does so by inducing the activity of E2F1 is controversial as it seems to be cell-type dependent, and not conserved in the mouse (Leone et al., 2001, Baudino et al., 2003). In addition to this mechanism, Bouchard and colleagues showed that MYC also activates ARF through the forkhead box class O (FOXO) family of transcriptions factors. Deregulated MYC expression induces accumulation of nuclear FOXO proteins, which binds to the *ARF* promoter, leading to increased ARF expression and suppression of MYC-driven lymphomagenesis in mice (Bouchard et al., 2007). A third mechanism has been recently proposed, in which MYC can interact with the ubiquitin ligase ULF and increases ARF protein stability, as ULF is responsible for ARF-ubiquitination and degradation (Chen et al., 2010). This latter mechanism is active upon oncogenic MYC expression, but not at physiological levels of MYC (Chen et al., 2013). Therefore, it is not completely clear, which of the mechanism(s) leads to ARF stabilization. Likewise, its activation by oncogenic MYC triggers p53-dependent apoptosis in almost all cases (Post et al., 2010), but this response appears to be cell-type, context and oncogene dependent. For instance, this pathway primarily elicits apoptosis upon MYC deregulation (Zindy et al., 1998), whereas when it is induced by oncogenic RAS, cells become senescent (Serrano et al., 1997). Thus, in response to MYC-oncogenic stress, activation of the ATM-MDM2-p53 DDR in parallel with the ARF-MDM2-p53 pathway can further cooperate to activate p53-TS apoptotic cell death response.

### 1.3.6. Ribosome biogenesis stress: 5S rRNA/RPL5/RPL11-MDM2-p53 pathway

Enhanced RiBi is an essential process to sustain the aberrant proliferation rates of cancer cells. Despite growing independently of external stimuli, uncontrolled cell proliferation cannot take place without increasing cell mass, which requires the production of a large amount of proteins, and that, in turn, requires more ribosomes (reviewed in Ruggero and Pandolfi, 2003). Indeed, nucleolar hypertrophy, reflecting increased rates of RiBi, has been widely recognized by physicians since the late 19$^{th}$ century as a hallmark of many cancers (Pianese, 1896, MacCarty, 1936). Importantly, many key tumor suppressors and proto-oncogenes regulate RiBi , such as p53 (Cairns and White, 1998, Zhai and Comai, 2000), ARF (Itahana et al., 2003), E2F1 (Ayrault et al., 2006), and MYC (van Riggelen et al., 2010). The loss of tumor suppressors or oncogene activation contribute to hyperactive RiBi ,which not only buffers tumor cells with sufficient amounts of proteins to sustain their high proliferation rates, but is essential for cancer initiation and progression (reviewed in Orsolic et al., 2016). However, RiBi is highly energy consuming (reviewed in Pelletier et al., 2018), such that altered RiBi activity is sensed by the cell as a cellular stress, leading to p53 stabilization. The potential existence of a checkpoint that sensed impaired RiBi was first described by our laboratory twenty years ago (Volarevic et al., 2000). Subsequently, it was demonstrated that the checkpoint was elicited by the induction of p53 (Pestov et al., 2001). The response was initially attributed to nucleolar disruption and the passive diffusion of several RPs from the nucleolus into the nucleoplasm, where they were able to bind and inhibit MDM2, triggering p53-dependent cell cycle arrest (Zhang and Lu, 2009). However, contrary to this argument, our group demonstrated that (**1**) deregulated RiBi leads to p53 stabilization in the absence of nucleolar disruption (Fumagalli et al., 2009), (**2**) only RPL5 and RPL11 , but not other proposed RPs, binds to and inhibits MDM2 upon altered RiBi (Fumagalli et al., 2012), and (**3**) that RPL5 and RPL11 carry out this function as part of a nascent pre-ribosomal complex which also contains 5S rRNA (Donati et al., 2013). Our findings, and that of others demonstrated that this precursor complex mediates p53 stabilization when an impairment to RiBi is encountered, ultimately leading to cell death, cell cycle arrest or senescence

(reviewed in Bursac et al., 2014). Given its function monitoring RiBi, we termed this response the **'Impaired Ribosome Biogenesis Checkpoint' (IRBC)** (Gentilella et al., 2017). Importantly, Macias et al., in 2010, provided the first evidence that this checkpoint is not only elicited upon RiBi impairment, but also under conditions of hyperactive RiBi such as upon oncogenic MYC expression. These studies demonstrated that, in the absence of this checkpoint, mice succumb much more rapidly to MYC-driven lymphomagenesis thus, suggesting the potential role of this checkpoint as a TS barrier against tumorigenesis (Macias et al., 2010). Many other aspects regarding this checkpoint, RiBi and its contribution to MYC-driven tumorigenesis will be discussed in detail in **Chapter 3**.

## 1.4. MYC-driven lymphomas

Abrogation of TS mechanisms allows deregulated MYC not only to initiate tumorigenesis but also to sustain malignant transformation (Adhikary and Eilers, 2005). Indeed, MYC deregulation is frequently acquired as a 'secondary event', that may explain why it is deregulated in the majority of human cancers, including colon, breast, prostate, lung and liver cancers, and in several pediatric cancers (Dang, 2008). In hematological malignancies, *MYC* gene is frequently altered in B-cell lymphomas, normally acquired as a secondary event, while rare in T-cell lymphomas. First evidence of the involvement of MYC in human cancer was observed in Burkitt's lymphoma (BL), a neoplasm from B-cell origin, in which MYC was identified consistently altered by chromosomal translocation (Dalla-Favera et al., 1982). *MYC* translocations or gene amplifications leading to MYC activation were subsequently detected in other mature B-cell lymphomas, frequently associated to the most aggressive forms of the disease (reviewed in Delgado and Leon, 2010, Ott et al., 2013). As displayed in **Table I-1** *MYC* genetic alterations are present in nearly 50% of plasmablastic lymphomas (PBL) and 5-15% of diffuse large B-cell lymphomas (DLBCL), frequently correlating with *BCL2* and/or *BCL6* translocations, which are denoted as 'double hit' or 'triple hit' lymphomas, the worst-case scenario. At a lower frequency, *MYC* alterations are also found in mantle cell lymphoma (MCL) and in B-cell acute lymphoblastic lymphoma/leukemia (B-ALL) (Delgado and Leon, 2010, Ott et al., 2013). Likewise, acquisition of *MYC* alterations is associated with transformation of

certain neoplasms to more aggressive subtypes as occurs in the transformation of the follicular lymphoma (FL) to the more aggressive DLBLC (Pasqualucci et al., 2014), and in the progression of the chronic lymphocytic leukemia (CLL) to the high-grade lymphoma known as Richter's syndrome (RS) (Scandurra et al., 2010). Also, in multiple myeloma (MM), one of the most common hematological cancers, progression from a premalignant stage to MM, as well as disease progression, is related to elevated MYC expression in 50% of the cases, frequently resulting from complex *MYC* locus rearrangements (Affer et al., 2014). Among T-cell lymphomas, *MYC* amplifications are found in 6% of T-ALLs (La Starza et al., 2014) and its expression is deregulated in anaplastic large-cell lymphoma (ALCL) due to the constitutive activation of the JAK/STAT3 signaling pathway (Weilemann et al., 2015). The contribution of *MYC* alterations to myeloid neoplasms has been less studied but it is frequently overexpressed in acute myeloid leukemia (AML), chronic myeloid leukemia (CML) and myelodysplastic syndrome (MDS), as a consequence of additional mutations upstream MYC, and also correlates with disease progression and worse prognosis. It is important to note that, although *MYC* alterations or deregulation are extremely frequent in human neoplasms, especially in B-cell lymphomas, its deregulation alone does not cause lymphoma. For instance, the translocation (t) of *MYC* found in patients of BL, the t(8;14), is present at low levels in blood and bone marrow (BM) of healthy individuals (Ott et al., 2013). Thus, induction of lymphomagenesis requires additional events that abrogate the stringent control of MYC expression. As MYC translocation and its subsequent deregulation is the primary event that drives BL, it has been a model of choice for the study of MYC tumorigenesis, especially through the development of MYC-driven mouse models, such as the E$\mu$-MYC-driven lymphoma mouse model (Adams et al., 1985).

**Table I-1. Oncogenic MYC in human hematological malignancies.**

| Neoplasm | Cell-of-origin | Primary 'hit' | Alterations in MYC Mechanism | Frequency | Additional oncogenic alterations* |
|---|---|---|---|---|---|
| **B-cell lymphomas/leukemias** | | | | | |
| B-ALL | Precursor B cell | Het | Translocations | 5% | *TEL1/2* translocations |
| BL | DZ GC cell | *MYC* translocation | Translocations<br>Point mutations in the TAD | >90%<br>60-70% | *TCF3*, *ID3*, *CCND3* mutations |
| DLBCL | DZ/LZ GC cell | Het | Translocations<br>Amplifications<br>Mutations | 5-15%<br>2% | *BCL2* and *BCL6* translocations |
| PBL | Plasmablast | Unknown | Translocations | 40-50% | *PRDM1* mutations |
| FL | LZ GC cell | *BCL2* translocation | Translocations, amplifications and point mutations | 30-40% | *CDKN2A/p16* inactivation, *BCL6* translocations |
| MCL | Naïve B cell | *CCND1* translocation | Translocations<br>Increased stability | rare | *ATM*, *BMI1*, *CDK4*, *BCL2* mutations |
| CLL | Mature/Post-GC B cells | Het | Translocations<br>Amplifications | <3% | *RPS15, MAP2K1, BRAF, RAS* mutations |
| MM | Plasma cell | Het | Translocations, complex rearrangements | 50% | Mutations in MAPK, NF-kB and DNA repair |
| *ALK*$^+$ LBCL | Plasmablast | *ALK* translocation | Upregulated by ALK-STAT3 signaling | ? | ER stress response? |
| **T-cell lymphomas/leukemias** | | | | | |
| T-ALL | Precursor T cell | *NOTCH1* mutations? | Amplifications<br>Downstream NOTCH1 | 6% | *NOTCH1* activating mutations (50%), *LEF1* inactivation |
| ALCL | Peripheral T cell | *ALK* translocation (*ALK*$^+$ ALCL) | Upregulated by ALK-STAT3 signaling | ? | Activation of JAK/STAT3 pathway, *TP63* rearrangements |
| **Myeloid leukemias** | | | | | |
| AML | HSC | Het | Amplifications and copy gain (trisomy 8)<br>Upregulated mRNA, increased stability due to *FLT3, NPM1* mutations | 1% | Trisomy 8 (9%), *FLT3* (25-30%), *NPM1, RUNX1* mutations |
| CML | HSC | *BCR-ABL1* fusion | Amplifications and copy gain (trisomy 8)<br>Upregulated mRNA downstream *BCR-ABL1* | ? | Trisomy 8, *PDGFRA*, *PDGFRB*, *FGFR1* rearrangements, *PCM1-JAK2* fusion |
| MDS | HSC/myeloid progenitor cell | Het | Amplifications<br>Upregulated mRNA | ? | Similar to AML |

(See next page)

**Table I-1. (continued)** *Abbreviations:* B-ALL, B-cell acute lymphoblastic lymphoma/leukemia; BL, Burkitt's lymphoma; DLBCL, diffuse large B-cell lymphoma; PBL, plasmablastic lymphoma; FL, follicular lymphoma; MCL, mantle cell lymphoma; CLL, chronic lymphocytic leukemia; MM, multiple myeloma; ALK, anaplastic lymphoma kinase; LBCL, large B-cell lymphoma; T-ALL, T-cell acute lymphoblastic lymphoma/leukemia; ALCL, anaplastic large-cell lymphoma; AML, acute myeloid leukemia; CML, chronic myeloid leukemia; MDS, myelodysplastic syndrome; DZ, dark zone; LZ, light zone; GC, germinal center; HSC, hematopoietic stem cell; ER, endoplasmic reticulum; Het, heterogeneous; FLT3, fms-like tyrosine kinase 3; NPM1, nucleophosmin. **TP53* mutations are also found at distinct frequencies.

### 1.4.1. Burkitt's Lymphoma

In brief, human BL is a highly aggressive, but curable human non-Hodgkin lymphoma (NHL), which originates in the B-cell linage. It has the fastest growing rate among human tumors, with a cell doubling time of only 25 hr. The first description of the disease was made by Sir Albert Cook in 1887, although it was not identified and defined until the 1950s by Dr. Denis Burkitt in African children living in areas endemic for malaria (Burkitt, 1958, Burkitt and O'Conor, 1961). It was the first human tumor found associated with a virus (Epstein et al., 1964) and one of the first tumors in which a chromosomal translocation that activates an oncogene was observed (Manolov and Manolova, 1972, Zech et al., 1976). The pathology is presented as three distinct clinical variants, endemic, sporadic and immunodeficiency-related BL (Jaffe, 2009). Endemic BL is associated with malaria endemicity and Epstein-Barr virus (EBV)-infection (Orem et al., 2007) and it is highly prevalent in 4 to 7 year-old children from equatorial Africa, with an incidence of 3-6 cases per 100,000 children per year (Magrath, 2012). The sporadic subtype occurs worldwide, predominantly in North America and Europe, and it is rarely associated with EBV infection (10-20% of the cases). The subtype accounts for 30-40% of pediatric NHL and for 1-2% of adult NHL in US and Europe, i.e., 2-3 cases per one million persons per year (Morton et al., 2006, Mbulaiteye et al., 2009, Sant et al., 2010). Finally, immunodeficiency-related BL occurs mainly in HIV+ adult patients, the infection increasing the risk of BL incidence around 1000 times more (Knowles, 2003, Ferry, 2006), but there is no evidence of EBV association. Overall, it is a rare disease, but its incidence and geographic distribution is heterogeneous and it is still one of the most frequent malignancies in present-day African children (Ferry, 2006). Clinically, BL presents a rapid lymph node enlargement (lymphadenopathy), most commonly at the head and

neck, and the growth of abdominal masses and hepatosplenomegaly. In sporadic BL, the most common site of presentation is the abdomen (60-80% cases) with frequent BM infiltration (30% cases) and dissemination to the Central Nervous System (CNS) in the worst cases, ∼15% (Swerdlow et al., 2008). By contrast, endemic BL is classically presented in the jaws and other facial bones (e.g. the orbit bones) but BM infiltration is rare. Finally, immunodeficiency-associated BL mainly involves lymph nodes together with BM and CNS infiltration, and in some cases, patients also present leukemic disease (Swerdlow et al., 2008).

Despite being an aggressive tumor, BL prognosis is generally favorable, with median 5-year survivals ∼70-90% with actual chemoimmunotherapy regimens (Costa et al., 2013, Mukhtar et al., 2017). However, there are significant differences among the distinct age groups, with 5-year survival reduced to 48% and 29% in adults and elderly patients, respectively, and an inferior outcome in black patients, likely reflecting unequal access to care. The current standard treatment for BL derives from a protocol developed by Magrath and colleagues in 1996, the CODOX-M protocol (Magrath et al., 1996) with minor modifications to minimize treatment-associated toxicities (Lacasce et al., 2004). However, as it is a rare disease, there is a lack of randomized studies and an optimal therapy is not clearly defined, presenting the possibility to apply distinct protocols, with comparable responses. These protocols are based on the administration of short and highly intensive chemotherapy regimens including CNS-penetrating agents, as high-dose methotrexate or cytarabine, in combination with intrathecal prophylaxis, to prevent the risk of CNS progression. Such aggressive regimens are associated with frequent adverse effects, including severe myelosuppression and mucositis, neuropathy, and even cases of treatment-related deaths due to tumor lysis syndrome, a complication derived from the rapid break down of cancer cells due to such aggressive chemotherapy that can lead to kidney failure, or sepsis (Mead et al., 2002, Blum et al., 2004). Minimization of these toxicities is required, especially for elderly patients. Furthermore, current treatments are sub-optimal for patients with poor prognosis at diagnosis or in the setting of relapse disease. Therefore, alternative therapies such as immunotherapy and molecular targeted-therapies, including antisense oligonucleotides against the *MYC* gene, proteasome inhibitors and CKIs, among others, are under investigation (Blum et al., 2004, Thomas et al., 2006, Mosse and Weck, 2010).

**Molecular pathology of Burkitt's lymphoma.** At the molecular level the three variants shared many morphologic, immunophenotypic and genetic features. The common hallmark among the subtypes is the translocation of *MYC* gene from the q24 arm of Chr 8 to one of the immunoglobulin (Ig) loci (Mosse and Weck, 2010). The translocation of *MYC* in BL was identified for the first time in 1982, when two independent groups found the gene rearranged to the Ig μ(mu) heavy chain gene (*IGH*) locus on Chr 14(q32) (Dalla-Favera et al., 1982, Taub et al., 1982). This translocation, denoted as t(8;14), is present in over 80% BL patients, regardless of the variant. In the remaining cases, MYC is rearranged to one of the Ig light chain loci, either to the Ig kappa light chain (*IGK*) promoter sequences t(2;8), in ∼15% of cases, or to the Ig lambda light chain (*IGL*) genes t(8;22), in the remaining cases (Hecht and Aster, 2000, Boxer and Dang, 2001). Both heavy and light chain loci are specifically active in mature B cells, thereby, translocated *MYC* allele is actively transcribed in BL, whereas normal *MYC* allele is transcriptionally silent (Boxer and Dang, 2001). Although there are distinct breakpoints on *MYC* gene, scattered over several hundred kb (Pelicci et al., 1986, Neri et al., 1988), exons 2 and 3 remain intact. However, the presence of different breakpoints, which cluster based on the BL variant, may indicate that translocation and neoplastic transformation occurs at different stages of B cell maturation, and that MYC may be differentially regulated in the distinct variants (Ferry, 2006, Mosse and Weck, 2010).

In addition to translocations, BL harbors additional alterations, such as *MYC* and *TP53* mutations, occurring in a 60 and a 40% of the cases, respectively, and recurrent somatic mutations in *TCF3*, *ID3* and/or *CCND3* genes (Ott et al., 2013). Most common MYC alterations are found in the translocated *MYC* allele, probably influenced by the presence of the hypermutable Ig locus (Boxer and Dang, 2001, Mosse and Weck, 2010). Frequently, mutations occur at one 'hot-spot' within the MBI TAD, which enhances MYC's oncogenic potential by distinct mechanisms, such as by increasing MYC protein stability or by impairing the induction of proapoptotic *BIM*, inhibiting the MYC-induced TS apoptotic response (Blum et al., 2004, Ott et al., 2013). One common 'hot-spot' is T58 residue (Blum et al., 2004, Mosse and Weck, 2010) whose mutation abolishes MYC proteasomal degradation allowing oncogenic MYC accumulation **(see Section 1.1.3.)**.

Regarding p53, approximately 35-40% of BL cases present inactivating mutations in the gene, which abrogates MYC-induced apoptosis. The apoptosis bypass in BL is also achieved through alterations in the ARF-p53-MDM2 pathway as well as genetic and epigenetic alterations that lead to the inactivation proapoptotic BIM (Mestre-Escorihuela et al., 2007, Richter-Larrea et al., 2010).

Other frequent synergistic mutations in BL include oncogenic mutations on *CCND3* (38%), which produce highly stable cyclin D3 isoforms that drives G1-to-S cell cycle transition; deletions or inactivating mutations in *CDKN2A*, encoding $p16^{INK4A}$ (17%), which also regulates the G1-to-S transition; and mutations involving *TCF3* or its negative regulator *ID3* (70%), which leads to the activation of the PI3K/AKT and the TCF3/ID3 pathways, promoting B-cell survival (Schmitz et al., 2012).

### 1.4.2. Modelling Burkitt's Lymphoma: the E*μ*-MYC mouse model

The t(8;14) of BL was recapitulated by Adams and colleagues in 1985 in the development of the E*μ*-MYC transgenic mouse model (Adams et al., 1985). In this model *MYC* gene is fused to the *IGH* gene promoter and enhancer (E*μ*), leading to B-cell specific MYC overexpression (Harris et al., 1988, Schmidt et al., 1988). It is considered a lymphoblastic lymphoma rather than a BL, but many histologic and cytologic features of the E*μ*-MYC lymphoma resemble human BL. Nevertheless, E*μ*-MYC tumors are very heterogeneous, exhibiting pre-B, immature B, or mixed immunophenotypes, whereas BL arises from more differentiated B cells from the dark zone (DZ) of the germinal center (GC) (Adams et al., 1985). Despite these differences, the E*μ*-MYC lymphoma is a reference model for studying MYC-driven lymphomagenesis and has allowed the identification of many genes implicated in the onset and progression of the disease. E*μ*-MYC tumors arise after a period of latency (2-5 months) in which there is an initial polyclonal expansion of pre-malignant undifferentiated B cells in the BM and peripheral blood of the mice (Langdon et al., 1986, Sidman et al., 1993). During this phase B cells are larger than their wild-type (wt) counterparts, exhibit increased protein synthesis and deregulated cell growth, and they do not differentiate. Then, these pre-malignant B cell precursors undergo rapid proliferation and turnover due to the activation of the ARF-MDM2-p53 pathway and changes in BCL2 family members, indicating that MYC overexpression

alone is not sufficient to transform lymphoid cells (Sidman et al., 1993, Jacobsen et al., 1994). Expansion of a lethal clone of pre-B and B-cell lymphomas requires additional genetic changes, such as the overexpression of *Bcl2* (Strasser et al., 1990), similarly to what is observed in many human MYC-driven B-cell neoplasms. The cooperation of MYC with BCL2 family members has been largely studied in this model, and it is now known that dysregulation of several members of the family accelerates E$\mu$-MYC lymphoma development (Egle et al., 2004, Michalak et al., 2009, Frenzel et al., 2010, Grabow et al., 2014), although it is not clear whether it occurs in spontaneous tumors. Likewise, disruption of the ARF-MDM-p53 pathway is also required to evade MYC-induced apoptosis and to initiate/maintain tumorigenicity in the E$\mu$-MYC model, similarly to what was shown in BL (Eischen et al., 1999). Indeed, the majority of E$\mu$-MYC tumors harbor mutations in the ARF-MDM2-p53 pathway, e.g. *Ink4a/Cdkn2a* locus deletions, overexpression of *Mdm2* or mutations on *Trp53* (Eischen et al., 1999, Meyer et al., 2006). Disruption of non-apoptotic TS mechanisms also cooperate in E$\mu$-MYC lymphomagenesis, in particular oncogene-induced senescence pathways and immune surveillance (Wall et al., 2013). Likewise, spontaneous oncogenic *Nras* mutations are also found in E$\mu$-MYC lymphomas (Alexander et al., 1989). Despite clear evidence of naturally-occurring mutations in *Trp53*, *Nras* and *Ink4a*/*Cdkn2a* in this model, it is not yet established which oncogenic lesions drive E$\mu$-MYC lymphoma development in up to half of the cases (Eischen et al., 1999).

# 2. Apoptotic cell death and antiapoptotic MCL1 in the E$\mu$-MYC-driven lymphoma

Intrinsic apoptotic cell death is a major feature of E$\mu$-MYC-driven lymphomagenesis. Overexpression of several antiapoptotic BCL2 family members, such as *Bcl2* (Strasser et al., 1990), *Bclxl* and *Mcl1* (Grabow et al., 2014), or deletion of proapoptotic BH3-only genes including *Bim*, *Bmf*, or *Bad* (Egle et al., 2004, Michalak et al., 2009, Frenzel et al., 2010), accelerate lymphoma development in the E$\mu$-MYC mouse. These members belong to the BCL2 family of proteins, named after the discovery of the chromosomal translocation of the *BCL2* gene in B-cell follicular lymphomas whose overexpression rather than promoting cell proliferation, as most previously discovered oncogenes, was found to inhibit of cell death (Youle and Strasser, 2008).

## 2.1. The BCL2 family

The major role of the BCL2 protein family is the regulation of the intrinsic apoptotic cell death at the OMM, primarily through direct interactions between them, which regulates MOMP, The ratio between anti- and proapoptotic members of this family governs cell fate, such that if the balance favors proapoptotic members, MOMP is promoted, resulting in the release of proapoptotic intermembrane space (IMS) proteins to the cytosol and the subsequent activation of the cysteine-dependent aspartate-specific protease (caspase) cascade, which rapidly drives the cell to commit suicide (Pop and Salvesen, 2009).

### 2.1.1. Structure and classification of the BCL2 family proteins

Classically, the distinct members of the BCL2 family are classified into three groups based on their function and structure: antiapoptotic proteins, proapoptotic effectors and proapoptotic BH3-only proteins **(Fig. I-7)**. Despite their structural differences, all contain at least one conserved BCL2 homology (BH) domain, the BH3 domain, comprised by the amino acid sequence 'LXXXGD', in which X represents any amino

acid. This short motif allows interactions among the distinct members of the family (Youle and Strasser, 2008).

**Antiapoptotic proteins.** Antiapoptotic BCL2 family members are structurally related multi-BH domain proteins. They are comprised of a globular bundle of nine α-helices (α1-α9), forming an exposed hydrophobic surface groove through helices α2-α5 capped by helix α8 (Moldoveanu et al., 2014). The groove, which contains residues from the BH1 and BH3 domains, is referred to as the BH3-surface groove as it binds the BH3 region of binding partners. The remaining α1 and α9 helices comprise the BH4 and the transmembrane (TM) domains, respectively, which are important for docking to several cell membranes, including the OMM and the endoplasmic reticulum (ER) membrane (Chipuk et al., 2010, Warren et al., 2019). The TM domain is also present in the proapoptotic effectors and in some BH3-only proteins, allowing them to anchor primarily to the OMM (Adams and Cory, 2018). Antiapoptotic BCL2 family proteins function either by antagonizing the BH3-only proteins BIM, PUMA and BH3-interacting-domaing death agonist (BID), or by inhibiting BAX and BAK effector proteins through direct protein interactions **(Fig. I-8)**. Depending on the cellular stress they can act through either mechanism or by both (Llambi et al., 2011). Their affinity for binding BAX and BAK proapoptotic effectors differs. For instance, BAX can be restrained by all five members, whereas BAK is primarily engaged by myeloid cell leukemia 1 (MCL1), BCL2-related protein A1 (human BFL1 or mouse A1, BFL1/A1 herein) and BCLxL.

**Proapoptotic effectors.** Proapoptotic BCL2 family effectors are also multi-BH domain proteins with conserved structures. Upon activation, they assemble into homo-oligomers within the OMM forming proteolipid pores that promote MOMP. The third member of the group, BCL2-related ovarian killer (BOK), is an unconventional proapoptotic effector that induces MOMP and apoptosis independently of other BCL2 proteins. BOK is regulated through ubiquitination and proteasomal degradation and it seems to play a role in apoptosis induced by ER-associated degradation (ERAD) (Llambi et al., 2016).

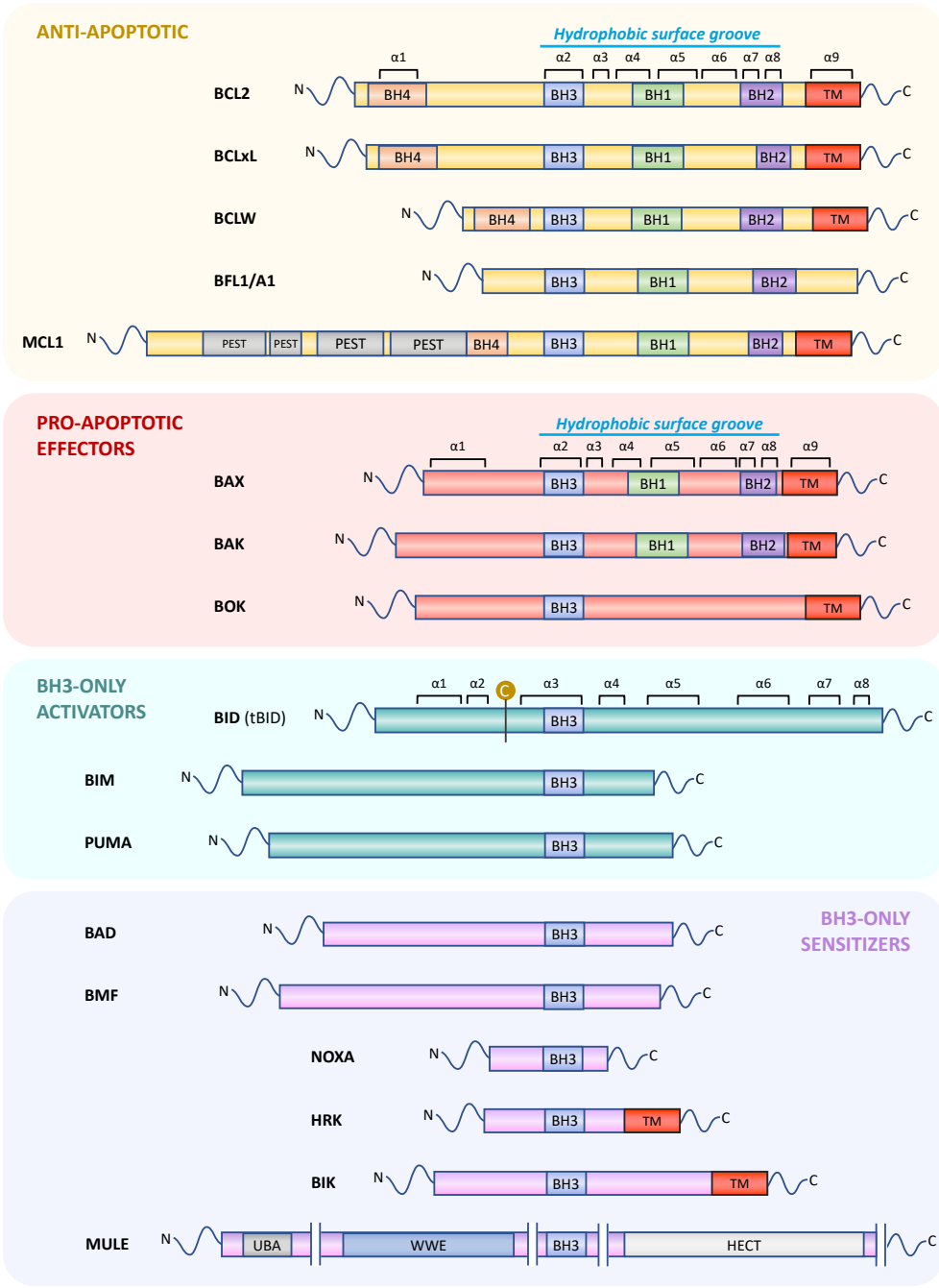


**Figure I-7. Core members of the BCL2 family of proteins.** (See next page)

**Figure I-7. (continued)** Major structural and functional domains of the distinct BCL2 family members are shown, including the BCL2 homology (BH) domains (denoted as BH1, BH2, BH3 and/or BH4) as well as the transmembrane (TM) domain, present in several members. The α-helices of the antiapoptotic members, proapoptotic effectors and of BID are indicated (α1-α9). The BH3 hydrophobic surface groove comprises α2-α8 and the TM domain contains α9. MCL1 N-terminus contains several PEST sequences. BID structure is similar to that of antiapoptotic members and of proapoptotic effectors. Its cleavage into the active 'truncated' BID (tBID) form, is indicated by a 'C'. MULE has additional domains to function as an E3 ligase, including a UBA domain, the WWE interaction module and a HECT E3 ubiquitin ligase domain. Adapted from Youle and Strasser (2008). *Abbreviations:* BCLW, BCL2-like protein 2; BFL1/A1, BCL2-related protein A1; MCL1, myeloid cell leukemia 1; BOK, BCL2-related ovarian killer; BID, BH3-interacting-domain death agonist; BAD, BCL2-antagonist of cell death; BMF, BCL2-modifying factor; HRK, harakiri; BIK, BCL2-interacting killer; MULE, MCL1 ubiquitin ligase E3; UBA, ubiquitin-associated; HECT, homologous to the E6-AP carboxyl terminus.

**Proapoptotic BH3-only proteins.** Nearly all proapoptotic BH3-only proteins are intrinsically unstructured proteins, until their BH3 domains engage to their partner (Adams and Cory, 2018). They do not share a common structure and they are not related to the other BCL2 family protein members, with the exception of BID, which resembles multidomain proteins. The BID BH3 domain is sequestered into its hydrophobic surface groove until it is exposed by proteolytic cleavage near its N-terminus, leading to the active form of the protein termed 'truncated' BID (tBID) (Chipuk et al., 2010). Despite their unrelated structures, all the members contain the conserved BH3 domain through which they can strongly interact with at least one antiapoptotic member. In addition, BH3-only proteins can be further classified as **'sensitizers'** or **'activators'** **(Fig. I-7)**. BH3-only activators, BIM, PUMA and tBID, can bind and inhibit all the antiapoptotic members and in addition, they can also bind and stimulate the activity of the proapoptotic effectors BAX and BAK. By contrast, BH3-only sensitizers cannot engage the proapoptotic effectors and they display more restricted binding affinities **(Fig. I-8)** (Giam et al., 2008, Martinou and Youle, 2011), thus, they are much less potent killers than the BH3-only activators (Youle and Strasser, 2008, Adams and Cory, 2018). They mainly function by competing for the binding of the BH3-surface groove of specific antiapoptotic BCL2 members, thereby relieving the inhibition of a direct activator or proapoptotic effector (Chipuk et al., 2010).

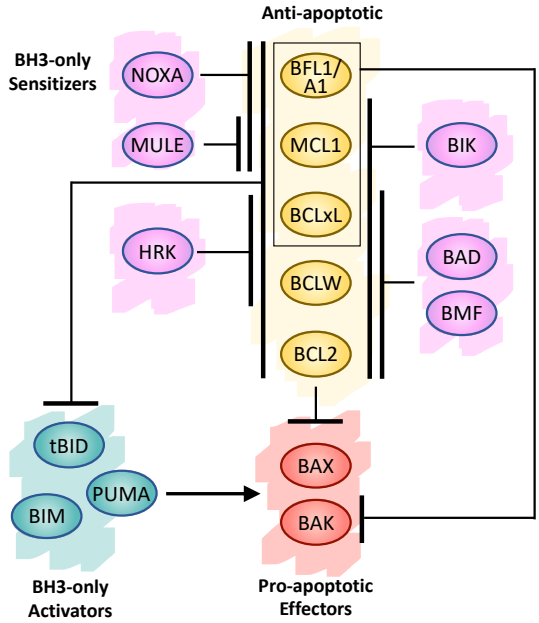


**Figure I-8. Selective binding profiles of the BCL2 family members.** Specific interactions of antiapoptotic BCL2 family members (yellow) with proapoptotic BH3-only activators (green), BH3-only sensitizers (pink) and proapoptotic effectors (red). Activators BIM, PUMA and tBID can bind to and neutralize the five antiapoptotic members comparably and they can additionally engage and activate the proapoptotic effectors BAX and BAK, promoting their oligomerization at the mitochondrial outer membrane. By contrast, the BH3-only sensitizers have more limited targets, as indicated on the figure. Among the antiapoptotic members, all of them can interact and inhibit BAX, whereas inhibition of BAK is mediated predominantly by MCL1, BFL1/A1 and BCLxL.

### 2.1.2. The BCL2 family in the regulation of the life/death switch

In healthy cells, activation of BAX and BAK is prevented by the interaction of antiapoptotic BCL2 family proteins. Stress signals trigger the activation of certain BH3- only proteins and, if the apoptotic stimulus is sufficient, the concentration of these molecules reaches a level at which they can neutralize the antiapoptotic proteins, leading to BAX and/or BAK activation, switching cell fate from survival to apoptosis. BH3-only activators also induce conformational changes in BAX and BAK, unfolding the proteins and leading to the exposure of their BH3 domains and of the TM domain of BAK, required for its translocation from the cytosol to the OMM. Unfolded and activated BAX/BAK monomers will form oligomers at the OMM,

resulting in MOMP and the initiation of the caspase cascade (Youle and Strasser, 2008, Adams and Cory, 2018). The best characterized mechanism of caspase activation is the promoted by the release of cyt *c* from the mitochondria. Once in the cytosol, cyt *c* binds to the C-terminal region of the apoptotic protease-activating factor 1 (APAF1), a cytosolic protein with an N-terminal caspase recruitment domain (CARD). The binding of cyt *c* facilitates the association of dATP with APAF1 and exposes its CARD, promoting its oligomerization and assembly into a heptameric protein ring termed an 'apoptosome'. This structure recruits and activates the initiator pro-caspase-9 (CASP9) via CARD-CARD interaction. Then, the apoptosome complex recruits the executioner caspase pro-caspase-3 (CASP3), which is subsequently cleaved and activated by the resident CASP9. Activated CASP3 initiates an amplification cascade by cleaving itself and many other key cellular substrates including (**1**) cytoskeletal proteins such as actin, the plasma membrane protein fodrin, leading to the loss of cell shape, and laminin, resulting in nuclear shrinkage, (**2**) nuclear proteins such as poly(ADP-ribose) polymerase (PARP), which abrogates its ability to sense DNA strand breaks thereby preventing DNA repair, and (**3**) DNases, including the caspase-activated DNase (CAD) and its inhibitor (ICAD), leading to the DNA fragmentation, or DNA laddering, characteristic of apoptotic cell death (Fulda and Debatin, 2006).

### 2.1.3. Signaling to the BCL2 family

The intrinsic apoptotic pathway is a type of caspase-dependent programmed cell death, given the major role that the BCL2 family exerts at the mitochondria **(Section 2.1.2.)**. This pathway is also referred as the BCL2-regulated or mitochondrial pathway (Youle and Strasser, 2008). The switch towards apoptosis requires the initial activation or abrogation of certain members of the family, which in turn largely depends on the type of apoptotic stimulus **(Fig. I-9)**. Developmental cues, removal of autoreactive B- and T cells during their development, or cytotoxic insults, such as viral infection, DNA damage or growth factor deprivation, initiate diverse but distinct signaling pathways that converge in the activation of specific BH3-only proteins, which has been addressed in genetically engineered mice.

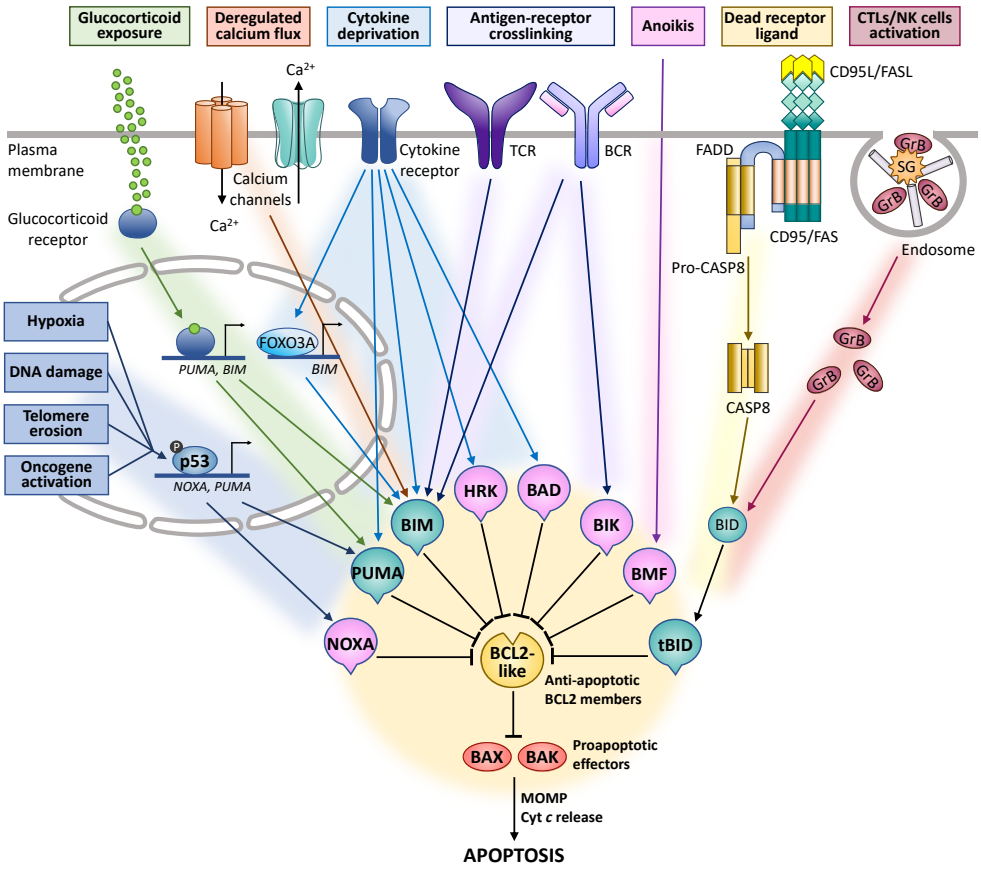


**Figure I-9. Signaling to the BCL2 family.** Activation of specific BH3-only proteins triggers apoptosis in response to distinct apoptotic stimuli. Oncogene activation, DNA damage, telomere shortening and hypoxia, frequent stress signals during tumorigenesis, drive p53-dependent apoptosis through the induction of PUMA, NOXA and BIM. The mechanism for the induction of BIM remains unclear. Glucocorticoids induce cell death through BIM and PUMA but independently of p53. Cytotoxic drugs, as staurosporine or phorbol ester (TPA), also drives p53-independent activation of PUMA (not shown). Cytokine deprivation activates BIM (through FOXO3A), PUMA, HRK and BAD, in a cell type-dependent manner. Antigen-dependent activation of B- and T-cell receptors, BCR and TCR, respectively, activate BIM, and possibly BIK in B cells. Anoikis activates BMF. Finally, apoptosis-induced in response to DDRR (CD95/FAS) stimulation, or in activated cytotoxic T lymphocytes (CTLs) or natural killer (NK) cells is mediated by tBID. Activation of these BH3-only proteins initiate apoptosis by neutralizing antiapoptotic BCL2 members, thus, unleashing proapoptotic effectors BAX and BAK, or even through the direct activation of these effectors, which results in MOMP, cyt *c* and cell death. Adapted from Strasser (2005), and Kelly and Strasser (2011). *Abbreviations:* DDRR, dead receptor; CD95L/FASL, CD95/FAS ligand; FADD, FAS-associated via death domain; CASP8, caspase-8; GrB, granzyme B; PFN, perforin; SG, serglycine; FOXO3A, forkhead box protein O3.

For instance, BIM is essential for preventing autoimmunity, as it is crucial for the removal of autoreactive lymphocytes during their development and for the termination of acute and chronic immune responses. BIM is also induced upon cytokine withdrawal and in response ER stress and abnormal calcium homeostasis. It also seems to play a role in DNA-damage-induced apoptosis, but the mechanism is not clear. By contrast, BID is activated by CASP8, in response to DDRR stimulation in fibroblasts and hepatocytes and to granzyme B (GrB) in cytotoxic T lymphocytes (CTLs). PUMA and NOXA are crucial p53 targets which are upregulated in response to DNA damage. The type of DNA damage, defines the mediators involved in the DDR and the particular cell type influences which member is induced. For instance, PUMA is essential for γ-radiation-induced apoptosis, while NOXA is essential for UV-radiation-induced apoptosis. Likewise, activation of NOXA is more restricted to certain cell types, including fibroblasts and intestinal epithelial cells. PUMA is also critical for apoptosis in response to hypoxia or MYC overexpression, in a p53-dependent manner, and in response to cytokine deprivation in hematopoietic and neuronal cells, or to treatment with glucocorticoids, phorbol ester (TPA) or staurosporine in lymphocytes, together with BIM, in a p53-independent manner (see reviews of Strasser, 2005, van Delft and Huang, 2006, Youle and Strasser, 2008, Chipuk et al., 2010, Kelly and Strasser, 2011).

Compared to BIM, BID or PUMA, which mediate apoptosis in response to many apoptotic stimuli, the other BH3-only proteins have milder killer effects and/or are more restricted to certain apoptotic stimuli or cell types. For instance, growth-factor-withdrawal-induced cell death is mediated by BCL2-antagonist of cell death (BAD) in fibroblasts, hematopoietic and mammary epithelial cells, and by harakiri (HRK) in certain neuronal populations. BCL2-modifying factor (BMF) is activated during anoikis, i.e. during apoptosis induced by cell detachment, while BCL2-interacting killer (BIK) is activated by B-cell receptor (BCR) crosslinking in human B cells, although other BH3-only proteins seem to be implicated in this apoptotic response (reviewed in Strasser, 2005, van Delft and Huang, 2006). Since certain apoptotic stimuli can activate more than one BH3-only protein, the functional overlapping of more than one BH3 member seems to be required to initiate a strong apoptotic signaling (Youle and Strasser, 2008).

BH3-only proteins are the major sentinels against cellular stress, but apoptotic signaling also regulates proapoptotic effectors by inducing changes in their stability (Chipuk et al., 2010). Under normal conditions, BAK and BAX expression levels seem to be sufficient to promote MOMP, but its proapoptotic activity is likely inhibited through post-translational modifications. For instance, survival signaling through ERK1/2 leads to BAX phosphorylation and inhibition of its proapoptotic activity. In addition, the BAX isoform β (BAXβ), which is ubiquitously expressed, is constitutively degraded in the absence of apoptotic stimuli to prevent non-desired apoptosis (Chipuk et al., 2010).

Antiapoptotic members can be also abrogated upon certain apoptotic stimuli (van Delft and Huang, 2006, Youle and Strasser, 2008). Among them, MCL1 is probably the most extensively studied, as it is the most potent antiapoptotic member, capable to neutralize a broad range of proapoptotic proteins **(Fig. I-8)**. It appears to function at an uppermost step in the pathway, as an 'apical' sensor, and therefore it must be eliminated or neutralized for apoptosis to proceed (Nijhawan et al., 2003). This is driven not only through protein-protein interactions between MCL1 and specific BH3-only members, such as NOXA, but also through the regulation of its transcription, translation, stability, cellular location and function (Thomas et al., 2010, Mojsa et al., 2014) **(see Section 2.2.3)**. Rapid neutralization or degradation of MCL1 in response to certain stress signals, as e.g. upon cytokine deprivation or UV radiation, is required to shift the threshold towards cell death, but in some cellular systems its loss is not sufficient to activate the mitochondrial apoptosis pathway (Nijhawan et al., 2003, Youle and Strasser, 2008, Senichkin et al., 2019).

### 2.1.4. Role of BCL2 family in lymphomagenesis

Regulation of the life/death switch by the BCL2 family is essential to maintain tissue homeostasis and immunity, with deregulation or defects in this sentinel network contributing to the development of several human diseases, such as autoimmunity and cancer (Strasser, 2005, Czabotar et al., 2014). Tumor development requires the acquisition of defects that allow nascent neoplastic cells to become self-sufficient for proliferation and insensitive to signals that normally restrain their growth (Kelly and Strasser, 2011) and thus, evasion of apoptosis is critical for the development and

progression of many cancers (Hanahan and Weinberg, 2011). During lymphomagenesis, cells encounter a broad range of stress stimuli, including oncogene activation, DNA damage, hypoxia, cytokine deprivation, and anoikis, all of which can elicit an apoptotic cell death response (Kelly and Strasser, 2011, Adams et al., 2018) **(Fig. I-9)**. Therefore, impairment of apoptosis presumably promotes lymphoma development by keeping cells alive long enough to acquire additional oncogenic mutations that drive their neoplastic progression (Czabotar et al., 2014). For instance, overexpression of antiapoptotic BCL2 members enable tumorigenic cells to survive even under stress conditions, such as limiting cytokines (Adams and Cory, 2007, Kelly and Strasser, 2011), while inactivation of certain BH3-only proteins is critical to evade apoptosis induced by oncogenes (Happo et al., 2012b), such as MYC **(see Fig. I-4 and Section 1.2.2.)**, thus facilitating tumor initiation and progression.

As mentioned in the previous chapter **(Section 1.4.2.)**, much of what we presently know about the role of the BCL2 family and its contribution to lymphomagenesis has been addressed by utilizing the E$\mu$-MYC transgenic mouse model (Adams et al., 1985). Additional genetic manipulations of this model, such as the enforced expression or the genetic knockout (KO) of certain genes of the BCL2 family, have provided experimental evidence of the individual roles of these members in lymphoma development (reviewed in Adams et al., 2018). The major functions of the pro and antiapoptotic BCL2 family members, as well as their cooperation in MYC-driven tumorigenesis and their alterations in different human B-cell lymphoid malignancies are summarized in **Table I-2**. In brief, inhibition of apoptosis through the loss of proapoptotic BCL2 family members such as *Bim* (Egle et al., 2004), *Puma* (Garrison et al., 2008, Michalak et al., 2009), *Bad* (Frenzel et al., 2010), *Bmf* (Frenzel et al., 2010) and *Bax* (Eischen et al., 2001a), accelerates MYC-driven tumorigenesis. However, the deletion of other members such as *Noxa* (Michalak et al., 2009) or *Bik* (Happo et al., 2012a), does not have an impact in MYC-driven tumorigenesis. In agreement with mouse models, homozygous deletion of *BIM* alleles are found in ~20% of MCL (Tagawa et al., 2005), while BIM (Richter-Larrea et al., 2010) or PUMA (Garrison et al., 2008) expression are strongly decreased in 40% of BL, mostly through the epigenetic silencing of their promoter.

**Table I-2. Alterations of BCL2 family members in mouse models and in human B-cell lymphomas**

| | | Phenotypic effects in mouse models | Cooperation with oncogenic MYC† | Alterations at mRNA or protein level in BL DLBCL FL MCL MZL MM CLL ALCL PCNSL |
|---|---|---|---|---|
| Antiapoptotic | BCL2 | KO mice die prematurely (fulminant lymphoid apoptosis) | Loss does not prevent lymphomagenesis | |
| | | OE cause B-cell accumulation (GC hyperplasia) | OE accelerates lymphomagenesis | + + + – |
| | BCLxL | KO mice are embryonic lethal. | Loss slightly delays lymphoma onset | |
| | | OE causes accumulation of mature lymphocytes | OE causes fatal B-ALL and MPC | + + + + + |
| | BCLW | KO male mice are sterile. | Loss strongly delays lymphomagenesis | |
| | | No other abnormalities. | OE accelerates myeloid leukemogenesis | + + + + + |
| | BFL1/A1 | KO mice are embryonic lethal. | No effect in lymphomagenesis | – |
| | MCL1 | KO mice are embryonic lethal. | Loss delays and even inhibits lymphomagenesis | |
| | | OE causes mature B and T lymphocytes accumulation and high incidence of lymphoma | OE accelerates lymphomagenesis | + + + +/– +/– + + + |
| BH3-only | BID | KO mice develop CMML | Unknown | Unknown |
| | BIM | KO mice accumulate lymphoid and myeloid cells and frequently develop autoimmune kidney disease | Loss markedly accelerates lymphomagenesis | – – * – * |
| | PUMA | KO mice develop normally with no tumor arising | Loss accelerates lymphomagenesis | – |
| | BAD | KO mice display mild thrombocytosis and low incidence of DLBCL at old age | Loss accelerates lymphomagenesis | Loss not observed in DLBCL. |
| | BMF | KO mice develop B-cell hyperplasia | Loss accelerates lymphomagenesis | – |
| | NOXA | Loss increases number of B cells | Loss has no effect in lymphomagenesis | – |
| | HRK | Loss has no impact on hematopoietic cells | Unknown | – |
| | BIK | Loss has no impact on hematopoietic cells | Loss has no effect in lymphomagenesis | – – – |
| Effector | BAK | KO mice have mild lymphoid hyperplasia | Loss accelerates lymphomagenesis | Unknown |
| | BAX | KO mice are phenotypically normal | Not reported | Unknown |
| | BOK | Unknown | Loss has no effect in lymphomagenesis | Unknown |

† Cooperation contributes to lymphoma development in the E$\mu$-MYC mouse, unless otherwise indicated. Dark-colored cells indicate alterations including overexpression (+), downregulation or loss (–), or single nt polymorphisms (*), found in human lymphomas which contribute to tumorigenesis. +/– indicates that overexpression (OE) is observed in some cases while it is downregulated in others. Adapted from Adams et al. (2018). *Abbreviations:* CMML, chronic myelomonocytic leukemia; MPC, plasmacytoma; MZL, marginal zone lymphoma; PCNSL, primary central nervous system lymphoma; KO, knockout.

Among the antiapoptotic BCL2 family members, BCL2 is overexpressed as a result of a chromosomal translocation, t(14;18), in 90% of FL, and in 20% of all the germinal center B-cell-like (GCB)-DLBCL subtype. In the activated B-cell-like (ABC)-DLBCL subset, BCL2 is also overexpressed, but due to copy number amplification (Adams et al., 2018). Overexpression of BCL2 is also frequent in E$\mu$-MYC-driven lymphomas and accelerates MYC-driven tumorigenesis, although it overexpression alone does not generate lymphomas (Strasser et al., 1990). Excluding FL and some cases of DLBCL, genetic alterations in BCL2 in human B-cell lymphomas are rare, as well as genetic and cytogenetic alterations in the other antiapoptotic members. Therefore, expression of one or more of these members under its endogenous regulatory system seems to be critical to maintain cell survival during the initial steps of neoplastic transformation, and to later sustain cancer survival and progression in a number of lymphoid malignancies (Kelly and Strasser, 2011). This issue has been addressed by gene KO studies in transgenic mice. Indeed, loss of *Bcl2* or of *Bcl2a1* (encoding BFL1/A1) were found to be dispensable for E$\mu$-MYC lymphoma initiation, development or maintenance (Kelly et al., 2007, Mensink et al., 2018). BCLxL and MCL1 were the next candidates investigated, since both antiapoptotic members are required for the survival of B-cell progenitors and precursors, and are expressed at high levels during several stages of B-cell development. In addition, they are amplified or overexpressed in several lymphoid neoplasias (Beroukhim et al., 2010) and their overexpression facilitates MYC-driven lymphomagenesis (Kelly and Strasser, 2011) **(Table I-2)**. KO studies addressed the critical role of MCL1 (Kelly et al., 2014, Grabow et al., 2016), BCLW (Adams et al., 2017), and to a lesser extent, BCLxL (Kelly et al., 2011), in the initial formation and expansion of E$\mu$-MYC-driven tumors. Strikingly, in contrast to BCLxL and BCLW, MCL1 was found to be essential for sustaining the subsequent growth of malignant E$\mu$-MYC lymphomas (Kelly et al., 2014, Grabow et al., 2016), as well as for the development of other hematological malignancies, such as AML (Xiang et al., 2010, Glaser et al., 2012) and BCR-ABL-driven B-ALL (Koss et al., 2013). These findings highlight the critical role that antiapoptotic MCL1 may possess in the initiation, progression and maintenance of many lymphoid/hematological tumors **(see also Section 2.3.1.)**.

## 2.2. Myeloid Cell Leukemia 1: MCL1

MCL1 was initially identified as an immediate-early response gene expressed during TPA-induced differentiation of the ML1 human myeloid leukemia cell line (Kozopas et al., 1993). It was also the first gene found to be homologous to BCL2 (Kozopas et al., 1993). It is a unique antiapoptotic member, which acts as an apical sensor for apoptotic stimuli and whose disappearance is required for the progression of downstream events of the apoptotic pathway, including BAX translocation to the OMM, BAX/BAK oligomerization, MOMP, cyt *c* release and caspase activation (Nijhawan et al., 2003). In addition MCL1 exerts specific physiological roles and displays particular tissue distribution distinct to that of its antiapoptotic relatives (Thomas et al., 2010). For instance, MCL1 is essential for early embryonic development (Rinkenberger et al., 2000) and for regulating cell survival of multiple cell linages in the adult (reviewed in Perciavalle and Opferman, 2013), including B and T lymphocytes (Opferman et al., 2003), plasma cells (Peperzak et al., 2013), hematopoietic stem cells (HSCs) (Opferman et al., 2005), neutrophils (Dzhagalov et al., 2007), hepatocytes (Vick et al., 2009), cardiomyocytes (Wang et al., 2013) and neurons (Arbour et al., 2008). Furthermore, like its BCL2 relatives, MCL1 regulates cell cycle progression through its interaction with CDK1, proliferating cell antigen (PCNA) and CHK1 (Thomas et al., 2010). Likewise, amplification of the MCL1 locus was identified in ~11% of human tumors of diverse types (Beroukhim et al., 2010), and its overexpression is frequent in many human cancers, such as MM and AML **(see Section 2.3. and Table I-2)**.

### 2.2.1. MCL1 general features: structure, cellular localization and variants

At the structural level, MCL1 is much larger than its antiapoptotic relatives (331 and 350 aa-long in mouse and human, respectively). It possess an extended unstructured N-terminal region, which is a critical regulatory region and whose sequence differs the most between human and mice (Thomas et al., 2010, Ertel et al., 2013). By contrast, its C-terminus contains a conserved BCL2 core with a high structural and functional homology with the other antiapoptotic relatives, particularly between residues 170-300. Within this region, MCL1 contains three BH homology domains (BH1, BH2 and BH3) and the TM domain **(Fig. I-7)**. Like its antiapoptotic relatives,

MCL1 structure is a globular group of α-helices, which form the characteristic hydrophobic surface binding groove or BH3-binding groove (Warren et al., 2019). In particular, the **MCL1 hydrophobic groove**, contained within helices α2-α4, has a more open conformation than that of the other antiapoptotic members, allowing the accommodation of BH3 domains from proapoptotic proteins with a wide range of affinities (Day et al., 2008, Campbell et al., 2010). In contrast, helix α9 contains the C-terminal **TM domain**, essential for the anchoring of MCL1 to distinct intracellular membranes, including the OMM, the nuclear membrane and the ER membrane (Thomas et al., 2010, Senichkin et al., 2019). Efficient targeting of MCL1 to the mitochondria additionally depends on the integrity of a **mitochondrial target sequence (MTS)** located within the first amino acids of its N-terminus (Perciavalle et al., 2012), an internal EELD sequence (residues 124-127), which facilitates its TOM70-dependent mitochondrial import (Chou et al., 2006), and the C-terminal TM domain (Akgul et al., 2000). On the other hand, within its unique, large (∼150 aa long) and unstructured **N-terminal regulatory region**, MCL1 contains in addition to the MTS, several PEST sequences and the BH4 homology domain (Senichkin et al., 2019, Warren et al., 2019). PEST sequences are regions enriched in proline (P), glutamate (E), serine (S) and threonine (T) residues commonly found in rapidly degraded proteins (Rechsteiner and Rogers, 1996). Indeed, MCL1 has a very rapid turnover and an estimated half-life of 1-3 hr (Senichkin et al., 2019), depending on the cell type and intracellular conditions, which significantly contrasts with the protein half-lives of the other antiapoptotic members such as BCL2 or BCLxL, which are ∼20 hr (Campbell et al., 2010). Within these PEST regions, MCL1 contains two cleavage sites for CASP3 and GrB, at two aspartate (D) residues, D127 and D157, **(Fig. I-10)** (Clohessy et al., 2004, Han et al., 2004, Herrant et al., 2004, Weng et al., 2005, Thomas et al., 2010), as well as specific phosphorylation sites, which modulate MCL1 stability and function (Mojsa et al., 2014, Warren et al., 2019).

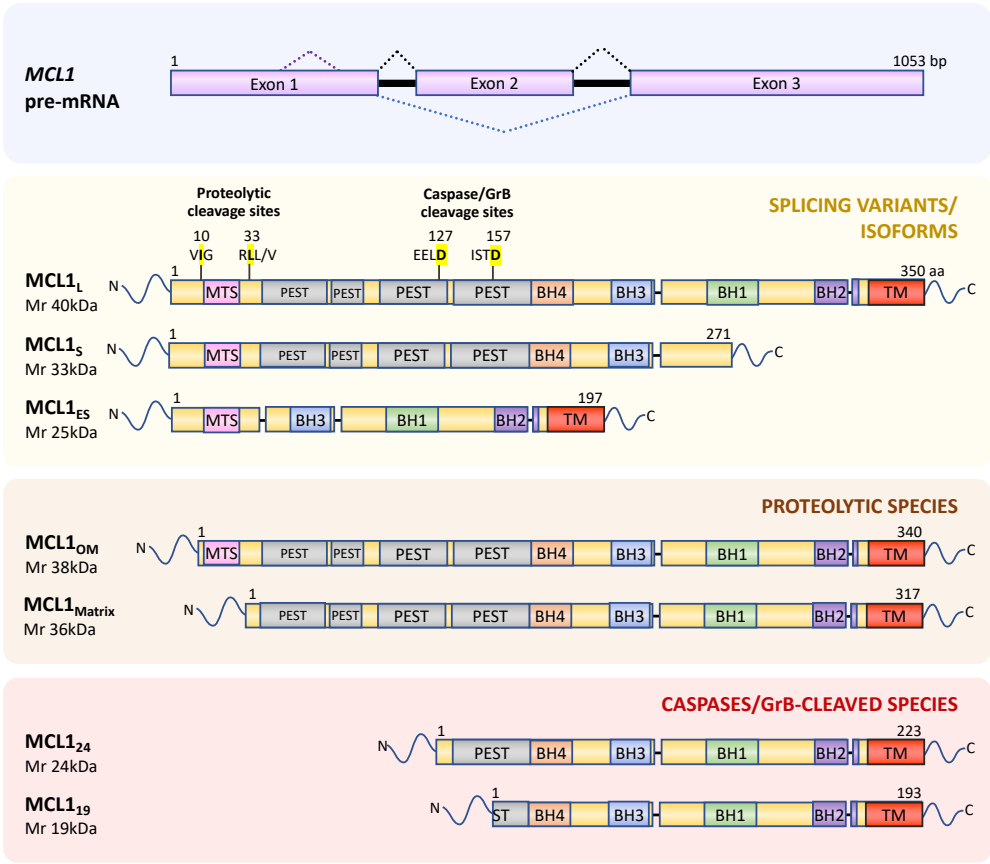


**Figure I-10. Structure of MCL1 pre-mRNA and MCL1 protein variants.** Alternative splicing of MCL1 pre-mRNA generates 3 isoforms: full-length MCL1 ($MCL1_L$ or just MCL1), 'short' MCL1 ($MCL1_S$) and 'extra-short' MCL1 ($MCL1_{ES}$), some which lack important MCL1 functional or regulatory domains. In addition, MCL1 can be further cleaved to generate distinct protein variants, $MCL1_{OM}$ and $MCL1_{Matrix}$, in reference to their cellular location at the OMM or in the mitochondrial matrix, respectively. Likewise, proteolytic cleavage by caspases or GrB, within MCL1 PEST sequences, generates two truncated forms of 24 and 19kDa referred as $MCL1_{24}$ and $MCL1_{19}$, respectively. The amino acid (aa) length, the relative molecular mass (Mr), in kDa, and the domains contained in each variant are displayed. Likewise, the distinct proteolytic cleavage sites are indicated above full-length MCL1. Further information about the location and function of these variants is shown in **Table I-3**. *Abbreviations:* MTS, mitochondrial targeting sequence; PEST, proline-glutamate-serine-threonine-rich region.

It is noteworthy that antiapoptotic MCL1 is not the only isoform of the gene. Indeed, the *MCL1* gene contains three exons and the translation of the full-transcript, containing all exons, gives rise to **full-length MCL1 or MCL1$_L$** (also referred as MCL1 for simplification), which exerts antiapoptotic activity (Senichkin et al., 2019, Warren et al., 2019). Two additional isoforms **MCL1 'short' (MCL1$_S$)**, of 33 kDa, and **MCL1 'extra-short' (MCL1$_{ES}$)**, of 25 kDa, **(Fig. I-10)**, result from alternative splicing of the pre-mRNA and, unlike full-length MCL1, they appear to function as proapoptotic proteins **(Table I-3)** (Bae et al., 2000, Kim et al., 2009). MCL1$_S$ is produced by skipping MCL1 exon 2, creating a frame shift in exon 3 that results in the loss of the BH1, BH2 and TM domains that localizes this isoform in the cytosol (Bae et al., 2000, Morciano et al., 2016). In contrast, alternative splicing within MCL1 exon 1, which occurs at lower frequency, generates MCL1$_{ES}$ isoform which misses a portion of the N-terminal regulatory region, including the PEST domains and the BH4 domain (Kim et al., 2009). Although it had been proposed that alternative splicing generated a 36 kDa antiapoptotic MCL1 variant in the mouse (Kojima et al., 2010), it was later demonstrated that ablation of the putative splice donor and acceptor still generates this species, thus, these alternative MCL1 isoforms appear to be absent in the mouse (Perciavalle et al., 2012). The two alternative human isoforms lack several BH domains required for the formation of the BH3-binding groove, despite maintaining an intact BH3 domain, so they are likely to act in a similar manner to that of the proapoptotic BH3-only proteins. Indeed, they are unable to bind proapoptotic BCL2 members, binding and inhibiting exclusively full-length MCL1 (Senichkin et al., 2019, Warren et al., 2019). Whereas MCL1$_S$ is known to induce apoptosis by binding and inhibiting full-length MCL1 (Bae et al., 2000), MCL1$_{ES}$ promotes cyt *c* release independently of BAX or BAK but requires its targeting to the mitochondria by MCL1 (Kim et al., 2009). However, little more is known about the proapoptotic roles of the two shorter MCL1 isoforms and their physiological relevance (Senichkin et al., 2019).

**Table I-3. MCL1 variants: structural features, intracellular location and function.**

| Name, generation | Length Mr | Domains included | Domains excluded | Cellular location | Function | H | M | References |
|---|---|---|---|---|---|---|---|---|
| **$MCL1_L$** Full transcript | 350 aa 40 kDa | All | None | OMM, ER, nuclear membrane | Antiapoptotic | ✓ | ✓ | (Kozopas et al., 1993) |
| **$MCL1_S$** E2 skipping | 271 aa 33 kDa | BH4, BH3, N-reg (MTS and PEST) | BH1, BH2 and TM | Cytosolic | Proapoptotic | ✓ | ✗ | (Bae et al., 2000, Morciano et al., 2016) |
| **$MCL1_{ES}$** Splice within E1 | 197 aa 25 kDa | BH1-BH3, TM | BH4, N-reg | OMM | Proapoptotic | ✓ | ✗ | (Kim et al., 2009) |
| **$MCL1_{OM}$** Proteolytic cleavage | 340 aa 38 kDa | BH1-BH4, TM, partial N-reg | Small portion of N-reg | OMM | Antiapoptotic | ✓ | ✓ | (Perciavalle et al., 2012) |
| **$MCL1_{Matrix}$** Proteolytic cleavage | 317 aa 36 kDa | BH1-BH4, TM partial N-reg | Portion of N-reg (MTS) | IMM, mit. matrix | Mitochondrial respiration | ✓ | ✓ | (Perciavalle et al., 2012) |
| **$MCL1_{24}$** CASP/GrB cleavage | 223 aa 24 kDa | BH1-BH4, TM | N-reg (MTS and PEST) | Cytosolic | Proapoptotic? | ✓ | ✓ | (Clohessy et al., 2004, Han et al., 2004, Herrant et al., 2004, Weng et al., 2005) |
| **$MCL1_{19}$** CASP/GrB cleavage | 193 aa 19 kDa | BH1-BH4, TM | N-reg (MTS and PEST) | Cytosolic | Proapoptotic? | ✓ | ✓ | |

*Abbreviations:* H, human; M, mouse; E1/2/3, exon 1/2/3; Mr, relative molecular mass; N-reg, N-terminal regulatory domain; OM/OMM, outer mitochondrial membrane; ER, Endoplasmic reticulum; IMM, inner mitochondrial membrane; mit., mitochondrial.

In parallel, two MCL1 species have been identified both in murine and human-derived tumor cell lines, generated by proteolytic cleavage of full-length MCL1, $MCL1_{OM}$ and $MCL1_{Matrix}$ **(Fig. 10)**, which refers to their mitochondrial sub-localization, at the OMM or in the mitochondrial matrix, respectively (De Biasio et al., 2007, Perciavalle et al., 2012) **(Table I-3)**. $MCL1_{OM}$, which lacks approximately the first 30 aa of MCL1 N-terminal region has a relative molecular mass (Mr) of 38 kDa, and prevents cell death in a similar way to full-length MCL1. $MCL1_{OM}$ it is the predominant specie observed in lymphoma cell lines from both mouse and human origin (De Biasio et al., 2007) and it is characterized by enhanced stability and inducing increased survival, possibly because it can evade interaction with its E3 ubiquitin ligase MULE (Warr et al., 2011). During mitochondrial import, MCL1 N-terminus undergoes further proteolytic cleavage giving rise to the shorter $MCL1_{Matrix}$ species, of Mr 36

kDa, which resides in the matrix tethered to the inner mitochondrial membrane (IMM). Unlike full-size MCL1 and $MCL1_{OM}$, $MCL1_{Matrix}$ does not prevent apoptosis but participates in maintaining normal IMM structure, regulates mitochondrial fusion and promotes the assembly of ATP synthase oligomers, thereby facilitating mitochondrial maintenance and bioenergetics (Perciavalle et al., 2012). In addition to these MCL1 species, activation of CASP3 upon tumor necrosis factor-related apoptosis-inducing ligand (TRAIL)-induced apoptosis (Weng et al., 2005) and in response to chemotherapeutics (Herrant et al., 2004) leads to the proteolytic cleavage and inactivation of MCL1 at D127 or D157. Each cleavage generates truncated fragments of 24 or 19 kDa respectively, referred as $MCL1_{24}$ or $MCL1_{19}$, which lack a large part of the N-terminal domain **(Fig. I-10)**. Likewise, paracellular secreted GrB can cleave MCL1 at these two sites during GrB-mediated apoptosis (Han et al., 2004). However, the precise role of these cleaved products is contradictory, with some suggesting that the cleavage impairs MCL1 antiapoptotic properties (Han et al., 2004, Herrant et al., 2004) or even converts it into a proapoptotic protein (Weng et al., 2005), whereas others argue that it is the process by which cells undergoing apoptosis, inactivating any residual MCL1 to further accelerate cell death (Mojsa et al., 2014).

### 2.2.2. MCL1 antiapoptotic function

Under resting conditions, MCL1 is predominantly located at mitochondria, although it can be also found at the cytosol where it presumably binds and inhibits BAX (Thomas et al., 2010, Mojsa et al., 2014). However, MCL1 binds with more strongly to BAK (Kale et al., 2018) and thus, its needs to be efficiently targeted to the mitochondria to fully counteract the proapoptotic activity of both BAX and BAK **(Fig. I-11)**. In addition, given the high plasticity of its BH3-binding groove (Day et al., 2008), MCL1 interacts with other members of the BCL2 family such as the BH3-only activators PUMA, BIM and tBID, and the BH3-only sensitizer NOXA (Kale et al., 2018). Its binding pattern differs to that of BCL2, BCLxL and BCLW antiapoptotic members **(Fig. I-8)**. For instance, MCL1 does not bind BAD but strongly binds and inhibits BAK. By contrast, BCL2 can bind BAD but only binds and inhibits BAX (Campbell et al., 2010). Depending on the cellular stress, MCL1 acts either by sequestering a direct BH3-only activator, by directly binding and inhibiting the proapoptotic effectors BAX

and/or BAK, or by both mechanisms **(Fig. I-11)**. Either mode of action ultimately leads to blocking of the MOMP and inhibition of apoptosis (Thomas et al., 2010, Mojsa et al., 2014). Importantly, among the BCL2 family, only two members belonging to the proapoptotic BH3-only group can antagonize MCL1 antiapoptotic function, the sensitizer NOXA together with the E3 ligase and BH3-only protein MULE **(Fig. I-11)**.

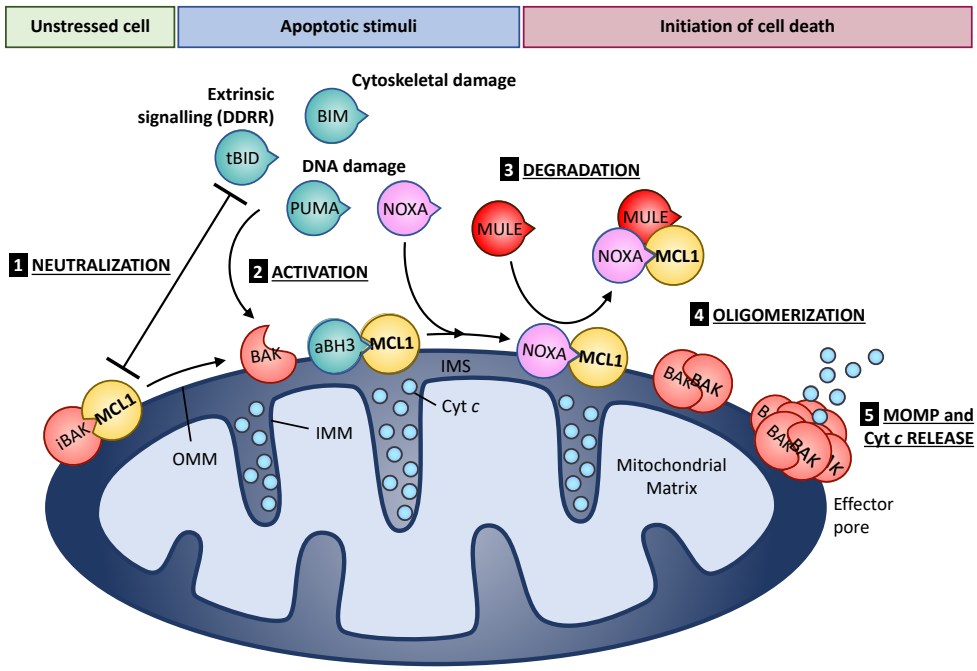


**Figure I-11. Model of MCL1 regulation of the intrinsic cell death pathway.** (1) Under resting conditions, MCL1 is constitutively bound to proapoptotic BAK when targeted to the OMM. Binding of MCL1 maintains BAK in an inactivate state (iBAK). Alternatively, MCL1 can sequester the proapoptotic BH3-only activators (aBH3) tBID, BIM and PUMA, preventing them from activating BAK. (2) When the apoptotic stimulus is sufficient, activation of BH3-only protein members is capable of disrupting MCL1/BAK complexes, releasing BAK. In addition, tBID, BIM and PUMA can directly activate BAK, promoting is homodimerization at the OMM. (3) On the other hand, certain apoptotic stimuli, such as those inducing DNA damage, lead to the activation of BH3-only sensitizer NOXA. NOXA relieves BAK by directly binding MCL1. NOXA:MCL1 complexes favor the association of the BH3-only protein and MCL1 E3 ubiquitin ligase MULE which, in turn, ubiquitinates MCL1 and directs its proteasomal degradation. (4) Once BAK, or BAX, are activated they form homodimers that further associate into oligomers leading to the formation of an effector pore at the OMM, promoting MOMP. (5) MOMP results in the release of cyt *c* to the cytosol, caspase activation and apoptosis. A similar mechanism is proposed for MCL1/BAX interactions at the cytosol, which upon an apoptotic stimulus, are targeted to the OMM for subsequent BAX activation. *Abbreviations:* IMS, intermembrane space.

NOXA promotes the dissociation of MCL1/BAK or MCL1/BAX inhibitory complexes by competition (Day et al., 2008, Mojsa et al., 2014) and enhances MCL1 proteasomal degradation by promoting its interaction with the E3 ubiquitin ligase MULE (Thomas et al., 2010, Gomez-Bougie et al., 2011). By contrast, binding of proapoptotic BH3-only BIM and PUMA stabilizes MCL1, despite sharing with NOXA the same BH3 binding site on MCL1 (Czabotar et al., 2007, Wuilleme-Toumi et al., 2007). This differential effect on MCL1 stability relies in a conformational change promoted by NOXA interaction, but not by BIM or PUMA, at a short QRN amino acid motif within MCL1 BH3 domain (aa 221-223), which favors its recognition by MULE (Song et al., 2016). By contrast, binding of BIM, and possibly PUMA, blocks the access of MULE to this motif (Song et al., 2016). In addition, MULE, which normally binds to MCL1 by docking its BH3 domain into the BH3-binding groove of MCL1 (Warr et al., 2005), engages MCL1 within a second interaction site within the first 30 aa of MCL1 N-terminus, when NOXA is bound (Warr et al., 2011, Mojsa et al., 2014).

### 2.2.3. MCL1 regulation

Given that MCL1 is critical for the survival of multiple linages in the adult tissue (Arbour et al., 2008, Vick et al., 2009, Perciavalle and Opferman, 2013, Wang et al., 2013), a strict control of its levels and normal function is crucial for cell function. Indeed, MCL1 is tightly regulated at multiple levels (reviewed in Thomas et al., 2010, Mojsa et al., 2014) **(Fig. I-12)**. Under physiological conditions, a large number of extracellular signals involved in survival and differentiation (e.g. factors involved in monocyte/macrophage differentiation and growth factors) can trigger transcriptional upregulation of *MCL1* (Le Gouill et al., 2004, Warr and Shore, 2008, Thomas et al., 2010). These extracellular factors act through signal transduction pathways that lead to the activation of transcription factors such as STAT3, in response to interleukin (IL)3, IL6, and VEGF that ultimately binds to the *MCL1* promoter and stimulates its transcription (Thomas et al., 2010). By contrast, stress signals, such as growth factor deprivation, genotoxic stress or cytotoxic drugs, lead to the inactivation of *MCL1* transactivating factors and/or to the activation of *MCL1* repressors such as E2F1 (Croxton et al., 2002, Thomas et al., 2010).

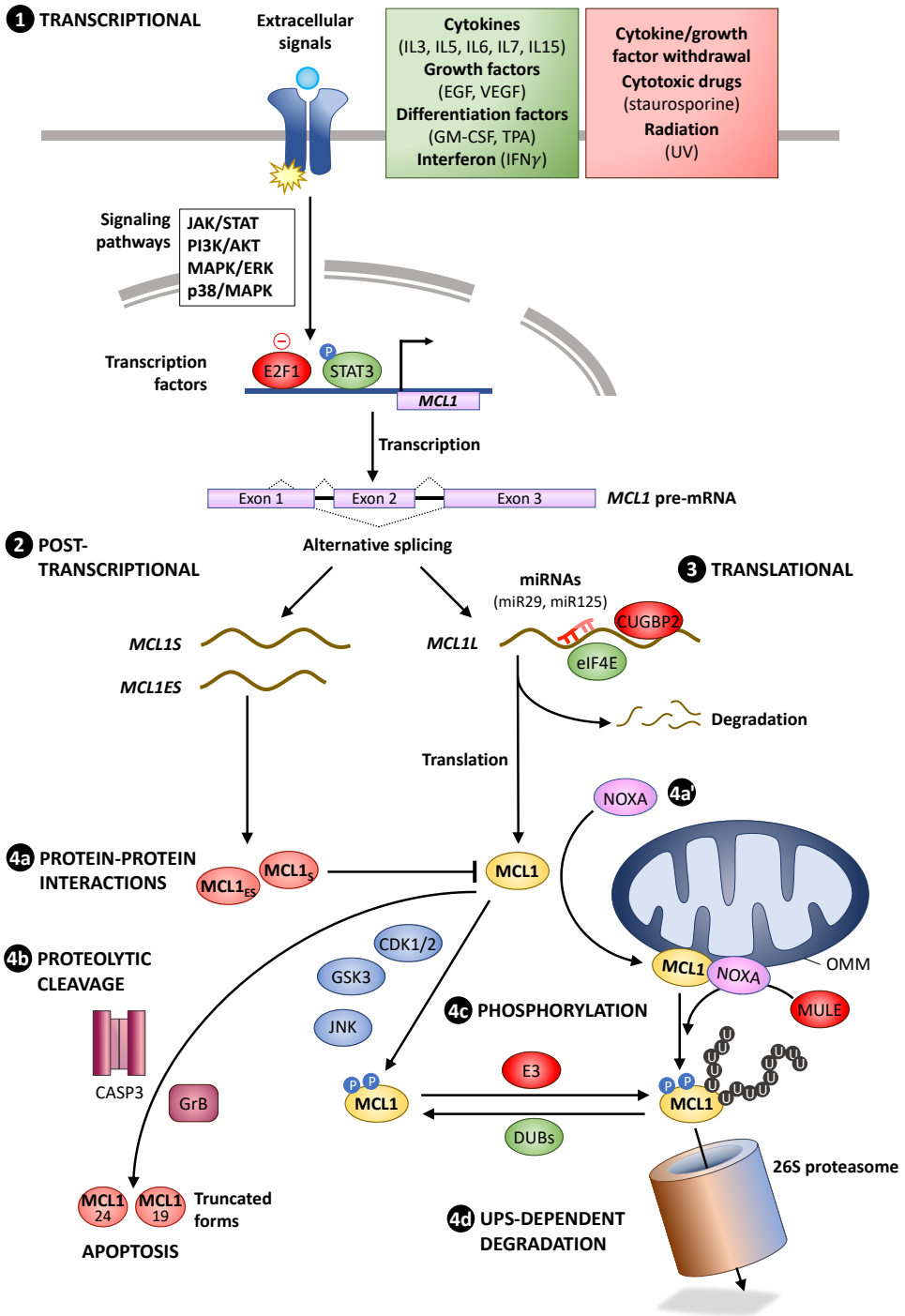


**Figure I-12. Overview of the molecular regulation of MCL1 at the (1) transcriptional, (2) post-transcriptional, (3) translational and (4) post-translational levels.** (See next page)

**Figure I-12. (continued)** (1) A wide variety of extracellular stimuli regulate *MCL1* transcription through the activation of transcription factors via one or more signal transduction pathways, which can induce (e.g. STAT3) or repress (e.g. E2F1) *MCL1* transcription. (2) *MCL1* pre-mRNA can be processed into three distinct mRNA species through alternative splicing giving rise to full-length (*MCL1L*), short (*MCL1S*) and extra short (*MCL1ES*) transcripts. (4a) Once translated, the shorter alternative isoforms, $MCL1_S$ and $MCL1_{ES}$ proteins become proapoptotic molecules and are able to bind and inactivate $MCL1_L$ referred to as MCL1 for simplification. (3) On the other hand, *MCL1L* mRNA has a short half-life and is degradation is further accelerated by several microRNAs (miR) and the RNA binding protein CUGBP2. By contrast, mTOR pathway (not shown) increases *MCL1L* translation through the activation of eIF4E. (4a') As shown in **Fig. I-11**, upon apoptotic stimuli, certain BH3-only proteins interact with MCL1, such as NOXA which promotes MCL1 degradation. (4b) Likewise, during apoptosis, MCL1 can be cleaved by CASP3 or by GrB into inactive the truncated forms $MCL1_{24}$ and $MCL1_{19}$, as shown in **Fig. I-10**. (4c) Phosphorylation of MCL1 by different kinases can accelerate or reduce the rate of MCL1 turnover. (4d) Degradation of MCL1 is mediated by the ubiquitin-proteasome system (UPS). Several E3 ubiquitin ligases (E3) and deubiquitinases (DUBs) direct or prevent, respectively, MCL1 degradation through the 26S proteasome.

In addition, *MCL1* pre-mRNA can be alternatively spliced to produce the shorter proapoptotic isoforms, as described above **(Section 2.2.1.)**. The ratio among the different isoforms can be altered under certain conditions, including during bacterial infection, where upregulation of $MCL1_S$ in infected macrophages promotes their rapid turnover, facilitating the rapid resolution of infection (Thomas et al., 2010). On the other hand, like the protein, *MCL1* mRNA has a very short half-life, estimated at ~2 hr (Yang et al., 1996), and its translation can be further accelerated or prevented. For instance, several miRNAs (Mott et al., 2007, Gong et al., 2013) and the RNA binding protein CUGBP2 (Subramaniam et al., 2008) target the 3'UTR of the *MCL1* transcript, inhibiting its translation and promoting its degradation. By contrast, activation of mTORC1 drives *MCL1* mRNA translation through eIF4E (Mills et al., 2008). Finally, MCL1 protein levels, intracellular localization and function are tightly regulated at the **post-translational level** (Thomas et al., 2010, Mojsa et al., 2014). Its long and unstructured N-terminus contains multiple sites susceptible of ubiquitination, phosphorylation and proteolytic cleavage **(Fig. I-13)** and such post-translational modifications alter MCL1 stability and rate of turnover. In addition, as stated earlier, MCL1 cleavage by CASP3 or GrB affects its function and localization **(Section 2.2.1.)**.

### 2.2.4. Regulation of MCL1 by the ubiquitin-proteasome system

Besides protease-mediated MCL1 degradation, the major mechanism responsible for the rapid degradation and turnover of MCL1 is the UPS **(Fig. I-12)**. Initially, the proteasome was found to mediate MCL1 degradation in two distinct scenarios: in cells undergoing apoptosis following UV irradiation (Nijhawan et al., 2003) and upon DNA-damage response induced by adenovirus infection (Cuconati et al., 2003). A few years later, the 13 lysine (K) residues, susceptible of ubiquitination, were identified and characterized **(Fig. I-13)** and thereby, MCL1 polyubiquitination was demonstrated (Zhong et al., 2005). To date, six E3 ligases have been identified and proposed to be involved in MCL1 ubiquitination: MULE (Zhong et al., 2005), $SCF^{\beta\text{-}TrCP}$ (Ding et al., 2007), $SCF^{FBW7}$ (Inuzuka et al., 2011), TRIM17 (Magiera et al., 2013), $APC/C^{CDC20}$ (Harley et al., 2010) and $SCF^{FBXO4}$ (Feng et al., 2017) **(Table I-4)**. Conversely, until recently, only one deubiquitinase (DUB), ubiquitin-specific peptidase 9X (USP9X), had been shown to mediate MCL1 deubiquitination (Schwickart et al., 2010). However, it was recently discovered that ubiquitin-specific peptidase 13 (USP13) (Zhang et al., 2018) and deubiquitinating protein 3 (DUB3) (Wu et al., 2019) are also able mediate MCL1 deubiquitination **(Table I-4)**. Although all of them can stabilize MCL1 by removing the conjugated K48-linked polyubiquitin chains from MCL1, they exhibit tissue-specific expression and none of them can completely reverse MCL1 ubiquitination in ubiquitination assays, suggesting that additional DUBs are implicated in MCL1 regulation (Wu et al., 2019).

Among the distinct MCL1 E3 ubiquitin ligases, the first one identified, by Zhong et al., in 2005, was **Mcl1 ubiquitin ligase E3 (MULE)**, already known as LASU1 or ARF-BP1 (Zhong et al., 2005). In parallel, MULE was identified as a BH3-only protein in a genome wide search for new BH3-containing proteins **(Fig. I-7)** (Warr et al., 2005). MULE is a large protein of 480 kDa that belongs to the HECT domain family of E3 ubiquitin-ligases (Zhong et al., 2005). As described in **Section 2.2.2.**, the BH3 domain of MULE docks into the BH3-binding groove of MCL1, subsequently targeting MCL1 for its proteasomal degradation (Warr et al., 2005, Zhong et al., 2005). However, binding affinity of MULE BH3 domain for MCL1 is very low compared to the BH3 motif of PUMA, BIM, tBID, BAK or NOXA, so the E3 ligase can be easily displaced from MCL1 BH3-surface groove in the presence of the proapoptotic molecules PUMA and BIM

(Warr et al., 2005, Czabotar et al., 2007, Wuilleme-Toumi et al., 2007, Warr et al., 2011). By contrast, binding of NOXA facilitates the engagement of MULE to MCL1 through the second interaction site within its N-terminus (Czabotar et al., 2007, Gomez-Bougie et al., 2011, Song et al., 2016), facilitating MULE-dependent MCL1 ubiquitination and subsequent proteasomal degradation (Warr et al., 2011, Mojsa et al., 2014) **(Figs. I-12 and I-13)**. However, it is controversial whether MULE-dependent MCL1 ubiquitination occurs constitutively or upon a specific apoptotic stimuli (Mojsa et al., 2014), as *Mule* deletion in mice does not alter MCL1 basal levels and B cell-specific *Mule*-deficient cells display impaired MCL1 degradation and resistance to apoptosis under genotoxic stress conditions (Hao et al., 2012).

**Table I-4. E3 ubiquitin ligases and deubiquitinases involved in MCL1 regulation.**

| Name | Type | Signal/Activator | References |
|---|---|---|---|
| **MULE** | HECT domain E3 ligase | Constitutive and stress-induced (UV, mitotic slippage, etc.)<br>**NOXA:MCL1 complexes** | Warr et al., 2005, Zhong et al., 2005, Czabotar et al., 2007, Wuilleme-Toumi et al., 2007, Gomez-Bougie et al., 2011 |
| **$SCF^{\beta\text{-}TrCP}$** | Multi-subunit RING-finger E3 ligase | Growth factor withdrawal, UV:<br>'Priming' **P-T163** by JNK,<br>**P-S155** and **P-S159** by GSK3 | Ding et al., 2007, Ren et al., 2013 |
| **$SCF^{FBW7}$** | Multi-subunit RING-finger E3 ligase | Growth factor withdrawal:<br>'Priming' **P-T163** by JNK,<br>**P-S155** and **P-S159** by GSK3<br>Mitotic arrest:<br>**P-S121** by p38, **P-S159** by CKII,<br>**P-T163** by JNK and **P-T92** by CDK1 | Inuzuka et al., 2011, Wertz et al., 2011 |
| **TRIM17** | Single-subunit RING-finger E3 ligase | Growth factor withdrawal:<br>'Priming' P-T163 by JNK,<br>P-S155 and P-S159 by GSK3 | Magiera et al., 2013 |
| **$APC/C^{CDC20}$** | Multi-subunit RING-finger E3 ligase | Mitotic arrest:<br>**P-T92** by Cyclin B1/ CDK1 | Harley et al., 2010 |
| **$SCF^{FBXO4}$** | Multi-subunit RING-finger E3 ligase | Chemotherapy? | Feng et al., 2017 |
| **USP9X** | DUB | Unknown | Schwickart et al., 2010, Gomez-Bougie et al., 2011 |
| **USP13** | DUB | Unknown | Zhang et al., 2018 |
| **DUB3** | DUB | Unknown | Wu et al., 2019 |

(See next page)

*Abbreviations:* MULE, MCL1 ubiquitin ligase E3; SCF, Skp1–Cullin–F-box-protein; β-TrCP, beta-transducin repeat-containing protein; FBW7, F-box and WD repeat domain-containing 7 protein; APC/C, anaphase-promoting complex/cyclosome; CDC20, cell-division cycle protein 20; FBXO4, F-box 4 protein; USP9X, ubiquitin-specific peptidase 9X; USP13, ubiquitin-specific peptidase 13; DUB3, deubiquitinating protein 3; JNK, c-Jun N-terminal kinase; GSK3, glycogen synthase kinase 3; CKII, casein kinase II; CDK1, cyclin-dependent kinase 1.

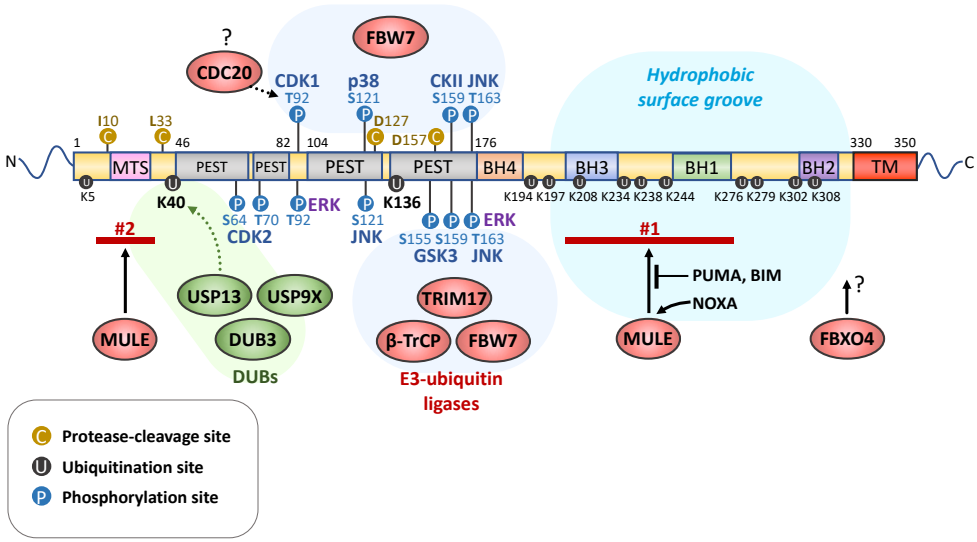


**Figure I-13. Regulation of MCL1 protein stability.** Major residues which can be phosphorylated (blue) or ubiquitinated (black), and the proteolytic-cleavage sites (yellow) on MCL1 are displayed. Among the 13 lysine (K) residues present in MCL1, ubiquitination of K40 and K136 are thought to be the most important for directing its proteasomal degradation. Phosphorylation by distinct protein kinases (in dark blue) at the indicated residues drives the recognition of several E3 ubiquitin ligases (in red), except phosphorylation by ERK (in purple) at T92 and/or T164, which promotes MCL1 stabilization. Dark-blue circles indicate the phosphorylation sites recognized by the E3 ligases. Direct ubiquitination of MCL1 by APC/C$^{CDC20}$ has not been demonstrated. MULE is the only E3 ligase that does not require a priming phosphorylation. MULE-interaction sites, as indicated by the red bars, fall into MCL1 BH3 groove (#1) or at MCL1 N-terminus (#2). Likewise, its interaction can be promoted or inhibited by several BH3-only proteins such as NOXA or PUMA and BIM. DUBs, which oppose MCL1 ubiquitination, are shown in green and its interaction can be inhibited by phosphorylation of MCL1 at specific residues. For instance, phosphorylation at S155, S159 and T163 inhibits the binding of USP9X to MCL1. Adapted from Mojsa et al. (2014).

The second E3 ubiquitin ligase identified was Skp1–Cullin–F-box-protein (SCF) E3 ligase complexed to the F-box protein β-TrCP, $SCF^{\beta\text{-}TrCP}$ (Ding et al., 2007). In response to certain apoptotic stimuli, such as cytokine withdrawal (Maurer et al., 2006) or UV irradiation (Morel et al., 2009), MCL1 is (**1**) phosphorylated at T163 (T144 in the mouse) by c-Jun N-terminal kinase (JNK). T163 phosphorylation primes subsequent phosphorylation of MCL1 (**2**) at S155 and S159 (S140 in the mouse) by GSK3, creating a phosphodegron which is recognized by β-TrCP and targets MCL1 for proteasomal degradation **(Fig. I-13 and Table I-4)**. Two additional E3 ubiquitin ligases also have been implicated in GSK3-dependent MCL1 ubiquitination, $SCF^{FBW7}$ and TRIM17 (Inuzuka et al., 2011, Magiera et al., 2013). However, TRIM17-dependent MCL1 ubiquitination and degradation appears to be restricted to neurons, mediating apoptosis upon survival factor deprivation (Magiera et al., 2013). On the other hand, $SCF^{FBW7}$ can also promote MCL1 ubiquitination in a GSK3-independent but p38-, casein kinase II (CKII)- and JNK-dependent manner (Wertz et al., 2011). Phosphorylation of MCL1 by these kinases at S121, S159 and T163, respectively, is indirectly enhanced by phosphorylation at T92 by CDK1 during prolonged mitotic arrest, promoting its recognition by FBW7 and its subsequent proteasomal degradation (Millman and Pagano, 2011, Wertz et al., 2011). Likewise, the RING-finger E3 ligase $APC/C^{CDC20}$, the major E3 ubiquitin ligase involved in cell cycle control, might also target MCL1 for degradation following cyclin B1/CDK1-dependent MCL1 phosphorylation at T92 during prolonged mitotic arrest (Harley et al., 2010). In addition, in cancer cells, both T163 and T92 can be phosphorylated by activated ERK in a GSK3-independent manner, conversely resulting in MCL1 stabilization and drug resistance (Ding et al., 2008). This opposing effect of ERK on MCL1 stability is likely to occur due to the impairment of the GSK3 pathway in many cancer cells (Nifoussi et al., 2012). Recently, another SCF ubiquitin ligase, $SCF^{FBXO4}$, has been identified to mediate MCL1 ubiquitination and degradation (Feng et al., 2017). This ubiquitin ligase is likely to play a major role in apoptosis of lung cancer cells following chemotherapy although whether it requires prior phosphorylation of MCL1 at a specific residue has not been addressed (Feng et al., 2017).

All the phosphorylations described above, within MCL1 N-terminus **(Fig. I-13)**, affect MCL1 stability and turnover, as the majority of E3 ubiquitin ligases promoting MCL1 degradation by the UPS recognize these residues, except phosphorylation of T92 and

T163 by ERK (Ding et al., 2008). Thus, phosphorylation-dependent ubiquitination constitutes the major mechanism of MCL1 regulation (reviewed in Mojsa et al., 2014). However, the effect of other phosphorylations on MCL1 stability are not completely determined, such as MCL1 phosphorylation at S121 and T163 by JNK. In addition, some phosphorylations may affect MCL1 function, such as the cell cycle-dependent phosphorylation of S64 by CDK1/2 and JNK which enhances its antiapoptotic function by increasing MCL1 interaction with proapoptotic BCL2 family members (Kobayashi et al., 2007). In response to DNA damage NOXA also promotes CDK2-mediated phosphorylation of MCL1 at S64 and T70, conversely resulting in ubiquitin-dependent MCL1 degradation (Nakajima et al., 2016). Overall, certain cellular stresses or apoptotic stimuli promote destabilization of MCL1 via phosphorylation and subsequent ubiquitin-dependent proteasomal degradation, switching the balance towards the proapoptotic members. Once apoptosis is initiated, active CASP3 can cleaved MCL1 to further contribute to MCL1 inactivation.

Of note, even in basal conditions, MCL1 undergoes rapid turnover, and MULE was the initial candidate proposed to mediate these effects (Zhong et al., 2005), although recent studies have questioned the involvement of MULE in MCL1 basal degradation (Hao et al., 2012). Surprisingly, MCL1 degradation may not even require ubiquitination, as shown by Stewart and coworkers, who generated a mutant form of MCL1 ($MCL1^{KR}$) in which all lysines (K) were mutated to arginines (R) and thus, could not be ubiquitinated. However, the mutant was degraded by the proteasome at a similar rate than the wt-MCL1 both under basal conditions and upon UV-induced apoptosis, suggesting that ubiquitin-independent pathways might play an important role in both constitutive and stress-induced MCL1 degradation (Stewart et al., 2010). Likewise, during mitotic slippage, MCL1 is degraded by the proteasome without the involvement of an E3 ligase (Sloss et al., 2016). It is possible that MCL1 is directed to the proteasome through a carrier or that, given the intrinsic disorder on its structure (~30%), the protein is degraded independently of ubiquitination, as has been reported for other proteins with intrinsically disorder regions, i.e. with unstructured regions of more than 30 aa in length, such as p21 or p53. (Jariel-Encontre et al., 2008, Ben-Nissan and Sharon, 2014). Therefore, MCL1 degradation pathway is not fully understood and its proteasomal degradation might occur in both a ubiquitin-dependent and independent manner.

## 2.3. MCL1 in cancer

Such stringent multi-level mechanisms of MCL1 regulation guarantees its function during early embryonic development (Rinkenberger et al., 2000) and in the survival of multiple adult cell lines (Arbour et al., 2008, Vick et al., 2009, Perciavalle and Opferman, 2013, Wang et al., 2013). Its many critical apoptotic roles confer on MCL1 a high oncogenic potential and it is not surprising that its expression is deregulated in many human cancers. However, its overexpression rarely results from a chromosomal translocation, but from gene amplification. Overall, MCL1 is found overexpressed both in hematological malignancies, especially in B-cell NHL, including CLL (Pepper et al., 2008) and ALL (Kaufmann et al., 1998) as well as in MM (Le Gouill et al., 2004, Wuilleme-Toumi et al., 2005), AML (Glaser et al., 2012) and CML (Aichberger et al., 2005) **(see also Table I-2)**, and solid tumors, as e.g. hepatocellular carcinoma (HCC) (Sieghart et al., 2006), cholangiocarcinoma (Isomoto et al., 2005), melanoma (Wong et al., 2008), non-small cell lung cancer (NSCLC) (Zhang et al., 2011) and breast cancer (BC) (Beroukhim et al., 2010 and reviewed in Quinn et al., 2011). In addition, its overexpression also correlates with poor prognosis, drug resistance and relapse (Song et al., 2005, Wuilleme-Toumi et al., 2005, Wei et al., 2006). For instance, *MCL1* gene amplifications or chromosomal gains are seen in 20-25% cases of ABC-DLBCL subset, one of the most aggressive types of NHL (Wenzel et al., 2013). Furthermore, elevated MCL1 mRNA or protein levels correlates with disease progression and severity in MM (Derenne et al., 2002, Wuilleme-Toumi et al., 2005), MCL (Khoury et al., 2003), and in FL (Cho-Vega et al., 2004). Elevation of MCL1 levels can result from (**1**) the constitutive activation of signal transduction pathways which upregulate *MCL1* transcription, as observed in MM (Le Gouill et al., 2004, Warr and Shore, 2008), CML (Aichberger et al., 2005) and CLL (Ertel et al., 2013), (**2**) the reduction or the loss of certain miRs such as miR29 (Mott et al., 2007) or miR125b (Gong et al., 2013), as observed in BL (Mazzoccoli et al., 2018), ALCL (Desjobert et al., 2011), DLBCL (Malumbres et al., 2009) and AML (Garzon et al., 2009), and (**3**) the alteration of certain post-translational mechanisms of MCL1 regulation, such as the increased expression of USP9X or the genetic inactivation of FBW7, which correlates with increased MCL1 protein levels in malignancies such as FL, DLBCL, MM and T-ALL (Schwickart et al., 2010, Inuzuka et al., 2011).

### 2.3.1. Cooperation of MCL1 with oncogenic MYC

Given the prevalence of MCL1 overexpression across human tumors, mouse models have been exploited to address the contribution of MCL1 in many of these malignancies (Ertel et al., 2013, Perciavalle and Opferman, 2013). First, it was shown that targeted *Mcl1* overexpression in mice within hematopoietic and lymphoid tissues led to an increased incidence of B-cell lymphomas over time (Zhou et al., 2001). By contrast, overexpression of other antiapoptotic BCL2 members as e.g. *Bcl2* is not able to cause lymphoma **(see also Table I-2)**. Likewise, MCL1 genetic ablation was shown to promote cell death in both tumor cell lines and mouse models (Moulding et al., 2000). For instance, in a mouse model of AML, MCL1 loss induces cell death regardless the complementary expression of the other antiapoptotic members, even in a heterozygous setting (Xiang et al., 2010, Glaser et al., 2012). Similarly, loss of *Mcl1* delays development of T-cell lymphomas (TCLs) in mice (Grabow et al., 2014) and causes cell death of tumor cells in BCR-ABL-driven B-ALL mouse model (Koss et al., 2013). These findings support a critical role for MCL1 in the development and the maintenance of specific malignancies. Indeed, overexpression of MCL1 cooperates with MYC to overcome oncogene-induced apoptosis in a mouse model of MYC-driven NSCLC (Allen et al., 2011), as occurs with other antiapoptotic BCL2 family members. Such cooperation was observed in a wide-genome screening of the most frequent somatic copy-number alterations across 26 distinct types of human cancers, which revealed that the gene most frequently co-amplified with *MCL1* was *MYC* (Beroukhim et al., 2010). Recently, cooperation of MCL1 with MYC has been also related to the acquisition of resistance to chemotherapy in triple-negative breast cancer (TNBC) cells (Lee et al., 2017b). Indeed, the dependency of MYC-driven tumors on MCL1 has been extensively studied in the E$\mu$-MYC mouse model, in which, as shown in **Table I-2**, its overexpression dramatically accelerates lymphomagenesis (Campbell et al., 2010). The many gene KO studies developed in the A. Strasser laboratory demonstrated the crucial role of MCL1 in the onset and the progression of this malignant MYC-driven B-cell lymphoma, as mentioned in **Section 2.1.4.**.

### 2.3.2. MCL1 inhibitors for the treatment of hematological malignancies

Given the pervasive role of MCL1 in cancer, its cooperation with oncogenic MYC signaling in both solid tumors and hematological malignancies, and its close correlation with cancer cell survival and patient outcome, it has become an attractive therapeutic target. The development of MCL1 inhibitors able to abrogate its antiapoptotic function has followed two main strategies: (**1**) downregulating MCL1 cellular levels through direct or indirect mechanisms; and (**2**) chemically inactivating its functional BH3 surface groove, i.e., disrupting its interaction with BAK/BAX through specific molecules, known as BH3 mimetics (see reviews of Warr and Shore, 2008, Akgul, 2009, Quinn et al., 2011 and Hird and Tron, 2019).

**Downregulating MCL1 cellular levels.** Multiple drugs cause MCL1 downregulation as part of their mechanism of action, even though not designed to target MCL1 (Quinn et al., 2011, Hird and Tron, 2019). Drugs that reduce MCL1 levels in an indirect manner include pan CKIs such as Flavopiridol, SNS,032, R-Roscovitine and Dinaciclib, selective CDK9 inhibitors, such as BAY1251152 and AZD4573, certain chemotherapeutic drugs, such as anthracyclines or global transcriptional inhibitors as e.g. high doses of Actinomycin D (ActD) or Triptolide (or Minnelide), the multikinase inhibitor Sorafenib and DUB inhibitors such as WP1130 **(Table I-5)** (Quinn et al., 2011, Wei et al., 2012, Hird and Tron, 2019). Antisense oligonucleotide strategies have also been designed against MCL1, but their poor stability in blood and the difficulty in targeting them to specific cell types have made it hard to translate their application into the clinic (Quinn et al., 2011). As shown in **Table I-5**, many of these compounds are currently under evaluation for the treatment of several hematological and solid tumors. However, as they affect multiple targets through distinct signaling pathways, they are less selective and potentially more toxic than specific MCL1 inhibitors. In addition, their pleiotropic effects make difficult to attribute the molecular mechanism underlying cell death to *MCL1* downregulation. Therefore, the second strategy, which involves the direct chemical antagonism of MCL1, has arisen as the most promising translational strategy in cancer.

**Development of specific BH3 mimetics.** From the early 2000s, great efforts have been made to develop small molecules that mimic the action of certain proapoptotic BH3-only proteins, termed 'BH3 mimetics'. This effort was initially based on the observation that abrogation of an antiapoptotic BCL2 family protein itself could lead to cancer regression, as was demonstrated by Letai et al. for the depletion of *Bcl2* in a murine model of leukemia (Letai et al., 2004). A few years later several compounds were identified, some of which displayed promising results for the treatment of certain malignancies, such as Navitoclax and Venetoclax, two BCL2 inhibitors developed by AbbVie (Tse et al., 2008, Souers et al., 2013). Both compounds were evaluated in clinical trials and their clinical efficacy was validated, especially of Venetoclax as a single-agent in relapsed CLL patients (Roberts et al., 2016). This provided the proof of principle for the application of BH3 mimetics for cancer treatment and indeed, Venetoclax was approved by the FDA in April 2016 in CLL patients with poor prognosis. Despite the outstanding results in certain cancers, such as CLL, other hematological tumors, such as AML, MM and B-cell NHL, as well as solid tumors, displayed heterogeneous responses or even acquired resistance to the compounds, frequently arising from the upregulation of MCL1 expression (van Delft et al., 2006, Quinn et al., 2011). The development of a selective MCL1 inhibitor, was challenging as its long shallow hydrophobic binding groove was more difficult to drug with a small molecule in comparison to its antiapoptotic relatives BCLxL and BCL2 (Hird and Tron, 2019). In addition, MCL1 inhibition could cause severe side effects, including hematopoietic toxicity (Opferman et al., 2003, Opferman et al., 2005, Dzhagalov et al., 2007, Perciavalle and Opferman, 2013), cardiotoxicity (Wang et al., 2013), neurotoxicity (Arbour et al., 2008), hepatotoxicity (Vick et al., 2009) and potentially mitochondrial respiration, through $MCL1_{matrix}$ inhibition (Perciavalle et al., 2012). Finally, many of the first compounds which potentially inhibited MCL1 were later found to exert their phenotypic effects through alternative mechanisms rather than MCL1 inhibition (R and Eastman, 2016, Chen and Fletcher, 2017). For instance, the pan-BCL2 inhibitor developed by GeminX GX15-070, also known as Obatoclax (Nguyen et al., 2007) was found to disrupt MCL1:BAK complexes (Li et al., 2008) and to overcome MCL1-mediated resistance to the proteasome inhibitor Bortezomib in melanoma and MCL cell lines (Nguyen et al., 2007, Perez-Galan et al., 2007), and to ABT-737 (an analog of Navitoclax) in BCL2-overexpressing cell lines (Nguyen et al.,

2007). The compound displayed cytotoxic activity in MM and NSCLC cell lines, and in several mouse tumor models (Nguyen et al., 2007, Trudel et al., 2007, Li et al., 2008) despite modest activity in other hematological tumors, such as CLL and AML (Schimmer et al., 2008, O'Brien et al., 2009, Schimmer et al., 2014). It was finally found that the compound decreased MCL1 expression through the induction of NOXA, instead of displacing its proapoptotic BH3-only partners from its BH3 surface groove, thus, it was erroneously characterized as a BH3 mimetic (Albershardt et al., 2011, R and Eastman, 2016).

**Specific MCL1 inhibitors.** The first specific and validated MCL1 inhibitor was an indole-2-carboxylic acid-derivative, the A-1210477 compound, developed by AbbVie **(Table I-5)** (Leverson et al., 2015). Despite displaying selective and strong binding to MCL1, its pharmacokinetic prolife was not favorable for its use *in vivo* (Opferman, 2016). With the aim of further improving the potency and reducing the binding to serum proteins of these indole-2-carboxylic acid derivatives, two additional molecules were developed VU661013, at Vanderbilt University, with cytotoxic activity in AML cell lines and antitumor efficacy *in vivo* (Ramsey et al., 2018), and AZD5991, developed by AstraZeneca (Tron et al., 2018). AZD5991 demonstrated potent and selective inhibition of MCL1, disrupting MCL1:BAK complexes and activating the intrinsic apoptotic pathway. The compound also displayed cytotoxic activity in hematological cell lines and in several subsets of NSCLC and BC cell lines (Tron et al., 2018, Koch et al., 2019), as well as anti-tumor response in preclinical studies in mouse and rat patient-derived xenograft (PDX) models for MM, AML and TCL (Tron et al., 2018, Koch et al., 2019). Given its successful preclinical results, this compound is currently undergoing phase I clinical in patients with relapsed or refractory (R/R) hematological malignancies, including MM, TCL, CLL/small lymphocytic leukemia (SLL), AML, ALL, MDS and RS (NCT03218683).

In parallel, non-indole acid-derived MCL1 inhibitors have been also developed, such as AMG-176, a potent MCL1 inhibitor produced by Amgen (Caenepeel et al., 2018). AMG-176 efficiently disrupts the interaction between MCL1 and proapoptotic BCL2 family members, resulting in increased MCL1 stability and BAK/BAX-dependent apoptotic cell death. It has also displayed potent cytotoxic activity in MM and AML cell lines and modest efficacy in BC and NSCLC cell lines (Caenepeel et al., 2018). As

it also demonstrated antitumoral activity in MM and AML orthotopic mouse models it is also being evaluated as a single agent in patients with R/R MM and AML (NCT02675452) and in a parallel study in combination with Venetoclax (NCT03797261). Likewise, its analog **AMG-397**, the first orally-available MCL1 inhibitor also developed by Amgen, is also undergoing a phase I clinical trial for patients with R/R MM, AML and DLBCL (NCT03465540).

Finally, a drug discovery collaboration established in 2007 between Vernalis and Servier culminated in the discovery of **S63845**. This compound was, indeed, the first-in-class MCL1 inhibitor which displayed strong activity and selectivity for MCL1, with ~20-fold higher affinity for MCL1 than A-1210477, and no activity towards BCL2 or BCLxL (Kotschy et al., 2016). It was found that engagement of the compound with MCL1 results in MCL1 protein stabilization and accumulation (without altering *MCL1* mRNA levels), and induction of BAK/BAX-dependent apoptotic cell death. In addition, it demonstrated apoptotic activity in several hematological cell lines, including MM, CML, AML and T-ALL cell lines (Kotschy et al., 2016, Li et al., 2019, Moujalled et al., 2019) and its administration led to complete tumor regression in MM and AML subcutaneous tumor models and in the E$\mu$-MYC lymphoma model (Kotschy et al., 2016). It also showed enhanced antitumor activity in combination with Venetoclax in AML and T-ALL *in vivo* models (Li et al., 2019, Moujalled et al., 2019). In solid tumors, generally more resistant to MCL1 inhibitors, it displayed moderate efficacy in NSCLC, BC and melanoma cell lines (Kotschy et al., 2016). However its combination with standard chemotherapy, in TNBC cell lines and PDX BC models, and with HER2-targeted therapies in HER2-amiplified BC models increased antitumor activity (Merino et al., 2017). Given these preclinical results and the safety features of the drug, a structural analog, named **S64315** (or MIK665) is now on phase I clinical trials in R/R DLBCL, MM, AML and MDS patients, as a single-agent, and in combination with Venetoclax in AML patients (NCT02979366, NCT02992483, NCT03672695).

**Table I-5. Specific and non-specific MCL1 inhibitors and current clinical status (i)**

| Compound, developer | Effects on MCL1 | Cytotoxic activity in | Current status (Clinical trials) | Patient criteria, treatment design | References |
|---|---|---|---|---|---|
| **Pan cyclin-kinase inhibitors** | | | | | |
| **Flavopiridol/ Alvocidib** (NCI, Tolero) | Decreased *MCL1* levels due to Pol II inhibition | MM cell lines | Phase I/II (Completed) NCT00445341 NCT00058240<br>Phase I (Completed) NCT00058227<br>Phase I (Recruiting) NCT03441555 | R/R MCL, DLCL; mono R/R CLL/SLL; mono MCL, CLL/SLL, FL, MZL; combo with fludarabine and rituximab<br>R/R AML; combo with venetoclax | (Gojo et al., 2002) |
| **SNS-032** (Sunesis) | Decreased *MCL1* levels due to Pol II inhibition | CLL cell lines | Phase I (Completed) NCT00446342 NCT00292864 | CLL, MCL, MM; mono Advanced BC, HM, NSCLC; mono | (Chen et al., 2009, Tong et al., 2010) |
| **Roscovitine/ Seliciclib** (CYCC) | Decreased *MCL1* levels due to Pol II inhibition | MM, MCL and CLL cell lines | Several Phase II trials<br>Phase II (Terminated) NCT00372073 | B-cell malignancies; mono<br>R/R NSCLC; combo with gemcitabine or cisplatin | (MacCallum et al., 2005) |
| **Dinaciclib** (AbbVie, Merck) | Decreased *MCL1* levels due to Pol II inhibition | MYC-driven B-cell lymphomas and AML cell lines | Phase II (Terminated) NCT00798213<br>Phase III (Completed) NCT01580228<br>Phase I/II (Completed) NCT00732810 | R/R AML, ALL; mono<br>R/R CLL; mono<br>Advanced BC and NSCLC; mono | (Gregory et al., 2015, Baker et al., 2016) |
| **Selective CDK9 inhibitors** | | | | | |
| **BAY1251152** (Bayer) | Decreased *MCL1* levels due to Pol II inhibition | AML cell lines and xenograft models | Phase I (Completed) NCT02745743<br>Phase I (On going) NCT02635672 | Advanced hematological tumors; mono<br>Advanced solid cancers; mono | (Lucking et al., 2017, Luecking et al., 2017) |
| **AZD4573** (Astra Zeneca) | Decreased *MCL1* levels due to Pol II inhibition | AML cell lines and xenograft models | Phase I (Recruiting) NCT03263637 | R/R AML, ALL, CLL, CML/SLL, MM, MDS, and RS; mono | (Cidado et al., 2018, Yeh et al., 2018) |
| **Global transcriptional repressors** | | | | | |
| **Triptolide/ Minnelide** (Minneamrita Therapeutics) | Decreased *MCL1* levels due to TR | NSCLC, BC, PC, CRC and AML cell lines and xenograft models | Phase I (Recruiting) NCT03760523<br>Phase II (Recruiting) NCT03117920 | R/R AML, mono<br>R/R PAC; mono | (Carter et al., 2006, Wei et al., 2012, Giri et al., 2019) |
| Anthracyclines: **Doxorubicin, Daunorubicin, Epirubicin** | Decreased *MCL1* levels due to TR* | NSCLC and BC cell lines | **Approved** as chemotherapeutic agents in many cancers. | AML, ALL, BL, DLBCL, FL, MM, SCLC, NB, sarcoma, thymoma, WT and some types of BC. | (Hortobagyi, 1997, Wei et al., 2012) |
| **Actinomycin D** (Rasna Therapeutics) | Decreased *MCL1* levels due to TR | NSCLC and BC cell lines | **Approved** for:<br>Phase II (On going) 2014-000693-18 | WT, RMS, EWS, TC, GTN and some types of OVC.<br>R/R NPM1 AML; mono | (Wei et al., 2012, Falini et al., 2015) |

**Table I-5. Specific and non-specific MCL1 inhibitors and current clinical status (ii)**

| Compound, developer | Effects on MCL1 | Cytotoxic activity in | Current status (Clinical trials) | Patient criteria, treatment design | References |
|---|---|---|---|---|---|
| **Multikinase inhibitors** | | | | | |
| **Sorafenib** (Bayer) | Inhibition of MCL1 translation due to eIF4E blockage | AML and CLL cell lines | **Approved** for:<br>Phase I (Completed) NCT01398501<br>Phase II (Completed) NCT00893373 | Metastatic HCC, thyroid and renal cell carcinoma<br>FLT3-ITD AML after allogeneic HSCT<br>AML; combo with standard chemotherapy | (Huber et al., 2011, Chen et al., 2014, Rollig et al., 2015) |
| **Deubiquitinase inhibitors** | | | | | |
| **WP1130/ Degrasyn** (Moleculin) | Decreased MCL1 levels due to USP9X inhibition | CML, HCC, NSCLC and BC cell lines | Preclinical status | *Not applicable* | (Sun et al., 2011, Liu et al., 2015, Fu et al., 2017) |
| **Pan BCL2 inhibitors (BH3 mimetics)** | | | | | |
| **GX15-070/ Obatoclax** (GeminX) | Decreased MCL1 protein levels due to induction of *NOXA* | NSCLC, MM, MCL, AML, BC, CC and CRC cell lines | Phase I/II (Completed) NCT00600964 NCT00438178<br>Phase II (Completed) NCT00684918 | CLL, mono<br>AML, MDS, CML, MF mono<br>AML; mono | (Nguyen et al., 2007, Trudel et al., 2007, Li et al., 2008) |
| **Selective MCL1 inhibitors (BH3 mimetics)** | | | | | |
| **A-1210477** (AbbVie) | MCL1 protein accumulation | MM and NSCLC cell lines | *No activity. in vivo* | *Not applicable* | (Leverson et al., 2015) |
| **VU661013** (Vanderbilt) | MCL1 protein accumulation | AML cell lines and PDXs. | *Not disclosed* | *Not applicable* | (Ramsey et al., 2018) |
| **AZD5991** (Astra Zeneca) | MCL1 protein accumulation | MM, AML, TCL, BC and NSCLC cell lines. AML and TCL PDXS. | Phase I (Ongoing) NCT03218683 | R/R MM, CLL/SLL, AML, ALL, MDS, RS; mono | (Tron et al., 2018, Koch et al., 2019) |
| **AMG-176** (Amgen) | MCL1 protein accumulation | MM, AML, BC, NSCLC cell lines. MM, AML mouse models | Phase I (Not Recruiting) NCT02675452<br>Phase I **(Suspended)** NCT03797261 | R/R MM, AML; mono and undefined combos<br>R/R AML; combo with venetoclax | (Caenepeel et al., 2018) |
| **AMG-397** (Amgen) | MCL1 protein accumulation | MM, AML, ALL and BL cell lines | Phase I (Not recruiting) NCT03465540 | R/R MM, AML, DLBCL; mono | |
| **S63845** (Novartis, Servier, Vernalis) | MCL1 protein accumulation | MM, AML, CML, T-ALL, NSCLC, HM, BC cell lines. MM, AML, T-ALL, E$\mu$-MYC mouse models | *Not selected* | *Not applicable* | (Kotschy et al., 2016, Li et al., 2019, Moujalled et al., 2019) |
| **S64315/ MIK665** (Novartis, Servier) | MCL1 protein accumulation | | Phase I (Recruiting) NCT02992483<br>Phase I (Not Recruiting) NCT02979366 NCT03672695 | R/R MM, DLBCL; mono<br>R/R AML, MDS; mono<br>R/R AML; combo with venetoclax | |

**Table I-5. (continued)** *Indicates no study regarding MCL1 repression. *Abbreviations:* ID, Identifier; NCI, National Cancer Institute; CYCC, Cyclacel Pharmaceuticals; TR, transcriptional repressor; PDX, patient-derived xenograft; R/R, relapsed or refractory; HSCT, human stem cell transplant; BC, breast cancer; CC, cervical cancer; CRC, colorectal cancer; EWS, Ewing's sarcoma; GTN, gestational trophoblastic neoplasia; HCC, hepatocellular carcinoma; HM, human melanoma; MF, myelofibrosis; NB, neuroblastoma; NSCLC, non-small cell lung cancer; OVC, ovarian cancer; PC, prostate cancer; RMS, rhabdomyosarcoma; RS, Richter's syndrome; SLL, small lymphocytic lymphoma; TC, testicular cancer; TCL, T-cell lymphoma; WT, Wilms tumor; mono, monotherapy; combo(s), combination(s). Review in Quinn et al. (2011), Hird and Tron (2019). *Last access to ClinicalTrials.gov on 1-10-2019*.

Therefore, four distinct MCL1 inhibitors are currently in ongoing phase I clinical trials: AZD5991, AMG-176, AMG-397 and S64315. All have shown on-target activity and preferential anti-tumor effects as single agents in hematological malignancies, even in those associated with poor outcomes, and modest efficacy in solid tumors, providing a rationale for testing them in the clinic. In addition, they have improved the efficacy and the duration of the anti-tumor response in combination with targeted therapies or with standard chemotherapy, even displaying activity in monotherapy-resistant models (Caenepeel et al., 2018, Ramsey et al., 2018, Tron et al., 2018, Koch et al., 2019, Moujalled et al., 2019). It is important to note that most of the preclinical studies of efficacy and tolerability of MCL1 inhibitors have been performed utilizing humanized MCL1 mouse strains (Brennan et al., 2018, Caenepeel et al., 2018), since these inhibitors weakly bind mouse MCL1, raising the question whether human non-tumoral cells will tolerate chronic MCL1 inhibition at the level required to see a therapeutic effect on tumor cells. Data from phase I clinical trials will be critical to address these issues and establish the therapeutic window of these inhibitors in humans.

# 3. Ribosome Biogenesis in MYC-driven tumors

The ribosome is the central component of the translational machinery in all extent life, responsible for translating the information of the genetic code into functional proteins. Ribosomes are relatively stable entities and their cellular content depends to a large extent on their rate of synthesis, which requires the coordination of multiple processes, including the synthesis of its functional and structural components, the ribosomal proteins (RPs) and rRNAs, and of the many factors required for the correct maturation, assembly and transport of these ribosomal components into functional ribosomes at the cytoplasm. As the rate of cell growth and proliferation, is largely dictated by the availability of ribosomes, growing cells rely in the production of new ribosomes at high rates, which can consume up to the 80% of the energy of a eukaryotic cell (Schmidt, 1999, Warner, 1999). For instance, in proliferating mammalian cells, ∼2000 new ribosomes are assembled per minute, such that the cell dedicates as much as 50% of its nuclear transcription to synthesize rRNAs, which in yeast cells is 80% (Moss and Stefanovsky, 2002). Likewise, yeast cells dedicate half of all Pol II transcription to the synthesis of RPs transcripts, and ∼30% of global translation to synthesize RPs and ribosome-associated factors (RAFs) (Warner, 1999). Although these numbers are not known in mammals, rRNA constitutes 80% of the total nucleic acids, and RPs are among the most abundant cellular proteins, representing a 6% of the human protein biomass (Pelletier et al., 2018). Indeed, proliferating cell spends about half its time in making proteins used for the synthesis of new ribosomes (MacInnes, 2016). Such demand of new ribosomes is essential to provide growing cells with sufficient protein translation machinery for the synthesis of the large amounts of proteins required to increase the biomass before undergoing cell division. Importantly, tumor cells, which are characterized by aberrant proliferation, strongly rely on increased rates of RiBi to sustain their growth and proliferation, and to double the ribosome content required to produce daughter cells, as will be discussed in detail below **(Section 3.3)**.

## 3.1. Ribosomal components and function

In eukaryotes, the 80S ribosome **(Fig. I-14)**, as defined by its sedimentation rate in Svedberg (S) units (Taylor and Storck, 1964), is composed of equimolar amounts of four rRNA species (18S, 28S, 5.8S and 5S rRNA) and 80 distinct RPs, assembled into two subunits (**1**) the small 40S ribosomal subunit, comprised by a single strand of 18S rRNA and 33 distinct RPs of the small subunit, or RPSs, and (**2**) the large 60S ribosomal subunit, formed by the 28S, 5.8S and 5S rRNAs together with 47 distinct RPs from the large subunit, or RPLs (Bassler and Hurt, 2019). Although the structure of the ribosomal subunits is conserved throughout evolution, ribosomes of higher eukaryotes are much larger and have a more complex architecture than bacterial ribosomes, as determined by X-ray crystallography, potentially in support of their more elaborated biogenesis program (Melnikov et al., 2012, Pelletier et al., 2018). Eukaryotic 80S ribosomes contain >5500 nt of rRNA and 80 RPs, whereas bacterial 70S ribosomes contain ~4500 nt of rRNA and 54 RPs (Wilson and Doudna Cate, 2012). Despite these differences in composition and in the rRNA/protein ratio, they share a highly conserved structural core that forms the major functional domains of the ribosome including the decoding site, the peptidyl transferase center (PTC) and the subunit interface, which contains the mRNA-binding and the tRNA-binding sites. Likewise, both bacterial and eukaryotic ribosomes and subunits function in a similar manner, in which the small subunit is responsible for unwinding and recognizing the 5' end of mRNAs, and initiating translation at the AUG start codon and the delivery of the initiating methionyl-tRNA (Met-tRNAi), the aminoacyl-tRNA (aa-tRNA) containing the first methionine specific for translation initiation, whereas the large subunit is responsible for decoding the mRNA sequence, catalyzing peptide bond formation through its peptidyl transferase ribozyme activity (Melnikov et al., 2012) and is involved in the quality control of nascent peptides (Brandman et al., 2012).

Therefore, both the 40S and 60S ribosomal subunits are critical for protein translation at the four stages of the process: (**1**) initiation, (**2**) elongation, (**3**) termination and (**4**) recycling of the ribosomal subunits **(Fig. I-15)**. Among them, regulation of initiation is most critical step , during the recognition of the start codon by the Met-tRNAi (reviewed in Sonenberg and Hinnebusch, 2009).

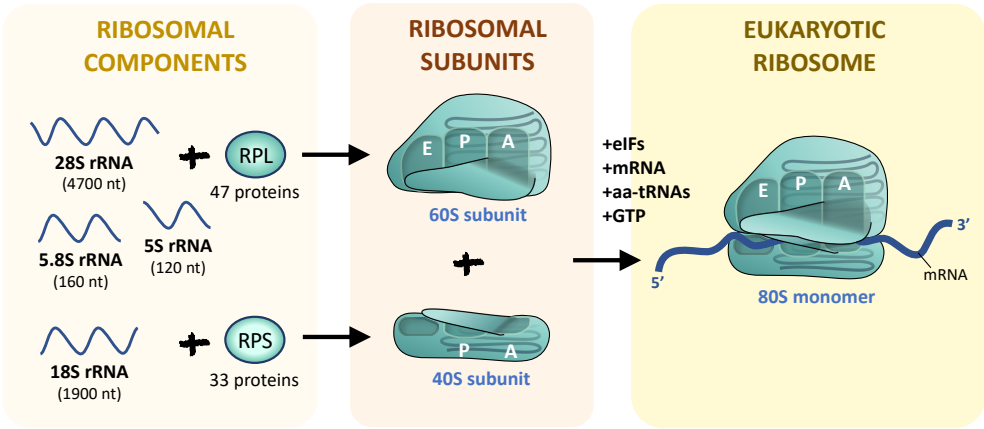


**Figure I-14. Eukaryotic 80S ribosome core.** See text for details. *Abbreviations*: RPL, ribosomal protein from the large (60S) subunit; RPS, ribosomal protein from the small (40S) subunit; eIFs, eukaryotic initiation factors; aa-tRNAs, aminoacyl tRNAs; P, peptidyl site; A, aminoacyl site; E, exit site.

As displayed in **Fig. I-15** the availability of the 40S ribosomal subunit together with eukaryotic initiation factors (eIFs) is essential for (1) **eukaryotic translation initiation**. Briefly, the 43S pre-initiation complex (43S PIC), which is comprised by the 40S subunit, a ternary complex formed by the eIF2 in its GTP-bound state and the Met-tRNAi, and other eIFs, has to be recruited to the capped 5' end of the mRNA to initiate the scanning of its 5'UTR for the AUG start codon (reviewed in Sonenberg and Hinnebusch, 2009). The eIF4F complex, which recruits the mRNA through the 7-methylguanosine ($m^7G$) cap at its 5' end via its cap-binding subunit eIF4E, also contains other eIFs that facilitates the 43S PIC assembly, forming the 48S PIC. This 48S PIC scans the 5'UTR of the mRNA, as successive triplets enter into the peptidyl (P)-site of the 40S subunit, and removes any inhibitory stem-loops. Once the start codon is encountered, the Met-tRNAi forms a codon-anticodon interaction, and the GTP of the eIF2 is hydrolyzed, resulting in the release of eIF2-GDP and other eIFs, and 60S subunit is joined to the 40S subunit to form the final 80S initiation complex (reviewed in Sonenberg and Hinnebusch, 2009). Immediately after the 80S complex is assembled at the start codon with the Met-tRNAi in the P-site, elongation begins (reviewed in Schuller and Green, 2018).

Of note, this mechanism of scanning the mRNA for the start codon, termed '**CAP-dependent translation initiation**' is considered the standard mode of initiation in eukaryotes under physiological conditions. However, under stress conditions that impaired CAP-dependent translation and repress global protein synthesis, such as mitosis, translation is driven by CAP-independent mechanisms, such as the internal ribosome entry sites (IRES)-dependent translation (Komar and Hatzoglou, 2011). **IRES elements** are highly complex RNA structural elements present in the 5'UTRs of ~10-15% of eukaryotic mRNAs, many of which encode proteins critical in cell survival, oncogenesis and tumor suppression, such as BCLxL, MYC and p53 (Spriggs et al., 2008, Komar and Hatzoglou, 2011). Under physiological conditions IRES-containing mRNAs are not efficiently translated but under stress conditions these they are selectively translated by directly recruiting the 48S PIC to the start codon, circumventing the scanning process in similar manner to the initiation of translation in bacteria (Sonenberg and Hinnebusch, 2009, Shatsky et al., 2018).

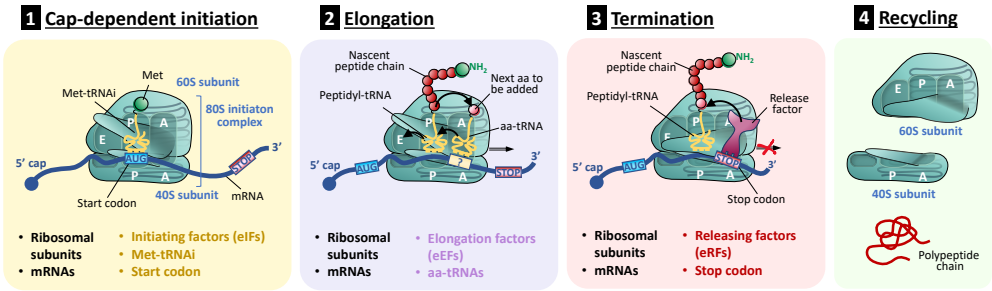


**Figure I-15. Major steps and components of eukaryotic translation.** Essential components of the translational machinery are indicated for each step. Components specific for a certain step are shown in color. See text for further details. *Abbreviations:* E, exit-site; P, peptidyl-site; A, aminoacyl-site; Met-tRNAi, initiating methionyl-tRNA; Met, methionine; aa, amino acid; aa-tRNA, aminoacyl-tRNA.

By contrast, (2) **elongation** is highly conserved. During this phase, the aminoacyl (A)-site of the 60S subunit is responsible for decoding the mRNA, i.e. for the incorporation of the corresponding amino acid in the nascent peptide chain as the aa-tRNAs are delivered into the A-site by the specialized eukaryotic elongation factor (eEF)1A in its GTP-bound state. When the appropriate tRNA is loaded, codon-anticodon interactions are sensed and the eEF1A GTPase mediates the binding of the aa-tRNA into the A-site, by hydrolyzing its bound GTP. Then the amino group of the incoming aa-tRNA 'attacks' the ester linkage on the peptidyl-tRNA loaded in the P-

site, allowing the transfer of the nascent peptide chain to the tRNA in the A-site to generate the nascent peptide +1 chain, unloading the tRNA located in the P-site. Following peptide bond formation, the ribosomal subunits rotate with respect to one another, and the tRNAs adopt an altered conformation which is recognized by a second GTPase, eEF2. Binding of eEF2 GTPase promotes the translocation of the mRNA-tRNA-nascent peptide complex from the A-site to the P-site and the translocation of the unloaded tRNA from the A site to the exit (E)-site, creating an open A-site for the next incoming aa-tRNA, while the ribosome scans the next triplet. The tRNA loaded on the E-site is released after translocation and the process is repeated until the ribosome reaches a stop codon, UAA, UAG or UGA. (3) Termination requires the recognition of any of these termination codons and the subsequent association of eukaryotic releasing factor (eRFs), which stimulate peptide release. Upon release of the final peptide, termination is completed. Finally, the (4) ribosome subunits disassemble and are either stored as free subunits or recycled by the ATP-binding cassette subfamily E member 1 (ABCE1) for a subsequent round of translation on a new mRNA (reviewed in Schuller and Green, 2018).

## 3.2. Ribosome biogenesis: the basics

The appropriate production of mature and functional ribosomal subunits is critical for the execution of translation, which allows the synthesis of all the repertoire of proteins required within a cell. Initial studies of the RiBi process were developed in the yeast *Saccharomyces cerevisiae*, benefiting from its powerful genetics and the conservation of the process in eukaryotes (Henras et al., 2008, Lafontaine, 2015). However, we now know that human RiBi is considerably more complex, as evidenced by the increased size of human ribosomes (Anger et al., 2013, Khatter et al., 2015), due to extensions on RPs and rRNA, and by the involvement of many additional components, in particular, the RAFs responsible for the correct assembly and maturation of the ribosomal subunits and the small nucleolar RNAs (snoRNAs) which guide rRNA modifications (Cerezo et al., 2019). Indeed, human ribosome contains 80 RPs, while yeast ribosomes are comprised by 79 RPs. Likewise, ∼290 human proteins have been identified as RAFs, many of which are not present in yeast, in which ∼200 RAFs have been described (Tafforeau et al., 2013). Regarding the snoRNAs, ∼200

have been identified in human, while only 75 in yeast (Lafontaine, 2015). Despite these additional layers of complexity, the basic principles of RiBi are conserved from yeast to human. Eukaryotic RiBi largely takes place in a specialized nuclear compartment, the nucleolus, and is orchestrated in a coordinated multi-step manner by the 4 rRNA species, the RPs, and thousands of RAFs involved in ribosomal processing, assembly or maturation, including endo- and exoribonucleases and the snoRNAs. Moreover, the three RNA polymerases, Pol I, Pol II and Pol III, are required to synthesize all the components which are involved in RiBi.

The process can be divided into five distinct steps: (**1**) the synthesis of the ribosomal components in the nucleolus (18S, 28S and 5.8S rRNA), the nucleus (5S rRNA and snoRNAs), or the cytoplasm (RPs and RAFs), (**2**) the import into the nucleus or the nucleolus of the RPs and the RAFs and the maturation of the 5S rRNA, (**3**) early rRNA processing and assembly of the 90S pre-ribosomal particle or 90S processome in the nucleolus and nucleus, (**4**) late rRNA processing, cleavage of the 90S processome into the 40S and 60S precursor ribosomal subunits, and (**5**) export and final maturation of the precursor ribosomal subunits in the cytoplasm, generating the mature translationally competent 40S and 60S subunits **(Fig. I-16)**.

### 3.2.1. Synthesis and maturation of the rRNA precursors: The nucleolus.

RiBi begins in **the nucleolus**, a specialized nuclear location whose major function is to "build ribosomes", and where the 18S, the 5.8S and the 28S rRNA species are transcribed by Pol I as a single polycistronic transcript, the 47S precursor ribosomal rRNA (47S pre-rRNA) (Boisvert et al., 2007). In eukaryotic cells, nucleoli are organized around clusters of rDNA units, commonly arranged as tandem repeats (Caburet et al., 2005), termed nucleolar organizer regions (NORs) **(Fig. I-17A)**. The NORs, containing the rDNA repeats, are located on the short arms of the five acrocentric chromosomes (Chr 13, 14, 15, 21 and 22) (Boisvert et al., 2007, Birch and Zomerdijk, 2008, Gibbons et al., 2015). There are ~two hundred copies of the rDNA genes in the human genome distributed along the NORs, although there is a substantial variability between individuals, as they are hotspots for recombination events (Stults et al., 2008, Gibbons et al., 2014). Nonetheless, it is the largest repetitive sequence and the most actively transcribed region in the human genome. However, the number of

rDNA genes which are actively transcribed is cell-type and species specific (Haaf et al., 1991). For instance, in human fibroblasts ~115 rDNA genes are actively transcribed per cell (Haaf et al., 1991). This balance between active and silent genes can be altered through epigenetic mechanisms but, on average, it is estimated only half of the rDNA genes are active (reviewed in McStay and Grummt, 2008).

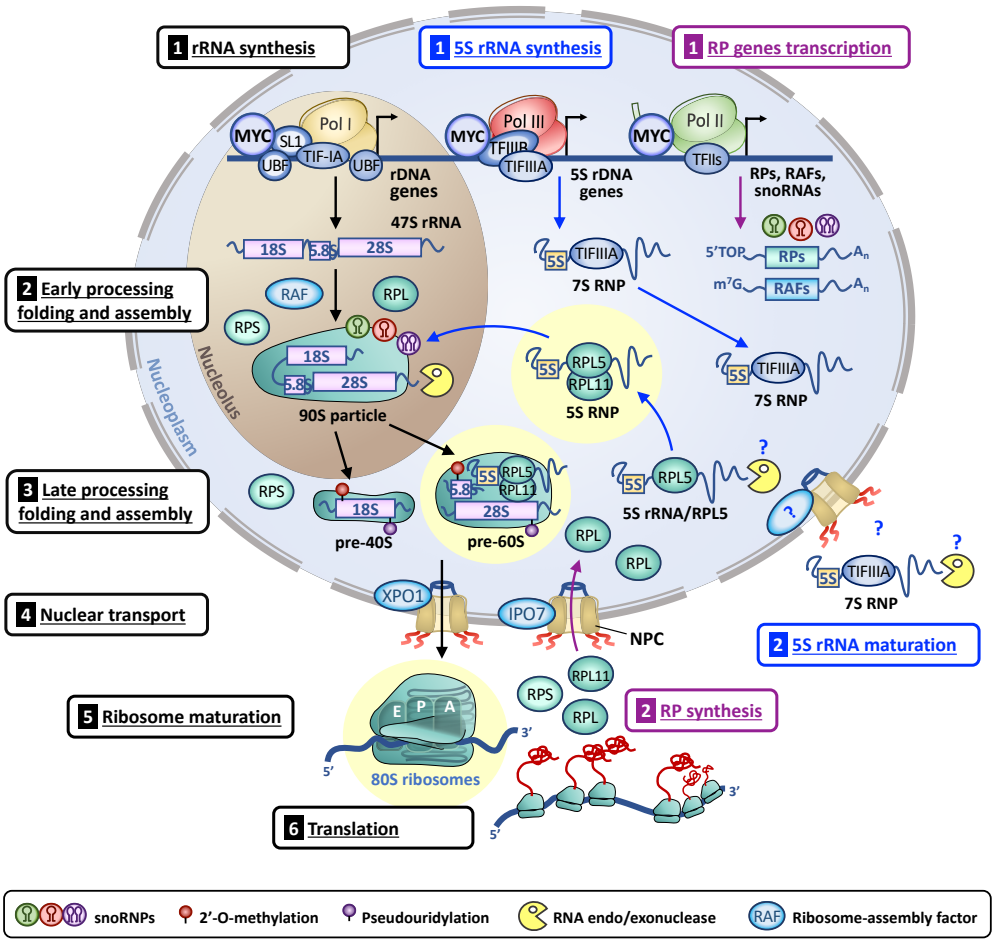


**Figure I-16. Overview of ribosome biogenesis.** Major steps of RiBi are indicated within the boxes. Black arrows and boxes indicate the steps of 47S pre-rRNA synthesis and maturation, RP assembly and ribosomal subunit maturation, to finally give rise to the mature 80S ribosome. Blue arrows and boxes indicate 5S rRNA biogenesis pathway and its assembly into the 90S processome. Purple arrows indicate the steps for snoRNAs, RPs and RAFs synthesis. *Abbreviations:* pre-40S/60S, 40S/60S precursor ribosomal subunit; snoRNPs, small nucleolar ribonucleoproteins; 5S/7S RNP, 5S/7S ribonucleoprotein; SL1, selectivity factor 1; UBF, upstream binding factor; TIF-IA, transcription initiation factor IA; XPO1, exportin 1; IPO7, importin 7; NPC, nuclear pore complex. See text for further details.

Each rDNA repeat of 43kb, contains an intergenic spacer (IGS) sequence of ~30kb with the transcription regulatory elements, and an rRNA coding region (CDR) of ~13kb **(Fig. I-17B)**. The CDR, encoding the 47S pre-rRNA, contains the sequences of the 18S, 5.8S and 28S rRNAs separated by two internal transcribed spacer (ITS) sequences, ITS1 and ITS2, respectively, and flanked by two external transcribed spacer sequences (ETS), 5'ETS and 3'ETS, respectively **(Fig. I-17C)**, all of which contain regulatory elements, such as promoters and enhancers (Pelletier et al., 2018). Multiple Pol I complexes bind to the CDR of each active rDNA unit and actively transcribe the rDNA genes, which can be visualized by electron microscopy as a chromatin spread **(Fig. I-17A)**. (Russell and Zomerdijk, 2005). Transcription by Pol I requires the association of the transcription initiation factor IA (TIF-IA), the selectively factor complex (SL1) and the upstream binding factor (UBF) (Russell and Zomerdijk, 2005).

In humans, the 47S pre-rRNA is fully transcribed before its processing (Cerezo et al., 2019). The post-transcriptional processing of the 47S pre-RNA includes the **cleavage of the ETS and ITS** sequences, mediated by endo- and exoribonucleolytic enzymes, as well as the **post-transcriptional modification** of the rRNA intermediates, mediated by small nucleolar ribonucleoproteins (snoRNPs) and other RAFs. The pre-rRNAs are modified at ~200 nt positions largely through methylations of the 2'-hydroxyl group of the ribose (2'-O-methylation) and pseudouridylations, which converts uridine into pseudouridine by isomerization (Lafontaine, 2015). 2'-O-methylations of the sugar backbone and uridine isomerization are catalyzed by the C/D box and the H/ACA box snoRNP families, respectively, which contain specific snoRNAs that recognize the substrate via base-pairing (reviewed in Watkins and Bohnsack, 2012, Lafontaine, 2015). Other RAFs catalyze additional modifications including methylation, acetylation and amino-carboxypropylation, independently of snoRNAs (Lafontaine, 2015). The majority of the pre-rRNA modifications cluster in functional regions of the ribosome, including the decoding and tRNA binding sites (A-/P-/E-sites), the PTC and the inter-subunit interface, thus post-transcriptional modifications are important not only for proper rRNA folding, but also for ribosome function (Lafontaine, 2015). The first modifications occur in parallel with the assembly of the first RPs, ~60-70 RAFs and specific snoRNPs, on the 47S pre-rRNA, to form the earliest 90S processome **(Fig. I-16)** (Kornprobst et al., 2016).

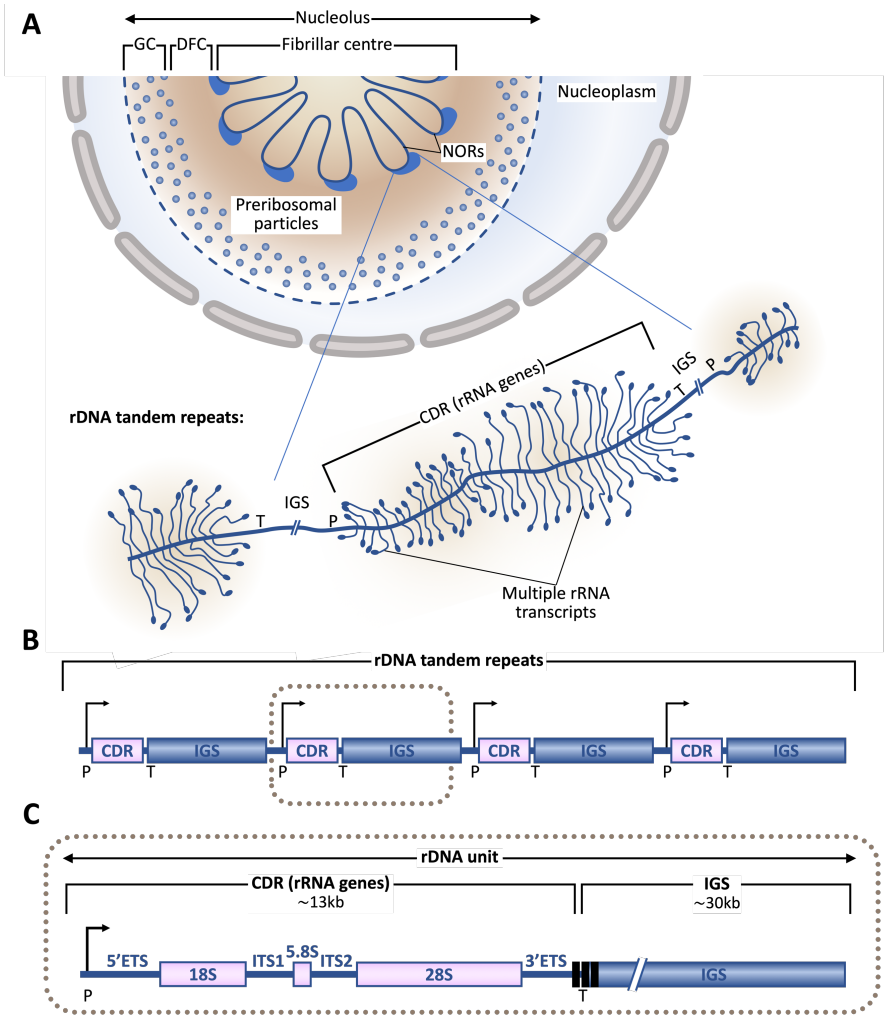


**Figure I-17. Organization of the rDNA genes. A.** Nucleolar localization and structure of the nucleolar organizer regions (NORs) containing arrays of the rDNA genes. Electron microscopy allows the visualization of the typical Christmas tree spread or "Miller" chromatin spread, showing the path of the gene with progressively longer nascent pre-rRNAs attached to the multiple RNA Pol I complexes while they move along the rDNA gene. **B.** Each rDNA repeat, oriented as head-to-tail tandem repeats in our representation, contains a rRNA coding region (CDR) and a non-transcribed intergenic spacer (IGS) region. **C.** The CDR region contains the sequences of the 18S, 5.8S and 28S rRNAs separated by two internal transcribed spacer (ITS) sequences, ITS1 and ITS2, and flanked by two external transcribed spacer (ETS) sequences, 5'ETS and 3'ETS. The IGS contains regulatory elements such as promoters (P), enhancers and terminators (T). *Abbreviations:* GC, granular component; DFC, dense fibrillar component. Adapted from https://www.mechanobio.info *(Accessed on 24-07-2019)*.

Within the 90S processome the pre-rRNA is folded and rapidly cleaved at both flanking regions, 5'ETS and 3'ETS, generating the first 45S pre-rRNA intermediate **(Fig. I-18)**. Then RiBi follows two pathways, a major pathway, in which the 45S pre-rRNA intermediate is first cleaved within ITS1 separating the early 40S and 60S precursor ribosomal particles, and a minor pathway, in which the 5'ETS is removed first and then ITS1 is cleaved producing early 40S precursor particles as first RPSs and RAFs assemble (reviewed in Cerezo et al., 2019). Then, the 40S precursor particle undergoes further endo- and exonucleolytic cleavage and association and dissociation of RAFs as it migrates towards the cytoplasm. Once at the cytoplasm, cleavage by NOB1, an endonuclease previously incorporated in the nucleoplasm, generates the mature 18S rRNA (reviewed in Cerezo et al., 2019). Maturation of the 60S subunit is more complex and the process is less understood, although recent studies in yeast are shedding light into the 60S biogenesis pathway (reviewed in Klinge and Woolford, 2019). In brief, after the ITS1 cleavage, early RPLs and RAFs are assembled with the 32.5S pre-rRNA, precursor of the 5.8S and 28S rRNAs, into the earliest 60S precursor particle. Maturation of the 60S particle requires further cleavage within the ITS2 to generate the 12S and 28S rRNA intermediates. These intermediates are gradually trimmed by the action of several exoribonucleases at the nucleoplasm (Klinge and Woolford, 2019). Finally, maturation of the 5.8S takes place in the cytoplasm, where its 3' end is processed generating either the short or long 5.8S rRNA ($5.8S_{S/L}$), which are the two distinct forms of the mature 5.8S rRNA, which only differ by a 7 or 8 nt extension at their 5' end (Lafontaine, 2015).

The transcription of the 18S, 5.8S and 28S rRNAs is particularly important, as it is one of the rate-limiting steps during RiBi, and the cellular abundance of ribosomes depends on the availability or rRNA (Moss and Stefanovsky, 2002). Many signaling pathways involved in cell growth and cell cycle progression, control the level of rDNA transcription through the direct or indirect activation of RNA Pol I, increasing the rate of transcription of each active rDNA gene (Russell and Zomerdijk, 2005) or by increasing the number of rDNA genes actively engaged in transcription through epigenetic mechanisms (reviewed in McStay and Grummt, 2008).

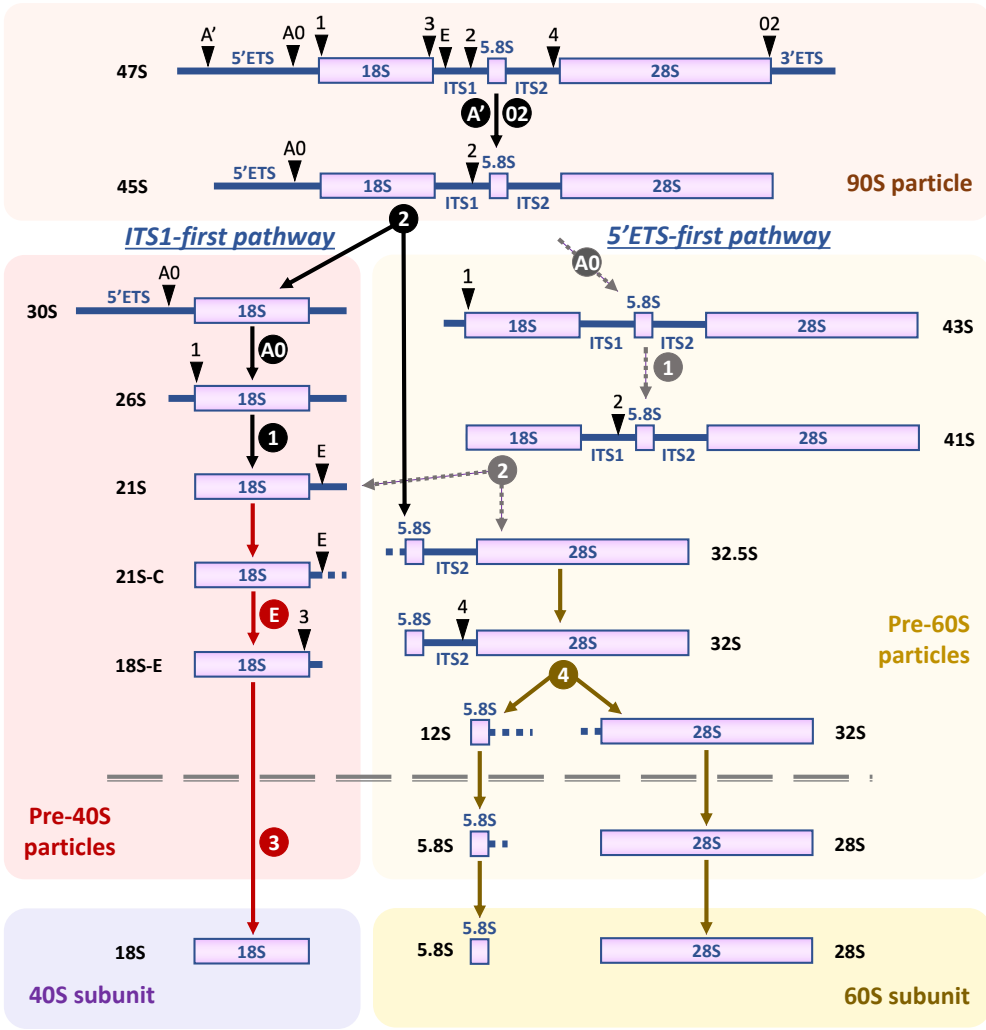


**Figure I-18. Major pathways of 47S pre-rRNA processing in human cells.** The 18S, 28S and 5.8S rRNA are transcribed by Pol I as a long primary transcript, the 47S pre-rRNA. Removal of spacer sequences (ETS and ITS sequences) follows two pathways: a major pathway termed 'ITS1-first pathway' (black arrows) and a minor pathway termed '5'ETS-first pathway' (grey dashed arrows), in reference to the spacer sequence which is removed first. Both pathways converge at a certain step of the maturation of the 40S (red arrows) and 60S (gold arrows) pre-ribosomal particles (pre-40S and pre-60S, respectively). Processing of the distinct rRNA intermediates is mediated by exo- and endoribonucleases (not shown). Steps mediated by exonucleases are displayed by the dashed ends of the rRNA intermediates. Steps mediated by endonucleases are those indicated by numbers, which also refer to the site at which the precursor is cleaved. The intermediate pre-rRNA generated are also annotated. Grey dashed bar represents the limit between the nucleus (above) and the cytoplasm (below) indicating that the last steps of processing take place at the cytoplasm.

### 3.2.2. The 5S rRNA

The 5S rRNA is encoded by ~two hundred gene copies clustered in tandem, exclusively distributed across Chr 1 (Stults et al., 2008, Gibbons et al., 2015), and, unlike rDNA genes, transcription of 5S rDNA genes is mediated by RNA Pol III in the nucleoplasm, in close proximity to the NORs (Ciganda and Williams, 2011, Fedoriw et al., 2012). Transcription of the 5S rRNA by RNA Pol III, which also mediates transcription of tRNAs and of several snoRNAs (Lafontaine, 2015), requires the recruitment and association of specific RNA Pol III cofactors TFIIIA, TFIIIB and TFIIIC (Kassavetis et al., 1990). TFIIIA is a key factor for transcription initiation but it also binds and stabilizes the emergent 5S rRNA product leading to the formation of a ribonucleic protein particle (RNP), known as the 7S RNP (Szymanski et al., 2003). This particle contains the precursor 5S rRNA which harbors a nucleotide extension (of 2-3 nt) at its 3' end. Maturation of the 5S rRNA requires the action of the exonuclease Rexo5 in *Drosophila*, which cleaves these 2-3 nt at the 5S rRNA 3' end (Gerstberger et al., 2017), but the exonuclease responsible for this function in human is not yet known. However, Rexo5 is evolutionary conserved, so that human REXO5 is likely to mediate 5S rRNA maturation in human cells. Interestingly, this exonuclease has prominent nucleolar localization (Gerstberger et al., 2017, Silva et al., 2017), suggesting that 5S rRNA maturation would take place in the nucleolus. In addition, the RPL5 (Sloan et al., 2013), an essential constituent of the 60S ribosomal subunit, seems to participate in the maturation of the 5S rRNA. In the *Xenopus oocyte* system, the 5S rRNA is exported into the cytoplasm as the 7S RNP where it can be stored either with TFIIIa or in complex with RPL5 (reviewed in Ciganda and Williams, 2011). However, this nucleocytoplasmic transport of the 5S rRNA seems to be specific for this system and the 5S rRNA export may not occur in somatic cells. Indeed, it has been recently shown that RPL5 binds the 5S rRNA at the nucleus (Kressler et al., 2012), and presumably at the nucleolus this 5S rRNA/RPL5 complex binds RPL11, another component of the 60S subunit (Sasaki et al., 2011), constituting the 5S rRNA/RPL5/RPL11 RNP or 5S RNP, which is then incorporated very early into the 90S processome **(Fig. I-16)** (Calvino et al., 2015). Recruitment of the 5S RNP on to the 90S processome is mediated by the RAFs BXDC1 and RRS1 (Donati et al., 2013, Sloan et al., 2013), the human orthologs of the yeasts Rpf2 and Rrs1 (Zhang et al., 2007). In addition another RAF, PICT1, which normally retains RPL11 in the nucleolus (Sasaki

et al., 2011), is also essential for the assembly of the 5S RNP into the nascent ribosomes (Sloan et al., 2013). Notably, ~40% of total 5S rRNA within mammalian cells is contained as a pool of free nucleoplasmic 5S rRNA/RPL5 suggesting a slow recruitment of the newly synthesized 5S rRNA into the ribosome (Sloan et al., 2013). Importantly, these ribosomal components, complexed as the 5S rRNA/RPL5/RPL11 RNP, have a critical role in RiBi regulation, constituting a regulatory checkpoint to ensure the fidelity of the RiBi process (Donati et al., 2013, Sloan et al., 2013), as it will be deciphered later **Section 3.4.1.**.

### 3.2.3. Ribosomal proteins and ribosomal-associated factors

Finally, RP-encoding genes are distributed on Chr X and Y, and in 20 of the 22 autosomes (Uechi et al., 2001). Like the 5S rRNA, RP mRNAs are transcribed in the nucleoplasm by Pol II, but they are exported into the cytoplasm, translated into RPs, co- and post-translationally folded (Pillet et al., 2017), and then re-imported into the nucleus. Nucleolar import is mediated by importins of the β-karyopherin family, such as importin β, transportin, Ran binding protein (RanBP)5 and RanBP7, or importin 7 (IPO7) (Jakel and Gorlich, 1998, Chook and Suel, 2011, Golomb et al., 2012), and its association to GTPases is required to drive the transport of the RPs across the nuclear pore complex (NPC) (Bange et al., 2013). Translocation of RPs into the nucleus occurs immediately after their synthesis, as RPs have a very short half-life in the cytoplasm, of only 2-3 min (Golomb et al., 2012). Once translocated, they shuttle between the nucleus and nucleolus (Warner et al., 1985) and bind to the distinct rRNA intermediates, participating in their processing while they assemble together into small or large pre-ribosomal particles as they migrate through the nucleoplasm (Kressler et al., 2010). Interestingly, RPs are synthesized in excess and only ~30% are incorporated into nascent ribosomes, while RPs not assembled into nascent ribosomal particles are rapidly degraded through the UPS in the nucleus (Lam et al., 2007, Badertscher et al., 2015). Indeed, the half-life of RPs as free nuclear proteins is of ~6 hr, but increases as much as 5-fold when incorporated into mature ribosomes, in which they possess half-lives of >30 hr (Boisvert et al., 2012). This excess can be explained given that in higher eukaryotes, unlike yeast, synthesis of RPs is independent from rRNA synthesis (Warner, 1977, Pierandrei-Amaldi et al., 1985, Granneman and Tollervey, 2007) and their production

is controlled at the post-transcriptional, translational and post-translational levels by mTOR under growing conditions (Gentilella et al., 2017). mTORC1 promotes translation of RPs through a specific motif located at the TSS of RPs mRNAs, the **5'TOP sequence**, a short motif which is also present in other components of the translational machinery such as eEFs (Gentilella and Thomas, 2012). Selective regulation of these 5'TOP mRNAs by mTORC1 involves the phosphorylation of 4EBPs and the subsequent release of eIF4E (Hsieh et al., 2012, Thoreen et al., 2012). The translational selectivity of mTOR for 5'TOP mRNAs challenges the classical view in which only long and highly structured 5'UTR-containing mRNAs are mTOR sensitive **(Section 1.1.3.)**. In support for the selective regulation of 5'TOP mRNAs by mTOR, it has been recently shown that a complex formed by the 40S ribosomal subunit together with La-related protein 1 (LARP1) controls their stability, providing a pool of stable RPs mRNAs upon unfavorable conditions (Gentilella et al., 2017). It may be that these 5'TOP mRNAs are stored and rapidly translated upon mitogen stimulation, whereas those containing long and highly structured 5'UTR must be first transcribed, such that their expression is only apparent at later times in cell cycle progression.

On the other hand, the RAFs and many snoRNAs are transcribed by Pol II. snoRNAs transcribed by Pol II are processed from pre-mRNA introns, while others can be transcribed from their own promoters by either Pol II or Pol III (Lafontaine, 2015). Then, snoRNAs are capped and modified in the nucleoplasm, and later assembled into the snoRNPs, together with the corresponding core proteins, in the nucleolus (Gerstberger et al., 2014). By contrast, the RAFs, including the snoRNP core proteins, are translated in the cytoplasm and re-imported into the nucleus or the nucleolus to associate with the emerging ribosomal particles. This association, despite transient, is necessary for many enzymatic, structural and regulatory functions. For instance, some RAFs catalyze the cleavage and removal of the ETS and ITS sequences from the pre-rRNA (endo- and exoribonucleases), its chemical modification (methyl- and acetyltransferases) or folding (helicases and chaperones). Other RAFs modify RPs (kinases, phosphatases, etc.), provide energy for the remodeling and assembly of the pre-ribosomal particles (ATPases and GTPases) or mediate the transport of the particles across the NPCs (nucleolar export factors) (Strunk and Karbstein, 2009, Kressler et al., 2010, Henras et al., 2015, Lafontaine, 2015, Aubert et al., 2018).

## 3.3. Ribosome biogenesis regulation by MYC and tumorigenesis

Considering the cooperation of several hundreds of molecules required to form competent ribosomes and the energetic expenditure (Warner, 1999, Moss and Stefanovsky, 2002), it is not surprising that RiBi subjected to an extensive regulation at multiple levels. Such regulation not only ensures the proper stoichiometry of all ribosomal components, but also the optimal production and activity of the many factors involved in the assembly of the ribosomal subunits (de la Cruz et al., 2018). Regulation of RiBi is intimately linked to signaling pathways which regulate cell growth in response to nutrients, growth factors and oncogenes, such as MYC (van Riggelen et al., 2010, Campbell and White, 2014).

### 3.3.1. MYC drives ribosome biogenesis and protein synthesis

Regulation of RiBi by MYC is of particular interest since its dysregulation and overexpression is a driver in many human cancers **(see Chapter 1, Section 1.4.)**. Its high oncogenic potential in sustaining tumor initiation and progression is attributed to its ability to upregulate RiBi (van Riggelen et al., 2010, Dang, 2012). Under physiological conditions, MYC controls RiBi by upregulating the transcription of rRNAs, both 47S pre-rRNA and 5S rRNA, and by regulating the expression of RPs and RAFs. In addition, MYC also regulates the expression of eIFs, thus promoting translation **(Fig. I-19)**. Genes involved in RNA processing, RiBi and cell growth have been identified as containing the primordial MYC core signature among MYC target genes (Ji et al., 2011), consistent with a major role for MYC in biomass accumulation. Indeed, MYC is able both promote RiBi and protein synthesis by stimulating the activity of the three RNA Pol (reviewed in van Riggelen et al., 2010, Campbell and White, 2014, Poortinga et al., 2015).

First, MYC increases the transcription of the 47S rDNA genes through three major mechanisms: (1) by promoting RNA Pol II-mediated transcription of Pol I machinery, both the subunit constituents and the associated cofactors (UBF, TIF-IA, etc.), as a heterodimer with MAX (Poortinga et al., 2004, Poortinga et al., 2011). Interestingly, upregulation of UBF promotes Pol I transcription by both regulating the epigenetic status of the rDNA chromatin to render rDNA genes transcriptionally active, and

through the recruitment of competent Pol I to the rDNA promoter elements, in association with SL1 (Poortinga et al., 2015). MYC also increases Pol I transcription (**2**) by directly binding E-boxes within rDNA promoter regions, which favors the direct interaction of Pol I with its specific cofactors, such as UBF and SL1, and improves chromatin accessibility through the recruitment of HATs and their coactivators, such as TRRAP (Arabi et al., 2005, Grandori et al., 2005), and (**3**) by binding to rDNA genes downstream regions to mediate looping between the promoter and termination regions, which also stimulates Pol I transcription (Shiue et al., 2009).

In parallel MYC also promotes Pol III activity thereby increasing the abundance of 5S rRNA. In this case MYC (**1**) promotes the synthesis of Pol III components in complex with MAX and in a Pol II-dependent manner (Poortinga et al., 2011), (**2**) recruits the coactivator TRRAP and the HAT GCN5 to the 5S rDNA promoter, resulting in the acetylation of histone H3 at the 5S rDNA promoter (Kenneth et al., 2007, and (**3**) stimulates Pol III transcription by directly binding to the Pol III cofactor TFIIIB (Gomez-Roman et al., 2003). The same mechanisms drive the transcription of tRNAs and of the subset of snoRNAs transcribed by Pol III (van Riggelen et al., 2010, Campbell and White, 2014). As seen in **Chapter 1, Section 1.1.2.**, the transactivation of both rDNA genes and tRNAs by MYC is counteracted by members of the MXD family, as a heterodimer with MAX (Poortinga et al., 2004).

Finally, many RPs and RAFs are transcriptional targets of MYC (van Riggelen et al., 2010). Many RAFs involved in rRNA processing and nuclear export are upregulated by MYC (Schlosser et al., 2003) such as nucleolin (NCL) (Ginisty et al., 1998), required for the early cleavage of the 47S pre-rRNA at its 5' end, nucleophosmin (NPM1) (Maggi et al., 2008), which has a role in rRNA processing and stability, in the nuclear export of ribosomal subunits and which also promotes SL1 recruitment to the rDNA gene promoters (Bergstralh et al., 2007), nucleolar protein 56 (NOP56), a component of the C/D box snoRNPs family (Schlosser et al., 2003), and exportin 1 (XPO1), required for the export of the pre-ribosomal subunits into the cytoplasm (Golomb et al., 2012). Likewise, numerous RPs are transcriptionally upregulated by MYC. In addition, MYC also promotes the translation of RPs mRNAs through their 5'TOP tract, which is mediated by the phosphorylation of 4EBP1 in an mTORC1-dependent manner as seen in **Section 3.2.3.** (Pourdehnad et al., 2013, Gentilella et al., 2015).

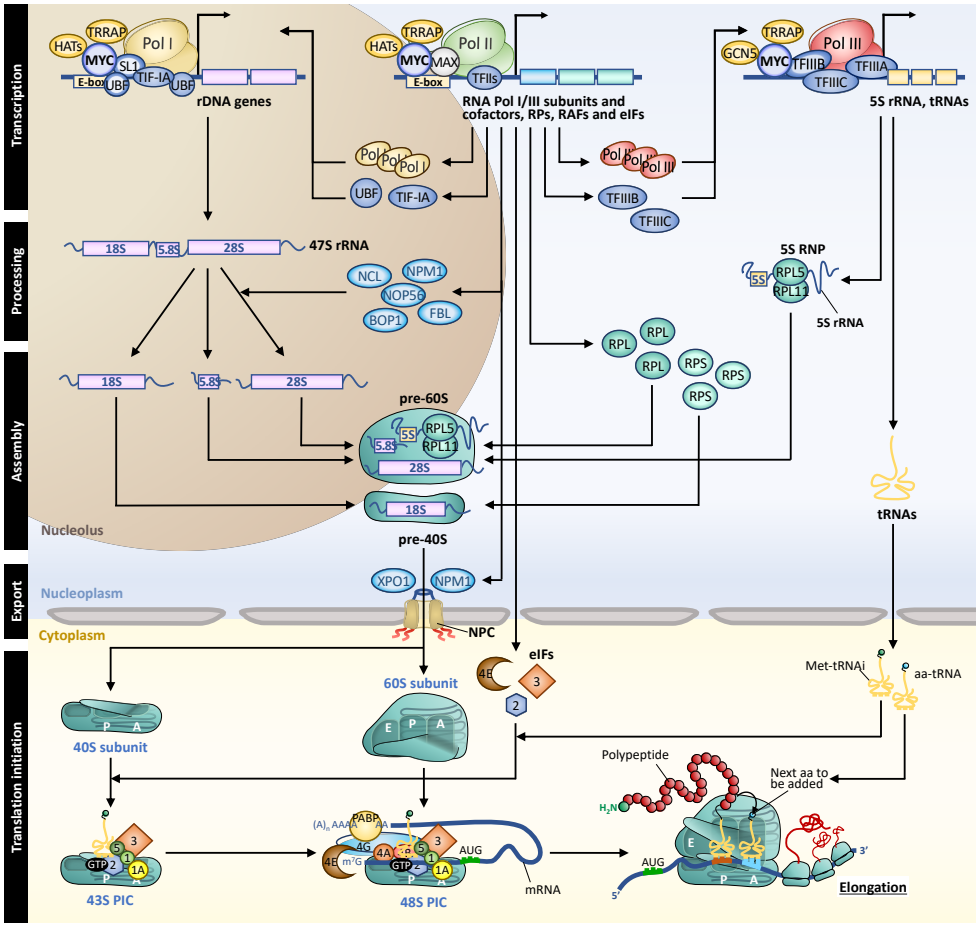


**Figure I-19. Regulation of ribosome biogenesis and mRNA translation by MYC.** MYC stimulates the activity of the three RNA Pol in part, through the recruitment of HATs (e.g. GCN5), and their coactivators (e.g. TRRAP), which acetylate histones, facilitating chromatin accessibility, and by upregulating the expression of Pol I and Pol III components via Pol II transcription. MYC also binds to E-boxes upstream rDNA genes and interacts with UBF and SL1 specific Pol I cofactors, stimulating Pol I activity. Binding of MYC downstream rDNA genes also facilitates Pol I transcription (not shown). Synthesis of 5S rRNA is also stimulated by MYC through the binding to TFIIIB. In addition, as a heterodimer with MAX, MYC upregulates the expression of RPs and of many RAFs (colored in light blue). MYC also promotes translation, not only by increasing RiBi and ribosome availability, but also by increasing the availability of other components of the translation machinery such as eIFs (via Pol II) and tRNAs (via Pol III). *Abbreviations:* HATs, histone acetyltransferases; TRRAP, transactivation/ transformation-associated protein; NCL, nucleolin; NPM1, nucleophosmin; NOP56, nucleolar protein 56; BOP1, block of proliferation protein 1; FBL, fibrillarin; PABP, polyadenylate-binding protein. See text for more details. Adapted from van Riggelen et al. (2010).

Beyond RiBi, MYC also regulates translation initiation by promoting the transcription of many translation initiation factors such as eIF4E, the α-subunit of eIF2, eIF4A and eIF4G (Rosenwald et al., 1993, Jones et al., 1996, Schmidt, 2004), and by directly promoting the methylation of the mRNA CAP structure, in cooperation with E2F1, which is required for eIF4E binding to the mRNA and for the recruitment of the 40S ribosome subunit (Cole and Cowling, 2009), as described in **Section 3.1.**.

### 3.3.2. Deregulated MYC promotes tumorigenesis due to aberrant ribosome biogenesis

Aberrant nucleolar hypertrophy, characterized by both an increase in the number and size of nucleoli, and resulting from hyper-activated rDNA transcription, has been used by pathologists as a marker of aggressive tumors since the late 19$^{th}$ century (Pianese, 1896). Indeed, increased levels of Pol I and Pol III subunits, cofactors and products, resulting in abnormally high rates of Pol I and Pol III transcription, are a feature of many cancers (White, 2008, Hannan et al., 2013). Accelerated rates of rDNA transcription in cancer do not appear to be due to 'gain of function' mutations in the Pol I and Pol III apparatus, but is a consequence of the activation of oncogenes or the loss of tumor suppressors (Bywater et al., 2013). The contribution of RiBi to tumorigenesis in the context of MYC overexpression was first studied in the E$\mu$-MYC mouse model. Tumor cells from this mouse displayed enhanced proliferation, protein synthesis and cell size (Iritani and Eisenman, 1999). Almost a decade later, Barna and co-workers demonstrated that the ability of MYC to drive hyperactive RiBi and thereby increased global protein synthesis, was determinant for MYC transforming capacity in the E$\mu$-MYC mouse model. Indeed, increased translation and aberrant protein synthesis rates were restored to normal levels when the E$\mu$-MYC mouse was crossed with the RPL24 hypomorphic mouse, a mouse model also referred as the Belly Spot and Tail (Bst) mouse (Oliver et al., 2004), in which one allele of the gene encoding a 60S subunit RPL24 is deleted (*Rpl24*$^{+/-}$) (Barna et al., 2008). In these E$\mu$-MYC *Rpl24*$^{+/-}$ mice delayed tumor onset and increased disease-free-survival were attributed to a reduction in RiBi and global protein synthesis capacity upon RPL24 haploinsufficiency (Barna et al., 2008). In addition, they demonstrated that MYC-accelerated RiBi aberrantly increased CAP-dependent translation, modulating

the translation of specific mRNAs and disrupting IRES-dependent translation, critical for accurate mitotic progression, leading to genome instability. Likewise, RPL24 haploinsufficiency was able to restore CAP-dependent translation and prevented the inhibition of IRES-dependent translation by deregulated MYC (Barna et al., 2008). Furthermore, excessive availability of competent ribosomes alters the pattern of mRNA translation, favoring translation of low affinity mRNAs, that possess long 5'UTRs with upstream open reading frames and/or stable secondary structures, many of which encode oncogenes, survival factors and cell cycle regulators critical for cancer progression (Kong and Lasko, 2012, Ruggero, 2013). The specific translation of certain mRNAs upon MYC-accelerated RiBi was corroborated by Cunnigham and co-workers, who demonstrated that overexpression of MYC increased the expression of phosphoribosyl-pyrophosphatase synthetase 2 (PRPS2), a rate-limiting enzyme involved in the synthesis of purines and pyrimidines and essential for MYC-driven tumorigenesis, whereas RPL24 haploinsufficiency restored the rate of *Prps2* mRNA translation (Cunningham et al., 2014).

Thus, aberrant RiBi driven by MYC overexpression leads not only to an increase in global protein synthesis capacity, but also alters the pattern of translation, favoring translation of low affinity mRNAs, and enhances CAP-dependent translation, all together contributing to genome instability, malignant transformation and tumor progression (Poortinga et al., 2015, Orsolic et al., 2016, Truitt and Ruggero, 2016).

## 3.4. Deregulated ribosome biogenesis and p53. The 'Impaired Ribosome Biogenesis checkpoint'.

### 3.4.1. Ribosomopathies

Conversely to the findings of Barna, who attributed E$\mu$-MYC tumor regression to a decreased global protein synthesis capacity and to the restoration of normal mRNA translation pattern, due to a restriction in nascent RiBi (Barna et al., 2008), others showed that the impairment of RiBi also leads to p53 activation. In this line, the group of Volarevic demonstrated that activation of p53 contributes to the pathogenesis of the Bst mouse model (Barkic et al., 2009). This model of RPL24 haploinsufficiency is used as a model for the human disease Diamond-Blackfan anemia (DBA) (Oliver et al., 2004), a congenital disorder caused by the depletion of a number of RPs, including RPL24, which belong to a subset of human disorders collectively termed ribosomopathies **(Table I-6)**. These disorders, most inherited, are characterized by an impaired ribosome production or function due to heterozygous mutations in RP genes or RiBi factors (Narla and Ebert, 2010). Although the distinct disorders have different clinical manifestations and display tissue-specific defects (Yelick and Trainor, 2015), in many of them, activation of p53 appears to be responsible for the aberrant phenotypes (Fumagalli and Thomas, 2011). In particular, involvement of p53 has been clearly demonstrated in the pathogenesis of the *5q-* syndrome (Pellagatti et al., 2010), a ribosomopathy caused by the sporadic monoallelic loss of a portion of the long arm of Chr 5 (del(5q)) which includes the *RPS14* and *LARP1* gene (Ebert et al., 2008, Gentilella et al., 2017), in which increased levels of p53 particularly in the erythroid progenitor cells, due to their inability to meet increased demand of ribosome during erythropoiesis, explains the severe anemia observed in patients (Dutt et al., 2011). Likewise, p53 activation cause apoptosis during facial development in Treacher Collins syndrome (TCS) (Jones et al., 2008), a ribosomopathy triggered by the mutations of several genes essential for RNA Pol I/Pol III transcription (Dauwerse et al., 2011, Bowman et al., 2012, Kadakia et al., 2014, Schaefer et al., 2014). In both pathologies, inactivation of p53 in mouse models largely rescues tissue-specific defects (Jones et al., 2008, Barlow et al., 2010b). In DBA, p53 upregulation also leads to apoptosis of the erythroid progenitors and

accumulation of nuclear p53 has been observed in bone marrow biopsies from DBA (Dutt et al., 2011), Schwachmann-Diamond syndrome (SDS) (Elghetany and Alter, 2002) and *5q-* syndrome (Pellagatti et al., 2010) patients, suggesting that p53 accumulation leads to the erythropoiesis defects characteristic of these diseases (Boultwood et al., 2012). However in DBA, the pathology and the implication of p53 is more complex, and in other diseases, such as X-linked Dyskeratosis congenita (DKC), the role of p53 is unknown or controversial (Chakraborty et al., 2011, Fumagalli and Thomas, 2011). For instance, in DKC, a ribosomopathy caused by a mutation in *DKC1* gene, encoding the nucleolar protein dyskerin involved in the pseudouridylation of rRNA (Heiss et al., 1998, Knight et al., 1999, Yoon et al., 2006), both p53 upregulation and downregulation have been observed (Gu et al., 2008, Bellodi et al., 2010). Paradoxically, these diseases are largely associated with an increased predisposition for cancer development later in life (Narla and Ebert, 2010).

**Table I-6. Ribosomopathies: implication of p53 (i)**

| Disease, prevalence | Inheritance | Alteration (frequency) | Protein function | Major clinical features | Role of p53 |
|---|---|---|---|---|---|
| **Diamond-Blackfan anemia (DBA)**<br>1:150,000 to 1:200,000 | Autosomal dominant | *RPS19 (25%)*<br>*RPL5 (7%)*<br>*RPS26 (6.6%)*<br>*RPL11 (5%)*<br>*RPL35a (3%)*<br>*RPS10 (2.5%)*<br>*RPS24 (2%)*<br>*RPS17 (1%)*<br>*RPL15 (<0.5%)*<br>*RPS28 (<0.1%)*<br>*RPS29 (<0.1%)*<br>*RPS7 (<0.1%)*<br>*RPS15 (<0.1%)*<br>*RPS27 (<0.1%)*<br>*RPL9 (<0.1%)*<br>*RPL18 (<0.1%)*<br>*RPL26 (<0.1%)*<br>*RPL27 (<0.1%)*<br>*RPL31 (<0.1%)* | 40S or 60S ribosomal components | Severe macrocytic anemia and reticulopenia<br>Growth retardation<br>Craniofacial defects<br>Thumb abnormalities<br>Cardiac tissue malformations<br>Kidney dysfunction<br>Predisposition to osteosarcoma, AML and MDS | Increased activity in erythroid precursors.<br>Suppression leads to phenotypic rescue in some DBA-models. |
| | X-linked recessive | *TSR2 (<0.1%)* | RPS26-dedicated chaperone | | |
| | | *GATA1 (<0.1%)* | Hematopoietic transcription factor | | |
| ***5q-* syndrome**<br>10-15% of patients with MDS or AML | Sporadic (Acquired) | *RPS14* (100%) | 40S ribosomal component | Severe macrocytic anemia<br>Hypolobulated megakaryocytes<br>Predisposition to AML | Increased activity<br>Suppression rescues normal phenotype in mouse model |
| | | *LARP1* (100%) | Stabilizes 5'TOP mRNAs | | |

(See next page)

**Table I-6. Ribosomopathies: implication of p53 (ii)**

| Disease, prevalence | Inheritance | Alteration (frequency) | Protein function | Major clinical features | Role of p53 |
|---|---|---|---|---|---|
| **Treacher Collins syndrome (TCS**)<br>1:10,000 or 1:50,000 | Autosomal dominant/ recessive | *TCOF1 (~90%)* | Treacle, nucleolar protein essential for Pol I transcription. Pol I/III components | Severe craniofacial defects<br>Mental retardation<br>Cancer predisposition not known | Upregulated p53 activity. Inhibition reverts phenotype in animal models. |
| **Schwachmann-Diamond syndrome (SDS)**<br>1:77,000 | Autosomal recessive | *SBDS (>95%)* | SDO1, involved in the maturation of the pre-60S particles at the cytoplasm | Neutropenia/ infections<br>Pancreatic insufficiency<br>Growth retardation<br>Anemia and thrombocytopenia<br>Predisposition to AML and MDS | Upregulated p53 activity |
| **X-linked dyskeratosis congenita (DKC)**<br>1:1,000,000 | X-linked recessive | *DKC1 (100%)* | Dyskerin, nucleolar protein involved in rRNA pseudoury-dilation | Cytopenia in the bone marrow<br>Skin hyper-pigmentation<br>Nail dystrophy<br>Oral leukoplakia<br>Predisposition to leukemia, solid tumors and pulmonary fibrosis | Controversial. Up/downregulated activity observed in mouse models and patients. Reduced p53 translation related to cancer. |
| **Cartilage-hair hypoplasia (CHH)**<br>1:1000 (Amish)†<br>1:23,000 (Finish)† | Autosomal recessive | *RMRP (100%)* | Component of RNase MRP complex, cleaves 47S pre-rRNA at early processing steps | Hypoplastic macrocytic anemia<br>Short limb dwarfism<br>Hypoplastic hair<br>Skeletal dysplasia<br>Predisposition to NHL and basal cell carcinoma (incidence increased 7-fold) | Not known |
| **Bowen-Conradi syndrome (BCS)**<br>1:355 (Hutterite)† | Autosomal recessive | *EMG1 (100%)* | Methylates a pseudouridine in the 90S particle | Microcephaly<br>Growth retardation<br>Psychomotor delay | Not known |
| **North American Indian childhood cirrhosis**<br>1:250 (Ojibway-Cree First Nations)† | Autosomal recessive | *CIRH1A (100%)* | UTP14,90S processome component involved in rRNA maturation | Cirrhosis (Liver disfunction) | Not known |

Prevalence is displayed per live births except if ethnicity indicated (†). Percentages indicate the frequency for each mutation. *, indicates the combined frequency for *POLR1D* and *POLR1C* mutations. Adapted from Fumagalli and Thomas (2011) and Aubert et al. (2018).

### 3.4.2. Defective ribosome biogenesis is monitored by the IRBC complex.

The first evidences of p53 stabilization following RiBi impairment were found more than a decade ago by using inhibitors of RNA synthesis such as ActD (Rubbi and Milner, 2003, Olson, 2004, Boisvert et al., 2007, Boulon et al., 2010). Given that these inhibitors cause nucleolar disruption, it was initially thought that perturbation of RiBi was sensed by the nucleolus as a stress signal that led to nucleolar disruption and to the passive diffusion of several RPs into the nucleoplasm, where they bound and inhibited MDM2, the E3 ubiquitin ligase of p53, leading to p53 stabilization (Zhang and Lu, 2009, Lindström and Latonen, 2013). A growing list of RPs were reported to bind and inhibit MDM2 and thus, to trigger p53 activation (Lohrum et al., 2003, Zhang et al., 2003, Dai and Lu, 2004, Dai et al., 2004, Jin et al., 2004, Dai et al., 2006, Chen et al., 2007, Yadavilli et al., 2009, Zhu et al., 2009, Zhang et al., 2010, Xiong et al., 2011, Daftuar et al., 2013, Zhou et al., 2013, He et al., 2016). However, our group first showed that the depletion of an essential RP of either subunit, which abrogates the biogenesis of either the 40S or 60S ribosomal subunits, led to p53 induction and cell cycle arrest without inducing nucleolar disruption (Fumagalli et al., 2009). Moreover, the induction of p53 was blocked by depletion of either RPL5 or RPL11, but not the other RPs proposed (Fumagalli et al., 2012). These observations argued that activation of p53 checkpoint was a regulated, rather than a passive, event (Fumagalli et al., 2009, Fumagalli et al., 2012). In contrast to the findings of our laboratory, many of the previous studies implicating other RPs in inhibiting MDM2 and in triggering p53 stabilization, used a distinct experimental paradigm. The implicated RP had been identified by either yeast two-hybrid screening or mass spectroscopy of MDM2 interacting proteins. To ascertain the functional importance of each candidate RP, they carried out loss- or gain-of-function studies. In the loss-of-function paradigm, rather than simply depleting the RP and looking at the effect on p53 stabilization, the authors treated control cells or cells depleted of the suspected RP with ActD to induce p53 after the candidate RP was depleted by RNAi. They found that the p53 response in cells depleted of the suspected RP was diminished as compared to control cells. However, they ignored that depletion of an essential RP over a period of time leads to a decrease in the number of ribosomes per cell and translation capacity, thus leading to lower levels of inducible p53. In the gain-of-function paradigm, they found that overexpression of the suspected RP led

to the induction of p53, but it was not considered that RPs are all highly basic proteins, which could artificially interact with the central acidic domain of MDM2 (Bursac et al., 2014). These two observations led to series of experiments showing that only RPL5 and RPL11 cooperatively mediate MDM2 inhibition and p53 stabilization, following RiBi impairment caused by the depletion of an essential RP (Fumagalli et al., 2012 Bursac et al., 2012). In further support of these findings, studies by Bursac and co-workers demonstrated that RPL5 and RPL11 are mutually protected from degradation following RiBi disruption with low-doses of ActD (Bursac et al., 2012), which specifically blocks Pol I transcription (Perry and Kelley, 1970). Therefore, the results together corroborated the existence of a regulated p53-dependent checkpoint in response to RiBi impairment, which was cooperatively mediated by RPL5 and RPL11, but not by the other proposed RPs, and independently of nucleolar disruption (Fumagalli et al., 2009, Bursac et al., 2012, Fumagalli et al., 2012).

Earlier studies searching for MDM2 interacting proteins by mass spectroscopy identified RPL5 and suggested the potential involvement of the 5S rRNA (Marechal et al., 1994), which, as explained previously in **Section 3.2.2.**, forms a pre-ribosomal complex with RPL5 and RPL11, the 5S RNP, which is incorporated into the 90S processome. Following the findings of Fumagalli, our laboratory subsequently demonstrated the implication of the 5S rRNA in mediating p53 stabilization. We demonstrated that RPL5, RPL11 and the 5S rRNA are mutually dependent on one another for inhibiting MDM2, since depletion of any of the three is sufficient to reverse the effects on RiBi impairment (Donati et al., 2013). Importantly, it was found that the depletion either RRS1 or BDXC1, the human orthologs of the yeast cofactors Rrs1 and Rpf2, respectively, involved in the assembly of the pre-ribosomal 5S rRNA/RPL5/RPL11 particle into the nascent 60S subunit, also induced p53 stabilization and that the response was reversed by co-depletion of either RPL5, RPL11 or 5S rRNA (Donati et al., 2013). These studies argued that the nascent pre-ribosomal 5S rRNA/RPL5/RPL11 particle was directed to the inhibition of MDM2 prior to its assembly into the 90S processome (Donati et al., 2013). Likewise, treatment with the mTOR inhibitor Rapamycin, which blocks 5'TOP translation and thus, the formation of the nascent pre-ribosomal 5S rRNA/RPL5/RPL11 particle **(see Section 3.2.3.)**, abrogates the induction of p53 by ActD, supporting its role of the nascent

pre-ribosomal complex in inhibiting MDM2 (Bursac et al., 2012). In support with this finding, the parallel study developed by Sloan et al. demonstrated that the reduction of nascent 5S rRNA levels, through the knock-down of the Pol III cofactor TFIIIA , rescued p53 stabilization induced by RiBi impairment (Sloan et al., 2013). In the studies of Sloan et al., they additionally identified the human RAFs involved in the nucleolar localization and the assembly of 5S RNP into the nascent 60S ribosome, RRS1 and BXDC1, and PICT1, (Sloan et al., 2013). They also found that oncogenic-stress-induced ARF-mediated p53 activation also involves the 5S RNP, suggesting that this pre-ribosomal complex coordinates a crosstalk between the cellular responses to ribosomal and oncogenic stress (Sloan et al., 2013).

Given that (**1**) only depletion of RPL5 and RPL11, and not the other RPs, reverses p53-mediated cell cycle arrest induced by RiBi impairment (Fumagalli et al., 2012), (**2**) the mutual protection of RPL11 and RPL5 from proteasomal degradation upon altered RiBi (Bursac et al., 2012) (**3**) previous studies in yeast demonstrating that RPL11 and RPL5 formed a pre-ribosomal complex with the 5S rRNA prior to the incorporation into the 90S processome (Zhang et al., 2007), (**4**) the latter identification of the 5S rRNA in mediating the inhibitory effect on MDM2 together with RPL11 and RPL5 in an inter-dependent manner and prior to the incorporation of the complex into the 90S processome (Donati et al., 2013, Sloan et al., 2013), and (**5**) that overexpression of MDM2 is not sufficient to induce the formation of this complex so that it is actively elicited upon RiBi impairment, led us to the define this response as the **'Impaired Ribosome Biogenesis Checkpoint' (IRBC)** (Gentilella et al., 2017).

As displayed in **Figure I-20**, many genetic and pharmacological stresses, or even pathological conditions, can activate the IRBC pathway, but the mechanism sensing the lesion in RiBi and driving the transition of the pre-ribosomal RPL5/RPL11/5S rRNA particle into the IRBC complex is still unknown. However, the recent resolution of the 3D structure of a portion of the RPL11/MDM2 complex has provided some insights (Zheng et al., 2015). In this 3D reconstruction it has been shown that MDM2 binds to RPL11 in a manner that mimics the 28S rRNA binding in the 60S ribosomal subunit, suggesting that upon insults to RiBi, the RPL11 binding region of 28S rRNA drives the association of the pre-ribosomal 5S rRNA/RPL5/RPL11 complex to MDM2 away from its assembly into the 90S processome (Zheng et al., 2015).

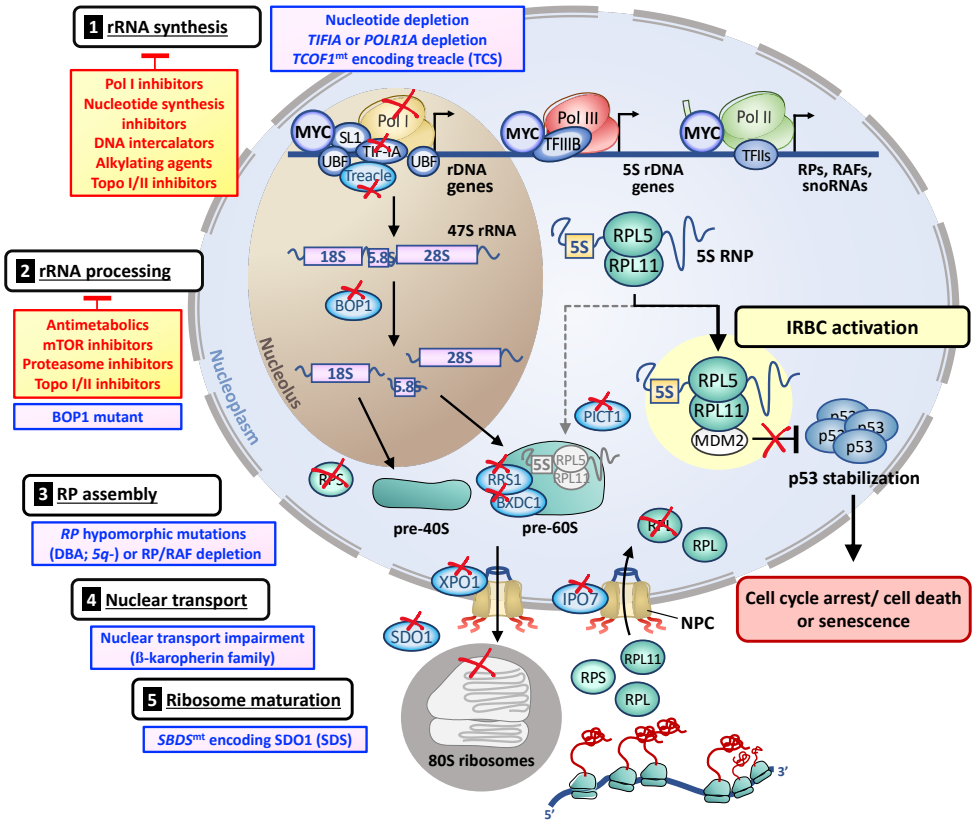


**Figure I-20. Ribosome biogenesis stress and the IRBC.** Perturbations on RiBi pathway either pharmacologically (yellow boxes), genetically or under certain pathological conditions (purple boxes) results in the redirection of the nascent pre-ribosomal 5S rRNA/RPL5/RPL11 complex (5S RNP) towards the binding and inhibition of MDM2, activating the IRBC, which leads to p53 stabilization and cell cycle arrest, cell death or senescence. RiBi can be abrogated at multiple levels: (**1**) Compounds that inhibit Pol I transcription (e.g. low-dose ActD, CX5461) or nt synthesis (e.g. MPA), Topo I/II inhibitors, and many chemotherapeutic drugs (e.g. doxorubicin, cisplatin, oxaliplatin), impair RiBi at the level of rRNA synthesis. Likewise, nt depletion or the depletion of a component or cofactor of the Pol I machinery (e.g. TIF-IA) disrupt rRNA synthesis. (**2**) Metabolic drugs (e.g. 5-FU), kinase inhibitors (e.g. rapamycin, sorafenib), proteasome inhibitors (e.g. MG132, bortezomib) or Topo I/II inhibitors, abrogate RiBi at the level of rRNA processing. Mutations in certain RAFs (e.g. BOP1, NMP1) also create a defect in the early rRNA processing. (**3**) Depletion of other RAFs (e.g. RRS1, BXDC1, PICT1) or mutations on RPs, as occur in certain ribosomopathies (see box), impair pre-40S or pre-60S ribosomal subunit assembly. (**4**) RiBi can be also abrogated due to the depletion of RAFs involved in the nuclear transport of ribosomal components (e.g. XPO1 or IPO7) or (**5**) due to mutations in RAFs (e.g. SDO1) involved in late ribosomal maturation. Details of RiBi pathway are omitted for simplifying. *Abbreviations:* MPA, mycophenolic acid; 5-FU, 5-fluorouracil; Topo, topoisomerase; POLR1A, DNA-directed RNA polymerase I subunit A.

### 3.4.3. The IRBC checkpoint as a tumor suppressor barrier against MYC-driven tumorigenesis

Importantly, recent studies suggested that the IRBC may also respond to hyperactive RiBi to prevent tumorigenesis *in vivo*, as was first demonstrated in a mouse model engineered by Macias and co- workers (Macias et al., 2010). They generated a *knock-in* mouse model expressing a mutant form of MDM2, C305F MDM2, which was first discovered in an osteosarcoma (Schlott et al., 1997). The mutation disrupts the interaction of RPL11 and RPL5 with MDM2 (Lindstrom et al., 2007) and thereby, fails to activate p53 in response to impaired RiBi induced by ActD, 5-fluoroacil (5-FU) and mycophenolic acid (MPA), but not in response to DNA damage (Macias et al., 2010). Likewise, they showed that ARF mediated inhibition of MDM2 was not affected in the mutant setting (Macias et al., 2010). Although retaining p53 ubiquitination and transcriptional repression activities, the C305F mutant displays impaired nuclear export, and appears to trap p53 in the nucleus, preventing its degradation (Lindstrom et al., 2007). Likewise, when these *Mdm2*$^{C305F/C035F}$ mice, with attenuated p53 degradation, were crossed with the E$\mu$-MYC mice, lymphomagenesis was greatly accelerated compared to that of E$\mu$-MYC mice harboring the wt *Mdm2* allele (Macias et al., 2010). Contrary to the findings of Barna and co-workers, who attributed tumor suppression to the decrease in global synthesis capacity (Barna et al., 2008), Macias studies provide strong evidence for a role of the IRBC checkpoint in safeguarding against MYC-induced tumorigenesis and supports a model in which the IRBC-MDM2-p53 and the ARF-MDM2-p53 pathways act in an independent, but parallel manner to protect against MYC-induced tumorigenesis (Macias et al., 2010). A crosstalk between both pathways was later demonstrated by the studies of Sloan et al., who suggested that ARF activation also induces the IRBC pathway by inhibiting RiBi (Sloan et al., 2013). Notably, *Mdm2*$^{C305F/C035F}$ mice do not present accelerated onset of tumorigenesis in other oncogenic contexts, such as inactivation of retinoblastoma or in a RAS mutant background (Pan et al., 2011), reinforcing the concept that the IRBC pathway is context-dependent and not a general response to oncogenic stress. In an opposite manner, Nishimura and co-workers recently suggested that the IRBC-MDM2-p53 pathway may prevent tumorigenesis by the induction of senescence following replicative and H-RAS/E2F1 oncogenic stress in mouse embryonic

fibroblasts (MEFs) and human BC cells, respectively (Nishimura et al., 2015). They showed that replicative stress, which delays rRNA processing, and oncogenic stress, which enhances rRNA transcription, deregulates RiBi, leading to accumulation of the 5S rRNA/RPL5/RPL11 complex in the free-ribosomal fraction, which binds and inhibits MDM2, resulting in p53 stabilization and cellular senescence (Nishimura et al., 2015). In addition, consistent with previous reports (Dai et al., 2012, Sloan et al., 2013), they showed a connection between ARF and the IRBC pathway, suggesting that under replicative stress, increased ARF expression may downregulate rRNA processing factors by inhibiting transcriptional activity of MYC, independently of p53 (Nishimura et al., 2015). Recently, the role of RPL5 and RPL11 in inhibiting MDM2 in MYC driven tumors has been extended to colorectal cancer (CRC) tumorigenesis, as C305F MDM2 mutation also accelerates tumor progression (Liu et al., 2017).

Importantly, previous studies showed that RPL5 and RPL11 were able to specifically inhibit MYC activity through several mechanisms (Dai et al., 2007, Dai et al., 2010, Liao et al., 2014). For instance, upon impairment of RiBi RPL11 binds the N-terminal transcriptional activation domain of MYC and competes for the recruitment of the transcriptional coactivator TRRAP to the promoters of MYC target genes (Dai et al., 2007, Dai et al., 2010). In addition, upon RiBi impairment both RPL5 and RPL11 regulate the expression and activity of MYC by guiding the RNA-induced silencing complex (RISC) to *MYC* mRNA, promoting its degradation (Liao et al., 2014). This negative feedback loop between MYC and the components of the IRBC was further corroborated in a separate study developed by Morgado-Palacin and co-workers, who demonstrated the upregulation of MYC target genes and an increase in MYC levels in bone marrow hematopoietic progenitor cells (HPCs) and a DBA mouse model, respectively, both harboring an inducible *Rpl11*-null allele (Morgado-Palacin et al., 2015). Furthermore, their studies reinforced the value of the IRBC as a tumor suppressor barrier, as mice harboring the inducible *Rpl11*-null allele, which recapitulated DBA pathological features, also displayed higher predisposition to cancer (Morgado-Palacin et al., 2015).

These findings support a role of the IRBC in MYC-induced tumorigenesis, not only in hematological malignancies, but also in solid tumors, which has driven an enormous interest in the development of inhibitors targeting this pathway in the tumor context **(Fig. I-21)**, as is discussed in the following section.

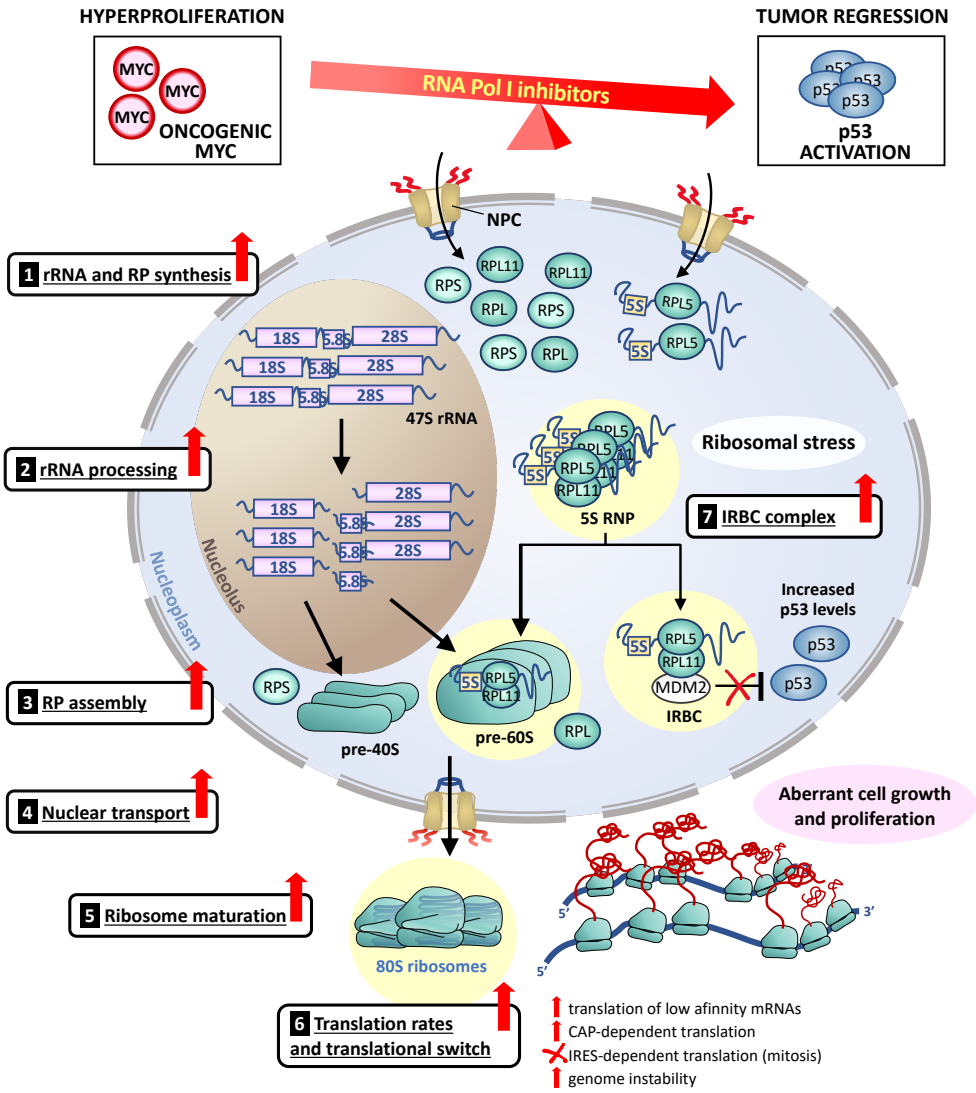


**Figure I-21. Targeting ribosome biogenesis in MYC-driven tumors.** In MYC-driven tumors oncogenic MYC (**1-5**) stimulates RiBi at every level, as shown in **Figure I-19**. (**6**) An increased availability of ribosomes, together with the induction of components of the translational machinery by MYC leads to aberrant rates of translation and promotes a switch in the translational pattern. (See next page)

**Figure I-21. (continued)** (**7**) In addition, oncogenic MYC expression actively drives the redirection of the 5S rRNA/RPL5/RPL11 RNP (5S RNP) to the binding an inhibition of MDM2, resulting in a basal activation of the IRBC and increased levels of p53 within MYC-driven tumors. Targeting RiBi, as e.g. by using Pol I inhibitors, will favor the formation of the IRBC complex and the activation of the IRBC, leading to further activation of p53 and tumor regression. See text for details.

## 3.5. Targeting ribosome biogenesis in MYC-driven cancer

Targeting RiBi pathway, in particular rRNA synthesis, the rate-limiting step in RiBi, has the potential double advantage of both inhibiting cell growth and inducing p53 **(Section 3.4.2.)**. In pursuing this goal, a number of new compounds have been developed, identified or older ones better characterized in their mode of action, with respect to suppressing RiBi (reviewed in Hannan et al., 2013, Hein et al., 2013, Quin et al., 2014, Pelletier et al., 2018).

### 3.5.1. RNA Pol I inhibitors: CX5461 and beyond

Targeting the IRBC checkpoint has brought interest in developing compounds that specifically impair the formation of the Pol I pre-initiation complex. One example is CX5461, developed by Cylene Pharmaceuticals (San Diego, CA, USA), a small molecule compound, orally available, which binds to G-quadruplex (G4) regions on DNA, higher order structures formed within G-rich regions (Duquette et al., 2004), whose function is to maintain chromatin structure in an open conformation that ensures active transcription (Wittner et al., 2011). Such structures are particularly enriched in rDNA genes, since they present a high-GC content, ~70% as compared to 42% in human genome in general (Willems et al., 1968, Galtier et al., 2001). The CX5461 demonstrates a 300-400-fold increased selectivity for inhibiting Pol I over that of Pol II and Pol III (Drygin et al., 2011). Its binding to rDNA genes prevents the binding of NCL or SL1 to the promoter of rDNA genes, thus impairing the formation of the rDNA PIC and rRNA transcription (Drygin et al., 2011, Bywater et al., 2012). Several preclinical studies have been carried out with this inhibitor for the treatment of MYC-driven tumors. For instance, the study of Bywater and co-workers showed that CX5461 rapidly induced IRBC complex formation and p53-dependent cell death of E$\mu$-MYC lymphoma B cells both *in vitro* and in the E$\mu$-MYC mouse model,

while maintaining a viable population of wt B cells of the same linage. The selectivity of CX5461 for malignant E$\mu$-MYC lymphoma B cells was attributed to the extremely high rates of RiBi in such cells (Bywater et al., 2012). Likewise, *TP53* wt human leukemia and lymphoma cell lines, also characterized by high rates of RiBi, displayed high sensitivity to CX5461 treatment, and showed p53 stabilization and apoptosis induction (Bywater et al., 2012). Given its particular potency, selectivity, and efficacy as a single agent in preclinical models of MYC-driven hematological tumors, possibly due to the addition of such tumors to RiBi (Bywater et al., 2012, Devlin et al., 2016), CX5461 is currently undergoing phase I clinical trials in patients with refractory blood cancers (ACTRN12613001061729; Harrison et al., 2015). Interestingly, the molecule also displayed promising results in a broad range of solid tumor models (Drygin et al., 2011, Rebello et al., 2016, Xu et al., 2017) and is also being tested in a phase I clinical trial in patients with advanced solid tumors (NCT02719977). Contrary to the non-genotoxic p53-dependent cytotoxic activity demonstrated in hematological malignancies, with moderate sensitivity of p53-deficient or p53-mutant cell lines (Bywater et al., 2012, Devlin et al., 2016), in solid tumors, CX5461 response seems to be independent of p53 status (Drygin et al., 2011, Rebello et al., 2016, Xu et al., 2017). Moreover, CX5461 triggers p53-independent senescence (Drygin et al., 2011) and induces cell cycle arrest in prostate tumors expressing high levels of MYC (*Hi-MYC*), but not in *PTEN*-null tumors, which display low levels of MYC, supporting the notion that MYC levels confer sensitivity to Pol I inhibitors in solid tumors (Rebello et al., 2016). In this context, even *Hi-MYC TP53* deficient tumors displayed moderate sensitivity to Pol I inhibition (Rebello et al., 2016). Consistent with these observations, recent studies have reported a p53-independent response upon Pol I inhibition (Lee et al., 2017a), with data demonstrating that Pol I inhibition triggers the activation of the DDR-mediated cell cycle arrest and subsequent apoptosis independently of p53 and suggesting that Pol I inhibition induces DNA damage (Negi and Brown, 2015). As seen in previous section, both RPL5 and RPL11 are able to inhibit MYC independently of p53 **(see Section 3.4.3.)**. Therefore, additional mechanisms may mediate cell death under conditions of oncogenic stress and when RiBi is compromised, even in the absence of p53.

A second selective RNA Pol I small molecule inhibitor, CX3543 (quarfloxin), also developed by Cylene Pharmaceuticals, and stabilizing G4 structures, has shown antitumor efficacy in a broad panel of cancer cell lines and in xenograft models of pancreatic and BC (Drygin et al., 2009). In addition, this molecule has completed phase I and II clinical trials in patients with advanced solid tumors (NCT00955786) and lymphoma, and in carcinoid and neuroendocrine malignancies (NCT00780663) respectively, providing preliminary evidences of the clinical benefit of targeting these structures. However, the compound was withdrawn from further trials due to bioavailability concerns (Balasubramanian et al., 2011). Promising results of a preclinical study published this year showed that quarfloxin, as well as CX5461, are cytotoxic in neuroblastoma cell lines expressing high levels of *MYC* or *MYCN* (Hald et al., 2019), the last also known to positively regulate the expression of genes involved RiBi and protein synthesis (Boon et al., 2001). Likewise, both compounds repressed the growth of *MYCN*-amplified neuroblastoma xenografts (Hald et al., 2019). Whereas the compounds induce p53 signaling and apoptosis in *TP53* wt neuroblastoma cell lines, *TP53* mutant cells undergo G2/M-phase cell cycle arrest but showed a less pronounced tumor growth suppression than tumors harboring *TP53* wt. Strikingly, despite effectively inducing cell cycle arrest, p53 signaling and cell death at low doses in *MYCN*-amplified neuroblastoma cell lines, they failed to induce a significant inhibition of RiBi (Hald et al., 2019). By contrast, a DNA damage response was observed (Hald et al., 2019), similarly to the previous observations by Xu et al., with both drugs causing synthetic lethality in BRCA1/2-deficient colon, breast and ovarian cancer cell lines, at doses which did not inhibit Pol I activity (Xu et al., 2017). Indeed, lethality was associated to a failure in homologous recombination and non-homologous end joining pathways in such cell lines, which are required for the DNA repair, thus indicating that both CX5461 and quarfloxin were inducing DNA damage (Xu et al., 2017). Therefore, contrary to previous reports characterizing these drugs as non-genotoxic Pol I inhibitors (Drygin et al., 2009, Drygin et al., 2011, Bywater et al., 2012), these studies demonstrated that these compounds induce replication-dependent ssDNA damage (i.e. genotoxic stress), activating the ATM/ATR signaling pathway responsible of the G2/M-phase cell cycle arrest in *TP53* mutant cells (Negi and Brown, 2015, Hald et al., 2019). Such induction of DNA-damage is likely mediated by the stabilization of G4 structures in

the genome, which impedes the progression of the DNA replication fork (Xu et al., 2017). In addition, stabilization of G4 structures in promoter regions has been shown to inhibit transcription (Balasubramanian et al., 2011, Rhodes and Lipps, 2015). Interestingly, both *MYC* and *MYCN* contain G4 motifs in their sequences, either on the *MYC* promoter (Siddiqui-Jain et al., 2002) or in a *MYCN* intronic region (Trajkovski et al., 2012), which is important for its transactivating function (Suenaga et al., 2009), thus, providing a potential mechanism of *MYC* gene targets suppression by these compounds.

Considering these findings, it will be important to determine which mechanism induced by these drugs, the IRBC or the DDR in response to G4 stabilization and genotoxic stress, is responsible for the antitumor effects. In addition, it has been suggested inhibition of rDNA synthesis might also elicit the DDR (Harding et al., 2015, van Sluis and McStay, 2015, Warmerdam et al., 2016), thus, it might be possible that the pathways converge and that both contribute to the antitumor efficacy of these drugs in a parallel manner.

### 3.5.2. Novel mode of action for classical chemotherapeutics

A second group of compounds have been identified or further characterized as Pol I inhibitors. This group includes agents that preferentially intercalate into the GC-rich regions of the rDNA genes and thus, prevent elongation of the pre-rRNA chains by Pol I (Peltonen et al., 2014). The best examples are the acridine derivatives, such as BMH-21, CID-765471, aminacrine and ethacridine, the two latter FDA-approved, as well as ActD, an antibiotic produced by the *Streptomyces* (Waksman and Woodruff, 1942), which has been widely used as an anticancer drug since its approval in 1954 and is still used for the treatment of Wilms tumors (WT), rhabdomyosarcoma (RBS) and Ewing's sarcomas (EWS) under the name of Cosmegen® (Hollstein, 1974, Jaffe et al., 1976, Malogolowkin et al., 2008).

BMH-21, identified by Peltonen and co-workers in 2010, in addition to binding GC-rich DNA regions, blocks Pol I transcription by inducing proteasome-mediated degradation of the largest Pol I subunit, RPA194 (Peltonen et al., 2014), which does not cause DNA damage but potently activates p53 (Peltonen et al., 2010). A recent

study demonstrated that BMH-21 directly impairs Pol I transcription elongation, inducing the pause of Pol I (Wei et al., 2018). A similar mechanism of action was attributed to the acridine-derivative CID-765471, characterized by Morgado-Palacin et al., who found that the compound, as well as aminacrine and ethacridine, causes the selective degradation of the RPA194 subunit of Pol I in the absence of DNA damage (Morgado-Palacin et al., 2014).

ActD is a potent inhibitor of global transcription (Bensaude, 2011), but when used at low doses, <10 nM, it preferentially binds to GC-rich DNA regions (Perry and Kelley, 1970), displaying selectivity for the rDNA genes and preventing rDNA transcription elongation (Fetherston et al., 1984). As a consequence of rRNA synthesis inhibition, ActD causes strong p53 stabilization and the disruption of nucleolar structures (Choong et al., 2009), which led to the concept of nucleolar stress or nucleolar disruption (Dai and Lu, 2004, Dai et al., 2004, Jin et al., 2004) Although it was later shown that at this range it actively induces the IRBC **(see Section 3.4.2.)**, the anti-tumor efficacy of ActD at low concentrations has not been extensively assessed *in vivo* (Merkel et al., 2012, Cortes et al., 2016), and its application in the clinic is limited due to its toxicity at high doses (Hill et al., 2014). Like many other chemotherapeutic drugs, ActD induces extensive DNA damage at high-doses (Ross and Bradley, 1981). A recent study has demonstrated that several chemotherapeutic drugs, generally considered as DNA-damaging agents, also inhibit RiBi at distinct levels (Burger et al., 2010). As shown in **Figure I-21**, some chemotherapeutic agents such as doxorubicin or ActD target rDNA transcription, others, such as camptothecin or 5-FU disrupt rRNA processing (Burger et al., 2010). Critically, in a recent study from Bruno and co-workers they unexpectedly found that certain platinum-based drugs, such as oxaliplatin and phenanthriplatin, do not do not cause DNA damage, but instead inhibit rDNA transcription, leading to p53 induction in a RPL11 dependent manner, presumably through activation of the IRBC (Bruno et al., 2017). In the case of ActD, it has been suggested that the specific inhibition of RNA Pol I by low dose ActD would not cause DNA damage, but induce p53 through the activation of the IRBC. In fact, two independent studies have shown the efficacy of low-doses of ActD in mouse models (Merkel et al., 2012, Cortes et al., 2016). In the study developed in our laboratory, it was demonstrated that ActD at low doses induces cell cycle arrest and cell death in *MYCN*-driven neuroblastoma cell lines, as well as tumor regression in

vivo in a subcutaneous neuroblastoma mouse model (Cortes et al., 2016). Importantly, high N-MYC levels, an indicator of bad prognosis, sensitizes neuroblastoma cells to ActD. Furthermore, ActD also displays efficacy in *TP53* null neuroblastoma cell lines, but to a much lesser extent (Cortes et al., 2016), which supports previous findings demonstrating ActD efficacy in both *TP53* wt, *TP53* mutant and *TP53* deficient CLL cell lines, patient derived tumors, as well as in a CLL-mouse model (Merkel et al., 2012).

From the clinics, it is known that, although treatment with ActD is often successful, patients frequently display treatment-associated toxicities, mainly related to hepatic toxicity or veno-occlusive disease (VOD) in up to 13.5% of cases (Hill et al., 2014). Both, liver toxicity, which frequently causes fever, anemia and thrombocytopenia (Davidson and Pritchard, 1998), and VOD, whilst undesirable, are usually reversible upon termination of treatment. However, VOD has been associated with some cases of patient death due to multi-organ failure (D'Antiga et al., 2001). Despite these adverse effects, as occurs for many other well-established drugs, dosing guidelines for ActD treatment in humans are founded largely on empirical experience, and are not based on the knowledge of the pharmacology of the drug, with only a few studies investigating the pharmacokinetic of ActD. Therefore, it is likely that the standard clinical doses are much higher than optimal. Regarding this concern, it would be necessary to better determine the pharmacokinetic profile of the drug, to re-evaluate the dosing guidelines in human patients and to assess lower dose therapeutic windows, with modified drug administration planning, that effectively inhibits Pol I transcription while minimizes non-specific side effects. The preclinical *in vivo* studies in the subcutaneous mouse model of neuroblastoma and in the CLL-mouse model highlight the clinical value of ActD for the treatment of a broad range of human MYC-driven malignancies, although it remains to be determined to which extent the IRBC is responsible for mediating cell cycle arrest and apoptosis in other cancer subtypes.

# RATIONALE OF THE STUDY

# Rationale of the study

Elevated MYC deregulated expression is observed in up to a 70% of human malignancies, frequently attributed to gene amplification or gene translocation (Hoffman and Liebermann, 2008, Dang, 2012). Elevated MYC protein levels are able to drive tumor initiation and progression, in cooperation with other oncogenic events, but importantly, overexpression of MYC is essential to maintain tumorigenesis and to avoid major cellular checkpoint mechanisms, globally referred to as the intrinsic TS response (Lowe et al., 2004). Indeed, partial inhibition of MYC can restore these regulatory checkpoints and promote cell cycle arrest, cell death or senescence, reverting malignant phenotype (Gabay et al., 2014). Its oncogenic potential together with the fact that it is virtually deregulated in almost all human cancers, has driven an immense interest in developing inhibitors against MYC for the treatment of cancer. However, MYC has traditionally been considered as an 'undruggable' target and inhibitors have remained elusive for many years (Dang et al., 2017). MYC is difficult to target given its predominant nuclear location, as the effective delivery of drugs into the nucleus is still challenging, its physiological function in normal cells, essential for tissue homeostasis, and importantly, because of the lack of a well-defined ligand-binding pocket, which could be traditionally targeted by small molecules inhibitors.

Therefore, an alternative strategy in the field is to target MYC cofactors and/or downstream effectors that play critical roles in tumor development or maintenance. In this regard, among the many cellular functions that MYC regulates, including cell growth, cell proliferation, differentiation, adhesion, metabolism, angiogenesis, metastatic dormancy and apoptosis (reviewed in Meyer et al., 2006, Hoffman and Liebermann, 2008, Meyer and Penn, 2008, Dang, 2012, Dang, 2013, McMahon, 2014), it appears that its role in controlling cell growth and proliferation, which is largely dictated by the availability of ribosomes (Poortinga et al., 2015), is critical for initiating and sustaining tumorigenesis and may serve as a potential drug target (van Riggelen et al., 2010, Dang, 2012). MYC is a master regulator of RiBi and protein synthesis (van Riggelen et al., 2010), enhancing the activity of the three RNA Pols, required for the synthesis of all the ribosomal components and RAFs (Gomez-Roman

et al., 2003, Campbell and White, 2014), promoting the stability and translation of ribosomal components mRNAs (Ji et al., 2011, Gentilella et al., 2015), as well as upregulating the expression of many RAFs involved in rRNA processing, ribosome assembly (Schlosser et al., 2003, Herter et al., 2015), nuclear export (Golomb et al., 2012), and translational initiation (Schmidt, 2004). Indeed, although MYC is a pleiotropic transcription factor, that regulates the transcription of at least 15% of the entire genome (Fernandez et al., 2003), genes involved in cell growth such as those involved in rRNA processing, RiBi and translation, form the most representative MYC transcriptional core signature (Ji et al., 2011, Sabo et al., 2014), suggesting that MYC relies on RiBi and protein synthesis to drive malignant transformation. In fact, this was demonstrated more than a decade ago in the studies of Barna et al. (2008), and since then, targeting RiBi, and in particular Pol I transcription, has arisen as a promising therapeutic strategy to treat MYC-driven tumors. The first evidence of the potential therapeutic benefit of pharmacological RiBi inhibitors was observed in the E$\mu$-MYC mouse model **(see Section 3.5.1.)** demonstrating that disruption of RiBi selectively kills E$\mu$-MYC lymphoma cells (Bywater et al., 2012). However, the molecular mechanism underlying this response is not yet clear and while initially it was argued that suppression of tumor growth was solely attributed to a global decrease in translation capacity (Barna et al., 2008), our laboratory and others, have shown that in response to RiBi impairment a p53-dependent tumor suppressor response is activated by a pre-ribosomal complex comprised of 5S rRNA/RPL5/RPL11 (Donati et al., 2013, Sloan et al., 2013). Upon distinct insults to RiBi, this complex, that we have recently termed the IRBC complex (Gentilella et al., 2017), is re-directed from the assembly into nascent 60S ribosomes to the binding and inhibition of MDM2, resulting in p53 stabilization and depending on the cellular context (Lowe et al., 2004, Pelletier et al., 2018) to cell cycle arrest (Macias et al., 2010), apoptosis (Bywater et al., 2012) or senescence (Nishimura et al., 2015). The first evidence that activation of this checkpoint could suppress tumor growth was provided by Macias et al., who generated a *knock-in* mouse model expressing a mutant form of MDM2 (*Mdm2*$^{C305F}$), which is unable to interact with RPL11 or RPL5. This MDM2 mutant fails to activate p53 in response to impaired RiBi, but not in response to the ARF mediated inhibition of MDM2, which is also activated upon MYC oncogenic stress (Macias et al., 2010). When the *Mdm2*$^{C305F}$ mice were crossed with E$\mu$-MYC mice,

lymphomagenesis was greatly accelerated compared to E$\mu$-MYC mice (Macias et al., 2010). In a following study from Bywater and co-workers, using the Pol I inhibitor CX5461, they demonstrated the role of the IRBC in mediating p53-dependent cell death and tumor regression in the E$\mu$-MYC lymphoma model upon RiBi impairment (Bywater et al., 2012). Interestingly, an antiapoptotic BCL2 family member, MCL1 (reviewed in Thomas et al., 2010), has been shown to be essential in the initiation, progression and maintenance of these tumors (Kelly et al., 2014). These studies carried out at A. Strasser's laboratory demonstrate that MCL1, but not other antiapoptotic BCL2 family member, is critical for sustaining E$\mu$-MYC-driven lymphomagenesis and its deletion promotes E$\mu$-MYC lymphoma regression (Kelly et al., 2014, Grabow et al., 2016). However, the role of MCL1 has never been clearly studied in the context of RiBi impairment but a potential linked between them has been suggested in a recent study (Merkel et al., 2012), showing that ActD, a potent inhibitor of transcription that binds to DNA and blocks RNA polymerases elongation, promotes the degradation of MCL1 in CLL cell lines when used at a nanomolar range, without affecting its mRNA levels. Despite that RiBi has not been addressed in this study, ActD preferentially binds to the GC-rich rDNA genes under such concentrations (Perry and Kelley, 1970, Fetherston et al., 1984), specifically inhibiting Pol I transcription and thereby inducing the IRBC (Bursac et al., 2012, Donati et al., 2013, Sloan et al., 2013), suggesting a potential link between RiBi impairment, p53 and MCL1 degradation.

Therefore, we set out to elucidate the unsolved paradigm concerning the role of the IRBC versus that of global translation inhibition following impaired RiBi in cells derived from E$\mu$-MYC B cell lymphomas and to decipher the downstream mechanism promoting tumor suppression, in the context of E$\mu$-MYC-driven lymphomagenesis.

# OBJECTIVES

# Objectives

The main goal of this Thesis is to determine the contribution of the IRBC and the underlying mechanism mediating tumor suppression in E$\mu$-MYC-driven B-cell lymphoma cell lines and to translate these results into a preclinical model.

To this end, we established the following specific objectives:

1. **To decipher whether the impact of RiBi impairment in E$\mu$-MYC lymphoma-cells growth is attributed to the activation of the IRBC checkpoint and/or to the decrease in translation capacity. To determine if these findings could be recapitulated pharmacologically by using ActD at nanomolar concentrations.**

2. **To decipher the molecular mechanism driving IRBC-dependent apoptosis in MYC-driven tumors. To identify the mechanism of degradation of antiapoptotic MCL1 isoform and its implication in ActD-mediated apoptosis.**

3. **To determine the antitumoral efficacy of low doses ActD through IRBC-mediated p53 stabilization and MCL1 degradation in the E$\mu$-MYC lymphoma *in vivo* model.**

# RESULTS

# Results

## 1. Depletion of RPL7a or RPL11 in E$\mu$-MYC lymphoma cells reduces nascent ribosome biogenesis and global protein synthesis to a similar extent

We first set out to determine in E$\mu$-MYC lymphoma cells if impairing RiBi led to the induction of the IRBC and p53 stabilization as previously demonstrated (Bywater et al., 2012, Donati et al., 2013). To address this question, we used an inducible tetracycline (Tet)-regulated miR30-shRNA system (Zuber et al., 2011) to stably deplete either RPL7a or RPL11, both essential RPs of the 60S ribosomal subunit, but the latter also a component of the IRBC complex (Donati et al., 2013). To induce shRNA expression, cells were treated for 22 hr with doxycycline (dox), resulting in the depletion of either RP mRNA levels to approximately 50% **(Fig. R-1A)**, similar to those predicted for the hypomorphic RPL24 mutation of the Bst mouse, *Rpl24*$^{Bst/+}$ mouse model (Barna et al., 2008, Barkic et al., 2009). In both cases, depletion of either *Rpl7a* or *Rpl11* mRNAs led to a selective decrease in native 60S ribosomes **(Fig. R-1B)** and nascent 28S rRNA biosynthesis, as measured on polysome profiles **(see Materials and Methods)** or by $^{3}$H-uridine pulse labeling of newly transcribed rRNAs, respectively **(Fig. R-1C)**. Consistent with the decrease in 60S ribosome subunit production, depletion of either RP led to a similar reduction in global protein synthesis, of approximately 35%, as measured by the incorporation of $^{3}$H-leucine into nascent protein **(Fig. R-2A)**, which was associated with a similar 50% reduction in cell proliferation in both RP-depleted cell lines, as compared to that of Ren control cells **(Fig. R-2B)**. Thus, the depletion of RPL7a or RPL11 display a similar apparent biological phenotype.

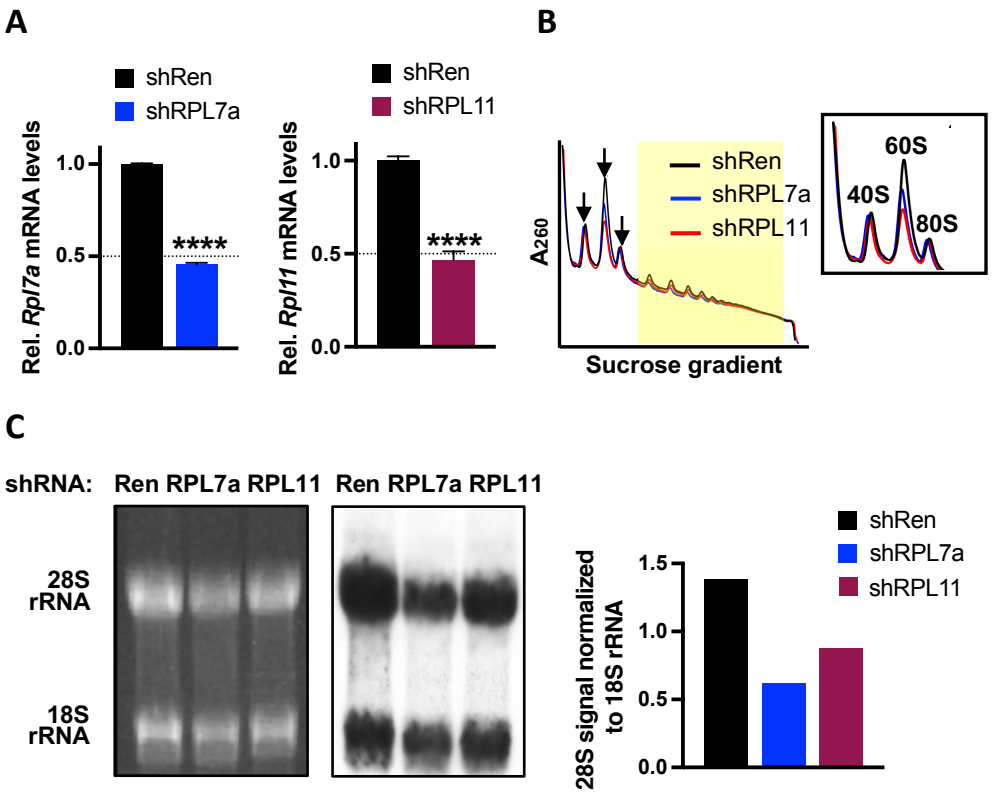


**Figure R-1. A 50% depletion of either *Rl7a* or *Rpl11* mRNAs causes a similar lesion in ribosome biogenesis in E$\mu$-MYC lymphoma cells.** E$\mu$-MYC cell lines expressing inducible RPL7a or RPL11 shRNA were treated for 22 hr with 1 µg/mL or 10 ng/mL of doxycycline (dox), respectively. Renilla shRNA (Ren control) cells, treated for 22 hr with 1 µg/mL dox, represent a non-silencing control. **A.** Quantitative real time-PCR (qRT-PCR) showing *Rpl7a* and *Rpl11* transcript levels in RPL7a- and RPL11-depleted cells, left and right panels respectively, relative to *Rpl7a* and *Rpl11* mRNA levels of Ren control cells and normalized to *beta-actin* (*ß-actin*) mRNA. Dotted line is set at a 50%. Each bar represents the average values ± SEM from 3 independent experiments (n=3). Student t-test was performed for statistical analyses: ****, P value (P)<0.0001. **B.** Polysome profile analyses showing the relative abundance of 40S and 60S ribosome subunits, 80S monosomes (indicated by arrows) and polysomes (yellow-shadowed area) in RPL7a- and RPL11-depleted E$\mu$-MYC cells, compared to Ren control cells. Inset of the peaks for 40S and 60S subunits and the 80S monosomes is shown on the right panel. **C.** Left panel: Ethidium bromide-stained agarose gel (left panel) and $^{3}$H-uridine autoradiogram (middle panel) of 18S and 28S rRNA. Right panel: Quantification of 28S rRNA signal normalized to 18S rRNA signal in RPL7a-, RPL11-depleted and Ren control E$\mu$-MYC cells.

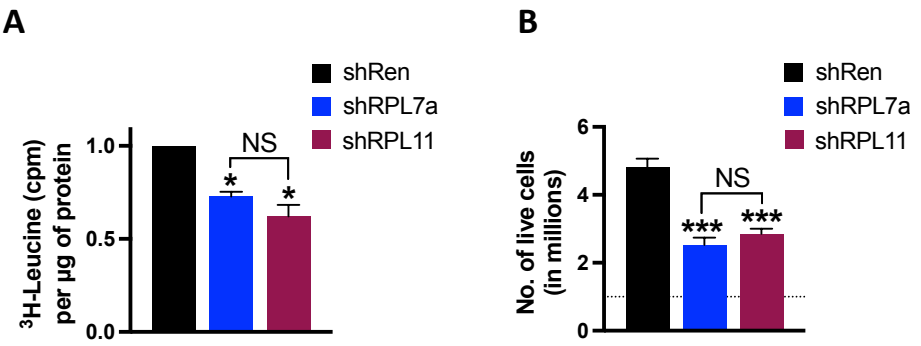


**Figure R-2. Depletion of *Rpl7a* or *Rpl11* mRNA in Eμ-MYC lymphoma cells reduces the rate of global protein synthesis and cell proliferation to a similar extent**. **A.** $^3$H-leucine labeling of nascent protein in RPL7a- and RPL11-depleted Eμ-MYC cells in comparison to Ren control cells after 22 hr of dox treatment. Results were normalized to the concentration of total proteins. **B.** Proliferation assay of Ren control, RPL7a- and RPL11-depleted Eμ-MYC cells after 22 hr of dox treatment. $1x10^6$ cells were seeded at time 0 ($t_0$), as indicated by the dotted line. Each graph displays the average values ± SEM from 3 independent experiments (n=3). One-way ANOVA tests were performed for statistical analyses: *, P<0.05; ***, P<0.001; NS, not significant (P>0.05).

## 2. Impaired ribosome biogenesis leads to the induction of the IRBC and p53 stabilization

Despite a similar reduction in 60S subunit production, global protein synthesis and the rate of cell proliferation, only depletion of *Rpl7a* mRNA, but not *Rpl11* mRNA, induced p53 stabilization, which was paralleled by increased p21 and emergence of cleaved caspase-3 (CASP3cv) **(Fig. R-3A)**, suggesting activation of the IRBC. To determine the role of the IRBC in mediating p53 stabilization, RPL5 was immunoprecipitated from Eμ-MYC cell lysates cleared of mature ribosomes by ultracentrifugation and the RPL5-associated proteins were analyzed on Western blots, as previously described (Morcelle et al., 2019). In parallel to p53 stabilization, we found increased amounts of MDM2 and RPL11 associated with RPL5 in RPL7a-depleted cell lysates compared to Ren control cells, with their association completely absent in RPL11-depleted cells **(Fig. R-3B)**.

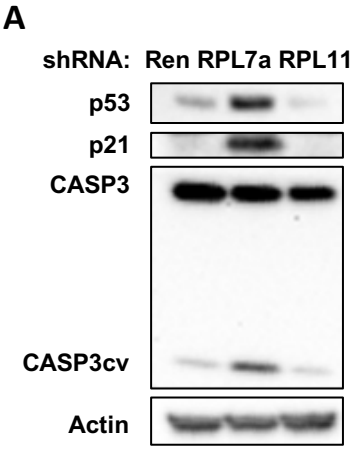


**Figure R-3. Only RPL7a depletion induces the IRBC, leading to p21 induction and caspase-3 cleavage in Eμ-MYC lymphoma cells.** **A.** Western blot showing expression of p53, p21 and full length and cleaved caspase-3 (CASP3cv) in RPL7a and RPL11-depleted cells compared to Ren control cells. Actin is shown as a loading control. **B.** Whole cell lysates (WCL) were subjected to high speed ultracentrifugation to clear mature ribosomes, followed by immunoprecipitation (IP) of supernatants with RPL5 or IgG control antibodies. Western blot shows the expression levels of MDM2, p53, RPL5 and RPL11 proteins in WCL, post-ultracentrifugation supernatants (Input), and in RPL5 IP and IgG IP control samples.

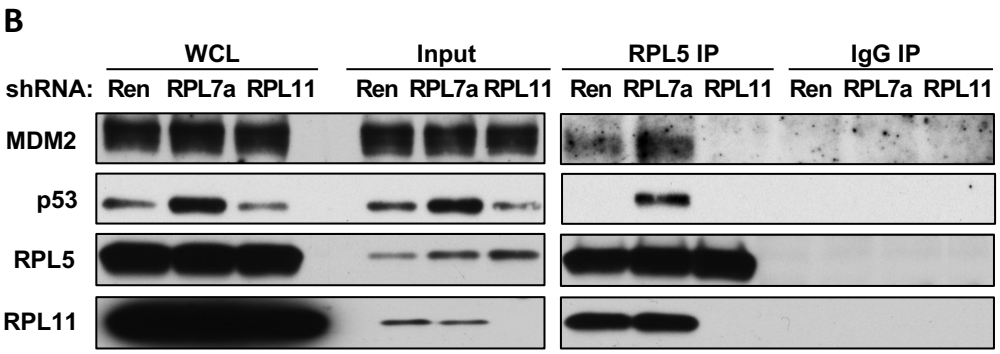


To follow the acute induction of the IRBC over time, Eμ-MYC cells were treated with Actinomycin D (ActD), a chemotherapeutic drug approved for cancer treatment, which at low nanomolar concentrations (<10 nM) specifically inhibits Pol I-mediated rDNA transcription in mammalian cells (Perry and Kelley, 1970). To test the role of ActD on the production of the Pol I mediated-transcription of 47S pre-rRNA, we measured by quantitative real time-PCR (qRT-PCR) amplification its internal transcribed spacer (*Its*)*1* **(see introduction Fig. I-17)**. The results show that *Trp53*$^{+/+}$ Eμ-MYC lymphoma cells treated with 5 nM ActD for increasing times results in the gradual reduction of *Its1* expression, over an 80% after 4 hr ActD-treatment **(Fig. R-4A)**. These strong inhibitory effects on rRNA synthesis were paralleled by p53 stabilization, and CASP3cv and cleaved PARP1 (PARP1cv), which was particularly evident at 4 hr post 5 nM ActD treatment **(Fig. R-4B)**. In parallel such treatment induced the formation of the IRBC complex, as shown by the co-immunoprecipitation

of MDM2 and RPL11 with RPL5 **(Fig. R-4C)**. These findings are consistent with those in hypomorphic RPL24 mice (Barkic et al., 2009), showing an elevation of p53 in RPL7a-depleted Eμ-MYC lymphoma cells, which appears to be mediated by the activation of the IRBC.

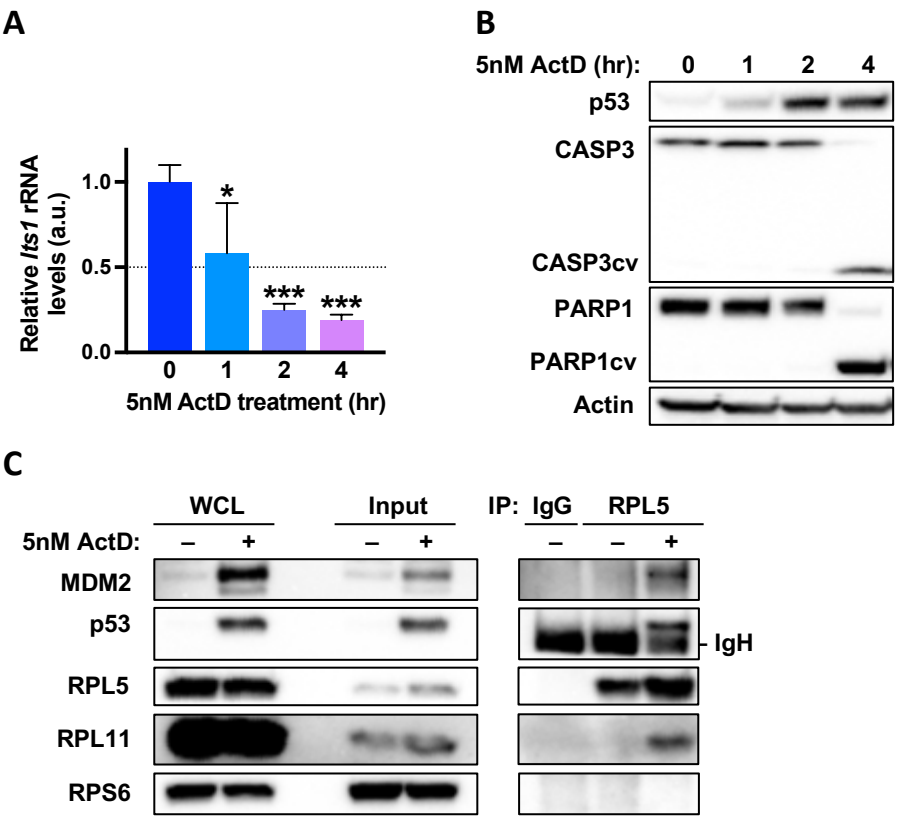


**Figure R-4. ActD treatment inhibits rRNA synthesis, induces the IRBC and causes p53 stabilization, leading to p21 induction and caspase-3 cleavage in Eμ-MYC lymphoma cells.** Cells were treated with 5nM ActD for 4 hr, unless otherwise indicated. **A.** qRT-PCR showing *Its1* rRNA levels in Eμ-MYC cells treated with ActD (1-4 hr) relative to non-treated cells (NT; $t_0$) and normalized to *beta-2 microglobulin* (*β2m*) mRNA. Dotted line is set at a 50%. Graph displays the average values ± SEM from 3 independent experiments (n=3). One-way ANOVA test was performed for statistical analysis: *, P<0.05; ***, P<0.001. **B.** Western blot analysis showing expression of p53, full length CASP3, CASP3cv, full length PARP1 and PARP1cv from WCL of Eμ-MYC cells treated with ActD (1-4 hr) compared to NT cells ($t_0$). Actin is shown as a loading control. **C.** WCL were subjected to high speed ultracentrifugation and RPL5 was immunoprecipitated as described in **Fig. R-3B**. Western blot showing expression levels of MDM2, p53, RPL5 and RPL11 proteins in WCL, inputs, RPL5 IP and IgG IP control samples. RPS6 is shown as a control for a RP not belonging to the complex.

## 3. Impaired ribosome biogenesis induces apoptosis upon IRBC-mediated p53 stabilization

Given that depletion of RPL7a leads to the induction of p53 and CASP3cv **(Fig. R-3A)**, we reasoned that such conditions would lead to enhanced apoptotic cell death. Compatible with this model, analyses by flow cytometry of E$\mu$-MYC lymphoma cells depleted of RPL7a for 22 hr, showed higher levels of Annexin V (AnnV) and Zombie Violet (ZV) co-staining, which allows the discrimination of apoptotic dead cells (Boersma et al., 2005, Vom Berg et al., 2013), as compared to RPL11-depleted cells or Ren control E$\mu$-MYC cells, **(Fig. R-5A)**. Furthermore, these effects were more pronounced at a later time point, following 48 hr RPL7a depletion **(Fig. R-5A)**. Inhibition of CASP3cv and PARP1cv with the pan-caspase inhibitor Z-Val-Ala-Asp-fluoromethylketone (ZVAD-FMK) **(Fig. R-5B)**, rescued the number of live cells upon RPL7a-depletion, which was particularly evident at 48 hr **(Fig. R-5C)**. To test whether apoptotic induction was p53-dependent, we performed the same analysis in *Trp53*$^{-/-}$ E$\mu$-MYC cells, using the same Tet-regulated miR30-shRNA protocol employed to generate *Trp53*$^{+/+}$ E$\mu$-MYC cells (Zuber et al., 2011). In the p53-deficient background, depletion of either RP mRNA levels, to an equivalent level as for the *Trp53*$^{+/+}$ E$\mu$-MYC cells **(Fig. R-6A)**, also decreases the rate of cell proliferation **(Fig. R-6B)**, compatible with earlier findings of Barna et al. (2008), but to a lesser extent than observed in *Trp53*$^{+/+}$ E$\mu$-MYC cells **(Fig. R-2B)**. Importantly, in this context, the depletion of RPL7a does not lead to enhanced apoptosis following 22 hr of dox treatment **(Fig. R-6C)**, although an increase in the number of apoptotic cells is observed following more profound RPL7a depletion, 48 hr after dox treatment **(Fig. R-6C)**. Consistent with these observations, the number of viable cells was markedly decreased in *Trp53*$^{+/+}$ E$\mu$-MYC cells following 12 hr of ActD treatment, while the impact of ActD treatment was significantly reduced in the p53-deficient background **(Fig. R-7A)**, which also correlates with increases in the amounts of CASP3cv and PARP1cv in the p53-wt background upon ActD treatment **(Fig. R-4B)**. We also observe that ActD treatment for 4 hr leads to the acute stabilization of p53 whose levels are increased by 5-fold, as measured by flow cytometry **(Fig. R-7B)**. This correlates with the upregulation of the p53 target genes *Puma*, *Noxa* and *p21* **(Fig. R-7C)**, as their expression were significantly increased in ActD-treated *Trp53*$^{+/+}$ E$\mu$-MYC lymphoma cells, but not in

their *Trp53*$^{-/-}$ counterparts. The results, taken together with RPL5 co-immunoprecipitation studies **(Fig. R-4C)** indicate that activation of the IRBC leads to p53-dependent apoptosis in response to ActD in E$\mu$-MYC lymphoma cells. The data also support the hypothesis that depletion of RPL7a or inhibition of Pol I-mediated transcription in *Trp53*$^{+/+}$ E$\mu$-MYC cells leads to p53 stabilization, CASP3cv and apoptosis through the activation of the IRBC and not due to a general decrease in global protein synthesis.

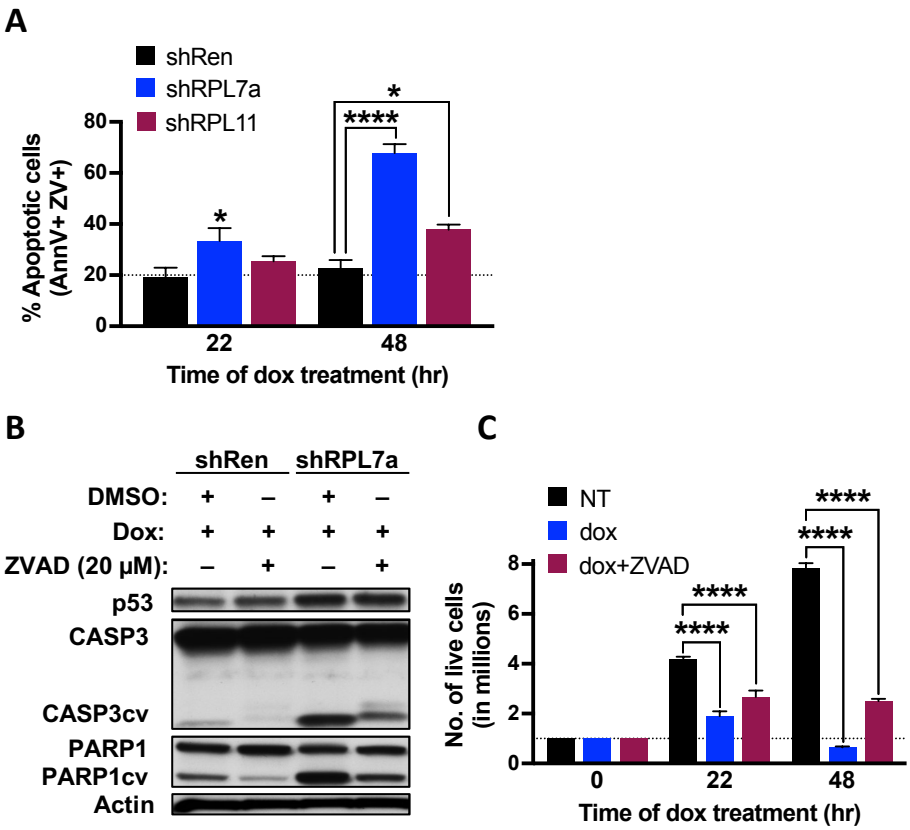


**Figure R-5. Depletion of RPL7a but not of RPL11, induces caspase-dependent cell death in E$\mu$-MYC lymphoma cells. A.** Flow cytometry analysis of Ren control, RPL7a-depleted and RPL11-depleted E$\mu$-MYC lymphoma cells following 22 hr and 48 hr dox treatment and staining with the apoptotic marker Annexin V (AnnV) and the cell membrane permeability dye Zombie violet (ZV). **B.** Western blot analysis of p53, full length CASP3, CASP3cv, full length PARP1 and PARP1cv in Ren control and RPL7a-depleted E$\mu$-MYC lymphoma cells treated with dox for 22 hr in parallel with the pan-caspase inhibitor Z-VAD-FMK (ZVAD) or DMSO. Actin is shown as a loading control. (See next page)

**Figure R-5. (continued) C.** Proliferation assay of the RPL7a-depleted Eμ-MYC lymphoma cells NT, or treated with dox, or treated with dox together with ZVAD. Live cells were counted at the indicated times. Dotted line indicates the number of cells seeded at $t_0$. Each graph displays the average values ± SEM from 3 independent experiments (n=3). Two-way ANOVA test was performed for statistical analyses: *, P<0.05; ****, P<0.0001.

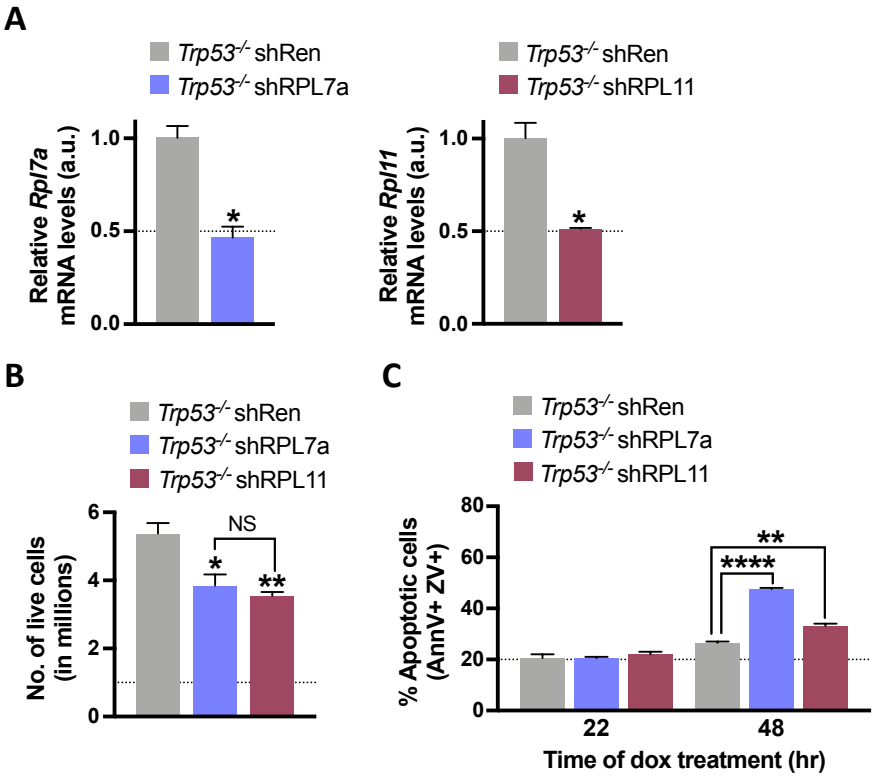


**Figure R-6. Induction of apoptotic cell death upon RPL7a-depletion is rescued in p53-deficient Eμ-MYC lymphoma cells, but not the reduced rate of proliferation.** All experiments were performed *Trp53*$^{-/-}$ Eμ-MYC cells stably transfected with a Renilla shRNA (shRen), or depleted of *Rpl7a* (shRPL7a) or *Rpl11* (shRPL11) and treated for 22 hr with dox. **A.** qRT-PCR showing *Rpl7a* and *Rpl11* transcript levels in RPL7a- and RPL11-depleted cells, left and right panel respectively, compared to their levels in Ren control cells and normalized to *β-actin* mRNA. Dotted line is set at a 50%. **B.** Proliferation assay of Ren control, RPL7a- or RPL11-depleted cells. 1x10$^6$ cells were seeded at $t_0$, as indicated with the dotted line. **C.** Flow cytometry analyses of Ren control, RPL7a- and RPL11-depleted cells following 22 hr and 48 hr dox treatment and staining with the apoptotic marker AnnV and the cell membrane permeability dye ZV. Dotted line is set at a 20%. For each graph the average values ± SEM from 3 independent experiments (n=3) are displayed. Student t-test (**A**), One-way ANOVA test (**B**) or Two-way ANOVA test (**C**) were performed for statistical analyses: *, P<0.05; **, P<0.01; ****, P<0.0001; NS, not significant (P>0.05).

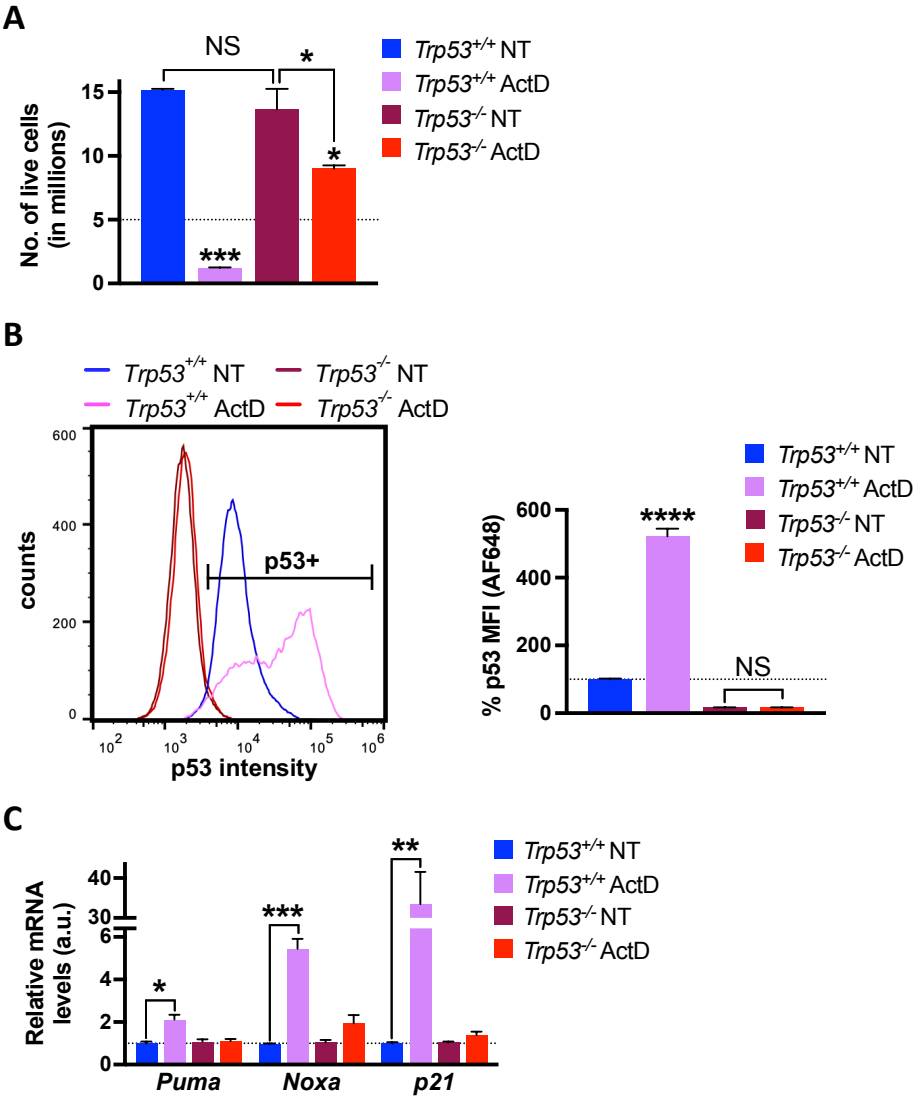


**Figure R-7. Induction of cell death by ActD treatment in Eμ-MYC lymphoma cells is rescued in the p53-deficient background. A.** Proliferation assay of *Trp53*$^{+/+}$ and *Trp53*$^{-/-}$ Eμ-MYC cells treated for 12 hr with 5 nM ActD and their corresponding NT controls. 5x10$^6$ cells were seeded at $t_0$, as indicated with the dotted line. **B.** The levels of p53 were assessed by flow cytometry in both *Trp53*$^{+/+}$ and *Trp53*$^{-/-}$ Eμ-MYC lymphoma cells treated for 4 hr with ActD and their corresponding NT controls. Left panel: Histogram showing cellular fluorescence intensity of p53 from one representative sample from each condition, as indicated above the graph. Right panel: representative graph showing mean fluorescence intensity (MFI) of p53 in the conditions displayed in the panel on the left **(see Materials and Methods)**. Values are relative to *Trp53*$^{+/+}$ NT control cells and representative from 2 independent experiments (n=2). Dotted line is set at 100% (See next page)

**Figure R-7. (continued) C.** Analysis by qRT-PCR of the mRNA levels of *Puma, Noxa* and *p21* in 4 hr ActD-treated *Trp53*$^{+/+}$ and *Trp53*$^{-/-}$ E$\mu$-MYC cells. Results were normalized to *β2m* mRNA and are shown as relative to the NT controls. Each graph displays the average values ± SEM from 2-3 independent experiments (n=2-3). One-way ANOVA test (**A**, **B**) or Kruskas-Wallis test (**C**) were performed for statistical analyses: *, P<0.05; **, P<0.01; ***, P<0.001; ****, P<0.0001; NS, not significant (P>0.05).

## 4. The antiapoptotic form of MCL1 is selectively lost in both RPL7a-depleted and ActD-treated *Trp53*$^{+/+}$ E$\mu$-MYC cells

Key mediators of p53-induced cell death include proapoptotic BH3-only containing proteins from the BCL2 family, including PUMA and NOXA, which indirectly activate the proapoptotic effectors BAX and BAK, through inhibition of the antiapoptotic members of the BCL2 family, BCL2, BCLxL, BCLW, BFL1/A1 and MCL1, despite PUMA been able to also directly activate BAX/BAK effectors (Youle and Strasser, 2008). As described in the introduction **(Section 2.1.)** activation of BAX/BAK leads to the induction of the caspase cascade and cell death response (Llambi et al., 2011), whereas an antiapoptotic response is essential for E$\mu$-MYC-driven lymphomagenesis (Kelly et al., 2011, Kelly et al., 2014).

Analysis of the levels of the three main antiapoptotic BCL2 family members, BCLxL, BCL2 and MCL1 by Western blot analysis, showed that the upper band of MCL1, Mr ~38 kDa, which corresponds to the antiapoptotic form of the protein, MCL1$_{OM}$ **(see Section 2.2.1. and Table I-3)** is selectively reduced in RPL7a-depleted cells, as compared to RPL11-depleted or Ren control cells **(Fig. R-8A)**. By contrast, there is little to no change in the levels of BCL2 or BCLxL **(Fig. R-8A)**. In contrast, MCL1 levels in *Trp53*$^{-/-}$ E$\mu$-MYC cells are not affected by RPL7a depletion, suggesting that loss of MCL1$_{OM}$ is p53 dependent **(Fig. R-8B)**. MCL1$_{OM}$ (Mr ~38 kDa), lacks approximately the first 30 aa of the N-terminal region (De Biasio et al., 2007, Warr et al., 2011), and is located at the OMM, where it prevents cell death by antagonizing BAK/BAX (Perciavalle et al., 2012). In contrast, the MCL1$_{Matrix}$ form (Mr ~36 kDa), likely generated by further cleavage of its N-terminus (Warr et al., 2011), is imported into the mitochondrial matrix where it plays a critical role in mitochondrial energy production (Huang and Yang-Yen, 2010, Perciavalle et al., 2012).

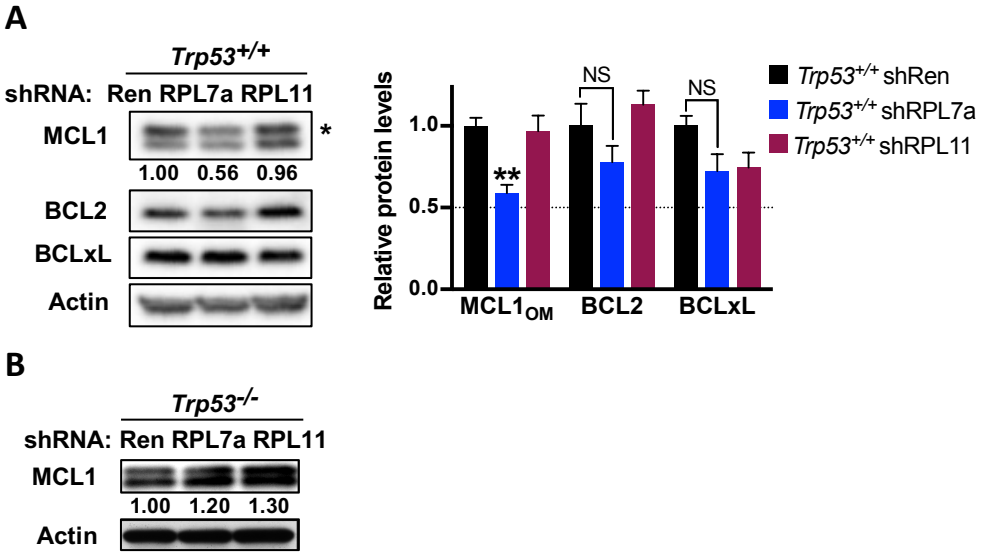


**Figure R-8. $MCL1_{OM}$ is selectively reduced in RPL7a-depleted *Trp53*$^{+/+}$ but not *Trp53*$^{-/-}$ Eμ-MYC lymphoma cells. A.** Left panel: Western blot analysis of MCL1, BCL2 and BCLxL in RPL7a- and RPL11-depleted *Trp53*$^{+/+}$ Eμ-MYC lymphoma cells compared to Ren control cells. Actin is shown as a loading control. Antiapoptotic $MCL1_{OM}$ (indicated by the *) was quantified by densitometry analysis using the NIH Image J software **(see Materials and Methods)** and their relative values in each condition are displayed below MCL1 blot. Right panel: Relative quantification the three antiapoptotic members in the conditions displayed in **A** from 3 independent experiments (n=3). Two-way ANOVA was performed for statistical analysis: **, P<0.01; NS, not significant (P>0.05). **B.** Western blot analysis of MCL1 levels in RPL7a- and RPL11-depleted *Trp53*$^{-/-}$ Eμ-MYC lymphoma cells compared to Ren control cells. Actin is shown as a loading control. Values represented under the MCL1 blot were calculated as in **A**.

A time course analysis showed that acute 5 nM ActD treatment led to the induction of p53 within 2 hr, which was followed within 4 hr by the selective loss of the antiapoptotic form of MCL1 and the activation of caspase-3, as detected by CASP3cv and PARP1cv **(Fig. R-9A)**. In contrast, none of these responses were detected in *Trp53*$^{-/-}$ Eμ-MYC cells **(Fig. R-9A)**. In line with our observations following RPL7a depletion, ActD treatment, at low concentrations, had little effect on the levels of the BCL2 family members, BCLxL or BCL2 **(Fig. R-9B)**. Thus, the $MCL1_{OM}$ form, is selectively reduced following RiBi impairment, in a p53 dependent manner **(Figs. R-8A and R-9A)**.

That the two protein bands, $MCL1_{OM}$ and $MCL1_{Matrix}$ are derived from MCL1, was confirmed by Western blot analysis of protein lysates from either wt-MEFs **(lane 1, Fig. R-9C)**, or from two distinct clones of *Mcl1* deleted (*Mcl1* KO) MEFs **(lanes 2-3, Fig. R-9C)**, compared to *Trp53*$^{+/+}$ E$\mu$-MYC lymphoma cells treated with or without ActD **(lanes 4-5, Fig. R-9C)**. Given that $MCL1_{OM}$ and $MCL1_{Matrix}$ are generated by proteolytic cleavage, our data suggests that ActD treatment has an impact on MCL1 at the post-translational level.

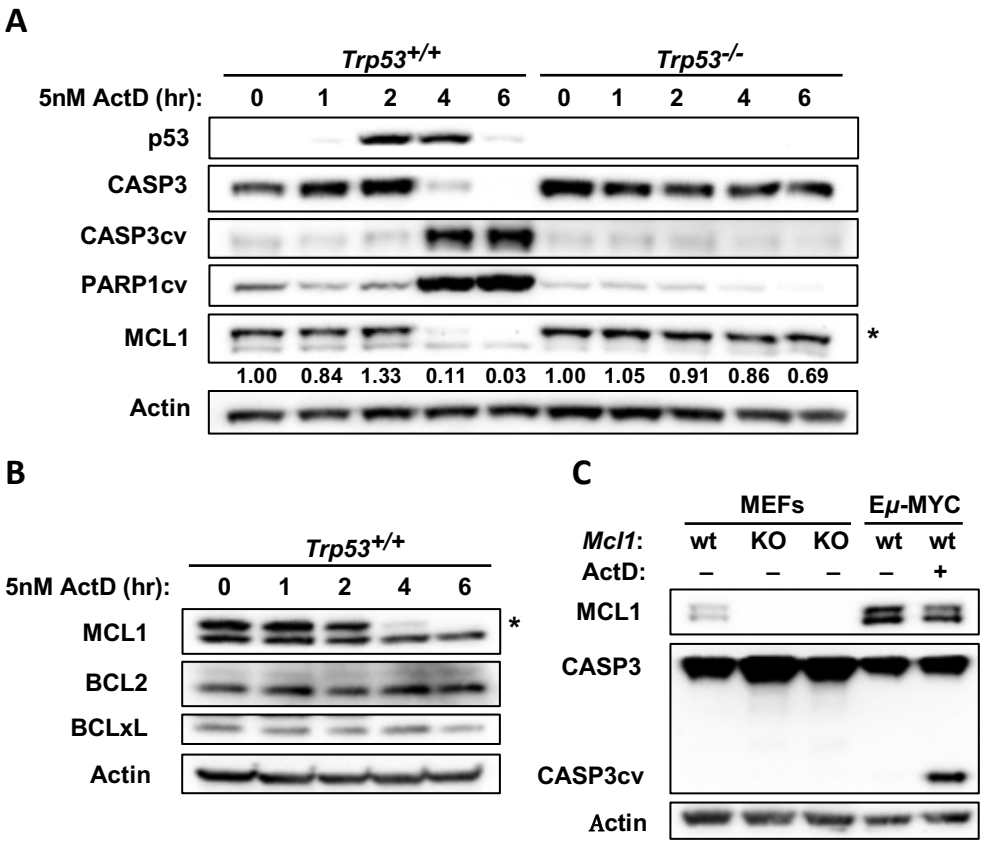


**Figure R-9. ActD treatment leads to the selective loss of $MCL1_{OM}$ in a p53 dependent manner. A.** Western blot analysis of p53, full length CASP3, CASP3cv, PARP1cv and MCL1 levels following the indicated times of ActD treatment in both *Trp53*$^{+/+}$ and *Trp53*$^{-/-}$ E$\mu$-MYC cells. Actin is shown as a loading control. Relative $MCL1_{OM}$ levels (indicated by the *) displayed below the MCL1 blot were calculated as in **Fig. R-8A**. **B.** Western blot analysis of MCL1, BCL2 and BCLxL protein levels following the indicated times of ActD treatment in *Trp53*$^{+/+}$ E$\mu$-MYC lymphoma cells. Actin is shown as a loading control. * indicates the band corresponding to antiapoptotic $MCL1_{OM}$ form. (See next page)

**Figure R-9. (continued) C.** Western blot analysis of MCL1, full length CASP3 and CASP3cv, in wt-MEFs (*Mcl1*$^{wt}$) and *Mcl1* KO MEFs, provided by Dr. Joseph T. Opferman (St. Jude Children's Research Hospital, Memphis, USA), in comparison to *Trp53*$^{+/+}$ E$\mu$-MYC lymphoma cells treated with or without 5 nM ActD for 4 hr. Actin is shown as a loading control.

## 5. MCL1 loss upon RPL7a-depletion or ActD treatment occurs at the post-translational level.

We confirmed that the loss of MCL1 observed following RiBi impairment was not regulated by either transcription or degradation of its mRNA, by measuring the amount of *Mcl1* mRNA by qRT-PCR in RPL7a-depleted cells as compared to Ren control cells **(Fig. R-10A)**, or in cells treated with ActD for 4 hr **(Fig. R-10B)**, which showed little differences as compared to non-treated (NT) cells.

Likewise, although selective translational control of *Mcl1* mRNA has been implicated in controlling its protein levels (Mills et al., 2008), there was no apparent re-distribution of *Mcl1* mRNA on actively translating polysomes in whole cell extracts from RPL7a-depleted cells compared to Ren control cells **(Fig. R-10C)**. The results show that RiBi impairment does not alter the transcription or translation of MCL1, and supported a post-translational event responsible for modulating MCL1 protein stability. To test this possibility, RPL7a-depleted *Trp53*$^{+/+}$ E$\mu$-MYC and Ren control lymphoma cells were treated with cycloheximide (CHX) to inhibit nascent protein synthesis, and whole cell lysates were analyzed for MCL1 protein levels over time. Western blot analysis showed that the half-life of MCL1$_{OM}$ (upper band) decreased from ~35 min Ren control cells to ~25 min in RPL7a-depleted cells **(Fig. R-10D)**. Together these studies demonstrate that IRBC-induced stabilization of p53 leads to accelerated MCL1 protein turnover and cell death.

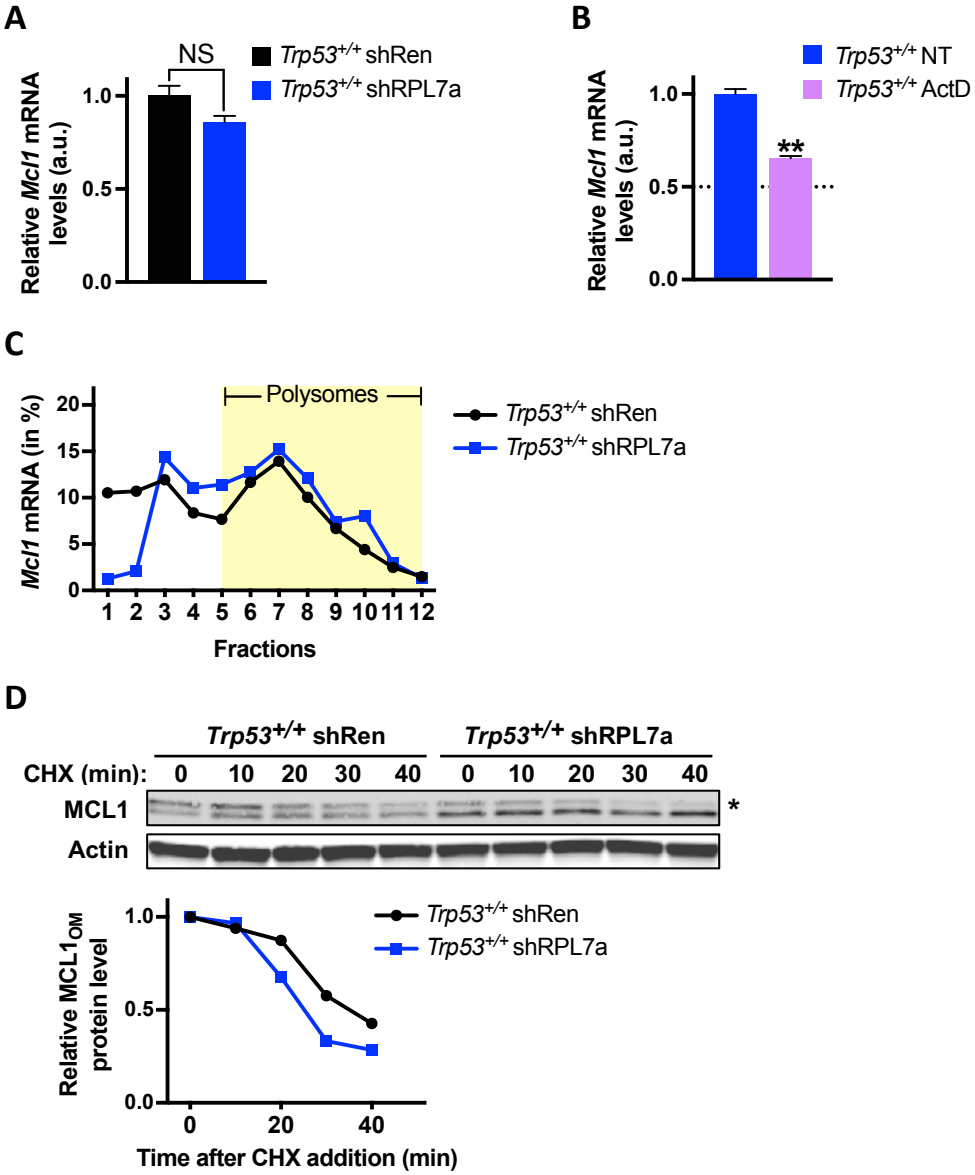


**Figure R-10. MCL1 loss following RPL7a-depletion occurs at the post-translational level.** **A.** Quantification of *Mcl1* mRNA levels by qRT-PCR in RPL7a-depleted *Trp53*$^{+/+}$ E$\mu$-MYC lymphoma cells, relative to *Mcl1* mRNA levels of Ren control cells following 22 hr dox treatment. Values were normalized to *ß-actin*. Graph displays average values ± SEM from 3 independent experiments (n=3). Student t test was performed for statistical analysis: NS, not significant (P>0.05). **B.** Quantification of *Mcl1* transcripts by qRT-PCR in 4 hr ActD-treated *Trp53*$^{+/+}$ E$\mu$-MYC cells relative to NT cells and normalized to *ß2m* mRNA. Graph displays average values ± SEM from 3 independent experiments (n=3). Student t test was performed for statistical analysis: **, P<0.01 (see next page).

**Figure R-10 (continued) C.** Polysome distribution of *Mcl1* mRNA transcript on a 10-50% sucrose gradient from E$\mu$-MYC lymphoma cells depleted of RPL7a or of Ren control lymphoma cells. *Mcl1* mRNA levels from each fraction were normalized to luciferase and plotted as the percentage of total mRNA from all 12 fractions. Fractions of *Mcl1* mRNA associated to actively translating polysomes are indicated in the graph and shadowed in yellow. **D.** Top panel: Western blot analysis showing expression of MCL1 protein in Ren control and RPL7a-depleted *Trp53*$^{+/+}$ E$\mu$-MYC lymphoma cells treated with dox for 22 hr followed by 100 µg/mL cycloheximide (CHX) chase, and harvested at the indicated time points. Actin is shown as a loading control. Bottom panel: Graph showing the fold decrease in $MCL1_{OM}$ levels, indicated by the * in the panel above, normalized to actin over time. Relative protein expression was determined by densitometry analysis using the NIH Image J software **(see Materials and Methods)**.

## 6. MCL1 loss is associated with increased ubiquitination and proteasomal degradation.

The short half-life of MCL1 in *Trp53*$^{+/+}$ E$\mu$-MYC lymphoma cells (~35 min) is consistent with previous studies, which estimated its half-life at ~1 hr but in a cell-type and cell-context dependent manner. This significantly contrasts with the stability of the other antiapoptotic BCL2 family members, including BCL2 or BCLxL, with half-lives of over 20 hr (Campbell et al., 2010, Senichkin et al., 2019). The short half-life of MCL1 protein, is explained in part, by its inherent instability **(see introduction Sections 2.2.3. and 2.2.4.)**, containing multiple PEST-rich regions (Rechsteiner and Rogers, 1996), and many lysine (K) residues targeted by distinct ubiquitin E3 ligases (Mojsa et al., 2014). Its rapid turnover is attributed to both proteasome-dependent and proteasome-independent-mediated degradation (Nijhawan et al., 2003, Clohessy et al., 2004, Han et al., 2004, Weng et al., 2005, Zhong et al., 2005). Treatment with the pan-caspase inhibitor QVD-OPh (Caserta et al., 2003) inhibited CASP3 activation (CASP3cv) induced by either RPL7a-depletion or ActD treatment but did not prevent the loss of MCL1 **(Figs. R-11A, B)**. In contrast, proteasome inhibition by MG132 treatment (Lee and Goldberg, 1998), at two distinct doses, partially rescued MCL1 protein levels, and CASP3 and PARP1 cleavage, following ActD treatment **(Fig. R-12A)**, suggesting that MCL1 degradation may be mediated by the UPS.

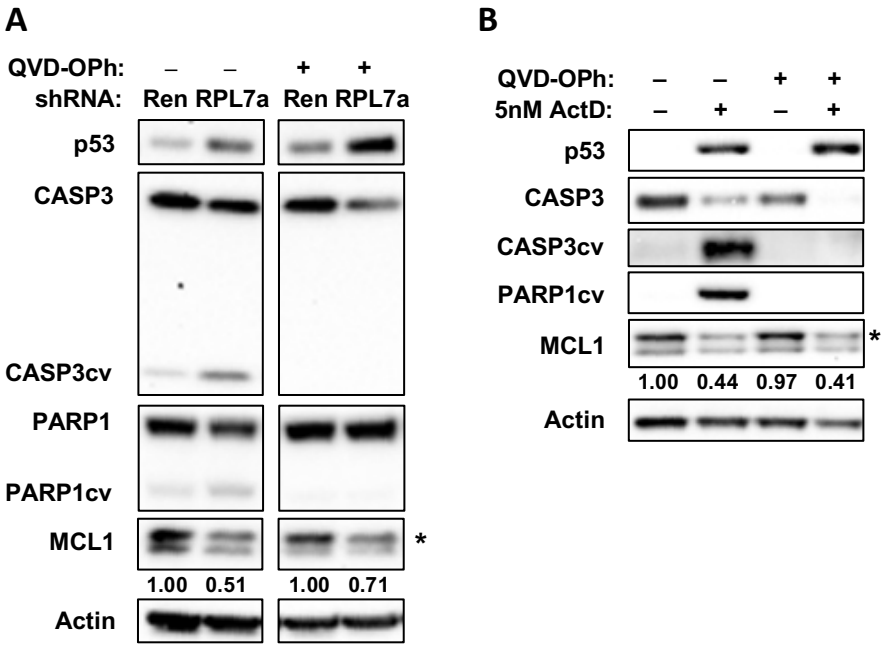


**Figure R-11. MCL1 degradation, following either RPL7a depletion or ActD treatment, is not mediated by caspase-3. A.** Western blot analysis of p53, full length CASP3, CASP3cv, full length PARP1, PARP1cv and MCL1 levels in RPL7a-depleted and Ren control *Trp53*$^{+/+}$ Eμ-MYC cells, following 22 hr dox treatment with or without 20 μM QVD-OPh. Actin is shown as a loading control. MCL1$_{OM}$ form, corresponding to the band indicated by the *, was quantified and normalized to tubulin and values are displayed below the MCL1 blot. **B.** Western blot analysis of p53, full length CASP3, CASP3cv, PARP1cv and MCL1 levels in 4 hr ActD-treated and NT control *Trp53*$^{+/+}$ Eμ-MYC cells, in the presence or absence of 20 μM QVD-OPh added 30 min prior ActD treatment. Actin is shown as a loading control. MCL1$_{OM}$ form levels (indicated by the *) were calculated as in **A** and values are displayed below the MCL1 blot.

Consistent with this possibility, we observed a dramatic increase in the amount of ubiquitinated proteins co-immunoprecipitating with MCL1 following a 22 hr dox treatment to deplete RPL7a in *Trp53*$^{+/+}$ Eμ-MYC lymphoma cells, as compared to Ren control cells **(Fig. R-12B, left panel)**. In contrast no such increase was observed in MCL1 immunoprecipitates from RPL7a-depleted *Trp53*$^{-/-}$ Eμ-MYC lymphoma cells as compared to Ren control **(Fig. R-12B, right panel)**. In parallel, acute treatment of *Trp53*$^{+/+}$ Eμ-MYC lymphoma cells with ActD led to a sharp increase in ubiquitinated protein levels associated with immunoprecipitated MCL1 **(Fig. R-12C, lanes 2 and 3)**, an effect not observed in MCL1 immunoprecipitates from ActD-treated *Trp53*$^{-/-}$ Eμ-

MYC lymphoma cells **(Fig. R-12C, lanes 5 and 6)**. These findings suggest a model in which IRBC-induced stabilization of p53 leads to the proteasomal degradation of MCL1 through the enhanced ubiquitination of MCL1 or one of its partner proteins, such as NOXA **(see introduction Section 2.2.2.)**, whose mRNA levels are increased by ActD treatment **(Fig. R-7C)**, as well as in RPL7a-depleted *Trp53*$^{+/+}$ E$\mu$-MYC as compared to Ren control cells **(Fig. R-12D)**, and which is known to favor the interaction of MULE with MCL1, promoting its ubiquitination and proteasomal degradation (Gomez-Bougie et al., 2011, Song et al., 2016).

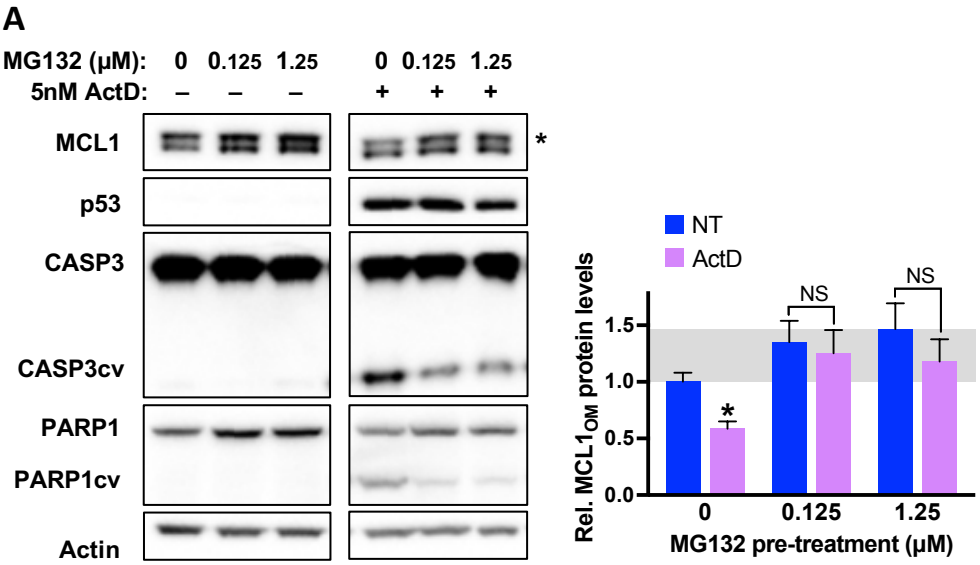


**Figure R-12. ActD treatment induces MCL1 proteasomal degradation, associated to enhanced levels of ubiquitination. A.** Left panel: Western blot analysis of MCL1, p53, full length CASP3, CASP3cv, full length PARP1 and PARP1cv levels in cells treated with the indicated dose of MG132 for 30 min, followed by treatment with ActD for 4 hr in *Trp53*$^{+/+}$ E$\mu$-MYC cells in comparison to NT control cells. Actin is shown as a loading control. * indicates antiapoptotic $MCL1_{OM}$ form. Right panel: Relative quantification of $MCL1_{OM}$ protein levels normalized to tubulin. Graph shows average values ± SEM from 2 independent experiments (n=2). Values are relative to NT cells in the absence of the MG132 inhibitor. Student t test was performed for statistical analysis: *, P<0.05; NS, not significant (P>0.05). Shadowed grey area represents the change in $MCL1_{OM}$ levels due to constitutive MCL1 degradation under basal conditions. (See next page)

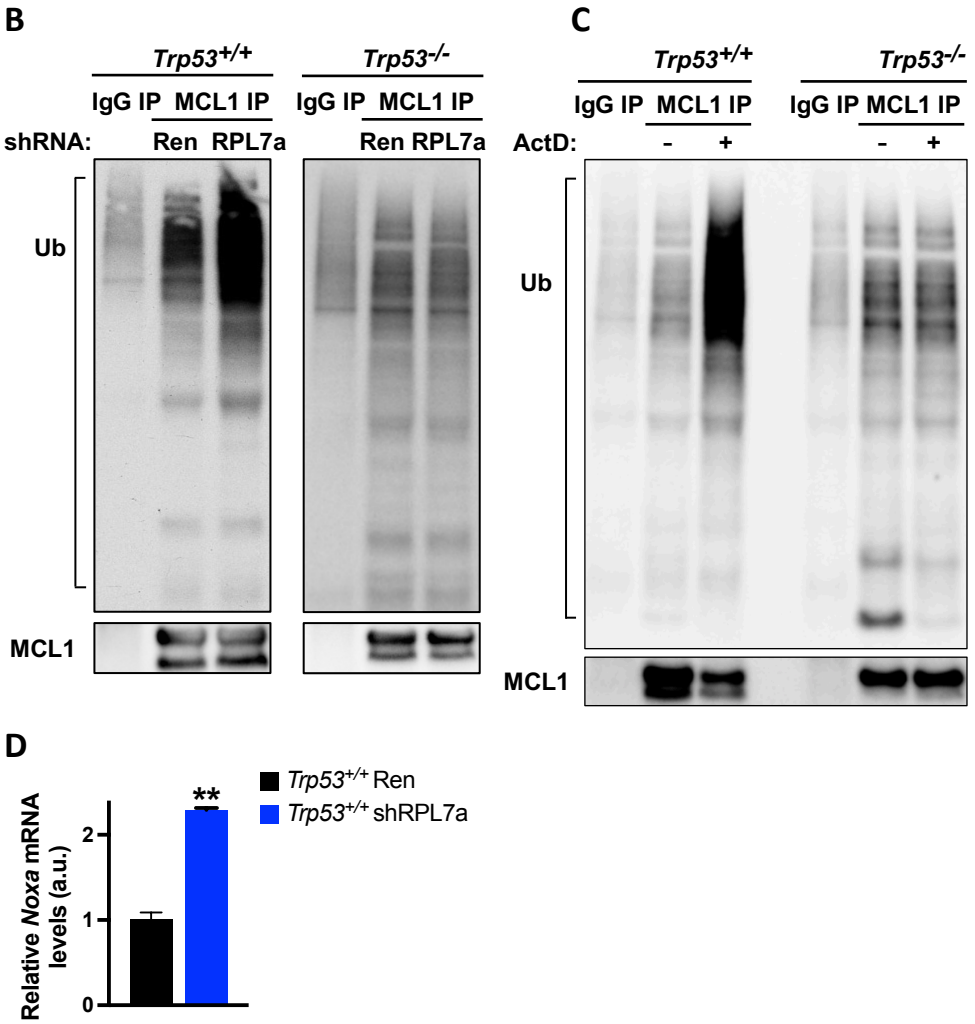


**Figure R-12. (continued) B.** Ubiquitination assay: MCL1 was immunoprecipitated (MCL1 IP) from total protein lysates of RPL7a-depleted or Ren control *Trp53*$^{+/+}$ (left panel) and *Trp53*$^{-/-}$ (right panel) E$\mu$-MYC cells. The immunoprecipitates were separated by SDS-PAGE, followed by Western blot analysis for ubiquitin (Ub) and MCL1. Rabbit IgG antibody was used as a control of immunoprecipitation (IgG). **C.** Ubiquitination assay: *Trp53*$^{+/+}$ and *Trp53*$^{-/-}$ E$\mu$-MYC cells were treated for 6 hr with ActD, and total protein lysates were treated as in **B**. **D.** Quantification of *Noxa* mRNA levels by qRT-PCR in RPL7a-depleted *Trp53*$^{+/+}$ E$\mu$-MYC lymphoma cells, relative to *Noxa* mRNA levels of Ren control cells following 22 hr dox treatment. Values were normalized to *β-actin* mRNA. Graph displays average values ± SEM from 2 independent experiments (n=2). Student t test was performed for statistical analysis: **, P<0.01.

## 7. MCL1 ubiquitin-resistant mutant is partially protected against ActD-induced cell death

To determine if the enhanced ubiquitination of MCL1 by ActD treatment has an impact on lymphoma cell survival, we used retrovirus infection to stably express in *Trp53*$^{+/+}$ E$\mu$-MYC lymphoma cells either an epitope 3X Flag-tagged murine MCL1 wt (Mcl1$^{wt}$) or MCL1 mutant (Mcl1$^{KR}$) form, in which all the lysines (K) have been converted to arginines (R), both constructs kindly provided by Dr. Joseph T. Opferman (St. Jude Children's Research Hospital, Memphis, USA). Consistent with the hypothesis that ubiquitination of MCL1 plays a role in its stability, we observed, in cells expressing comparable amounts of exogenous MCL1, that the Mcl1$^{wt}$ variant was more sensitive to ActD-induced MCL1 degradation than those expressing the Mcl1$^{KR}$ mutant, despite ActD stabilizing p53 to similar levels and showing a similar reduction of endogenous MCL1 **(Fig. R-13A)**. In addition, the expression of the Mcl1$^{KR}$ mutant reduced PARP1 and CASP3 cleavage **(Fig. R-13A)**, and enhanced the protection of *Trp53*$^{+/+}$ E$\mu$-MYC lymphoma cells against cell death in a dose and time dependent manner **(Figs. R-13B, C)**. Indeed, the $EC_{50}$ dose of ActD was 2-fold higher in the mutant Mcl1$^{KR}$-overexpressing population ($EC_{50}$=1.34 nM), compared to that of either Flag control or Mcl1$^{wt}$-overexpressing cells ($EC_{50}$=0.64 and 0.77 nM, respectively) **(Fig. R-13B, left panel)**. Taken together these results are compatible with ActD treatment leading to enhanced polyubiquitination of MCL1, which triggers its degradation and induces apoptosis of E$\mu$-MYC-driven lymphoma cells.

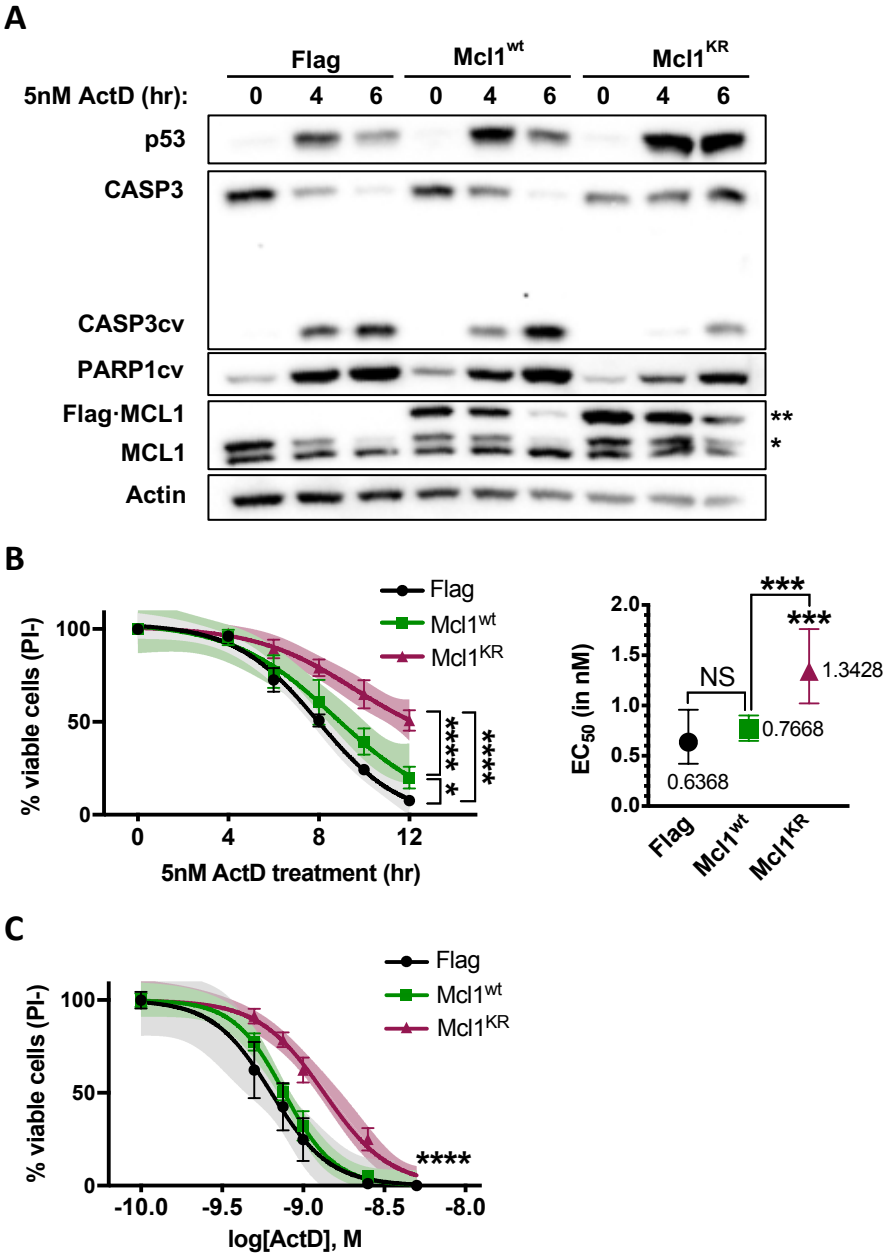


**Figure R-13. Ubiquitination-resistant MCL1 mutant (Mcl1$^{KR}$) confers partial protection against ActD-induced MCL1-degradation and increased resistance of E$\mu$-MYC lymphoma cells to cell death. A.** Western blot analysis of p53, full length CASP3, CASP3cv, PARP1cv, endogenous MCL1 (indicated by the *) and Flag-tagged MCL1 (indicated by the **) levels in 3X Flag-tagged empty vector (Flag), or 3X Flag-tagged Mcl1$^{wt}$- and Mcl1$^{KR}$-overexpressing E$\mu$-MYC lymphoma cells in the absence or presence of ActD for the indicated time (See next page)

**Figure R-13. (continued) B.** Left panel: Dose-dependent response to ActD. Flag control, $Mcl1^{wt}$- and $Mcl1^{KR}$-overexpressing E$\mu$-MYC cells were treated with increasing concentrations of ActD (0.5-5 nM) for 12 hr. Cell death was determined by propidium iodide (PI) staining and flow cytometry analysis. Each point represents the average ± SEM of 3 independent experiments (n=3) and shadowed areas display 95% confidence interval (CI) for each data. Curves were statistically compared analyzing best-fitted values by extra-sum-of-squares F test: ****, P<0.0001. Right panel: $EC_{50}$ values of the different cell lines in response to ActD. One-way ANOVA was performed for statistical analysis: ***, P<0.001; NS, not significant (P>0.05). **C.** Time-dependent response to ActD. Flag control, $Mcl1^{wt}$- and $Mcl1^{KR}$-overexpressing E$\mu$-MYC cells were treated with 1.5 nM ActD for different times (4-12 hr), and cell death was determined as in **B**. Each point represents the average ± SEM of 3 independent experiments (n=3) and shadowed areas display 95% CI for each data. Extra-sum-of-squares F test was performed to statistically compare the curves: *, P<0.05; ****, P<0.0001.

## 8. Single dose administration of ActD reduces tumor burden of Eμ-MYC lymphoma cells bearing wt-*Trp53.*

Considerable efforts have been made to develop BH3 binding mimetics which selectively target MCL1 **(see Chapter 2, Section 2.3.2.)**. In parallel, a number of Pol I inhibitors are being developed and tested in specific cancers, including the small Pol I inhibitor CX5461 **(see Chapter 3, Section 3.5.1.)**. The findings that ActD, a clinically approved anti-cancer drug, may lead to both ribosome biogenesis inhibition and the selective loss of the antiapoptotic form of MCL1 in a p53 dependent manner is clinically relevant. To test the potential efficacy of low dose ActD in the treatment of MYC-driven lymphomas, we generated *Trp53*$^{+/+}$ E$\mu$-MYC or *Trp53*$^{-/-}$ E$\mu$-MYC lymphomas by lateral tail-vein injection of either lymphoma cell line in congenic C57BL/6 Ly5.1 mice. For the analysis of the acute effects of ActD, *Trp53*$^{+/+}$ E$\mu$-MYC lymphoma bearing mice with established disease were treated with a single dose of ActD or vehicle. Following 6 hr treatment with ActD there was a reduction in the number of *Trp53*$^{+/+}$ E$\mu$-MYC lymphoma cells in the spleen, decreasing from ~65% in vehicle-treated mice to 55% in the ActD-treated mice **(Fig. R-14A)**. Consistent with these results, relative spleen weights were significantly lower in mice treated with ActD compared to the vehicle treated mice **(Fig. R-14B)**. Likewise, we observed that ActD induced p53, CASP3cv and PARP1cv in the spleens of recipient mice harboring *Trp53*$^{+/+}$ E$\mu$-MYC lymphoma cells **(Fig. R-14C)**.

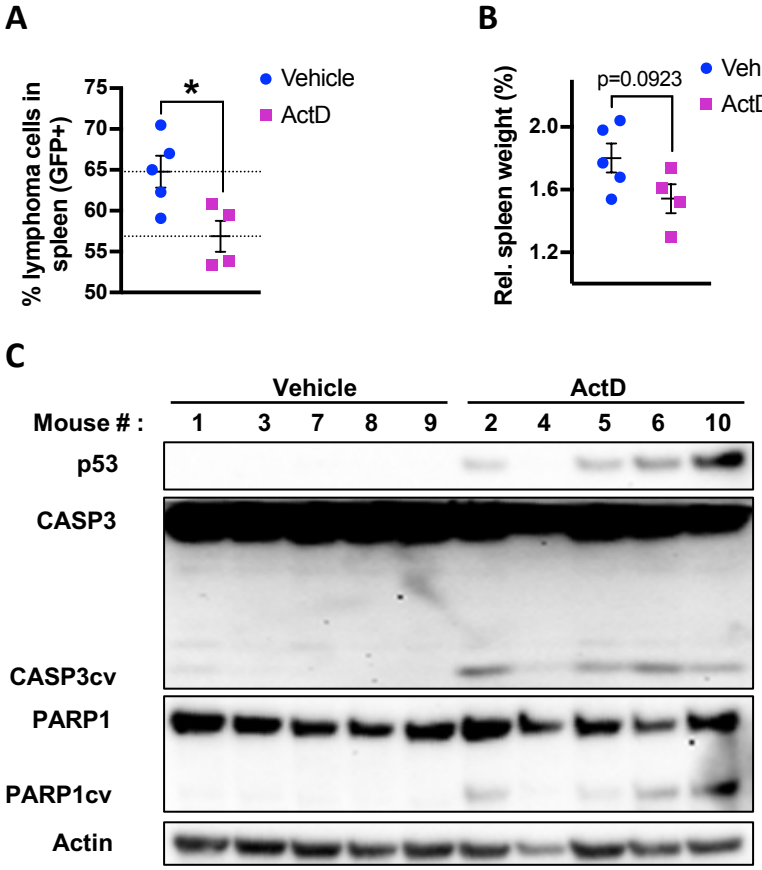


**Figure R-14. Single administration of ActD leads to a decrease in the *Trp53*$^{+/+}$ Eμ-MYC-lymphoma cell population by inducing cell death in a p53-dependent manner.** *Trp53*$^{+/+}$ Eμ-MYC-lymphoma recipient mice were treated with either ActD or vehicle and spleens were collected 6 hr after treatment administration. **A.** Flow cytometry analysis of the percentage of GFP+ viable (PI-) B (B220+) cells, corresponding to *Trp53*$^{+/+}$ Eμ-MYC lymphoma cells, present in the spleen of mice. Dotted lines are set at the average values of each cohort **B.** Spleens weight displayed as a percentage relative to total body weight of mice analyzed in **A**. **C.** Western blot analysis of p53, full length CASP3, CASP3cv, full length PARP1 and PARP1cv levels in the spleens of *Trp53*$^{+/+}$ Eμ-MYC-transplanted mice analyzed in **A**. Each lane corresponds to the spleen homogenate of an individual mouse (n=5 per treatment group). Actin is shown as loading control. Each graph displays individual values and the mean ± SEM of 4-5 mice per treatment group. Student t-test was performed for statistical analysis: *, P<0.05.

Further analysis of mice harboring *Trp53*$^{+/+}$ Eμ-MYC lymphomas demonstrated that after a single administration of ActD for 6 hr, effectively blocks Pol I transcription, as measured by the reduced qRT-PCR amplification of the 47S pre-rRNA *Its1* **(Fig. R-**

**15A)**. Notably, by flow cytometry we detected a dramatic increase of p53 levels in the spleen, ~300% **(Fig. R-15B)**, and ~250% in the lymph nodes **(Fig. R-15C)** of ActD-treated mice compared to vehicle-treated mice, 6 hr post-treatment, consistent with our previous observations by Western blot analysis **(Fig. R-14C)**. Activation of p53 was corroborated by measuring the mRNA levels of the p53 target genes *Puma*, *Noxa* and *p21*, which were significantly increased in the spleen of ActD-treated mice as compared to those of vehicle-treated mice **(Fig. R-15D)**. Likewise, we observed by Western blot analysis, that induction of p53 leads to a decrease in antiapoptotic $MCL1_{OM}$, in spleen lysates collected from mice treated with ActD for 6 hr **(Fig. R-15E)**.

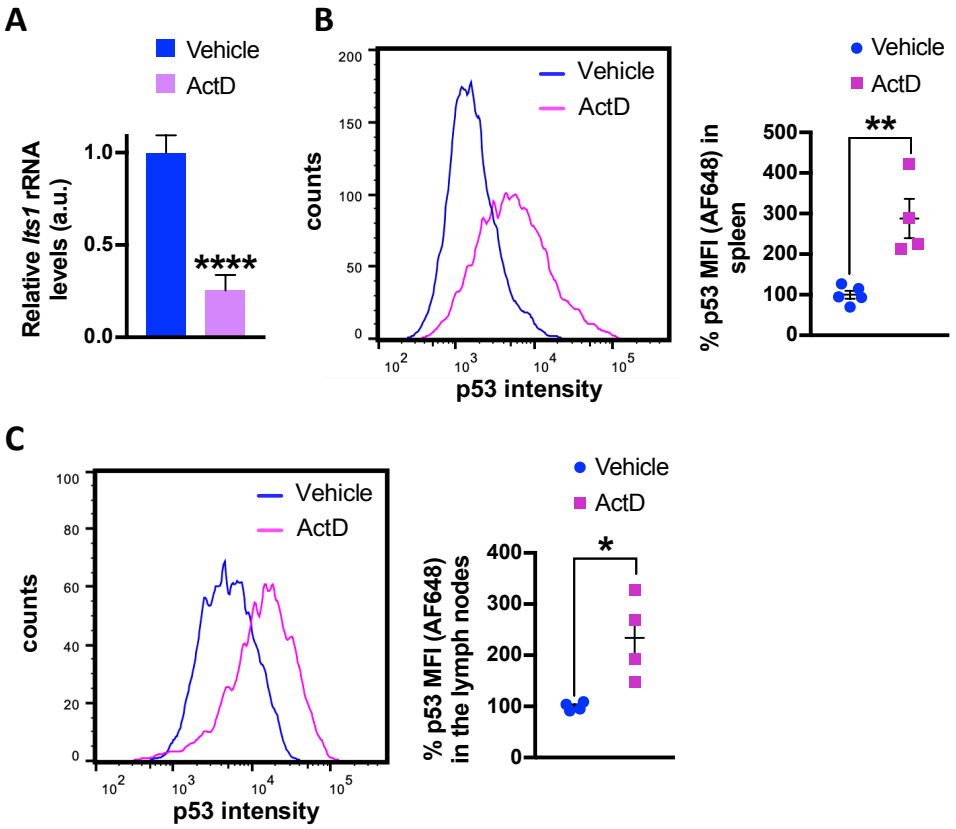


**Figure R-15. Single administration of ActD inhibits Pol I-mediated transcription, inducing p53 activation and antiapoptotic MCL1 degradation in the *Trp53*$^{+/+}$ Eμ-MYC-lymphoma cell population. A.** Quantification of the 47S rRNA *Its1* levels by qRT-PCR from spleen homogenates of mice analyzed in **Fig. R-14**, collected 6 hr after administration of ActD or vehicle. Values are relative to vehicle-treated cohort and normalized against *β2m* mRNA levels. (See next page)

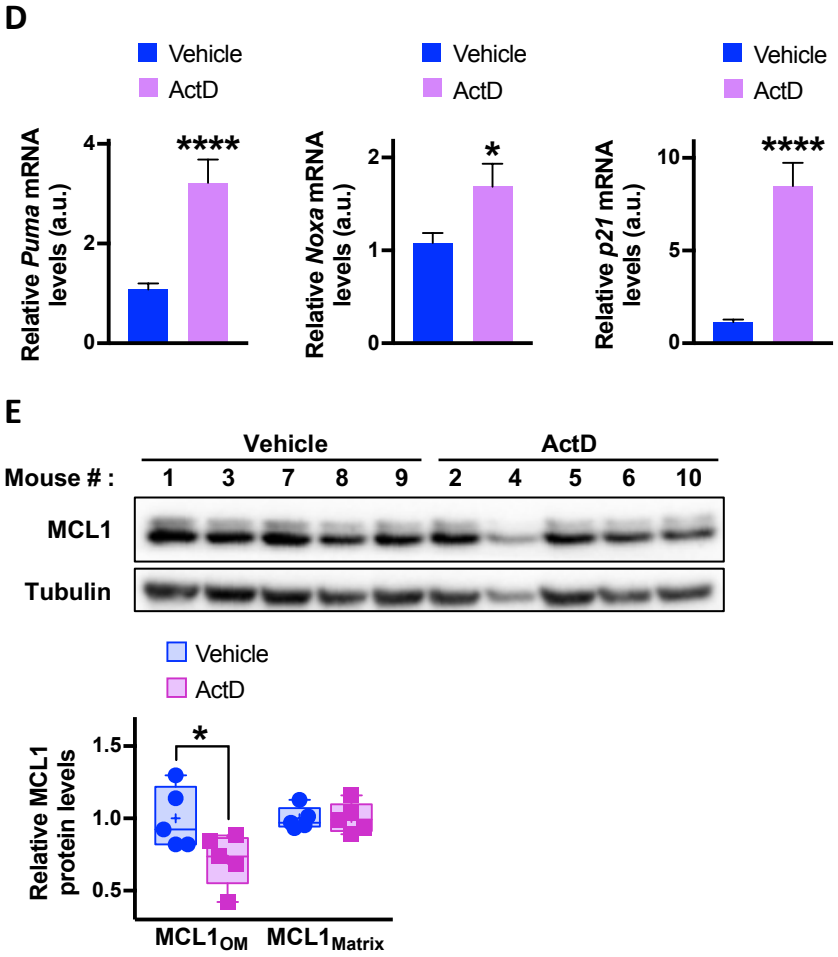


**Figure R-15. (continued) B, C.** Left panels: Histograms showing p53 fluorescence intensity acquired by flow cytometry from the *Trp53*$^{+/+}$ E$\mu$-MYC lymphoma cells (GFP+) present in the spleen (**B**) or the lymph nodes (**C**) of one representative mouse per treatment group. Right panels: graphs showing p53 mean fluorescence intensity (MFI) from the GFP+ cells, corresponding to the E$\mu$-MYC lymphoma cells, present in the spleen (**B**) or the lymph nodes (**C**) of mice analyzed in **A** acquired by flow cytometry and relative to the p53 MFI of the correspondent vehicle cohort. **D.** Relative quantification of *Puma, Noxa* and *p21* mRNA levels, respectively, from samples analyzed in **A** normalized against *ß2m* mRNA levels. **E.** Top panel: Western Blot analysis of MCL1 from samples analyzed in **A**. Each lane corresponds to the spleen homogenate of an individual mouse (n=5 per treatment group). Tubulin is shown as a loading control. Bottom panel: Quantification of both antiapoptotic ($MCL1_{OM}$, upper band) and non-apoptotic ($MCL1_{Matrix}$, lower band) MCL1 forms normalized to tubulin and relative to vehicle-treated controls. All graphs display the mean ± SEM of 4-5 mice per treatment group. Student t-test (**A-D**) and Two-way ANOVA test (**E**) were performed for statistical analyses: *, P<0.05; **, P<0.01; ****, P<0.0001.

## 9. ActD treatment suppresses lymphomagenesis and extends survival of *Trp53*$^{+/+}$ E$\mu$-MYC-lymphoma bearing mice

To further determine the therapeutic effects of ActD on lymphomagenesis, C57BL/6 Ly5.1 mice harboring either *Trp53*$^{+/+}$ or *Trp53*$^{-/-}$ E$\mu$-MYC lymphoma cells were administrated with either the vehicle or 0.100 mg/kg ActD daily. After three days, animals were evaluated by flow cytometry for white blood cells (WBCs) count **(Fig. R-16A)**, lymphocytes number **(Fig. R-16B)**, and circulating *Trp53*$^{+/+}$ or *Trp53*$^{-/-}$ E$\mu$-MYC lymphoma cells **(Fig. R-16C)**. The three parameters were significantly reduced in mice harboring *Trp53*$^{+/+}$ E$\mu$-MYC lymphoma cells treated with ActD, but there was no impact on those harboring *Trp53*$^{-/-}$ E$\mu$-MYC lymphoma cells **(Figs. R-16A-C)**. This was particularly true in the case of circulating *Trp53*$^{+/+}$ E$\mu$-MYC lymphoma cells, which were undetectable after ActD treatment **(Figs. R-16C, D)**. Finally, ActD treatment appears to be selective for malignant cells, since it had no deleterious effect on the wt-B cell population nor on non-B cell populations of neither *Trp53*$^{+/+}$ nor *Trp53*$^{-/-}$ E$\mu$-MYC-lymphoma bearing mice **(Figs. R-16D, E)**.

Strikingly, C57BL/6 Ly5.1 recipient mice harboring *Trp53*$^{+/+}$ E$\mu$-MYC lymphomas dramatically benefited from ActD treatment, increasing their lifespan ~3-fold during the treatment period, as compared to their corresponding vehicle-treated controls **(Fig. R-17A)**. Indeed, median survival of non-treated cohort was achieved before any of the ActD-treated mice started to succumb to lymphomas **(Fig. R-17A)**. By contrast, ActD did not confer any survival advantage in *Trp53*$^{-/-}$ E$\mu$-MYC lymphoma-transplanted mice, which all succumbed to lymphomas 14 days after the initial tail-vein injection **(Fig. R-17A)**. ActD administration was scheduled in three discontinuous cycles separated by drug holidays as a function of decreased body weight **(Fig. R-17B)**. With the exception of one animal, all ActD-treated *Trp53*$^{+/+}$ E$\mu$-MYC lymphoma-transplanted mice started to succumb to lymphomas around one week after treatment cessation **(Fig. R-17A)**. Therefore, ActD treatment selectively kills *Trp53*$^{+/+}$ lymphoma cells and promotes lymphoma regression and extends the survival of E$\mu$-MYC-lymphoma bearing mice in a p53-dependent manner.

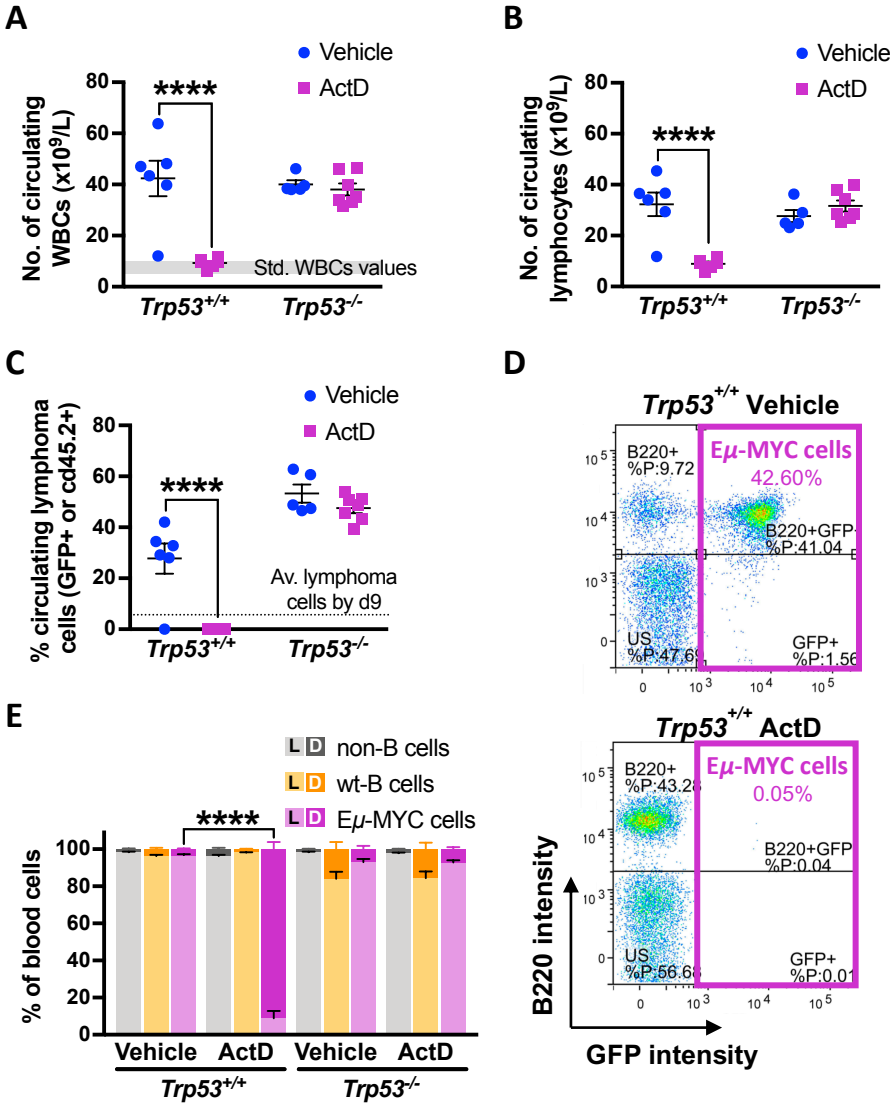


**Figure R-16. ActD treatment promotes lymphoma regression in *Trp53*$^{+/+}$ but not in *Trp53*$^{-/-}$ Eμ-MYC-transplanted mice by selectively killing *Trp53*$^{+/+}$ Eμ-MYC lymphoma cells.** **A.** White blood cells (WBCs) count, **B.** lymphocytes count and **C.** percentage of lymphoma cells at 13 days (d13) post-transplant. Tumor burden was determined by flow cytometry as the percentage of viable (PI-) *Trp53*$^{+/+}$ (B220+ GFP+) or *Trp53*$^{-/-}$ Eμ-MYC cells (B220+ cd45.2+) in peripheral blood of *Trp53*$^{+/+}$ or *Trp53*$^{-/-}$ Eμ-MYC-bearing mice, respectively, treated with either vehicle or ActD. Normal WBCs values in non-transplanted C57BL/6 mice are shadowed in grey (**A**), and % of lymphoma cells at d9 post-transplant (**C**) are indicated. **D.** Representative FACS plots from peripheral blood of *Trp53*$^{+/+}$ Eμ-MYC-bearing mice treated with vehicle (top panel) or ActD (bottom panel) at 13 days (d13) post-transplant. Gates indicate the Eμ-MYC lymphoma cell population (PI- B220+ GFP+ cells). (See next page)

**Figure R-16. (continued) E.** Graph displaying percentage of live (PI-) and dead (PI+) wt-B (B220+ GFP- or B220+ cd45.2-), non-B (B220- GFP- or Cd45.2-) and E$\mu$-MYC lymphoma (GFP+ or cd45.2+) cells determined by flow cytometry analyses in the peripheral blood of mice analyzed in **A**. D and L refer to dead and live cells, respectively. In all graphs mean ± SEM is indicated (n=5-7 mice per treatment group). Student t-test (**A-C**) or Two-way ANOVA test (**E**) were performed for statistical analyses: ****, P<0.001.

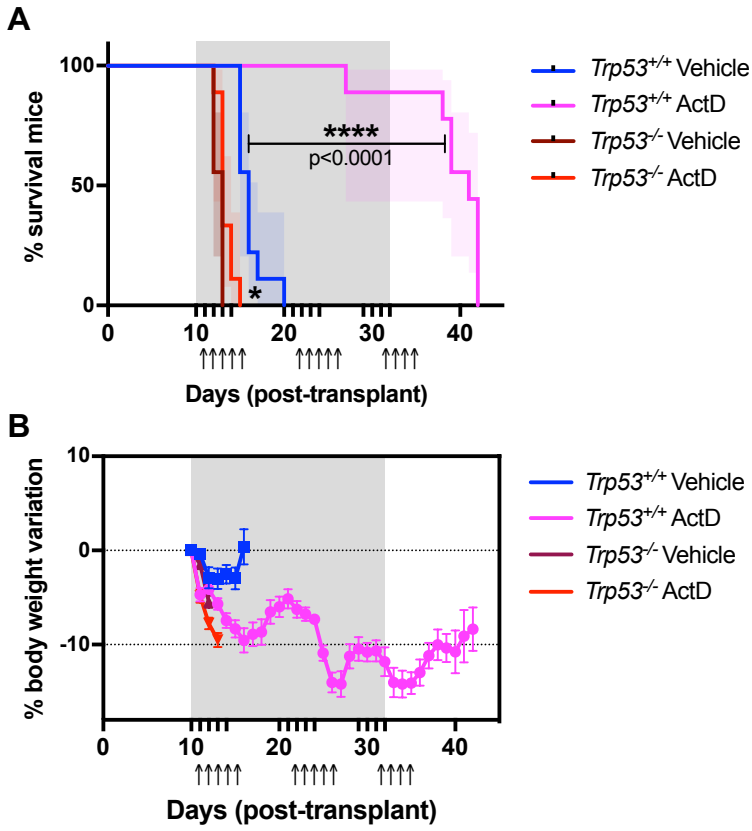


**Figure R-17. ActD treatment extents survival of *Trp53*$^{+/+}$, but not of *Trp53*$^{-/-}$ Eμ-MYC-lymphoma transplanted mice. A.** Kaplan-Meier survival curve of C57BL/6 Ly5.1 mice transplanted with either *Trp53*$^{+/+}$ or *Trp53*$^{-/-}$ Eμ-MYC lymphoma cells treated with ActD (0.100 mg/kg) or its corresponding vehicle, as indicated. **B.** Body weight variation of C57BL/6 Ly5.1 mice harboring *Trp53*$^{+/+}$ or *Trp53*$^{-/-}$ Eμ-MYC lymphoma cells following ActD-treatment, as indicated. For the *Trp53*$^{-/-}$ Eμ-MYC lymphoma cohort, only 3-4 days were recorded as they succumbed to the lymphoma by day 13-14, as displayed in **A**. Data shows average values ± SEM (n=9 mice per treatment group). Grey shadowed zone denotes treatment period with arrows indicating dosing days. For **A**, 95% confidence interval (CI) for each curve is shadowed in its respective color. Statistical analysis was carried out for each pair of vehicle and ActD-treated group by using the log-rank (Mantel-Cox) and Gehan-Breslow-Wilcoxin test: *, P<0.05; ****, P<0.0001.

# DISCUSSION

# Discussion

Earlier studies have shown that MYC-driven B-cell lymphomas rely on elevated levels of RiBi to drive aberrant rates of protein synthesis required for the accelerated growth an proliferation of malignant cells (Barna et al., 2008, van Riggelen et al., 2010). This opened an avenue for therapeutic intervention targeting RiBi. However, it is unclear whether RiBi inhibition induces MYC-tumor regression by decreasing translational capacity (Barna et al., 2008) and/or by stabilizing the tumor suppressor p53 (Macias et al., 2010) mediated by the IRBC, as we have shown for the depletion of other RPs (Donati et al., 2013). Here, we address the paradigm concerning the role of the IRBC in the context of impaired RiBi by generating a model in which we could induce an shRNA to either RPL7a or RPL11, the latter an essential component of the IRBC, in E$\mu$-MYC lymphoma cells. We demonstrate that: (**1**) Partial depletion of either 60S RPL7a or RPL11, to a similar level to that of the Bst mouse employed by Barna and co-workers, reduced protein synthesis, RiBi and proliferation equivalently, however, (**2**) only RPL7a depletion, but not RPL11, leads to p53 stabilization, caspase-3 cleavage and apoptosis mediated by the activation of the IRBC. Furthermore, we show that (**3**) the IRBC induced apoptosis is associated with the selective degradation of antiapoptotic form of MCL1 and (**4**) in a preclinical setting that low concentrations of ActD, an FDA approved drug for cancer which disrupts RiBi, efficiently kills *Trp53*$^{+/+}$, but not *Trp53*$^{-/-}$ E$\mu$-MYC lymphoma cells, extending their mouse survival. Overall, activation of this checkpoint in the context of MYC-driven tumors elicits a strong p53-dependent apoptotic response which is mediated by the loss of antiapoptotic MCL1.

## Activation of the IRBC pathway in response to RiBi impairment

### *What are the cellular consequences of RiBi impairment in Eμ-MYC cells?*

The first evidence of the existence of a checkpoint monitoring RiBi came at the beginning of the century, when our laboratory reported that the conditional deletion of the 40S RPS6 in the liver of adult mice impairs hepatocytes proliferation after hepatectomy, failing to restore the loss liver mass, but not the growth of resident hepatocytes following a nutrient fasting-refeeding regime (Volarevic et al., 2000). These findings suggest that ribosome content is not limiting for protein synthesis and liver growth, but that RiBi inhibition triggers an active cell cycle checkpoint that arrests the proliferation of hepatocytes. A similar response was observed in normal T lymphocytes, where the deletion of one *Rps6* allele led to G1-to-S-phase cell cycle arrest correlating with an increase in p21 expression (Sulic et al., 2005), as we observed in the context of RPL7a-depleted E$\mu$-MYC cells **(Fig. R-3A)**. In line with prior observations, total protein content of T cells was not affected following reduction of RPS6 (Sulic et al., 2005). Like in hepatocytes, despite the lesion in nascent 40S RiBi, the number of residual ribosomes is sufficient for normal cell growth in T cells. Here, we show in E$\mu$-MYC lymphoma cells that partial depletion of either 60S RP, RPL7a or RP11, induces a lesion in 60S RiBi **(Figs. R-1B, C)** sufficient to cause a significant reduction in nascent protein synthesis **(Fig. R-2A)**. Therefore, it appears that in the MYC tumorigenic context, the number of pre-existing ribosomes is insufficient to maintain both increased aberrant proliferation and protein synthesis, supporting the strong dependency of MYC-driven tumors on increased levels of RiBi, as previously suggested by Barna et al., in 2008.

Later studies performed in our laboratory demonstrated that the cell cycle checkpoint elicited upon RPS6 depletion, was mediated by the stabilization of p53 and that it is not the number of ribosomes that the cell monitors, but nascent RiBi (Fumagalli et al., 2009). The p53 response could be recapitulated in cell culture by the depletion of other RPs of either the 40S or 60S ribosomal subunit, but not by depletion of RPL5 or RPL11. Moreover co-depletion of either RPL5 or RPL11 prevented the p53 response induced by the depletion of other RPs, without further affecting protein synthesis capacity (Fumagalli et al., 2009, Fumagalli et al., 2012,

Teng et al., 2013). Finally subsequent studies showed that three components that make up the pre-ribosomal complex, RPL5, RPL11 and 5S rRNA, which are normally incorporated into the 60S ribosomal subunit, mediated this anti-proliferative response (Donati et al., 2013). The model argues that conditions that disrupt RiBi, such as the depletion of an essential RP, promotes the redirection the nascent 5S rRNA/RPL5/RPL11 RNP, from its incorporation into the nascent 90S processome, to the binding and inhibition of MDM2. Binding of this complex, that we termed the IRBC complex (Gentilella et al., 2017), to MDM2 inhibits its E3-ligase activity towards p53, promoting p53 stabilization, which leads to cell cycle arrest, cell death or senescence, depending on the cell context. In support of this model we show that activation of the IRBC, elicits p53-dependent apoptosis in the context of MYC-driven tumors, suggesting that the IRBC, has as important role in mediating tumor suppression, as discussed later.

Despite proliferation rates being reduced to a similar extent in both RPL7a and RPL11 E$\mu$-MYC lymphoma cells, in the latter, the IRBC is not involved, as we do not observe its activation, p53 stabilization or p21 induction **(Fig. R-3A)**. Therefore, it is likely that upon RPL11 depletion proliferation of E$\mu$-MYC lymphoma cells is not arrested, but its rate is delayed. As there is a lesion on RiBi, new ribosomes are supplied at a lower rate, decreasing the pace of translation, as observed by the reduction of nascent protein synthesis **(Fig. R-2A)**. A reduced translation capacity delays the progression of these cells through the cell cycle. This is consistent with previous observations made in our laboratory in primary human fibroblasts, in which depletion of RPL11 does not induce cell cycle arrest, but slows down progression of cells through all phases of the cell cycle (Teng et al., 2013). Two conclusions arose from the Teng et al. study, (**1**) ribosome content, depending on cell context, can be limiting for protein synthesis capacity in proliferating mammalian cells, as occurs in yeast (Shah et al., 2013), and (**2**) upon reduced translation capacity cells adapt by adjusting the rate of proliferation. Our findings corroborate the first observation of Teng, but in contrast to his second observation in primary human fibroblasts, we observed that prolonged depletion of RPL11 leads to apoptosis in *Trp53*$^{+/+}$ E$\mu$-MYC lymphoma cells **(Fig. R-5A)**, presumably without p53 stabilization. Thus, it is likely that MYC tumor cells cannot overcome a chronic reduction in their translation rates, and undergo apoptosis through a p53-independent mechanism. MYC is known to directly regulate certain

members of the BCL2 family. Among them, it has been recently found that the proapoptotic BH3-only member, BIM, is able to induce apoptosis in a p53-independent manner in response to DNA damage (Delbridge et al., 2016). Thus, it might be a potential candidate to mediate p53-independent cell death upon prolonged RiBi impairment in the absence of the IRBC. In addition, it seems that the two mechanisms act in an orchestrated, time-dependent manner, ultimately leading to MYC tumor regression but that, as the RiBi lesion triggers the IRBC, the second mechanism does not have sufficient time to be evoked.

### *What is sensed by the cell to elicit the IRBC?*

Notably, even a partial reduction in RPL7a synthesis induces the IRBC although the 60S ribosomal subunits are still synthesized, but to a lesser extent **(Figs. R-1A, B)**, which supports the hypothesis that the IRBC is exerted at initial time points following impaired RiBi. How is the 5S rRNA/RPL5/RPL11 redirected to the IRBC in this context? The homologue of RPL7a in yeast, Rpl7a, is involved in the early steps of assembly of the 60S pre-ribosomal subunit (de la Cruz et al., 2015) and we previously showed that defects in RPL7a synthesis block subsequent maturation of the 60S ribosomal subunit in mammalian cells (Fumagalli et al., 2009). Therefore, if RPL7a synthesis is reduced, the rate of production of functional 60S ribosomal subunits is also decreased. The remaining RPs, which are likely to be synthesized at normal rates, will be rapidly degraded by the UPS if they cannot be incorporated into the nascent 60S ribosomal subunit (Lam et al., 2007, Sung et al., 2016), with the exception of RPL5 and RPL11, which under conditions that disrupt RiBi, are protected from degradation (Bursac et al., 2012) in a complex together with 5S rRNA (Donati et al., 2013, Sloan et al., 2013). Therefore, it has been assumed that the accumulation of this nascent pre-ribosomal 5S rRNA/RPL5/RPL11 complex is redirected to bind and inhibit MDM2, resulting in the activation of the IRBC. However, as we previously showed, depletion of a 40S RP inhibits the production of 40S ribosomal subunits and induces the IRBC without altering the production of the 60S subunit and thus the continuous incorporation of the pre-ribosomal 5S rRNA/RPL5/RPL11 complex into the nascent large subunit (Fumagalli et al., 2009, Fumagalli et al., 2012). How is the checkpoint elicited if the synthesis of the 60S subunit is not delayed and the nascent 5S rRNA/RPL5/RPL11 complex is incorporated into the 60S subunit at normal rates? The

studies developed by our laboratory demonstrated that impaired 40S RiBi leads to the translational upregulation of RPL11, generating sufficient RPL11 protein to bind MDM2, while upon impairment of 60S RiBi, such upregulation is not observed. However, as no new 60S ribosomes are produced, there is no competition for RPL11 (Fumagalli et al., 2009). These findings suggest that the IRBC is regulated in an independent manner depending on which subunit is affected. In support to this hypothesis, we later showed that abrogation of both 40S and 60S RiBi results in translational upregulation of RPL11, a more potent inhibition of MDM2, an additive effect on p53 stabilization and a more severe cell cycle arrest (Fumagalli et al., 2012). Although the additive effect on p53 stabilization and the stronger inhibition of MDM2 is consistent with an independent regulation of the IRBC depending on the initial insult, a recent study developed in our laboratory demonstrated that the model proposed by Fumagalli regarding RPL11 translational regulation was incorrect. Contrary to his observations, depletion of a RP from either subunit results in a similar re-distribution of *RPL11* mRNA on the polysomal fractions, whose mean size is globally decreased as compared to control cells (Gentilella et al., 2017). These findings suggest that abrogation of RiBi of either subunit conversely results in a reduction of 5'TOP mRNAs translation, i.e., in a decrease in the synthesis of RPs, including that of RPL5 and RPL11 (Gentilella et al., 2017). Therefore, the accumulation of the IRBC complex, following abrogation of either 40S or 60S RiBi, appear to result from an enhanced protection of RPL5 and RPL11 against degradation, as reported by Bursac and colleagues (Bursac et al., 2012). It may be possible that the differential components that make-up the IRBC complex, in comparison to the nascent 5S rRNA/RPL5/RPL11 complex which is incorporated into the 90S processome, are responsible for the stabilization of RPL5 and RPL11 following RiBi impairment. To address this question, it will be critical to decipher the mechanism(s) leading to the conversion of the 5S rRNA/RPL5/RPL11 complex into the IRBC complex, to identify the novel components associated and/or whether it is post-translationally modified, and if such changes vary depending on the RiBi insult.

### *Why partial RPL11-depletion does not trigger the IRBC? What do we know about the assembly of RPL11 onto the 90S processome?*

Intriguingly, partial depletion of RPL11, which reduces the rate of 60S ribosome subunit synthesis to a similar extent to that of partial RPL7a depletion **(Fig. R-1C)**, does not trigger the IRBC **(Fig. R-3B)**, despite the continued synthesis of RPL11 at a lower rate. This observation is consistent with a previous study developed by Morgado-Palacin et al., who showed that deletion of one *Rpl11* allele in MEFs, did not apparently induce the IRBC, as basal levels of p53 did not rise, despite 50% of RPL11 synthesis remaining and the apparent lesion in RiBi, shown by the accumulation of the unprocessed 32S precursor rRNA (Morgado-Palacin et al., 2015). It could be argued that the remaining 60S ribosomal subunit biogenesis consumes all the available RPL11 and thus, the complex cannot be formed. Likewise, partial RPL5 depletion in mouse embryonic stem cells (mESCs) and in human BC cell lines fail to elicit a p53 response (Singh et al., 2014, Fancello et al., 2017), presumably due to a failure in the formation of the IRBC. It seems that alterations in any of the components of the IRBC complex are not sensed by this mechanism. Therefore, when RPL11 or RPL5 are partially depleted, the 5S rRNA/RPL5/RPL11 complex continues assembling in the 90S processome but at a lower rate, which slows-down the rate of 60S RiBi and thereby delays the maturation of the 60S subunit. In this context, the remaining RPLs, produced at a normal rate, are likely degraded by the UPS (Lam et al., 2007, Sung et al., 2016) but the IRBC fails to be elicited. By contrast, when a RP from either subunit, except RPL5 and RPL11, is insufficient, alterations in the rate of 40S or 60S RiBi are sufficient to actively redirect a certain amount of this 5S rRNA/RPL5/RPL11 complex to bind an inhibit MDM2. Indeed, even if 60S RiBi is affected the complex is accumulated in the free-ribosomal fraction, protected from degradation (Bursac et al., 2012), which evidences that the IRBC is elicited in an active manner and that it possibly requires the association of a distinct set of proteins than those required for the assembly of the 5S rRNA/RPL5/RPL11 complex into the 90S processome.

### *How the RiBi stress signal is transduced to trigger the IRBC?*

Recently, Zheng and co-workers resolved the crystallographic structure of the RPL11-MDM2 complex, showing that MDM2 mimics the 28S rRNA binding site for RPL11 on the 90S processome (Zheng et al., 2015). Thus, how is the decision whether RPL11 will bind to the 28S rRNA or MDM2 made? It might be possible that, upon conditions that impair RiBi, the RPL11-binding region of 28S rRNA becomes less accessible, favoring the binding of RPL11 to MDM2. Further studies in yeast led to the identification of a protein termed Symportin 1 (Syo1) as the chaperone that protects the pre-ribosomal 5S rRNA/RPL5/RPL11 complex until it is delivered to the 90S processome in the nucleolus (Kressler et al., 2012). Syo1 binds independently RPL5 and RPL11 in the cytoplasm and the Syo1/RPL5/RPL11 complex is then recognized by importin Kap104, which mediates its nuclear import. In the nucleus, Kap104 is released and, concomitantly, the 5S rRNA is incorporated in the complex constituting the pre-ribosomal 5S rRNA/RPL5/RPL11/Syo1 particle (Kressler et al., 2012). Structural data suggest that the binding of 5S RNA induces a conformational change of both RPL11 and RPL5 which allows its assembly into the 90S processome (Calvino et al., 2015). The integration of the 5S rRNA/RPL5/RPL11 complex in the 90S processome is mediated by a complex formed by the RAFs Rpf2 and Rrs1 in yeast (Zhang et al., 2007), which presumably induce the dissociation of Syo1, unmasking the binding site on RPL11 for the 25S pre-rRNA, corresponding to the human 28S rRNA (Calvino et al., 2015). Notably, Syo1 and the 25S pre-rRNA bind RPL11 at the same site as MDM2 (Zheng et al., 2015). Therefore, it is likely that Syo1 preferentially directs the pre-ribosomal 5S rRNA/RPL5/RPL11 complex to the assembly into the 90S processome and not towards the IRBC complex. However, it will be important to determine whether in the absence of Syo1 and upon conditions that impaired RiBi the IRBC complex can or not bind MDM2, to determine whether Syo1 is necessary for the IRBC formation and likewise, whether its mammalian homolog, HEAT repeat-containing protein 3 (HEATR3), has analogous function.

In human cells BDXC1 and RRS1, the homologs of the RAFs Rpf2 and Rrs1 in yeast, also mediate 5S rRNA/RPL5/RPL11 assembly into the 90S processome together with the tumor suppressor PICT1, which binds the pre-ribosomal 5S rRNA/RPL5/RPL11 complex via 5S rRNA (Sloan et al., 2013). Like in yeast, the incorporation of this pre-

ribosomal complex into the 90S processome is required for the maturation of the 60S subunit. However, neither PICT1, nor BDXC1 or RRS1 appear to mediate the binding of the 5S rRNA/RPL5/RPL11 complex to MDM2, as their depletion efficiently induces p53 (Donati et al., 2013, Sloan et al., 2013).These studies and those of the Volarevic laboratory (Bursac et al., 2012) show that the branch point for redirection of the nascent pre-ribosomal 5S rRNA/RPL5/RPL11 complex to MDM2, resides upstream before its assembly into the 90S processome. Therefore, the characterization of the mediators that redirect the 5S rRNA/RPL5/RPL11 complex towards MDM2 prior to its assembly into the 90S processome will be important to decipher the mechanism of activation of this checkpoint.

## The role of the IRBC in human pathology

### *What are the consequences of defective RiBi?*

Ribosomes are constituted by stoichiometric amounts of RPs, although 'specialized ribosomes', containing distinct RP composition or distinct modifications of rRNA, are present in certain conditions and/or cell types, and are believed to translate specific repertoires of mRNA (reviewed in Xue and Barna, 2012, Genuth and Barna, 2018). The existence of ribosome heterogeneity under physiological conditions was disregarded for many years, as such heterogeneity had been only observed in certain human disorders globally referred as ribosomopathies. For instance, heterozygous mutations in RP genes, which are known to cause DBA **(see introduction, section 3.4.1.)**, were firstly identified in 1999, concretely in the gene encoding RPS19 (Draptchinskaia et al., 1999). RP haploinsufficiency impairs production or function of the ribosome which induces the tissue-specific defects observed in DBA (Narla and Ebert, 2010). However, the first direct evidence of functional heterogenous ribosomes came from the studies of Shi and co-workers in mESCs, in which ribosomes containing substoichometric amounts of several core RPs were argued to be specialized in the translation of a specific repertoire of mRNAs (Shi et al., 2017). This differential translation had been already suggested for RP deficiencies or defects in RAFs which result in defective ribosome assembly or alter the stability or composition of the fully assembled ribosomes depending on which particular RP or step of RiBi is affected (Steffen et al., 2012). Such defects lead to changes in the

quantity of ribosomes, their fidelity or selectivity in translating mRNAs, which may have a direct impact on the cell's pattern of protein synthesis. First demonstration that a change in the ratio of ribosomes to mRNA modify the pattern of proteins synthesized was provided by Lodish for the synthesis of the distinct hemoglobin chains (Lodish, 1974). Then, our laboratory were the first to state that the p53-mediated checkpoint monitoring RiBi was placed to prevent alternations in the pattern of translation (Volarevic et al., 2000). Now-a-days, two non-mutually exclusive models have emerged to explain how changes in cellular ribosome content or function may directly impact selective translation (reviewed in Mills and Green, 2017). First, alterations in the ratio of ribosomes per mRNA may cause changes in the pattern of translation based on competition of the mRNA pool for the available ribosomes, primarily impacting mRNAs with lower initiation rates (Khajuria et al., 2018). On the other hand, substoichometric amounts of a specific RP may lead to the presence heterogeneous ribosomes that interact with distinct affinities to a subset of mRNAs. If a certain RP has a specialized function in recruiting particular mRNAs to the ribosome, its depletion or mutation will lead to a decreased translation of those mRNAs and thereby an altered pattern of translation. In support to this hypothesis Kondrashov et al. showed that during mouse embryogenesis, depletion of *Rpl38* did not affect global protein synthesis rates but altered the translation of a subset of mRNAs that encoded *homeobox* genes (Kondrashov et al., 2011). Likewise, the leukemia-associated mutation in *RPL10* drives specific and constitutive IRES-mediated overexpression of antiapoptotic BCL2 (Kampen et al., 2019), and the DBA-associated heterozygous mutations in *RPLS19* and *RPL11* reduce IRES-mediated translation of several erythroid differentiation factors in mouse models and patient samples (Horos et al., 2012). Although it is more likely that these alterations result from the reduction in the quantity of ribosomes, the possibility that RP-deficient ribosomes actively translate a distinct set of mRNAs cannot be excluded. Importantly, an altered pattern of translation might affect essential cellular functions, including cell growth, metabolism, proliferation, differentiation and/or survival and such defects might be transmitted to daughter cells leading to pathophysiological consequences, as those observed in ribosomopathies. In addition, changes in the pattern of translation can promote malignant transformation and tumor development in the longer term (reviewed in Ruggero, 2013). Indeed,

ribosomopathies, characterized by an impaired RiBi, are associated to an increased predisposition for cancer development later in life. In several of these pathologies, such as DKC, a higher risk of tumor development has been attributed to alterations in the pattern of translation. In DKC, mutations in the gene encoding the nucleolar protein dyskerin, which catalyzes pseudouridylation of rRNA, perturb rRNA modifications leading to defects in the translation of specific IRES-containing mRNAs involved in cell cycle and apoptosis, such as p53 (Bellodi et al., 2010, Jack et al., 2011). Therefore, it is likely that cells are not able to sense changes in the pattern of translation, but do through alterations in RiBi, thus the IRB is placed to prevent from the transmission of altered ribosomes to daughter cells, which may give rise to protein synthesis infidelity and eventually to malignant transformation and thereby evidencing a role for the IRBC in preventing tumorigenesis.

In the context of the studies summarized above it must also be noted that RiBi is the most energy-consuming process in a cell (Schmidt, 1999, Warner, 1999), the IRBC checkpoint might be elicited to preserve energy and cellular resources expenditure when an imbalance in ribosomal components occur. However, in this context, the direct shut-down of the production of ribosomal subunits by the IRBC would be more efficient, which is not the case. It is likely that ribosomal subunits or certain RPs, have additional extra-ribosomal functions critical for proper cell function, beyond the those described here for RPL5 and RPL11 in the regulation of p53 stability (reviewed in Warner and McIntosh, 2009, Zhou et al., 2015). For instance, RPS25 plays a specialized role in translation initiation of specific IRES-dependent mRNAs (Hertz et al., 2013). RPL5, RPL11 and RPS14 are also involved in the regulation of MYC activity and stability. RPL11 binds MYC at promoter regions of *MYC*-target genes, inhibiting their transcription (Dai et al., 2007, Dai et al., 2010). Also, together RPL5 and RPL11 bind to the *MYC* mRNA and guide it to the RISC for degradation (Liao et al., 2014). A similar role has been described for RPS14 (Zhou et al., 2013). These findings provide important evidence for extra-ribosomal functions of RPs in preventing tumorigenesis. Therefore, the identification of other roles of specific RPs, or of the 40S and 60S ribosomal subunits beyond translation, may help to understand what is sensed by the cell as a damage to RiBi. Likewise, such an understanding would provide insights into the mechanism of pathogenesis of certain diseases such as ribosomopathies and cancer.

### *Is the IRBC involved in the defects observed in Ribosomopathies?*

In the past decade the RiBi process and its regulation has gained prominent attention due to its emerging role in specific cellular processes and human pathology. The severe, and sometimes lethal, consequences of RiBi defects are well-reflected in ribosomopathies, such as *5q-* syndrome and DBA. Both pathologies are characterized by severe macrocytic anemia and bone marrow failure and are largely caused by the heterozygous loss-of-function mutations in certain RP genes, resulting in RP haploinsufficiency (Narla and Ebert, 2010, Fumagalli and Thomas, 2011). In both syndromes, RP haploinsufficiency selectively reduces the number of erythroid progenitor cells in the bone marrow of patients and compromises the production of hemoglobin, leading to the accumulation of free heme in these cells. Free heme is highly toxic for the cells, as it catalyzes the generation of reactive oxygen species (ROS) (Jeney et al., 2002). It has been proposed that accumulation of ROS produces oxidative damage that causes apoptosis of the erythroid progenitors and the severe anemia characteristic of these pathologies (Keel et al., 2008). However, it is not clear whether heme-induced oxidative stress is linked to the accumulation of p53 observed in bone marrow samples of DBA patients (Dutt et al., 2011), as heme-induced erythroid cell death is likely independent of p53 (Doty et al., 2019). The importance of elevated p53 levels in the apoptotic phenotype of these precursors has been demonstrated in different model systems of DBA (Danilova et al., 2008, Barlow et al., 2010a, Jaako et al., 2011, McGowan et al., 2011). In such models, deletion of p53 was found to reverse not only the hematopoietic defects, but also other tissue-specific morphological defects, such as brain/craniofacial abnormalities, growth retardation (Danilova et al., 2008) and skin hyperpigmentation (McGowan et al., 2011), all associated with RP haploinsufficiency. In support of a key role of activated p53 in this pathology, as a consequence of RPs haploinsufficiency, a later study by Jaako et al., reported that crossing *Rps19*-deficient mice with *Mdm2*$^{C305F}$ *knock-in* mice partially prevented p53-dependent erythropoietic dysfunction (Jaako et al., 2015). The study also demonstrates the contribution of IRBC to the erythroid pathology (Jaako et al., 2015). However, as the rescue was only partial, the involvement of other pathways to the induction of p53 and the erythroid pathology in DBA patients, besides the IRBC , cannot be discarded. Whether a p53-independent

mechanism is involved in the erythroid pathology must still rigorously validated (Torihara et al., 2011, Singh et al., 2014). In addition, mutations in RPL5 and RPL11, the two RP components of the IRBC, have been also identified in DBA patients, correlating with more severe developmental defects (Gazda et al., 2008). It might be possible that, in the case of DBA caused by RPL5 or RPL11 haploinsufficiency, p53 accumulates through a distinct mechanism. Indeed, accumulation of p53 might be attributed to the upregulation of ARF-MDM2 signaling, as was previously reported in HPCs derived from DBA patients (Gazda et al., 2006), or to the upregulation of the DNA damage response, as reported in RPS19-deficient human cells and in zebrafish models of DBA caused by a deficiency in RPL11 (Danilova et al., 2014). Altered nucleotide metabolism and ROS might also contribute to p53 activation upon RP-depletion (Danilova and Gazda, 2015). Therefore, distinct mechanisms might cooperate to induce p53 under RP insufficiency depending on the species and/or on which particular RP is involved. In the case of DBA caused by mutations in RPL5 or RPL11, it is also possible that p53-independent mechanism(s) contribute(s) to the pathogenesis. The pathological manifestations of the disease might therefore be attributed to a global or selective inhibition of protein synthesis or to defects in pre-rRNA processing and 60S ribosome assembly finally leading to erythroid progenitor cells death. A recent study developed by Khajuria and colleagues, shed some light on the subject. They found that, alterations in translation, due to reduced ribosome content in cells with DBA-associated lesions, were responsible for the erythroid defects although the failed to examine p53 (Khajuria et al., 2018). In their hands, RP haploinsufficiency results in a decreased translation of important transcripts involved in the differentiation of the erythroid linage, among them *GATA1*, whose downregulation impairs commitment of human hematopoietic stem and progenitor cells (HSPCs) into the erythroid lineage (Khajuria et al., 2018). Likewise, impaired translation of specific transcripts may also play a role in mediating DBA-associated phenotypes non-related to the hematopoietic tissue, such as thumb abnormalities and other congenital defects (Gazda et al., 2008). Therefore, alteration of translation may play a prominent role in DBA patients with RPL5 or RPL11 defects, as they tend to have congenital phenotypes more severe than those observed with other RP gene mutations (Gazda et al., 2008). It will be important to further establish the role of the IRBC and of p53 activation in DBA and why certain tissues or cell types, such as

erythroblasts, are much more sensitive to ribosome haploinsufficiency and p53 activation.

### *Why certain cell types are more sensitive to RiBi impairment?*

Recent observations have provided some evidence concerning the cause of the selective sensitivity of the erythroid precursors in DBA pathogenesis. First, Dutt el al. demonstrated in 2011 a selective effect of RP haploinsufficiency on p53 activation in human CD34+ HSPCs induced to differentiate along the erythroid linage (Dutt et al., 2011). Cells committed to differentiate require higher levels of protein synthesis than their corresponding undifferentiated stem cells and thus, differentiation implies a dramatic change in protein synthesis rates (Buszczak et al., 2014, Signer et al., 2014). Although few studies have queried this aspect, translational output is likely to play a key role in the upregulation of protein expression during embryonic stem cell (ESC) differentiation, in addition to transcription reprogramming (Sampath et al., 2008, Ingolia et al., 2011, Khajuria et al., 2018). Efficiency of translation largely depends on the availability of translational machinery components such as translational factors, tRNAs and aa-tRNA synthetases and the availability of ribosomes. Initiation is assumed to be the rate-limiting step for translation, which largely depends on the availability of mature 40S ribosomal subunits, as they are the key hub for subsequent association of eIFs, mRNAs, and the 60S ribosomal subunit (Strunk et al., 2012). In certain cells, such as progenitor cells committed to differentiate, in which the demand of active ribosomes is especially high and which are extremely sensitive to changes in translational rates, the production of competent ribosomes is crucial (Zhang et al., 2014, Sanchez et al., 2016). This may explain why such cells are particularly sensitive to alterations in the RiBi pathway although the contribution of additional factor, such as environmental cues, to the enhanced susceptibility of erythroid precursor cells to p53 activation cannot be excluded. In parallel, the study developed by Morgado-Palacin et al. in mESCs, showed that these cells, as well as induced pluripotent stem cells (iPSCs), characterized by extremely rapid proliferation rates with doubling times of 8-10 hr or even lower, are particularly susceptible to alterations in RiBi (Morgado-Palacin et al., 2012). Thus, the IRBC is placed as a quality checkpoint to sense whether a cell is ready to undergo intense proliferation and/or to conditions which demand a highly active production of new ribosomes. This role

for the IRBC explains the selectivity of certain cell types to RiBi and p53 activation, as is the case of the Eμ-MYC lymphoma cells, whose fast proliferation strongly depends on high rates of RiBi, and which are also extremely sensitive to RiBi impairment, rapidly undergoing IRBC-induced p53-dependent cell death within only 4 hr following rRNA synthesis inhibition by ActD **(Figs. R-4A-C)**.

### *Is the IRBC an active mechanism against MYC-driven tumorigenesis?*

In 2010, Macias et al. provided the first evidence of the role of the IRBC as a tumor suppressor barrier, when they showed that Eμ-MYC mice harboring the C305F mutation in MDM2, which impedes the binding to RPL11 and the inhibitory effect of the IRBC complex, succumbed much earlier to lymphoma than their wt counterparts (Macias et al., 2010). The same mutation has been related to accelerated tumor development in the distal colon of *Apc+/min* mice, induced by deregulated MYC signaling (Liu et al., 2017). Thus, the checkpoint not only monitors defective RiBi but also exacerbated ribosome production, as that induced by oncogenic MYC. Likewise, a study by Nishimura et al. in 2015 suggested that the IRBC might prevent tumorigenesis via induction of senescence upon replicative and oncogenic stress (Nishimura et al., 2015). In support to Macia's hypothesis, we observed a constitutive association of MDM2 with RPL5 and RPL11 in the free non-ribosomal fraction of control Eμ-MYC cells **(Fig. R-3B)**, which correlates with a basal activation of p53 and basal levels of apoptosis in these cells **(Figs. R-3A and 4B)**. To explain these findings, it has been suggested that, in MYC-driven tumors, MYC induces the overexpression of RPL11, RPL5 and the increased transcription of 5S rRNA, resulting in the accumulation of the free pre-ribosomal 5S rRNA/RPL5/RPL11. This complex, then may bind MDM2 and promote IRBC-mediated p53 stabilization, suppressing MYC-driven oncogenesis, but not to a level sufficient to counteract its full oncogenic potential. However, if MYC drives to the same extent all RPs, all the available RPL5 and RP11 would be expected to be consumed in the generation of new ribosomes as are other RPs, inhibiting IRBC formation, as suggested by others (Donati et al., 2011, Brighenti et al., 2014).. However, a study developed by our group this year shed light on the role of the IRBC in response to MYC-induced tumorigenesis. In a MYC-inducible system in the presence of serum, the oncogene induces the expression of RPL5 and RPL11, which correlates with an increased RiBi. In parallel, induction of MYC

leads to the activation of p53 and to slower rates of proliferation, consistent with the passive activation of the IRBC as part of an intrinsic tumor suppressor response. However, such treatment, does not lead to the accumulation of RPL5 and RPL11 in the free ribosomal fraction, but does induce an increase in the formation of the IRBC, as shown by the dramatic enhancement of the co-immunoprecipitation of MDM2, RPL11 and 5S rRNA with endogenous RPL5 (Morcelle et al., 2019). These studies argue for an active mechanism leading to the formation of the IRBC complex upon conditions of hyperactive RiBi (Morcelle et al., 2019).

Intriguingly, we observe that following RPL7a-depletion or ActD treatment, p53 is associated with the IRBC complex **(Figs. R-3B and 4C)**, thus, the binding of the IRBC complex to MDM2 does not disrupt p53-MDM2 interaction, while the inhibition of the E3 ligase activity of MDM2 is sufficient to stabilize p53. Can p53 bind to its target gene promoters when bound to MDM2? Is it possible that it transactivates distinct targets than the p53 protein unbound to MDM2? Is it finally released from the MDM2 in order to transactivate its target genes? The study developed by Bursac and co-workers, in 2012, provided some insights regarding these questions. They found increased levels of acetylated p53 re-localizing to the nucleoli following RiBi impairment, associated together with MDM2, RPL5, RPL11 and nucleolar promyelocytic leukemia (PML) protein (Bursac et al., 2012). PML is a nuclear matrix-bound protein which organizes particular subnuclear structures termed 'nuclear bodies' and that contains binding motifs for p53 and MDM2 (Salomoni and Pandolfi, 2002). PML is known to regulate p53 acetylation at several lysine residues through the recruitment of CBP under certain stress conditions, increasing DNA binding and transcriptional activity of p53 (Pearson et al., 2000, Salomoni and Pandolfi, 2002). Thus, PML-mediated acetylation of p53 within the IRBC complex is likely to mediate p53 transcriptional activation in response to RiBi impairment. Further characterization of the partners associated to the IRBC complex and of the modifications to which p53 is subjected, will help to solve this paradigm and may provide clues in the differential responses elicited by p53 in response to the activation of the IRBC.

### *Why does RP haploinsufficiency cause cancer?*

Paradoxically, patients with ribosomopathies, in which loss-of-function mutations of certain RPs or RAFs genes inhibits cell proliferation, have increased predisposition to both solid and hematological tumors through their lifetimes (Narla and Ebert, 2010, Vlachos et al., 2012), up to 200-fold for certain cancer types (Sulima et al., 2019). Likewise, somatic mutations and deletions affecting RPs genes are frequently found in certain cancers such as T-ALL, accounting for a 20% of the cases, and CLL, among others, with the most frequent mutations affecting RPL10, RPL22, RPL5 and RPL11 in T-ALL, and RPS15 in CLL (Fancello et al., 2017). However, how cells bearing a deficiency in a RP which growth slow and normally triggers p53 and cell cycle arrest, as observed in most ribosomopathies, can survive in the presence of wt cells, which could out grow them, and finally favor the development of a disease such as cancer? First question was addressed by a study developed by Schneider et al., who observed that the expression of proteins involved in innate immune system activation are induced in erythroblasts, monocytes and macrophages from mice bearing a heterozygous deletion of *Rps14* in HSPCs, which recapitulate *5q-* MDS (Schneider et al., 2016). Activation of these proteins in erythroblasts blocks terminal erythroid differentiation and induces p53-dependent apoptosis of the erythroid progenitor cells, recapitulating the erythropoietic defects observed in patients with *5q-* syndrome (Schneider et al., 2016). By contrast its increased expression in macrophages and monocytes contributes to the release of pro-inflammatory cytokines that exerts negative effects on erythropoiesis and hematopoiesis, as observed in serum of individuals with MDS (Schepers et al., 2013). Thus, chronic inflammatory stimulation in both HSPCs and bone marrow microenvironment may be central to promote tumorigenesis (Schneider et al., 2016). On the other hand, chronic activation of p53 upon RP haploinsufficiency, may also favor the selection of clones which overcome IRBC-dependent p53 function by either inactivating RPL11, RPL5, or p53 or by deregulating MDM2 expression. Indeed, mutations on *TP53* are considered a prognostic factor for *5q-* patients and to be a critical step for the progression of the *5q-* syndrome to AML (Jadersten et al., 2011, Saft et al., 2014). In addition, the extraribosomal functions of certain RPs may be important for preventing tumorigenesis. For instance, haploinsufficiency of RPL5 and RPL11 might

also promote tumorigenesis by enhancing MYC's oncogenic potential, given their roles in the feed-back regulation of MYC expression and function (Dai et al., 2007, Dai et al., 2010, Liao et al., 2014).

Another possibility arises from the recent observation that mutations in RPs and/or ribosome biogenesis factors alters the pattern of translation, especially affecting IRES-mediated translation. This has been reported for DKC1 gene mutations that suppress p53 expression by altering IRES-mediated translation (Bellodi et al., 2010, Jack et al., 2011) **(See Discussion, pg.165)**, for mutations in *RPS25* (Hertz et al., 2013), or for T-ALL-associated *RPL10* mutations driving IRES-mediated overexpression of the antiapoptotic factor BCL2 (Kampen et al., 2019). Therefore, prolonged alterations in the pattern of translation, due to RP haploinsufficiency or modifications in RPs or in rRNAs, may favor the expression of growth-promoting genes while disfavor tumor-suppressing factors, such as p53.

Finally, accumulation of ROS and oxidative stress, observed in samples from DBA patients and in mouse models of DBA, have also been argued to contribute to the progression of cancer-derived DBA, by generating DNA damage and genomic instability (Kapralova et al., 2017), although the mechanism by which defective ribosomes lead to elevated ROS and oxidative damage is poorly understood. Interestingly, only ribosomopathies leading to hematopoiesis defects show increased risk of blood cancer suggesting that the sensitivity of the hematopoietic system to oxidative stress, due to the failure of the erythroid precursors to produce hemoglobin may eventually predispose to cancer (De Keersmaecker et al., 2015, Sulima et al., 2019). It will be of interest to determine to which extent the loss of the IRBC, alterations in the pattern of translation or the production of ROS contributes to tumor progression in these pathologies.

## Antiapoptotic MCL1 links enhanced sensitivity to RiBi impairment to cell death in MYC-driven tumors

One of the major findings presented here is the identification of antiapoptotic MCL1 as a critical mediator of the IRBC-MDM2-p53 apoptotic response in E$\mu$-MYC lymphomas. Intriguingly, such a strong apoptotic response observed in this system by us **(Fig. R-9)** and others (Bywater et al., 2012) is not recapitulated in all tumor models, as perturbation of RiBi can conversely result in senescence or autophagy (Drygin et al., 2011, Nishimura et al., 2015). Although in general, RiBi impairment in solid tumors results in p53-dependent non-apoptotic responses, apoptosis is the major response in cell lines derived from hematologic malignancies. The mechanism(s) underlying these differential responses is not known. Is it possible that the strong reliance on MCL1 sensitizes cells to apoptosis? In MYC-driven lymphoma, MCL1 is a well-established critical factor for both lymphoma initiation and survival (Kelly et al., 2014) but, is MCL1 overexpression required to counteract TS response in other MYC-driven tumor models?

### *Does MYC overexpression correlate with MCL1 increased expression?*

In addition to the dependency of E$\mu$-MYC lymphomagenesis on MCL1 expression, MCL1 was found to cooperate with MYC-driven tumorigenesis in a model of AML (Xiang et al., 2010) and in a MYC-driven model of NSCLC (Allen et al., 2011). Importantly, genetic studies suggest such a cooperation in human patients, where 60-70% of tumors displaying *MCL1* gene copy number amplification also harbor *MYC* gene amplifications (Beroukhim et al., 2010). *MCL1* lies on an amplification peak within Chr 1 and, together with *BCL2L1* (encoding BCLxL), are the only two antiapoptotic members whose dysregulation frequently arise from copy-number change (Beroukhim et al., 2010). Therefore, somatic amplification of *MCL1* seems to be a common target for MYC-driven tumors to evade oncogene induced apoptosis. In addition, MCL1 expression is critical for the survival of multiple adult cell linages, as proliferating human HSPCs (Delbridge et al., 2015), and during the differentiation pro-B and pro-T cells into B- and T lymphocytes (Opferman et al., 2003). It might be possible that tumor cells arising from normal cell counterparts, in which MCL1

expression is already high are more prone to dysregulate this member rather than other. For instance, the malignant E$\mu$-MYC lymphoma arises after a latency period, in which B-cell precursors undergo rapid proliferation and turnover, from the clonal expansion of these proliferating B-cell progenitors **(see Introduction, Section 1.4.2.)**. It may be that, at early stages of E$\mu$-MYC tumorigenesis, oncogenic and replicative stresses lead to the upregulation of the proapoptotic BH3-only member BIM, whose expression limits the expansion of proliferating premalignant B-cells precursors (Egle et al., 2004, Lee et al., 2013). Progression into malignant lymphoma cells, which requires additional alterations, seems to strongly depend in the deregulation of BCL2 family members, and in particular dysregulation of MCL1 expression may be critical to neutralize BIM-mediated apoptotic response and thus, to transform the premalignant progenitor cells.

MCL1 expression is also critical in other cancers, as has been demonstrated in many KO mouse models **(see Introduction, Section 2.3.)**. For instance, genetic loss of *Mcl1* delays the development of AML, driven by distinct oncogenes (Xiang et al., 2010, Glaser et al., 2012) and of BCR-ABL-driven B-ALL (Koss et al., 2013). In contrast to MYC-driven E$\mu$-MYC lymphoma, in which loss of one *Mcl1* allele is sufficient to promote lymphoma regression (Grabow et al., 2016) in these tumor models both alleles must be deleted in order to delay tumor progression (Xiang et al., 2010, Glaser et al., 2012, Koss et al., 2013). Such observations reinforce the importance of MCL1 overexpression in the context of MYC-driven tumors. However, it remains unclear why MCL1 dysregulation is more frequent or more essential in these cells than its antiapoptotic relatives (BCL2, BCLxL, BCLW and BFL1/A1). It has been speculated that the rapid turnover of MCL1 is critical for the removal of the proapoptotic BH3-only proteins induced by MYC (Grabow et al., 2016). It is also possible that as it is the most promiscuous antiapoptotic member, i.e. able to interact and neutralize more proapoptotic family members than its antiapoptotic partners, once overexpressed it is able to counteract MYC-induced apoptosis in most cases, while dysregulation of any other antiapoptotic relative, with more restricted binding affinities, fails to overcome MYC-induced TS response.

### *Which mechanism drives MCL1 reduction following IRBC activation?*

The cooperation between MYC and MCL1 in tumorigenesis led us to the question whether the apoptotic response mediated by the IRBC might be a common mechanism in all MYC-driven tumors. Importantly, although MCL1 overexpression seems to be essential to initiate E$\mu$-MYC tumorigenesis by neutralizing proapoptotic BIM, which BH3-only protein drives MCL1 degradation in the context of the IRBC is unknown. PUMA and NOXA are the most plausible candidates to mediate this response given that (**1**) they are two well-known p53 targets (Youle and Strasser, 2008); (**2**) they can both interact with MCL1 with high affinity (Kale et al., 2018) and (**3**) they are upregulated following RiBi impairment in our system **(Figs. R-7C, 12D and 15E)**. Whereas NOXA-MCL1 interaction has been shown to promote MCL1 degradation via enhanced MCL1 ubiquitination by MULE (Gomez-Bougie et al., 2011, Song et al., 2016), PUMA-MCL1 interaction increases MCL1 stability. However, PUMA may not prevent MCL1 degradation, since its PEST region is still exposed (Mei et al., 2005). Given that we observed a rapid loss of the antiapoptotic form of MCL1 associated with increased ubiquitination levels upon RiBi impairment **(Figs. R-12B, C)**, possibly corresponding to MCL1, we speculated that NOXA may be a key factor driving IRBC-dependent MCL1 degradation. However, we cannot discard that PUMA may cooperate with NOXA to further neutralize MCL1 or its antiapoptotic relatives, or by directly activating BAX/BAK proapoptotic effectors, thus, contributing to E$\mu$-MYC lymphoma cell death. It would be of critical interest to decipher the contribution of these two BH3-only members in the IRBC-mediated MCL1 degradation and apoptotic response.

As seen in the Introduction **(Chapter 2, Section 2.2.4.)**, among the distinct E3 ligases which can ubiquitinate MCL1, MULE is thought to be the major E3 ligase responsible for ubiquitin-dependent proteasomal degradation of MCL1 in normal conditions, as well as under certain apoptotic stimuli (reviewed in Mojsa et al., 2014). In addition, MULE was identified as the E3 ligase responsible for MCL1 degradation upon interaction of NOXA (Gomez-Bougie et al., 2011, Park et al., 2016). Together with our observations that NOXA is upregulated under conditions that impair RiBi both *in vitro* and *in vivo*, may suggest that MULE is the E3 ligase responsible for MCL1-degradation, resulting from the IRBC activation in E$\mu$-MYC lymphoma cells.

However, the enhanced ubiquitination levels observed in the immunoprecipitated fractions following RiBi impairment might also correspond to a MCL1-interacting protein **(Figs. R-12B, C)**, particularly given that the ubiquitin-resistant MCL1-mutant form ($Mcl1^{KR}$) does not completely protect against IRBC-induced cell death **(Figs. 13A-C)**. It might be that NOXA acts as a 'carrier' protein for MCL1, targeting it to the proteasome. Indeed, NOXA is a labile protein which is degraded in a proteasome-dependent manner via a degron sequence on its C-terminal tail (Pang et al., 2014). This discrete region of NOXA is also responsible for triggering MCL1 degradation (Czabotar et al., 2007), suggesting it may act as a scaffold for a common E3 ligase and promote co-degradation of MCL1. In addition, NOXA can be degraded by the proteasome independently of its ubiquitination status (Craxton et al., 2012, Pang et al., 2014), as has been observed for other BCL2 members in *in vitro* systems, including for MCL1 (Stewart et al., 2010, Wiggins et al., 2011). Therefore, it is also possible that NOXA:MCL1 complexes are targeted to the proteasome independently of an E3 ligase, although the increased ubiquitin levels observed following activation of the IRBC favors the hypothesis of a ubiquitin-dependent mechanism directing MCL1 proteasomal degradation.

In brief, we purpose that targeting RiBi induces the IRBC, which results in p53 stabilization, with the subsequent upregulation of p53 targets (p21, PUMA, NOXA, etc.), cell cycle arrest and E$\mu$-MYC tumor cell death through the degradation of antiapoptotic MCL1 **(Fig. D-1)**. Increased p21 levels may induce G1-to-S phase arrest, while NOXA may be the candidate more likely to mediate antiapoptotic $MCL1_{OM}$ degradation. By contrast non-apoptotic MCL1 ($MCL1_{Matrix}$), inside the mitochondrial matrix, is not affected **(Figs.R-9A, B)**. Degradation of $MCL1_{OM}$ may allow PUMA to neutralize other antiapoptotic BCL2 members and/or to activate BAX/BAK, which ultimately leads to MOMP, CASP3 activation and tumor cell death.

### *What drives cell death upon RiBi impairment in the absence of p53?*

In our model, sensitivity of E$\mu$-MYC lymphoma cells to RiBi inhibitors relies on the integrity of the IRBC-p53 pathway, but what would happen in the context of p53-deficient tumors? As observed in the $Trp53^{+/+}$ RPL11-depleted E$\mu$-MYC cells, in which the IRBC is not elicited, we expect that $Trp53^{-/-}$ E$\mu$-MYC cells, in which RiBi is inhibited,

would undergo cell death at later time points given the reduced number of ribosomes. In such a setting the preexisting pools of ribosomes could not cope with the high protein synthetic demand, potentially leading to replicative stress and activation of the DDR. Indeed, we showed that prolonged ActD treatment also reduces the number of live cells in the p53-deficient background at longer time points **(Fig.R-7A)**. Moreover, a recent study by Devlin and co-workers identified another BH3-only member, BMF, responsible for mediating E$\mu$-MYC cells cell death in a p53-independent manner following treatment with AKT/mTOR inhibitors. Targeting the PI3K-AKT-mTOR pathway leads to translation inhibition and also to the downregulation of rDNA synthesis, but as it also decreases the synthesis of RPL5 and RPL11 the IRBC is not induced (Devlin et al., 2016a), a similar situation to what is observed in RPL11-deficient E$\mu$-MYC cells. Therefore, alternative pathways may drive cell death following prolonged RiBi impairment, when the IRBC response is abrogated, such as when RPL11 or p53 are lost. However, this response per se would not be sufficient to induce tumor regression *in vivo*, as ActD-treated mice bearing *Trp53*$^{-/-}$ E$\mu$-MYC lymphomas succumb to lymphomagenesis at the same rate than their vehicle counterparts **(Fig.R-17A)**. It is likely that if the IRBC cannot trigger p53-dependent cell cycle arrest or apoptosis, alterations in translation, replicative stress or DNA damage, leading to the activation of alternative cell death pathways, are not elicited quick enough to counteract the rapid expansion of the *Trp53*$^{-/-}$ E$\mu$-MYC cells.

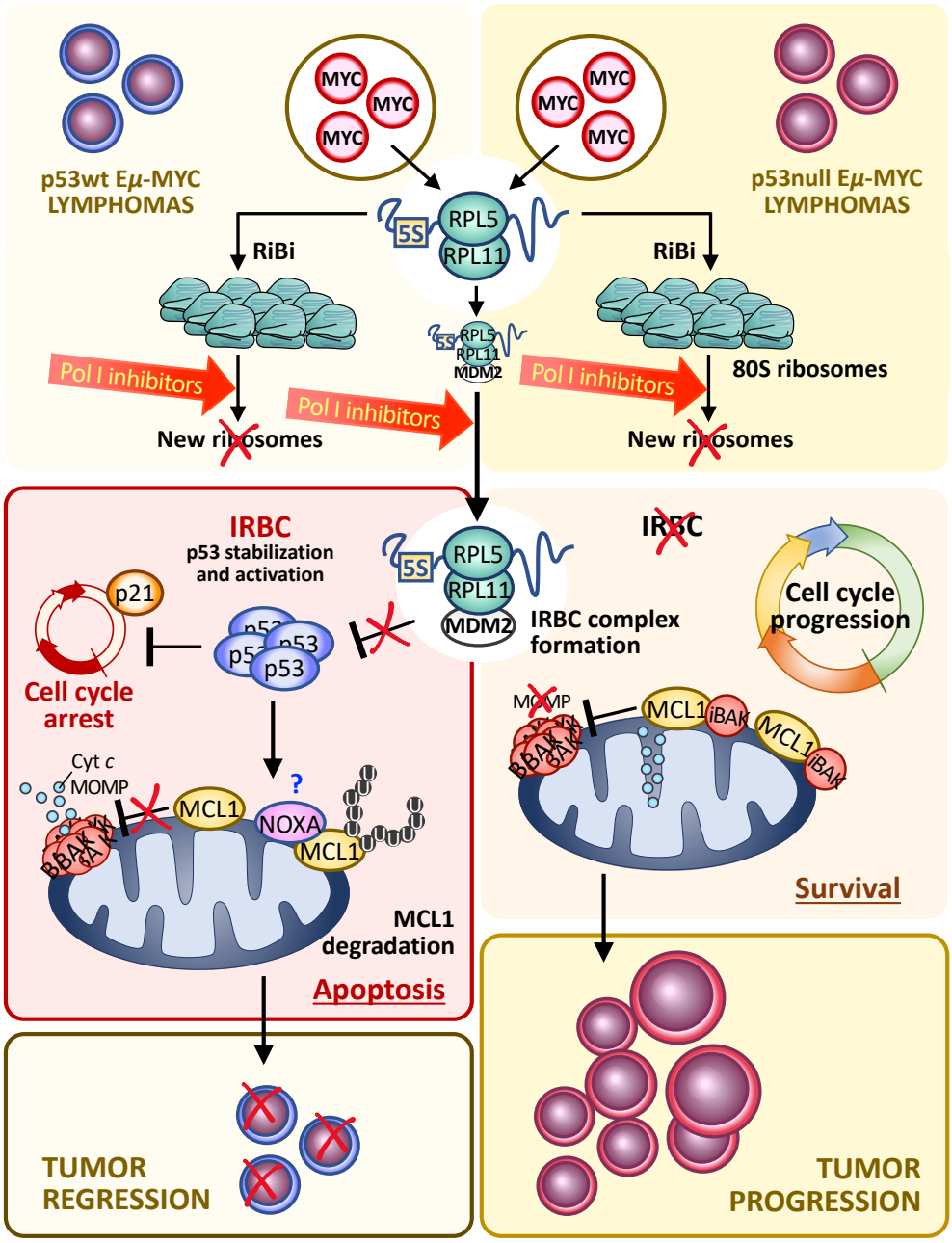


**Figure D-1. Model: Targeting RiBi and activation of the IRBC in Eμ-MYC-driven lymphomas.** In Eμ-MYC-driven lymphomas, elevated MYC expression upregulates RiBi at every level. Increased synthesis of RPs and rRNAs not only drives RiBi but also leads to increased levels of free pre-ribosomal 5S rRNA/RPL5/RPL11 complex. (See next page)

**Figure D-1. (continued)** Besides its assembly into nascent 60S ribosomes, the complex is also actively directed to the IRBC complex, activating the IRBC at basal levels but not sufficient to fully drive the IRBC response. However, impairment of RiBi, e.g. by targeting Pol I-mediated rRNA synthesis with Pol I inhibitors (red arrows), further induces the formation of the IRBC complex and now the amount of the complex effectively binds and inhibits MDM2, activating the IRBC. Once activated, p53 gets stabilized and drives cell cycle arrest and cell death through the degradation of antiapoptotic MCL1, ultimately leading to E$\mu$-MYC tumor regression. By contrast, IRBC activation in p53-deficient E$\mu$-MYC tumors fails to induce p53-dependent response and MCL1 expression is sufficient to sustain survival and progression of E$\mu$-MYC lymphomas even in the context of impaired RiBi. Abbreviations: iBAK, inactive BAK.

## Targeting RiBi for the treatment of MYC-driven hematological malignancies

### *Can we take advantage of the IRBC in the clinic?*

The apparent addiction of E$\mu$-MYC cells to increased rates of RiBi is a proof of concept opening an avenue for therapeutic intervention of MYC-driven tumors. The evidence supported by the studies of Barna et al. and Bywater et al., demonstrating that aberrant rates of RiBi in E$\mu$-MYC tumor cells are required for MYC's oncogenic potential (Barna et al., 2008, Bywater et al., 2012), have led to development of specific Pol I inhibitors which are currently being tested in clinical trials (Drygin et al., 2009, Bywater et al., 2012). Here, we demonstrate the benefits of therapeutically targeting RiBi pathway in *Trp53*$^{+/+}$ E$\mu$-MYC-driven B-cell lymphomas by using ActD at a low dose, which is known to inhibit Pol I-mediated transcription **(Fig. R-17A)**. Translation of this approach into the clinic seems very feasible, as compared to the novel first-in-class Pol I inhibitors employed in previous studies such as CX3543 (Drygin et al., 2009) and CX5461 (Bywater et al., 2012). Moreover, ActD not only harbors a potential for the treatment of human MYC-driven blood-borne tumors such as BL, but also for the treatment of MM, aggressive subtypes of DLBCL or double-hit lymphomas, transformed FL, high-risk CLL or AML, among others, in which MYC deregulation is a common event that correlates with disease progression, resistance or relapse **(see Chapter 1, Section 1.4.)**. Our results demonstrate the selectivity of ActD for E$\mu$-MYC lymphoma cells, as wt-B cell population was not affected **(Figs. R-16C, E)**. In addition, our findings highlight the importance of the p53 status and of the functionality of the p53-MDM2 pathway, which are critical to the

strong anti-tumor response, and argue for a need of patient stratification based on the expression and mutational status of the IRBC-MDM2-p53 pathway for the use of ActD in the clinic. The major advantage over the novel Pol I inhibitors is that ActD is a chemotherapeutic drug already approved by the FDA for over a half a century, currently used with high efficacy as a key agent in the multimodal treatment of rare tumors mostly occurring in children, such as WT (Malogolowkin et al., 2008), RMS (Jaffe et al., 1973) and EWS (Jaffe et al., 1976), but also in GTN in adult women (Goldstein and Berkowitz, 2012). As its associated-toxicities and risk-profile are already well established (Hill et al., 2014), the trials for the application of ActD for the treatment of human MYC-driven blood-borne tumors could be rapidly performed and with reduced risks of toxicity. Critically, we used ActD at a 5-fold lower concentration than that generally used in previous studies, of ∼0.500 mg/kg (Robinson and Waksman, 1942, Dipaolo et al., 1957), with one single administration being sufficient to effectively inhibit Pol I transcription *in vivo* **(Fig. R-15A)** and to induce apoptosis of *Trp53*$^{+/+}$ E$\mu$-MYC lymphoma tumor cells within 6 hr **(Figs. R-14A, C)**. Moreover, at these low doses, tumor regression largely results from the specific inhibition of rRNA synthesis and not from global transcription inhibition. Consistent with this notion, the preclinical studies developed by Siboni et al. demonstrated that ActD administration in mice at 0.125-0.25 mg/kg, doses higher than that we used in our studies (0.100 mg/kg) and much lower than the human equivalent dose (HED) used as standard treatment in humans, does not affect global transcription (Siboni et al., 2015). To extrapolate the HED we used a body surface area normalization method, which is recommended when entering phase I and II clinical trials (Reagan-Shaw et al., 2008). The method applies a conversion factor, or Km, specific to each species (Freireich et al., 1966). The HEDs corresponding to our ActD administration studies are of 0.012 mg/kg for children and 0.0081 mg/kg for adults, below the current standard dosages of treatment, which vary between 0.015 and 0.045 mg/kg for children and adults, respectively. Therefore, we used a dose over 5-fold lower than the dose administrated for treatment of WT in standard adult patients (body weight average = 60 kg), which should dramatically reduce its associated toxicities without compromising its efficacy. In addition, daily administration of ActD during 5 days is the standard regimen for treatment of pediatric RMS (Ortega et al., 1997) and adult GTN (Goldstein and Berkowitz, 2012), which reinforces the safety and

tolerability of the drug. Our preclinical data are very promising and highlight the importance to determine the clinical efficacy of ActD at this range in MYC-driven hematological malignancies and to assess whether its effects are driven through the selective inhibition of Pol I transcription and the activation of the IRBC.

In further support of the use of ActD over the novel Pol I inhibitors (CX5461 and CX3543), some discrepancies regarding their mechanism of action have recently arose. While both CX5461 and C3543 were characterized as selective non-genotoxic Pol I inhibitors (Drygin et al., 2009, Bywater et al., 2012), now it is being questioned whether they largely function by generally stabilizing G4 structures on the DNA rather than through the specific inhibition of Pol I. The stabilization of G4 DNA structures is thought to negatively impact the progression of DNA replication complexes, leading to DNA damage and activation of ATM/ATR signaling (Rodriguez et al., 2012). Activation of ATM/ATR pathway with CX5461 has been observed in immortalized human fibroblasts (Quin et al., 2016) and in a panel of ALL cell lines (Negi and Brown, 2015). A recent study published this year corroborates that CX5461 induces DNA damage in the absence of Pol I inhibition (Hald et al., 2019). Furthermore, an independent study by Xu et al., in 2017, demonstrated that both compounds, CX5461 and CX3543 induced DNA damage at doses in the nanomolar range (>10 nM) at which they failed to inhibit rDNA transcription, contrarily to ActD. Likewise, they observed an increase in G4 structures *in vivo* (Xu et al., 2017). Therefore, the selectivity of these compounds for inhibiting Pol I is questionable, strengthening the clinical use of ActD, whose selectivity for Pol I inhibition at low doses, has been largely demonstrated.

### *How can we combine ActD?*

Combination therapies have become the standard of care for the treatment of many cancers. It offers the possibility to target key pathways in a synergistic or additive manner. Thus, we can expect that other chemotherapeutic agents used in combination with ActD would improve patient's clinical outcome. Such benefit of multi-modal treatment was evidenced by the studies of Devlin in 2016, who reported a marked benefit in E$\mu$-MYC lymphoma bearing-mice survival by combining CX5461, with AKT/mTOR inhibitors, in comparison with each agent alone (Devlin et al., 2016).

The AKT/mTOR pathway is a known activator of both RiBi and mRNA translation (reviewed in Gentilella et al., 2015). Indeed, through the phosphorylation of S6K1, the AKT/mTOR pathway upregulates rDNA transcription at several levels (Hannan et al., 2003, Mayer et al., 2004, Ben-Sahra et al., 2013). Furthermore, recent studies have shown that AKT cooperates with MYC to stimulate RiBi and cancer progression (Chan et al., 2011, Devlin et al., 2013). Thus, it is expected that the combination of ActD with AKT/mTOR inhibitors would have a clinical benefit over the administration of ActD alone in MYC-driven tumors. In addition, it would be interesting to further enhance the activity of p53 by directly disrupting MDM2-p53 interaction, e.g. by combining low-dose ActD, which leads to the IRBC-mediated MDM2 inhibition, with inhibitors such as nutlins (Vassilev et al., 2004) or CGM097 (Holzer et al., 2015), which compete with high affinity with p53 on the MDM2 p53-binding pocket. The use of such inhibitors is of particular interest for the treatment of hematological malignancies, given the low frequency of mutations or deletions of the *TP53* gene, 10-20% overall (Imamura et al., 1994, Stengel et al., 2017), but in which *MDM2* and/or its paralog *MDM4* are frequently found amplified/overexpressed (Konikova and Kusenda, 2003, Tisato et al., 2017). Therefore, it will be critical to address the efficacy of the ActD/MDM2 inhibitors combination in eliciting a cytotoxic response and promoting further tumor regression in cell lines and mouse models of MYC-driven hematological malignancies, as e.g. BL, MM or FL.

### *Do we expect resistance?*

*TP53* gene mutations are rare at diagnosis in common cancers of hematopoietic origin, such as MM, AML or CLL (Imamura et al., 1994, Stengel et al., 2017), supporting a therapeutic application of ActD for the treatment of such pathologies. However, we cannot exclude the possibility that resistance will arise. It might be possible that prolonged and chronic activation of p53 results in the emergence of resistant clones with deregulated MDM2 expression, or direct mutations on p53 that would bypass the IRBC-mediated antitumor response. This mechanism of resistance has been proposed for *5q-* patients, in which mutations on *TP53* seem to be the critical event for the progression of the syndrome to AML (Jadersten et al., 2011, Saft et al., 2014). In addition, as described before, deficient RiBi leads to alterations in the translational pattern (Khajuria et al., 2018), with a number of studies reporting cases

where such changes favor the expression of growth-promoting genes (Kampen et al., 2019), while disfavoring tumor suppressor genes (Bellodi et al., 2010, Jack et al., 2011). It might be of interest to determine if there is a common translational reprogramming upon RiBi impairment and whether cells can reverse these changes or bypass the IRBC and adapt in the absence of nascent RiBi, and thus to become resistant to therapies targeting RiBi.

### *Can ActD be applied as an indirect MCL1 inhibitor?*

In support of a therapeutic application of ActD for the treatment of human neoplasms such as BL, MM or AML, the novel selective MCL1 inhibitors S63845 (developed by Sevier in collaboration with Novartis) and both AMG176 and AMG397 (developed by Agmen), which displayed promising antitumor activity in preclinical models (Caenepeel et al., 2018, Li et al., 2019, Moujalled et al., 2019) are currently on Phase I clinical trials. S63845 is being evaluated as single agent (NCT02979366 and NCT02992483) for patients with AML and MDS, and for patients with relapsed or refractory DLBCL and MM, respectively, or in combination with Venetoclax in AML patients (NCT03672695). Similarly, AMG176 and AMG397 are being assessed in phase I clinical trials for patients with relapsed or refractory DLBCL, MM and/or AML (NCT02675452 and NCT03465540) and AMG176 is also being evaluated in combination with Venetoclax in AML patients (NCT03797261) **(see Chapter 2, Section 2.3.2. and Table I-5)**. However, on the 12$^{th}$ of September this year, Amgen published an update about the status of their current programs, including those for the MCL1 inhibitors (https://www.amgen.com/amgen-highlights-new-data-from-kyprolis-carfilzomib-and-oncology-pipeline-at-imw-2019/; *Accessed on 1-10-2019*). Surprisingly, two of the clinical trials with these inhibitors, NCT03465540 and NCT02675452, are on hold due to safety issues. Although the company has not disclosed cardiac toxicity in any of the studies, the phase I study with AMG397 (NCT03465540) has been handed out by the FDA to evaluate a 'safety signal for cardiac toxicity' and during the phase I trial with AMG176 (NCT02675452) there were two fatal adverse events, one of which was due to the treatment (Spencer et al., 2019), and thus, the program has been voluntary halted by Agmen. Furthermore, the phase I clinical trial with AMG176 inhibitor in combination with Venetoclax (NCT03797261) is also suspended to evaluate safety. Given that ActD treatment

appears to be selective for tumor cells, as it does not affect wt-B-cell population **(Fig. R-16E)**, and since cardiotoxicity is not a reported adverse effect of ActD treatment (Hill et al., 2014), it may be applied as a safer therapeutic approach to target MCL1 in AML, MM and DLBCL. In addition, other blood-borne tumors which strongly depend on MCL1 expression, such as BCR-ABL-driven B-ALL (Koss et al., 2013), or T-ALL (Grabow et al., 2016), and certain solid tumors such as NSCLC, melanoma or BC, in which *MCL1* amplifications are a frequent event (Beroukhim et al., 2010), are also potential targets of ActD treatment. Indeed, many of these tumors displayed deregulated MYC expression which reinforces the use of ActD as a treatment. In addition, for some of these tumors, such as NSCLC, BC and melanoma cell lines, S63485 has displayed moderate efficacy (Kotschy et al., 2016). It might be possible that ActD displays higher efficacy, as it leads to the effective degradation of MCL1. By contrast, S63485 neutralizes, but does not trigger MCL1 degradation. This differential effect, together with the ability of ActD to inhibit RiBi, suggests a more potent effect of ActD for the treatment of these malignancies than that of the recently developed MCL1 inhibitors

Therefore, it will be important to determine in these models the sensitivity to ActD and whether MCL1 degradation is a common mechanism triggered by the IRBC, to further support the clinical application of ActD for the treatment of these malignancies.

# CONCLUSIONS

# Conclusions

From the work developed during this Thesis, we have reached the following conclusions:

1. Partial depletion of a RP causes a lesion in ribosome biogenesis that leads to a reduction of cell proliferation and protein synthesis in E$\mu$-MYC lymphoma cells.

2. Impaired ribosome biogenesis triggers cell death through the activation of the IRBC and not the reduction in protein synthesis rates induces apoptosis of E$\mu$-MYC-driven lymphoma cells.

3. Apoptotic response induced through the activation of the IRBC is dependent on p53 expression.

4. When RPL11, a component of the IRBC complex, is decreased, the checkpoint is not elicited.

5. Degradation of MCL1 is responsible for the rapid cell death of E$\mu$-MYC cells following ribosome biogenesis impairment.

6. Low doses of ActD effectively induce IRBC-mediated-p53-dependent cell death and MCL1 degradation in E$\mu$-MYC cells.

7. Low-doses of ActD effectively kills p53-wt E$\mu$-MYC lymphoma cells *in vivo* and extents survival of mice harboring p53-wt E$\mu$-MYC lymphomas but not of mice harboring p53-deficient E$\mu$-MYC lymphomas.

.

# MATERIALS AND METHODS

# Materials and methods

## Cell culture

Eμ-MYC lymphoma *Trp53*$^{+/+}$ (clones #4242 and *Gfp*-tagged 4242) and *Trp53*$^{-/-}$ (clones #KA540 and 3239) cell lines were kindly provided by Dr. R. Pearson (Peter MacCallum Cancer Centre, Melbourne, VIC, Australia) and maintained in Anne-Kelso medium, containing Dulbecco's modified Eagle medium (DMEM) supplemented with 10% heat-inactivated fetal bovine serum (FBS, Sigma-Aldrich, St Louis, MO, USA), 200 mM GlutaMAX™ (Gibco, Thermo Fisher Scientific, Waltham, MA, USA), 100 μM L-Asparagine (Sigma), 0.5% 2-mercaptoethanol and Penicillin/Streptomycin (Gibco) Bywater et al., 2012. Cells were maintained in 20% $O_2$, 10% $CO_2$, at 37 ºC and 90-95% of relative humidity.

## Reagents and plasmids

The antibodies used are listed in **Table M-1**. Actinomycin D (ActD) was purchased from BioVision (BioVision, Inc., Milpitas, CA, USA) and dissolved in dimethyl sulfoxide (DMSO). Doxycycline (dox), Iodoacetamide (IAA), cycloheximide (CHX), Z-VAD-FMK (ZVAD) and MG132 were also purchased from Sigma and either dissolved in $H_2O$ MilliQ (dox and IAA) or DMSO (CHX, ZVAD and MG132). QVD-OPh was purchased from Selleckchem (Selleck Chemicals, Houston, Texas, *USA)* and dissolved in DMSO. Lipofectamine 2000, TRIzol RNA extraction reagent, random hexamers and Moloney Murine Leukemia Virus Reverse Transcriptase (M-MLV RT) were purchased from Invitrogen (Invitrogen, Carlsbad, CA, USA). The SYBR Green kit was purchased from Roche (Basel, Switzerland). EN$^3$HANCE autoradiography enhancer, $^3$H-leucine and $^3$H-uridine were purchased from PerkinElmer (PerkinElmer, Inc., Waltham, MA, USA). The BCA protein assay kit was purchased from Pierce (Pierce Biotechnology Inc., Rockford, IL, USA). Magna ChIP™ Protein A/G magnetic beads were purchased from Millipore (Millipore corp., Billerica, MA, USA). Retroviral vectors were obtained from Addgene (Addgene, Watertown, MA, USA), except pMSCV-puro-3X Flag-derived plasmids, which were a gift from Dr. J. T. Opferman (St. Jude Children's Research

Hospital, Memphis, TN, USA) **(Table M-2)**. Plasmid amplification was carried out in *Escherichia coli* DH5α in the presence of Ampicillin.

**Table M-1. List of antibodies**

| Antibody | Origin | Clone | Dilution | Used by | Source | Cat. # /Ref. |
|---|---|---|---|---|---|---|
| α-Tubulin | M | B-5-1-2 | 1:10000 | WB | Sigma | T6074 |
| β-Actin | M | AC-74 | 1:5000 | WB | Sigma | A2228 |
| BCL2 | M | C-2 | 1:500 | WB | SCBT | sc-7382 |
| BCLxL | Rb | 54H6 | 1:1000 | WB | CST | 2764 |
| CASP3 | Rb | *N.A.* | 1:1000 | WB | CST | 9662 |
| FLAG | M | M2 | 1:1000 | WB | Sigma | F1804 |
| MCL1 | Rb | Y37 | 1:500 | WB/IP | Abcam | ab32087 |
| MDM2 | M | 2A10 | 1:500 | WB | Abcam | ab16895 |
| Normal Rb IgG | Rb | *N.A.* | *N.A.* | IP | SCBT | sc-2027 |
| p21 (H) | M | SXM30 | 1:1000 | WB | BDB | 556431 |
| p21 (M) | M | SX118 | 1:500 | WB | SCBT | sc-53870 |
| P53 | M | 1C12 | 1:1000 | WB | CST | 2524S |
| PARP1 | M | C2-10 | 1:2000 | WB | SCBT | sc-53643 |
| RPL5 (uL18) | Rb | *N.A.* | 1:1000 | WB/IP | Bethyl | A303-933A |
| RPL11 (uL5) | M | 3A4A7 | 1:1000 | WB | Invitrogen | 373000 |
| RPS6 | M | *N.A.* | 1:10000 | WB | Gifted* | Bursac et al. (2012) |
| Ub-HRP | M | P4D1 | 1:500 | WB | SCBT | sc-8017 |
| B220-APC | R | RA3-6B2 | 1:400 | FACS | BDB | 553092 |
| cd45.2-FITC | M | 104 | 1:400 | FACS | BDB | 553772 |
| p53-AF647 | M | 1C12 | 1:200 | FACS | CST | 2533 |

*RPS6 antibody is a gift from Dr. S. Volarevic. *Abbreviations:* Cat. #, catalog number; Ref., reference; H, human; M, mouse; Rb, rabbit; R, Rat; Ub-HRP, horseradish peroxidase-linked ubiquitin; APC, allophycocyanin; FITC, fluorescein isothiocyanate; PE, phycoerythrin; AF647, Alexa Fluor 647; WB, western blot; IP, immunoprecipitation; FACS, flow cytometry; SCBT, Santa Cruz Biotechnologies; CST, Cell Signaling Technologies; BDB, BD (Becton, Dickinson and Company) Biosciences; *N.A.*, Not available/applicable.

**Table M-2. List of retroviral vectors**

| Vector name | Gene/ Insert | Description | Provider; cat. # | Reference |
|---|---|---|---|---|
| Gag/Pol | *Gag Pol* | Gag, Pol | Addgene #14887 | Reya et al., 2003 |
| pMD2.G | *VSV-G* | Envelope | Addgene #12259 | Barde et al., 2010 |
| TRMPVIR | shRen | Renilla | Addgene #27994 | Zuber et al., 2011 |
| pMSCV-puro-3X Flag | *3X Flag* | Flag control | Dr. J. T. Opferman | Stewart et al., 2010 |
| pMSCV-puro-3X Flag-mMcl1 | *3X Flag-Mcl1$^{WT}$* | MCL1$^{WT}$ | Dr. J. T. Opferman | Stewart et al., 2010 |
| pMSCV-puro-3X Flag-mMcl1 KR | *3X Flag-Mcl1$^{KR}$* | MCL1$^{KR}$ | Dr. J. T. Opferman | Stewart et al., 2010 |

## Stable cell lines

The stable cell lines expressing tetracycline (Tet)-inducible shRNA against Renilla (Ren), RPL7a, or RPL11 were generated using a retroviral vector, TRMPVIR (Zuber et al., 2011). The shRNA sequences were selected using the Designer of Small Interfering RNA (http://biodev.cea.fr/DSIR/DSIR.html) program and cloned into TRMPVIR vector as previously described (Zuber et al., 2011). A minimum of five shRNA sequences were screened for each target gene. shRNA encoding retroviruses were generated using Platinum-E retroviral packaging cell lines provided by Dr. D. R. Plas (University of Cincinnati, Cincinnati, Ohio, USA). Briefly, 3.5 µg of TRMPVIR plasmid containing RPL7a, RPL11 or Renilla shRNA and 1.5 µg of Gag/Pol and pMD2.G plasmids were transfected into HEK293T cells using Lipofectamine 2000 reagent (Invitrogen) and virus supernatants were collected at 48 hr and filtered (0.45 µm filter) to remove cellular debris. The virus supernatants were plated on Retronectin (Takara Bio, Kusatsu, Japan)-coated plates for 5 hr at 37 °C, to facilitate binding of virus to the plate, and then, supernatant was replaced by Anne-Kelso media-containing $0.5x10^6$ E$\mu$-MYC lymphoma cells supplemented with 4 µg/mL Polybrene (Sigma). After 24 hr of transduction, the cells were grown in complete medium for another 48 hr and then treated with dox to induce shRNA expression. The shRNA expressing cells were then single cell sorted for dsRED positive cells by fluorescence-activated cell sorting (FACS Vantage SE cell sorter, BD Biosciences, Franklin Lanes, NJ, USA). Single cell colonies were grown, treated with dox and mRNA levels were quantified by qRT-PCR.

For the generation of the stable 3X Flag-tagged MCL1 wt ($Mcl1^{wt}$), 3X Flag-tagged KR mutant ($Mcl1^{KR}$) and 3X Flag-tagged control (Flag) E$\mu$-MYC cell lines, retroviral packaging was performed in HEK293T cells as described above. Viral supernatants, collected at 48 hr, were used for transduction of E$\mu$-MYC lymphoma cells cultured in Anne-Kelso media supplemented with Polybrene. After the second transduction (48 hr), cells were incubated in fresh media in the presence of puromycin (Sigma) during four passages, and tested for stable expression of Flag-tagged MCL1 proteins by Western blot analysis.

## Drug treatment, cell lysis and RNA extraction

Ren and shRPL7a cells were treated with 1 µg/mL dox, and shRPL11 cells with 10 ng/mL dox to achieve an approximate 50% depletion of respective transcript levels. ActD was used at a concentration of 5 nM; ZVAD, at 20 µM; CHX, at 100 µg/mL; QVD-OPh, at 20 µM; and MG132, at 0.125 and 1.25µM, for the times indicated in the text. Following either treatment, cells were harvested by centrifugation at 1,300 rpm for 5 min, rinsed in ice-cold PBS and lysed on ice-cold extraction buffer: 50 mM Tris-HCl, pH 8.0, 250 mM NaCl, 1% Triton X-100, 0.25% sodium deoxycholate, 0.05% SDS, supplemented with 1 mM dithiothreitol (DTT) and protease inhibitors cocktail (Roche). Total RNA was extracted with TRIzol reagent (Invitrogen) according to the manufacturer's instructions.

## Quantitative real time-PCR

Total RNA was quantified using NanoDrop 1000 spectrophotometer (Thermo Fisher Scientific, Waltham, MA, USA) and treated with DNase I to remove DNA (Sigma) following the manufacturer's instructions. Reverse transcription was performed after DNase treatment using random hexamers and M-MLV RT (Invitrogen), as previously described (Fumagalli et al., 2009). Diluted cDNA samples (1:10-1:40) were analyzed in triplicate by qRT-PCR using the LightCycler® 480 SYBR Green I Master kit (Roche) with a Roche LightCycler® 96 or 480 II detection system (Roche), using the following conditions: first a 5-min incubation at 95 ºC, followed by 45 amplification cycles of 15 seconds (s) at 95 ºC, 15 s at 58 ºC, and 20 s at 72 ºC, acquiring the SYBR Green signal at the end of each cycle. Melting curve analyses were performed after each

amplification cycle to verify that a single PCR product was amplified. Relative mRNA expression was calculated using the comparative $C_T$ method ($2^{-\Delta\Delta CT}$) as previously reported (Donati et al., 2013). For each experiment, the average values of the corresponding control sample(s) ($\Delta C_T$ values) was used to calculate the variation of the sample replicates ($\Delta\Delta C_T$ values), and their expression was normalized to the levels of either β-*actin* or β*2m*, the latter widely used as a control in E$\mu$-MYC lymphoma cell lines (Bywater et al., 2012). The sequences of the primers for *Rpl7a*, *Rpl11*, *Its1*, *p21*, *Puma*, *Noxa*, *Mcl1*, β-*actin*, β*2m* and *Firefly luciferase* (*F-luc*) mRNA are reported in **Table M-3.** Negative controls were included to ensure that we had no contamination.

**Table M-3. List of qRT-PCR primer sequences**

| Target | Forward primer | Reverse primer |
|---|---|---|
| β-actin | 5' CTACAATGAGCTGCGTGTGGC 3' | 5' CAGGTCCAGACGCAGGATGGC 3' |
| β2m | 5' TTCACCCCCACTGAGACTGAT 3' | 5' GTCTTGGGCTCGGCCATA 3' |
| F-luc | 5' ACAGATGCACATATCGAGGTG 3' | 5' GATTTGTATTCAGCCCATATCG 3' |
| ITS1 | 5' CCGGCTTGCCCGATTT 3' | 5' GCCAGCAGGAACGAAACG 3' |
| MCL1 | 5' GTGCCTTTGTGGCCAAACACT 3' | 5' AGCACATTTCTGATGCCGCCT 3' |
| NOXA | 5' ACCACCTTAAATCCAGCTGTCCCA 3' | 5' CCCTTCAGCCCTTGATTGCTTGTT 3' |
| p21 | 5' CCAGACATTCAGAGCCACAGG 3' | 5' GGTCGGACATCACCAGGATT 3' |
| PUMA | 5' GAGCGGCGGAGACAAGAA 3' | 5' GGCGTCCCATGAAGAGATTGTACAT 3' |
| RPL7a | 5' AAGTCCCTCCTGCCATTAACCAGT 3' | 5' TTTGCCAGCAGCTTTCTTTCAGC 3' |
| RPL11 | 5' AGCCAAGGCAGAGGAAATTCTGGA 3' | 5' ATGCTTGGGTCGTATTTGATGCCC 3' |

*Abbreviations:* F-luc, Firefly luciferase

## Protein analysis

Protein concentrations from cell extracts and tissue homogenates for Western blot analysis was determined using the Pierce BCA protein assay kit following the manufacturer's instructions. Equal protein amounts (20-30 µg) were resuspended in 1X SDS loading buffer (375 mM Tris-HCl, 9% SDS, 50% Glycerol and bromophenol blue) and, after incubation at 95 ºC for 5 min, resolved by electrophoresis by 10% SDS-PAGE (Bio-Rad, Bio-Rad Laboratories Inc., Hercules, CA, USA) or by 4-12% Nu-PAGE Bis-Tris (Invitrogen) and transferred onto PVDF membranes (Millipore). PVDF

membranes were stained with amido black to confirm equal loading and transfer of proteins and subsequently probed with the indicated primary antibodies **(Table M-1)** as previously described (Fumagalli et al., 2009). Immunoblots were developed using a secondary horseradish peroxidase (HRP)-coupled polyclonal antibody, which was either swine anti-rabbit or rabbit anti-mouse (Agilent, Santa Clara, CA, USA) and an enhanced chemiluminescence (ECL) detection kit (GE Healthcare). Signal was detected using iBright™ CL1000 imaging system (Thermo Fisher Scientific, Waltham, MA, USA) and quantification of band intensities by densitometry was carried out as explained bellow.

## Densitometry analysis

Relative protein expression was determined by densitometry analysis using the NIH Image J software (U.S. National Institute of Health, NHI, https://imagej.nih.gov/ij/). For each picture, background was first subtracted and each band corresponding to the protein to quantify was manually selected. Then, intensity curves from each selected band were plotted and the area under each curve was calculated. Same analysis was done for tubulin to normalize the expression of the protein of interest. Images with saturated pixels were excluded for quantification.

## Polysome profile analysis

Preparation of cellular extracts, polysome profiles and fraction collection for MCL1 mRNA association with polysomes were performed as described previously (Fumagalli et al., 2009), except for minor modifications. Briefly, cells were treated for 22 hr with dox and then, CHX (Sigma) was added to the medium at 37 °C for 5 min at a concentration of 100 µM. Cells were washed twice with ice-cold PBS supplemented with 100 µg/ml CHX, pelleted by centrifugation at 3,000 rpm for 3 min and resuspended in 250 µL of hypotonic lysis buffer (1.5 mM KCl, 2.5 mM $MgCl_2$, 5 mM Tris-HCl, pH7.4, 1% sodium deoxycholate, 1% Triton X-100) supplemented with 100 µg/ml CHX, 1 mM DTT, protease inhibitors (Sigma) and 100 U/mL RNase inhibitor (Invitrogen). After incubation on ice for 5 min, the extract was homogenized and centrifuged at 3,000 x *g* for 10 min at 4ºC to remove nuclei, and the resulting supernatant was made 1 mg/mL in heparin (heparin was omitted in the analysis of

*Mcl1* mRNAs polysomal association due to its inhibitory effect on the PCR). 500 μg of cytoplasmic extract were applied to a linear 17.1-51% (w/v) sucrose gradient containing 300 mM NaCl, 10 mM $MgCl_2$, 50 mM Tris-HCl, pH 7.5, 1 mM DTT and 10 U/ml RNase inhibitor and centrifuged in a SW41 Beckman rotor at 36,000 rpm for 2 hr at 4 ºC (Beckman Coulter, Brea, CA, USA). Twelve sucrose gradient fractions of 1 mL were collected by upward displacement, ranging from light to heavy sucrose, into 100 μL proteinase K buffer containing 100 mM Tris-HCl, pH 7.5, 50 mM EDTA and 5% SDS. Each fraction was treated with 100 μg/mL proteinase K for 30 min at 37 ºC. After incubation, 100 pg *F-luc* mRNA spike (catalog #L4561; Promega, Madison, WI, USA) and 10 μg of glycogen (catalog #AM9510; Invitrogen) were added to each fraction to control for mRNA extraction and PCR efficiency, and to improve RNA recovery, respectively. RNA was subjected to phenol/chloroform extraction and isopropanol precipitation as described previously (Gentilella et al., 2017). Equal volumes of RNA from each fraction were reverse-transcribed and subjected to qRT-PCR analysis. *Mcl1* mRNA quantification on each fraction was normalized to luciferase mRNA and plotted as the percentage of total mRNA from all 12 fractions.

## De novo protein synthesis by $^3$H-leucine incorporation

Cells were labeled with $^3$H-leucine as previously described (Fumagalli et al., 2012) with minor modifications. Briefly, cells were treated for 22 hr with dox and then incubated for 30 min with 10 μCi/mL of $^3$H-leucine (PerkinElmer). Cells were washed with PBS, then incubated in 1 mL ice-cold 10% trichloroacetic acid (TCA) for 10 min and precipitated at 10,000 x *g* 4 ºC for 15 min. The TCA-insoluble proteins were washed twice with 5% TCA and solubilized in 250 μL of 0.1 M NaOH. A 200 μL aliquot of each sample was transferred into a scintillation vial together with 4 mL of scintillation liquid, and then the amount of $^3$H-leucine was determined in each sample using a liquid scintillation counter Tri-Carb® 2100TR (PerkinElmer). The remaining aliquot was used for protein quantification as previously described and, for each sample, the number of counts per minute (cpm) was normalized to total amount of protein (μg). Cycloheximide (CHX), at a concentration of 100 μg/mL for 2 hr, was used as a background control of protein synthesis.

## $^{3}$H-uridine pulse chase for rRNA synthesis

To label newly synthesized rRNA, after 22 hr dox treatment, cells were pulse labeled for 40 min with 1.0 µCi/mL of [$^{5,6}$-$^{3}$H]-uridine (PerkinElmer). Pulsed-labeled cells were then washed and chased for 3 hr at 37 ºC in 10% $CO_2$ in Anne-Kelso medium containing 1 mM non-radioactive uridine (Sigma). Following RNA extraction (see above), 10 µg of total RNA was resolved by electrophoresis on a formaldehyde-containing 0.8% agarose gel and transfer to Hybond N+ membrane (GE Healthcare, Chicago, IL, USA) for Northern blot analysis. After UV crosslinking, the membranes were sprayed with the liquid EN$^{3}$HANCE (PerkinElmer) and exposed to Kodak BioMax MS film (Kodak) at -80 ºC during 1 week for autoradiography.

## Cell viability assays and flow cytometry analysis

After treatment, cells were collected by centrifugation at 1,300 rpm for 5 min, washed twice with PBS, and resuspended in Annexin V (AnnV) binding buffer (catalog #422201; BioLegend, San Diego, CA, USA). The cells were then incubated for 15 min at room temperature with Alexa Fluor (AF)680-conjugated AnnV (catalog #A35109; Invitrogen) and Zombie violet (catalog #423113; BioLegend), and then analyzed by FACS on a BD LSRII analyzer (BD Biosciences). For propidium iodide (PI) staining, after the washes with PBS, cells were resuspended in FACS buffer (2% FBS in PBS) containing 1 µg/mL PI (catalog #P4170; Sigma) for 15 min at room temperature before FACS analysis, using a Gallios analyzer (Beckman Coulter). For intracellular staining of p53, after the washes with PBS, cells were fixed with ice-cold 4% paraformaldehyde (PFA, catalog #252931; PanReac Química S.L.U., Barcelona, Spain) for 20 min, washed and permeabilized in FACS buffer containing 0.1% saponin (Sigma) for 20 min at room temperature. Permeabilized cells were then incubated with AF647-conjugated mouse anti-p53 antibody **(Table M-1)** for 1 hr at room temperature and analyzed by FACS on the Gallios analyzer. The data were analyzed using FlowJo software v.10.5.3 (FlowJo, LLC, Ashland, OR, USA, https://www.flowjo.com/).

## Immunoprecipitation

After treatment, cells grown in 15-cm dishes were washed twice in PBS and harvested in ice-cold immunoprecipitation lysis (IP) buffer (50 mM Tris-HCl, pH 7.5, 150 mM KCl, 5 mM $MgCl_2$, 1 mM EGTA, 0.8% NP40, 10% glycerol) supplemented with 1 mM DTT, 1 mM PMSF and EDTA-free protease inhibitor cocktail (Roche), and then subjected to immunoprecipitation as previously described (Morcelle et al., 2019). Briefly, after 5 min incubation in a rotatory shaker, lysates were mechanically sheared by passing them 4-5 times through a 25 G-needle (BD Plastipak, BD Biosciences Franklin Lanes, NJ, USA) and cleared by centrifugation at 16,000 x *g* for 15 min at 4 ºC. Whole cell lysates were quantified by the BCA assay (Pierce) and ribosomes were pelleted by ultracentrifugation at 200,000 x *g* for 2 hr at 4 ºC using a Fiberlite F50-24 x 1.5 rotor (Thermo Scientific) to obtain post-ribosomal supernatants. Equivalent amounts of protein (1 mg) were pre-cleared with Magna ChIP™ Protein A/G magnetic beads (Millipore) for 1 hr and then incubated overnight at 4 ºC in IP buffer with either rabbit polyclonal anti-RPL5 or control rabbit IgG **(Table M-1)** to a final concentration of 4 µg antibody per mg of sample. Magna ChIP™ Protein A/G magnetic beads were added to the IP samples and incubated for an additional 2 hr at 4 ºC with rotation. Beads were washed four times with IP buffer, eluted in protein loading buffer by boiling at 95 ºC for 10 min and loaded on SDS-PAGE gel for Western blot analysis with MDM2, p53, RPL5 and RPL11 antibodies **(Table M-1)**, as described above.

## Ubiquitination assay

For the ubiquitination assay, cells were lysed in ice-cold RIPA buffer (50 mM Tris-HCl, pH 7.5, 150 mM NaCl, 2 mM EDTA, 1% NP40, 0.1% Sodium deoxycholate) supplemented with 1 mM DTT, 1 mM PMSF, protease inhibitors (Roche) and 5 mM of de DUB inhibitor IAA (Gentilella and Khalili, 2011). The lysates were cleared by centrifugation, protein quantified by the BCA Assay and 2 mg of each protein lysate was pre-cleared with Magna ChIP™ Protein A/G magnetic beads for 1 hr and then incubated with rotation overnight at 4 ºC in RIPA buffer with either anti-MCL1 or normal rabbit IgG **(Table M-1)** at a ratio of antibody to sample of 4 µg/mg. Magna ChIP™ Protein A/G magnetic beads were added to the IP samples and incubated by

rotation for an additional 3 hr at 4 ºC. Beads were washed four times with IP buffer, eluted in protein loading buffer and resolved on 10% NuPAGE Bis-Tris gel for Western blot analysis with ubiquitin or MCL1 antibody **(Table M-1)**.

## Generation of animal models and mice treatment

All *in vivo* studies were performed with the approval of either the Peter MacCallum Cancer Centre Animal Experimentation Ethics Committee (Melbourne, VIC, Australia) or the IDIBELL's Animal Care and Use Committee and the Generalitat de Catalunya (Barcelona, Spain). Four-week-old male C57BL/6 Ly5.1 mice were obtained from the Garvan Institute of Medical Research (Sydney, NSW, Australia) or purchased to Charles River Laboratories (Calco, Italy). To generate the E$\mu$-MYC lymphomas, six-to-eight-week-old mice were intravenously injected with 200,000 E$\mu$-MYC B-cell lymphoma cells, either *Trp53*$^{+/+}$ (clone #4242-*Gfp*) or *Trp53*$^{-/-}$ (clone # 3239), in sterile PBS (Gibco) as previously described (Bywater et al., 2012, Devlin et al., 2016). When the number of lymphoma cells in peripheral blood was 20-30% (~10-13 days post-injection), as assessed by tail-vein bleeding (see below), mice were treated with the pharmacological inhibitor ActD (BioVision) or with the corresponding vehicle control. ActD was prepared in 1:1 polyethylene glycol (PEG)400/1X PBS and administrated intraperitoneally (*i.p.*) at a dose of 0.100 mg/kg mouse.

## Acute analysis of *in vivo* on-target effects

A single dose of either ActD or vehicle was administrated 6 hr before sacrifice to 4-5 mice per treatment group (n=4-5). Peripheral blood samples (50 µL blood) were collected by tail-vein bleed and added to 10 µL EDTA in 1.5 mL Eppendorf tubes for the assessment of tumor burden. 20 µL from each sample were diluted in 500 µL PBS and white blood cells (WBCs) and lymphocytes number were determined using an ADVIA 120 automated hematology analyzer (Bayer Diagnostics, Tarrytown, NY). After cervical dislocation, inguinal nodes, axillary lymph nodes, brachial nodes and the spleen were either collected into 12-well plates containing 1-2 mL of FACS buffer for flow cytometer analysis, or snap-frozen for protein/RNA analysis. For FACS analyses, single cell suspensions were generated by crushing spleens and lymph nodes with the end of a 10 mL-syringe and filtered through a 40 µm-mesh cell strainer (Corning,

Inc., NY, USA). WBCs were isolated from remaining blood samples and spleens by incubation in red-blood-cell (RBC) lysis buffer (144 mM $NH_4Cl$, 17 mM Tris-HCl, pH 7.65) at 37 ºC for 5 min, centrifugation at 300 x *g* for 5 min, and were resuspended in FACS buffer. WBCs (from both blood and spleen) and one million lymph node cells were analyzed by FACS. Briefly, samples were washed twice with FACS buffer and incubated on ice with APC-conjugated rabbit anti-B220 antibody for 20 min **(Table M-1)**, then washed and incubated with a mouse anti-cd45.2-FITC antibody (used only for *Trp53*$^{-/-}$ E$\mu$-MYC cells) for another 20 min, washed again and then resuspended in FACS buffer containing 1 µg/mL PI for 15 min at room temperature before FACS analysis on a BD LSRII analyzer (BD Biosciences). For intracellular staining of p53, one million WBCs from spleens or lymph node cells, collected from either vehicle-treated or ActD-treated *Trp53*$^{+/+}$ E$\mu$-MYC lymphoma-bearing mice (n=4-5 mice per treatment group), were fixed with PFA, permeabilized in FACS buffer and incubated with AF647-conjugated mouse anti-p53 antibody **(Table M-1)**, as described above, and subsequently analyzed by FACS on a Gallios analyzer (Beckman Coulter).

## Survival analysis

For survival (Kaplan-Meier) analyses, 10 days post-transplant mice were treated with either vehicle or 0.100 mg/kg/day ActD (n=9 mice per treatment group). Treatment was administrated via *i.p.* in a first cycle of 5 days on/6 days off and two additional cycles of 4 days on/4 days off. Peripheral blood analysis was assessed the day before and 3 days after treatment initiation to follow-up disease progression. Mice were weighted and monitored daily, and sacrificed at an ethical end-point; hunched posture, ruffled fur, enlarged lymph nodes, labored breathing, weight loss (equal to 20% of body weight at treatment initiation), limited mobility or paralysis.

## Statistical analysis

Statistical analysis was performed using GraphPad Prism v.7.0a for MAC (GraphPad Software, San Diego, CA, USA, https://www.graphpad.com/). Data are displayed as mean ± SEM, for the indicated 'n' independent experiments. Shapiro-Wilk test was performed to assess normal distribution of the data. Experimental data sets were compared using the indicated statistical test as follows:

Two-sampled, two-tailed Student's t-test: two experimental conditions. Data with normal-distribution and equal variance.

One-way ANOVA test: more than two conditions with one independent factor. Data samples normally distributed and with equal variance. Multiple comparisons corrected using Tukey's test.

Two-way ANOVA test: more than two conditions with two independent factors. Data samples normally distributed and with equal variance. Multiple comparisons corrected using Sidak's test.

Kruskal-Wallis test: more than two conditions. No normal distribution. Multiple comparisons corrected using Dunn's test.

Extra-sum-of-squares F test: comparison of the best-fitted values of distinct sigmoidal curves.

Log-ran (Mantel-Cox) test and Gehan-Breslow-Wilcoxin test: comparison of survival curves from two or more groups.

Statistical significance was considered for p values (P) below 0.05: *, $P<0.05$; **, $P<0.01$; ***, $P<0.001$ and ****, $P<0.0001$. P above 0.05 were considered not significant (NS).

# REFERENCES

ADAMS, C. M., CLARK-GARVEY, S., PORCU, P. & EISCHEN, C. M. 2018. Targeting the Bcl-2 Family in B Cell Lymphoma. *Front Oncol,* 8**,** 636.

ADAMS, C. M., KIM, A. S., MITRA, R., CHOI, J. K., GONG, J. Z. & EISCHEN, C. M. 2017. BCL-W has a fundamental role in B cell survival and lymphomagenesis. *J Clin Invest,* 127**,** 635-650.

ADAMS, J. M. & CORY, S. 2007. The Bcl-2 apoptotic switch in cancer development and therapy. *Oncogene,* 26**,** 1324-37.

ADAMS, J. M. & CORY, S. 2018. The BCL-2 arbiters of apoptosis and their growing role as cancer targets. *Cell Death Differ,* 25**,** 27-36.

ADAMS, J. M., HARRIS, A. W., PINKERT, C. A., CORCORAN, L. M., ALEXANDER, W. S., CORY, S., PALMITER, R. D. & BRINSTER, R. L. 1985. The c-myc oncogene driven by immunoglobulin enhancers induces lymphoid malignancy in transgenic mice. *Nature,* 318**,** 533-8.

ADHIKARY, S. & EILERS, M. 2005. Transcriptional regulation and transformation by Myc proteins. *Nat Rev Mol Cell Biol,* 6**,** 635-45.

AFFER, M., CHESI, M., CHEN, W. G., KEATS, J. J., DEMCHENKO, Y. N., ROSCHKE, A. V., VAN WIER, S., FONSECA, R., BERGSAGEL, P. L. & KUEHL, W. M. 2014. Promiscuous MYC locus rearrangements hijack enhancers but mostly super-enhancers to dysregulate MYC expression in multiple myeloma. *Leukemia,* 28**,** 1725-1735.

AICHBERGER, K. J., MAYERHOFER, M., KRAUTH, M. T., SKVARA, H., FLORIAN, S., SONNECK, K., AKGUL, C., DERDAK, S., PICKL, W. F., WACHECK, V., SELZER, E., MONIA, B. P., MORIGGL, R., VALENT, P. & SILLABER, C. 2005. Identification of mcl-1 as a BCR/ABL-dependent target in chronic myeloid leukemia (CML): evidence for cooperative antileukemic effects of imatinib and mcl-1 antisense oligonucleotides. *Blood,* 105**,** 3303-11.

AKGUL, C. 2009. Mcl-1 is a potential therapeutic target in multiple types of cancer. *Cell Mol Life Sci,* 66**,** 1326-36.

AKGUL, C., MOULDING, D. A., WHITE, M. R. & EDWARDS, S. W. 2000. In vivo localisation and stability of human Mcl-1 using green fluorescent protein (GFP) fusion proteins. *FEBS Lett,* 478**,** 72-6.

ALBERSHARDT, T. C., SALERNI, B. L., SODERQUIST, R. S., BATES, D. J., PLETNEV, A. A., KISSELEV, A. F. & EASTMAN, A. 2011. Multiple BH3 mimetics antagonize antiapoptotic MCL1 protein by inducing the endoplasmic reticulum stress response and up-regulating BH3-only protein NOXA. *J Biol Chem,* 286**,** 24882-95.

ALEXANDER, W. S., BERNARD, O., CORY, S. & ADAMS, J. M. 1989. Lymphomagenesis in E mu-myc transgenic mice can involve ras mutations. *Oncogene,* 4**,** 575-81.

ALLEN, T. D., ZHU, C. Q., JONES, K. D., YANAGAWA, N., TSAO, M. S. & BISHOP, J. M. 2011. Interaction between MYC and MCL1 in the genesis and outcome of non-small-cell lung cancer. *Cancer Res,* 71**,** 2212-21.

ANGER, A. M., ARMACHE, J. P., BERNINGHAUSEN, O., HABECK, M., SUBKLEWE, M., WILSON, D. N. & BECKMANN, R. 2013. Structures of the human and Drosophila 80S ribosome. *Nature,* 497**,** 80-5.

ARABI, A., WU, S., RIDDERSTRALE, K., BIERHOFF, H., SHIUE, C., FATYOL, K., FAHLEN, S., HYDBRING, P., SODERBERG, O., GRUMMT, I., LARSSON, L. G. & WRIGHT, A. P. 2005. c-Myc associates with ribosomal DNA and activates RNA polymerase I transcription. *Nat Cell Biol,* 7**,** 303-10.

ARBOUR, N., VANDERLUIT, J. L., LE GRAND, J. N., JAHANI-ASL, A., RUZHYNSKY, V. A., CHEUNG, E. C., KELLY, M. A., MACKENZIE, A. E., PARK, D. S., OPFERMAN, J. T. & SLACK, R. S. 2008. Mcl-1 is a key regulator of apoptosis during CNS development and after DNA damage. *J Neurosci,* 28**,** 6068-78.

ASLANIAN, A., IAQUINTA, P. J., VERONA, R. & LEES, J. A. 2004. Repression of the Arf tumor suppressor by E2F3 is required for normal cell cycle kinetics. *Genes Dev,* 18**,** 1413-22.

AUBERT, M., O'DONOHUE, M. F., LEBARON, S. & GLEIZES, P. E. 2018. Pre-Ribosomal RNA Processing in Human Cells: From Mechanisms to Congenital Diseases. *Biomolecules,* 8.

AYER, D. E. & EISENMAN, R. N. 1993. A switch from Myc:Max to Mad:Max heterocomplexes accompanies monocyte/macrophage differentiation. *Genes Dev,* 7**,** 2110-9.

AYRAULT, O., ANDRIQUE, L. & SEITE, P. 2006. Involvement of the transcriptional factor E2F1 in the regulation of the rRNA promoter. *Exp Cell Res,* 312**,** 1185-93.

BADERTSCHER, L., WILD, T., MONTELLESE, C., ALEXANDER, L. T., BAMMERT, L., SARAZOVA, M., STEBLER, M., CSUCS, G., MAYER, T. U., ZAMBONI, N., ZEMP, I., HORVATH, P. & KUTAY, U. 2015. Genome-wide RNAi Screening Identifies Protein Modules Required for 40S Subunit Synthesis in Human Cells. *Cell Rep,* 13**,** 2879-91.

BAE, J., LEO, C. P., HSU, S. Y. & HSUEH, A. J. 2000. MCL-1S, a splicing variant of the antiapoptotic BCL-2 family member MCL-1, encodes a proapoptotic protein possessing only the BH3 domain. *J Biol Chem,* 275**,** 25255-61.

BAKER, A., GREGORY, G. P., VERBRUGGE, I., KATS, L., HILTON, J. J., VIDACS, E., LEE, E. M., LOCK, R. B., ZUBER, J., SHORTT, J. & JOHNSTONE, R. W. 2016. The CDK9 Inhibitor Dinaciclib Exerts Potent Apoptotic and Antitumor Effects in Preclinical Models of MLL-Rearranged Acute Myeloid Leukemia. *Cancer Res,* 76**,** 1158-69.

BALASUBRAMANIAN, S., HURLEY, L. H. & NEIDLE, S. 2011. Targeting G-quadruplexes in gene promoters: a novel anticancer strategy? *Nat Rev Drug Discov,* 10**,** 261-75.

BANGE, G., MURAT, G., SINNING, I., HURT, E. & KRESSLER, D. 2013. New twist to nuclear import: When two travel together. *Commun Integr Biol,* 6**,** e24792.

BARDE, I., SALMON, P. & TRONO, D. 2010. Production and titration of lentiviral vectors. *Curr Protoc Neurosci,* Chapter 4**,** Unit 4 21.

BARKIC, M., CRNOMARKOVIC, S., GRABUSIC, K., BOGETIC, I., PANIC, L., TAMARUT, S., COKARIC, M., JERIC, I., VIDAK, S. & VOLAREVIC, S. 2009. The p53 tumor suppressor causes congenital malformations in Rpl24-deficient mice and promotes their survival. *Mol Cell Biol,* 29**,** 2489-504.

BARLOW, J. L., DRYNAN, L. F., HEWETT, D. R., HOLMES, L. R., LORENZO-ABALDE, S., LANE, A. L., JOLIN, H. E., PANNELL, R., MIDDLETON, A. J., WONG, S. H., WARREN, A. J., WAINSCOAT, J. S., BOULTWOOD, J. & MCKENZIE, A. N. 2010a. A p53-dependent mechanism underlies macrocytic anemia in a mouse model of human 5q- syndrome. *Nat Med,* 16**,** 59-66.

BARLOW, J. L., DRYNAN, L. F., TRIM, N. L., ERBER, W. N., WARREN, A. J. & MCKENZIE, A. N. 2010b. New insights into 5q- syndrome as a ribosomopathy. *Cell Cycle,* 9**,** 4286-93.

BARNA, M., PUSIC, A., ZOLLO, O., COSTA, M., KONDRASHOV, N., REGO, E., RAO, P. H. & RUGGERO, D. 2008. Suppression of Myc oncogenic activity by ribosomal protein haploinsufficiency. *Nature,* 456**,** 971-5.

BASSLER, J. & HURT, E. 2019. Eukaryotic Ribosome Assembly. *Annu Rev Biochem,* 88**,** 281-306.

BAUDINO, T. A., MACLEAN, K. H., BRENNAN, J., PARGANAS, E., YANG, C., ASLANIAN, A., LEES, J. A., SHERR, C. J., ROUSSEL, M. F. & CLEVELAND, J. L. 2003. Myc-mediated proliferation and lymphomagenesis, but not apoptosis, are compromised by E2f1 loss. *Mol Cell,* 11**,** 905-14.

BELLODI, C., KOPMAR, N. & RUGGERO, D. 2010. Deregulation of oncogene-induced senescence and p53 translational control in X-linked dyskeratosis congenita. *EMBO J,* 29**,** 1865-76.

BELTRAN, H. 2014. The N-myc Oncogene: Maximizing its Targets, Regulation, and Therapeutic Potential. *Mol Cancer Res,* 12**,** 815-22.

BEN-NISSAN, G. & SHARON, M. 2014. Regulating the 20S proteasome ubiquitin-independent degradation pathway. *Biomolecules,* 4**,** 862-84.

BEN-SAHRA, I., HOWELL, J. J., ASARA, J. M. & MANNING, B. D. 2013. Stimulation of de novo pyrimidine synthesis by growth signaling through mTOR and S6K1. *Science,* 339**,** 1323-8.

BENCHIMOL, S. 2001. p53-dependent pathways of apoptosis. *Cell Death Differ,* 8**,** 1049-51.

BENSAUDE, O. 2011. Inhibiting eukaryotic transcription: Which compound to choose? How to evaluate its activity? *Transcription,* 2**,** 103-108.

BERGSTRALH, D. T., CONTI, B. J., MOORE, C. B., BRICKEY, W. J., TAXMAN, D. J. & TING, J. P. 2007. Global functional analysis of nucleophosmin in Taxol response, cancer, chromatin regulation, and ribosomal DNA transcription. *Exp Cell Res,* 313**,** 65-76.

BEROUKHIM, R., MERMEL, C. H., PORTER, D., WEI, G., RAYCHAUDHURI, S., DONOVAN, J., BARRETINA, J., BOEHM, J. S., DOBSON, J., URASHIMA, M., MC HENRY, K. T., PINCHBACK, R. M., LIGON, A. H., CHO, Y. J., HAERY, L., GREULICH, H., REICH, M., WINCKLER, W., LAWRENCE, M. S., WEIR, B. A., TANAKA, K. E., CHIANG, D. Y., BASS, A. J., LOO, A., HOFFMAN, C., PRENSNER, J., LIEFELD, T., GAO,

Q., YECIES, D., SIGNORETTI, S., MAHER, E., KAYE, F. J., SASAKI, H., TEPPER, J. E., FLETCHER, J. A., TABERNERO, J., BASELGA, J., TSAO, M. S., DEMICHELIS, F., RUBIN, M. A., JANNE, P. A., DALY, M. J., NUCERA, C., LEVINE, R. L., EBERT, B. L., GABRIEL, S., RUSTGI, A. K., ANTONESCU, C. R., LADANYI, M., LETAI, A., GARRAWAY, L. A., LODA, M., BEER, D. G., TRUE, L. D., OKAMOTO, A., POMEROY, S. L., SINGER, S., GOLUB, T. R., LANDER, E. S., GETZ, G., SELLERS, W. R. & MEYERSON, M. 2010. The landscape of somatic copy-number alteration across human cancers. *Nature,* 463**,** 899-905.

BHATIA, K., HUPPI, K., SPANGLER, G., SIWARSKI, D., IYER, R. & MAGRATH, I. 1993. Point mutations in the c-Myc transactivation domain are common in Burkitt's lymphoma and mouse plasmacytomas. *Nat Genet,* 5**,** 56-61.

BIEGING, K. T., MELLO, S. S. & ATTARDI, L. D. 2014. Unravelling mechanisms of p53-mediated tumour suppression. *Nat Rev Cancer,* 14**,** 359-70.

BIRCH, J. L. & ZOMERDIJK, J. C. 2008. Structure and function of ribosomal RNA gene chromatin. *Biochem Soc Trans,* 36**,** 619-24.

BISHOP, J. M. 1982. Retroviruses and cancer genes. *Adv Cancer Res,* 37**,** 1-32.

BLACKFORD, A. N. & JACKSON, S. P. 2017. ATM, ATR, and DNA-PK: The Trinity at the Heart of the DNA Damage Response. *Mol Cell,* 66**,** 801-817.

BLUM, K. A., LOZANSKI, G. & BYRD, J. C. 2004. Adult Burkitt leukemia and lymphoma. *Blood,* 104**,** 3009-20.

BOERSMA, H. H., KIETSELAER, B. L., STOLK, L. M., BENNAGHMOUCH, A., HOFSTRA, L., NARULA, J., HEIDENDAL, G. A. & REUTELINGSPERGER, C. P. 2005. Past, present, and future of annexin A5: from protein discovery to clinical applications. *J Nucl Med,* 46**,** 2035-50.

BOISVERT, F. M., AHMAD, Y., GIERLINSKI, M., CHARRIERE, F., LAMONT, D., SCOTT, M., BARTON, G. & LAMOND, A. I. 2012. A quantitative spatial proteomics analysis of proteome turnover in human cells. *Mol Cell Proteomics,* 11**,** M111 011429.

BOISVERT, F. M., VAN KONINGSBRUGGEN, S., NAVASCUES, J. & LAMOND, A. I. 2007. The multifunctional nucleolus. *Nat Rev Mol Cell Biol,* 8**,** 574-85.

BOON, K., CARON, H. N., VAN ASPEREN, R., VALENTIJN, L., HERMUS, M. C., VAN SLUIS, P., ROOBEEK, I., WEIS, I., VOUTE, P. A., SCHWAB, M. & VERSTEEG, R. 2001. N-myc enhances the expression of a large set of genes functioning in ribosome biogenesis and protein synthesis. *EMBO J,* 20**,** 1383-93.

BOUCHARD, C., LEE, S., PAULUS-HOCK, V., LODDENKEMPER, C., EILERS, M. & SCHMITT, C. A. 2007. FoxO transcription factors suppress Myc-driven lymphomagenesis via direct activation of Arf. *Genes Dev,* 21**,** 2775-87.

BOULON, S., WESTMAN, B. J., HUTTEN, S., BOISVERT, F. M. & LAMOND, A. I. 2010. The nucleolus under stress. *Mol Cell,* 40**,** 216-27.

BOULTWOOD, J., PELLAGATTI, A. & WAINSCOAT, J. S. 2012. Haploinsufficiency of ribosomal proteins and p53 activation in anemia: Diamond-Blackfan anemia and the 5q- syndrome. *Adv Biol Regul,* 52**,** 196-203.

BOWMAN, M., OLDRIDGE, M., ARCHER, C., O'ROURKE, A., MCPARLAND, J., BREKELMANS, R., SELLER, A. & LESTER, T. 2012. Gross deletions in TCOF1 are a cause of Treacher-Collins-Franceschetti syndrome. *Eur J Hum Genet,* 20**,** 769-77.

BOXER, L. M. & DANG, C. V. 2001. Translocations involving c-myc and c-myc function. *Oncogene,* 20**,** 5595-610.

BRANDMAN, O., STEWART-ORNSTEIN, J., WONG, D., LARSON, A., WILLIAMS, C. C., LI, G. W., ZHOU, S., KING, D., SHEN, P. S., WEIBEZAHN, J., DUNN, J. G., ROUSKIN, S., INADA, T., FROST, A. & WEISSMAN, J. S. 2012. A ribosome-bound quality control complex triggers degradation of nascent peptides and signals translation stress. *Cell,* 151**,** 1042-54.

BRENNAN, M. S., CHANG, C., TAI, L., LESSENE, G., STRASSER, A., DEWSON, G., KELLY, G. L. & HEROLD, M. J. 2018. Humanized Mcl-1 mice enable accurate preclinical evaluation of MCL-1 inhibitors destined for clinical use. *Blood,* 132**,** 1573-1583.

BRIGHENTI, E., CALABRESE, C., LIGUORI, G., GIANNONE, F. A., TRERE, D., MONTANARO, L. & DERENZINI, M. 2014. Interleukin 6 downregulates p53 expression and activity by stimulating ribosome biogenesis: a new pathway connecting inflammation to cancer. *Oncogene,* 33**,** 4396-406.

BRUNO, P. M., LIU, Y., PARK, G. Y., MURAI, J., KOCH, C. E., EISEN, T. J., PRITCHARD, J. R., POMMIER, Y., LIPPARD, S. J. & HEMANN, M. T. 2017. A subset of platinum-containing chemotherapeutic agents kills cells by inducing ribosome biogenesis stress. *Nat Med,* 23**,** 461-471.

BURGER, K., MUHL, B., HARASIM, T., ROHRMOSER, M., MALAMOUSSI, A., ORBAN, M., KELLNER, M., GRUBER-EBER, A., KREMMER, E., HOLZEL, M. & EICK, D. 2010. Chemotherapeutic drugs inhibit ribosome biogenesis at various levels. *J Biol Chem,* 285**,** 12416-25.

BURKITT, D. 1958. A sarcoma involving the jaws in African children. *Br J Surg,* 46**,** 218-23.

BURKITT, D. & O'CONOR, G. T. 1961. Malignant lymphoma in African children. I. A clinical syndrome. *Cancer,* 14**,** 258-69.

BURSAC, S., BRDOVCAK, M. C., DONATI, G. & VOLAREVIC, S. 2014. Activation of the tumor suppressor p53 upon impairment of ribosome biogenesis. *Biochim Biophys Acta,* 1842**,** 817-30.

BURSAC, S., BRDOVCAK, M. C., PFANNKUCHEN, M., ORSOLIC, I., GOLOMB, L., ZHU, Y., KATZ, C., DAFTUAR, L., GRABUSIC, K., VUKELIC, I., FILIC, V., OREN, M., PRIVES, C. & VOLAREVIC, S. 2012. Mutual protection of ribosomal proteins L5 and L11 from degradation is essential for p53 activation upon ribosomal biogenesis stress. *Proc Natl Acad Sci U S A,* 109**,** 20467-72.

BUSZCZAK, M., SIGNER, R. A. & MORRISON, S. J. 2014. Cellular differences in protein synthesis regulate tissue homeostasis. *Cell,* 159**,** 242-51.

BYWATER, M. J., PEARSON, R. B., MCARTHUR, G. A. & HANNAN, R. D. 2013. Dysregulation of the basal RNA polymerase transcription apparatus in cancer. *Nat Rev Cancer,* 13**,** 299-314.

BYWATER, M. J., POORTINGA, G., SANIJ, E., HEIN, N., PECK, A., CULLINANE, C., WALL, M., CLUSE, L., DRYGIN, D., ANDERES, K., HUSER, N., PROFFITT, C., BLIESATH, J., HADDACH, M., SCHWAEBE, M. K., RYCKMAN, D. M., RICE, W. G., SCHMITT, C., LOWE, S. W., JOHNSTONE, R. W., PEARSON, R. B., MCARTHUR, G. A. & HANNAN, R. D. 2012. Inhibition of RNA polymerase I as a therapeutic strategy to promote cancer-specific activation of p53. *Cancer Cell,* 22**,** 51-65.

CABURET, S., CONTI, C., SCHURRA, C., LEBOFSKY, R., EDELSTEIN, S. J. & BENSIMON, A. 2005. Human ribosomal RNA gene arrays display a broad range of palindromic structures. *Genome Res,* 15**,** 1079-85.

CAENEPEEL, S., BROWN, S. P., BELMONTES, B., MOODY, G., KEEGAN, K. S., CHUI, D., WHITTINGTON, D. A., HUANG, X., POPPE, L., CHENG, A. C., CARDOZO, M., HOUZE, J., LI, Y., LUCAS, B., PARAS, N. A., WANG, X., TAYGERLY, J. P., VIMOLRATANA, M., ZANCANELLA, M., ZHU, L., CAJULIS, E., OSGOOD, T., SUN, J., DAMON, L., EGAN, R. K., GRENINGER, P., MCCLANAGHAN, J. D., GONG, J., MOUJALLED, D., POMILIO, G., BELTRAN, P., BENES, C. H., ROBERTS, A. W., HUANG, D. C., WEI, A., CANON, J., COXON, A. & HUGHES, P. E. 2018. AMG 176, a Selective MCL1 Inhibitor, Is Effective in Hematologic Cancer Models Alone and in Combination with Established Therapies. *Cancer Discov,* 8**,** 1582-1597.

CAIRNS, C. A. & WHITE, R. J. 1998. p53 is a general repressor of RNA polymerase III transcription. *EMBO J,* 17**,** 3112-23.

CALVINO, F. R., KHARDE, S., ORI, A., HENDRICKS, A., WILD, K., KRESSLER, D., BANGE, G., HURT, E., BECK, M. & SINNING, I. 2015. Symportin 1 chaperones 5S RNP assembly during ribosome biogenesis by occupying an essential rRNA-binding site. *Nat Commun,* 6**,** 6510.

CAMPANER, S. & AMATI, B. 2012. Two sides of the Myc-induced DNA damage response: from tumor suppression to tumor maintenance. *Cell Div,* 7**,** 6.

CAMPBELL, K. J., BATH, M. L., TURNER, M. L., VANDENBERG, C. J., BOUILLET, P., METCALF, D., SCOTT, C. L. & CORY, S. 2010. Elevated Mcl-1 perturbs lymphopoiesis, promotes transformation of hematopoietic stem/progenitor cells, and enhances drug resistance. *Blood,* 116**,** 3197-207.

CAMPBELL, K. J. & WHITE, R. J. 2014. MYC regulation of cell growth through control of transcription by RNA polymerases I and III. *Cold Spring Harb Perspect Med,* 4.

CARTER, B. Z., MAK, D. H., SCHOBER, W. D., MCQUEEN, T., HARRIS, D., ESTROV, Z., EVANS, R. L. & ANDREEFF, M. 2006. Triptolide induces caspase-dependent cell death mediated via the mitochondrial pathway in leukemic cells. *Blood,* 108**,** 630-7.

CASERTA, T. M., SMITH, A. N., GULTICE, A. D., REEDY, M. A. & BROWN, T. L. 2003. Q-VD-OPh, a broad spectrum caspase inhibitor with potent antiapoptotic properties. *Apoptosis,* 8**,** 345-52.

CASEY, S. C., BAYLOT, V. & FELSHER, D. W. 2017. MYC: Master Regulator of Immune Privilege. *Trends Immunol,* 38**,** 298-305.

CEREZO, E., PLISSON-CHASTANG, C., HENRAS, A. K., LEBARON, S., GLEIZES, P. E., O'DONOHUE, M. F., ROMEO, Y. & HENRY, Y. 2019. Maturation of pre-40S particles in yeast and humans. *Wiley Interdiscip Rev RNA,* 10**,** e1516.

CHAKRABORTY, A., UECHI, T. & KENMOCHI, N. 2011. Guarding the 'translation apparatus': defective ribosome biogenesis and the p53 signaling pathway. *Wiley Interdiscip Rev RNA,* 2**,** 507-22.

CHAN, J. C., HANNAN, K. M., RIDDELL, K., NG, P. Y., PECK, A., LEE, R. S., HUNG, S., ASTLE, M. V., BYWATER, M., WALL, M., POORTINGA, G., JASTRZEBSKI, K., SHEPPARD, K. E., HEMMINGS, B. A., HALL, M. N., JOHNSTONE, R. W., MCARTHUR, G. A., HANNAN, R. D. & PEARSON, R. B. 2011. AKT promotes rRNA synthesis and cooperates with c-MYC to stimulate ribosome biogenesis in cancer. *Sci Signal,* 4**,** ra56.

CHEN, D., KON, N., ZHONG, J., ZHANG, P., YU, L. & GU, W. 2013. Differential effects on ARF stability by normal versus oncogenic levels of c-Myc expression. *Mol Cell,* 51**,** 46-56.

CHEN, D., SHAN, J., ZHU, W. G., QIN, J. & GU, W. 2010. Transcription-independent ARF regulation in oncogenic stress-mediated p53 responses. *Nature,* 464**,** 624-7.

CHEN, D., ZHANG, Z., LI, M., WANG, W., LI, Y., RAYBURN, E. R., HILL, D. L., WANG, H. & ZHANG, R. 2007. Ribosomal protein S7 as a novel modulator of p53-MDM2 interaction: binding to MDM2, stabilization of p53 protein, and activation of p53 function. *Oncogene,* 26**,** 5029-37.

CHEN, H., LIU, H. & QING, G. 2018. Targeting oncogenic Myc as a strategy for cancer treatment. *Signal Transduct Target Ther,* 3**,** 5.

CHEN, L. & FLETCHER, S. 2017. Mcl-1 inhibitors: a patent review. *Expert Opin Ther Pat,* 27**,** 163-178.

CHEN, R., WIERDA, W. G., CHUBB, S., HAWTIN, R. E., FOX, J. A., KEATING, M. J., GANDHI, V. & PLUNKETT, W. 2009. Mechanism of action of SNS-032, a novel cyclin-dependent kinase inhibitor, in chronic lymphocytic leukemia. *Blood,* 113**,** 4637-45.

CHEN, Y. B., LI, S., LANE, A. A., CONNOLLY, C., DEL RIO, C., VALLES, B., CURTIS, M., BALLEN, K., CUTLER, C., DEY, B. R., EL-JAWAHRI, A., FATHI, A. T., HO, V. T., JOYCE, A., MCAFEE, S., RUDEK, M., RAJKHOWA, T., VERSELIS, S., ANTIN, J. H., SPITZER, T. R., LEVIS, M. & SOIFFER, R. 2014. Phase I trial of maintenance sorafenib after allogeneic hematopoietic stem cell transplantation for fms-like tyrosine kinase 3 internal tandem duplication acute myeloid leukemia. *Biol Blood Marrow Transplant,* 20**,** 2042-8.

CHENG, Q. & CHEN, J. 2010. Mechanism of p53 stabilization by ATM after DNA damage. *Cell Cycle,* 9**,** 472-8.

CHIPUK, J. E., BOUCHIER-HAYES, L., KUWANA, T., NEWMEYER, D. D. & GREEN, D. R. 2005. PUMA couples the nuclear and cytoplasmic proapoptotic function of p53. *Science,* 309**,** 1732-5.

CHIPUK, J. E., MOLDOVEANU, T., LLAMBI, F., PARSONS, M. J. & GREEN, D. R. 2010. The BCL-2 family reunion. *Mol Cell,* 37**,** 299-310.

CHO-VEGA, J. H., RASSIDAKIS, G. Z., ADMIRAND, J. H., OYARZO, M., RAMALINGAM, P., PARAGUYA, A., MCDONNELL, T. J., AMIN, H. M. & MEDEIROS, L. J. 2004. MCL-1 expression in B-cell non-Hodgkin's lymphomas. *Hum Pathol,* 35**,** 1095-100.

CHOOK, Y. M. & SUEL, K. E. 2011. Nuclear import by karyopherin-betas: recognition and inhibition. *Biochim Biophys Acta,* 1813**,** 1593-606.

CHOONG, M. L., YANG, H., LEE, M. A. & LANE, D. P. 2009. Specific activation of the p53 pathway by low dose actinomycin D: a new route to p53 based cyclotherapy. *Cell Cycle,* 8**,** 2810-8.

CHOU, C. H., LEE, R. S. & YANG-YEN, H. F. 2006. An internal EELD domain facilitates mitochondrial targeting of Mcl-1 via a Tom70-dependent pathway. *Mol Biol Cell,* 17**,** 3952-63.

CHUNG, H. J. & LEVENS, D. 2005. c-myc expression: keep the noise down! *Mol Cells,* 20**,** 157-66.
CIDADO, J., PROIA, T., BOIKO, S., SAN MARTIN, M., CRISCIONE, S., FERGUSON, D., SHAO, W. & DREW, L. 2018. AZD4573, a novel CDK9 inhibitor, rapidly induces cell death in hematological tumor models through depletion of Mcl1 [Abstract]. *Cancer Res,* 78**,** Abstract nr 310.
CIGANDA, M. & WILLIAMS, N. 2011. Eukaryotic 5S rRNA biogenesis. *Wiley Interdiscip Rev RNA,* 2**,** 523-33.
CLEVELAND, J. L. & SHERR, C. J. 2004. Antagonism of Myc functions by Arf. *Cancer Cell,* 6**,** 309-11.
CLOHESSY, J. G., ZHUANG, J. & BRADY, H. J. 2004. Characterisation of Mcl-1 cleavage during apoptosis of haematopoietic cells. *Br J Haematol,* 125**,** 655-65.
COLE, M. D. & COWLING, V. H. 2009. Specific regulation of mRNA cap methylation by the c-Myc and E2F1 transcription factors. *Oncogene,* 28**,** 1169-75.
CONACCI-SORRELL, M., MCFERRIN, L. & EISENMAN, R. N. 2014. An overview of MYC and its interactome. *Cold Spring Harb Perspect Med,* 4**,** a014357.
CORTES, C. L., VEIGA, S. R., ALMACELLAS, E., HERNANDEZ-LOSA, J., FERRERES, J. C., KOZMA, S. C., AMBROSIO, S., THOMAS, G. & TAULER, A. 2016. Effect of low doses of actinomycin D on neuroblastoma cell lines. *Mol Cancer,* 15**,** 1.
COSTA, L. J., XAVIER, A. C., WAHLQUIST, A. E. & HILL, E. G. 2013. Trends in survival of patients with Burkitt lymphoma/leukemia in the USA: an analysis of 3691 cases. *Blood,* 121**,** 4861-6.
COWLING, V. H., CHANDRIANI, S., WHITFIELD, M. L. & COLE, M. D. 2006. A conserved Myc protein domain, MBIV, regulates DNA binding, apoptosis, transformation, and G2 arrest. *Mol Cell Biol,* 26**,** 4226-39.
CRAXTON, A., BUTTERWORTH, M., HARPER, N., FAIRALL, L., SCHWABE, J., CIECHANOVER, A. & COHEN, G. M. 2012. NOXA, a sensor of proteasome integrity, is degraded by 26S proteasomes by an ubiquitin-independent pathway that is blocked by MCL-1. *Cell Death Differ,* 19**,** 1424-34.
CROXTON, R., MA, Y., SONG, L., HAURA, E. B. & CRESS, W. D. 2002. Direct repression of the Mcl-1 promoter by E2F1. *Oncogene,* 21**,** 1359-69.
CSIBI, A., LEE, G., YOON, S. O., TONG, H., ILTER, D., ELIA, I., FENDT, S. M., ROBERTS, T. M. & BLENIS, J. 2014. The mTORC1/S6K1 pathway regulates glutamine metabolism through the eIF4B-dependent control of c-Myc translation. *Curr Biol,* 24**,** 2274-80.
CUCONATI, A., MUKHERJEE, C., PEREZ, D. & WHITE, E. 2003. DNA damage response and MCL-1 destruction initiate apoptosis in adenovirus-infected cells. *Genes Dev,* 17**,** 2922-32.
CUNNINGHAM, J. T., MORENO, M. V., LODI, A., RONEN, S. M. & RUGGERO, D. 2014. Protein and nucleotide biosynthesis are coupled by a single rate-limiting enzyme, PRPS2, to drive cancer. *Cell,* 157**,** 1088-103.
CZABOTAR, P. E., LEE, E. F., VAN DELFT, M. F., DAY, C. L., SMITH, B. J., HUANG, D. C., FAIRLIE, W. D., HINDS, M. G. & COLMAN, P. M. 2007. Structural insights into the degradation of Mcl-1 induced by BH3 domains. *Proc Natl Acad Sci U S A,* 104**,** 6217-22.
CZABOTAR, P. E., LESSENE, G., STRASSER, A. & ADAMS, J. M. 2014. Control of apoptosis by the BCL-2 protein family: implications for physiology and therapy. *Nat Rev Mol Cell Biol,* 15**,** 49-63.
D'ANTIGA, L., BAKER, A., PRITCHARD, J., PRYOR, D. & MIELI-VERGANI, G. 2001. Veno-occlusive disease with multi-organ involvement following actinomycin-D. *Eur J Cancer,* 37**,** 1141-8.
DAFTUAR, L., ZHU, Y., JACQ, X. & PRIVES, C. 2013. Ribosomal proteins RPL37, RPS15 and RPS20 regulate the Mdm2-p53-MdmX network. *PLoS One,* 8**,** e68667.
DAI, M. S., CHALLAGUNDLA, K. B., SUN, X. X., PALAM, L. R., ZENG, S. X., WEK, R. C. & LU, H. 2012. Physical and functional interaction between ribosomal protein L11 and the tumor suppressor ARF. *J Biol Chem,* 287**,** 17120-9.
DAI, M. S. & LU, H. 2004. Inhibition of MDM2-mediated p53 ubiquitination and degradation by ribosomal protein L5. *J Biol Chem,* 279**,** 44475-82.
DAI, M. S., SEARS, R. & LU, H. 2007. Feedback regulation of c-Myc by ribosomal protein L11. *Cell Cycle,* 6**,** 2735-41.

DAI, M. S., SHI, D., JIN, Y., SUN, X. X., ZHANG, Y., GROSSMAN, S. R. & LU, H. 2006. Regulation of the MDM2-p53 pathway by ribosomal protein L11 involves a post-ubiquitination mechanism. *J Biol Chem,* 281**,** 24304-13.

DAI, M. S., SUN, X. X. & LU, H. 2010. Ribosomal protein L11 associates with c-Myc at 5 S rRNA and tRNA genes and regulates their expression. *J Biol Chem,* 285**,** 12587-94.

DAI, M. S., ZENG, S. X., JIN, Y., SUN, X. X., DAVID, L. & LU, H. 2004. Ribosomal protein L23 activates p53 by inhibiting MDM2 function in response to ribosomal perturbation but not to translation inhibition. *Mol Cell Biol,* 24**,** 7654-68.

DALLA-FAVERA, R., BREGNI, M., ERIKSON, J., PATTERSON, D., GALLO, R. C. & CROCE, C. M. 1982. Human c-myc onc gene is located on the region of chromosome 8 that is translocated in Burkitt lymphoma cells. *Proc Natl Acad Sci U S A,* 79**,** 7824-7.

DANG, C. 2008. The interplay between MYC and HIF in the Warburg effect. *Oncogenes Meet Metabolism.* Springer.

DANG, C. V. 2012. MYC on the path to cancer. *Cell,* 149**,** 22-35.

DANG, C. V. 2013. MYC, metabolism, cell growth, and tumorigenesis. *Cold Spring Harb Perspect Med,* 3.

DANG, C. V., O'DONNELL, K. A., ZELLER, K. I., NGUYEN, T., OSTHUS, R. C. & LI, F. 2006. The c-Myc target gene network. *Semin Cancer Biol,* 16**,** 253-64.

DANG, C. V., REDDY, E. P., SHOKAT, K. M. & SOUCEK, L. 2017. Drugging the 'undruggable' cancer targets. *Nat Rev Cancer,* 17**,** 502-508.

DANI, C., BLANCHARD, J. M., PIECHACZYK, M., EL SABOUTY, S., MARTY, L. & JEANTEUR, P. 1984. Extreme instability of myc mRNA in normal and transformed human cells. *Proc Natl Acad Sci U S A,* 81**,** 7046-50.

DANILOVA, N., BIBIKOVA, E., COVEY, T. M., NATHANSON, D., DIMITROVA, E., KONTO, Y., LINDGREN, A., GLADER, B., RADU, C. G., SAKAMOTO, K. M. & LIN, S. 2014. The role of the DNA damage response in zebrafish and cellular models of Diamond Blackfan anemia. *Dis Model Mech,* 7**,** 895-905.

DANILOVA, N. & GAZDA, H. T. 2015. Ribosomopathies: how a common root can cause a tree of pathologies. *Dis Model Mech,* 8**,** 1013-26.

DANILOVA, N., SAKAMOTO, K. M. & LIN, S. 2008. Ribosomal protein S19 deficiency in zebrafish leads to developmental abnormalities and defective erythropoiesis through activation of p53 protein family. *Blood,* 112**,** 5228-37.

DANOVI, D., MEULMEESTER, E., PASINI, D., MIGLIORINI, D., CAPRA, M., FRENK, R., DE GRAAF, P., FRANCOZ, S., GASPARINI, P., GOBBI, A., HELIN, K., PELICCI, P. G., JOCHEMSEN, A. G. & MARINE, J. C. 2004. Amplification of Mdmx (or Mdm4) directly contributes to tumor formation by inhibiting p53 tumor suppressor activity. *Mol Cell Biol,* 24**,** 5835-43.

DANSEN, T. B., WHITFIELD, J., ROSTKER, F., BROWN-SWIGART, L. & EVAN, G. I. 2006. Specific requirement for Bax, not Bak, in Myc-induced apoptosis and tumor suppression in vivo. *J Biol Chem,* 281**,** 10890-5.

DAUWERSE, J. G., DIXON, J., SELAND, S., RUIVENKAMP, C. A., VAN HAERINGEN, A., HOEFSLOOT, L. H., PETERS, D. J., BOERS, A. C., DAUMER-HAAS, C., MAIWALD, R., ZWEIER, C., KERR, B., COBO, A. M., TORAL, J. F., HOOGEBOOM, A. J., LOHMANN, D. R., HEHR, U., DIXON, M. J., BREUNING, M. H. & WIECZOREK, D. 2011. Mutations in genes encoding subunits of RNA polymerases I and III cause Treacher Collins syndrome. *Nat Genet,* 43**,** 20-2.

DAVIDSON, A. & PRITCHARD, J. 1998. Actinomycin D, hepatic toxicity and Wilms' tumour--a mystery explained? *Eur J Cancer,* 34**,** 1145-7.

DAY, C. L., SMITS, C., FAN, F. C., LEE, E. F., FAIRLIE, W. D. & HINDS, M. G. 2008. Structure of the BH3 domains from the p53-inducible BH3-only proteins Noxa and Puma in complex with Mcl-1. *J Mol Biol,* 380**,** 958-71.

DE BIASIO, A., VRANA, J. A., ZHOU, P., QIAN, L., BIESZCZAD, C. K., BRALEY, K. E., DOMINA, A. M., WEINTRAUB, S. J., NEVEU, J. M., LANE, W. S. & CRAIG, R. W. 2007. N-terminal truncation of

antiapoptotic MCL1, but not G2/M-induced phosphorylation, is associated with stabilization and abundant expression in tumor cells. *J Biol Chem,* 282**,** 23919-36.

DE KEERSMAECKER, K., SULIMA, S. O. & DINMAN, J. D. 2015. Ribosomopathies and the paradox of cellular hypo- to hyperproliferation. *Blood,* 125**,** 1377-82.

DE LA CRUZ, J., GOMEZ-HERREROS, F., RODRIGUEZ-GALAN, O., BEGLEY, V., DE LA CRUZ MUNOZ-CENTENO, M. & CHAVEZ, S. 2018. Feedback regulation of ribosome assembly. *Curr Genet,* 64**,** 393-404.

DE LA CRUZ, J., KARBSTEIN, K. & WOOLFORD, J. L., JR. 2015. Functions of ribosomal proteins in assembly of eukaryotic ribosomes in vivo. *Annu Rev Biochem,* 84**,** 93-129.

DELBRIDGE, A. R., OPFERMAN, J. T., GRABOW, S. & STRASSER, A. 2015. Antagonism between MCL-1 and PUMA governs stem/progenitor cell survival during hematopoietic recovery from stress. *Blood,* 125**,** 3273-80.

DELBRIDGE, A. R., PANG, S. H., VANDENBERG, C. J., GRABOW, S., AUBREY, B. J., TAI, L., HEROLD, M. J. & STRASSER, A. 2016. RAG-induced DNA lesions activate proapoptotic BIM to suppress lymphomagenesis in p53-deficient mice. *J Exp Med,* 213**,** 2039-48.

DELGADO, M. D. & LEON, J. 2010. Myc roles in hematopoiesis and leukemia. *Genes Cancer,* 1**,** 605-16.

DERENNE, S., MONIA, B., DEAN, N. M., TAYLOR, J. K., RAPP, M. J., HAROUSSEAU, J. L., BATAILLE, R. & AMIOT, M. 2002. Antisense strategy shows that Mcl-1 rather than Bcl-2 or Bcl-x(L) is an essential survival protein of human myeloma cells. *Blood,* 100**,** 194-9.

DESJOBERT, C., RENALIER, M. H., BERGALET, J., DEJEAN, E., JOSEPH, N., KRUCZYNSKI, A., SOULIER, J., ESPINOS, E., MEGGETTO, F., CAVAILLE, J., DELSOL, G. & LAMANT, L. 2011. MiR-29a down-regulation in ALK-positive anaplastic large cell lymphomas contributes to apoptosis blockade through MCL-1 overexpression. *Blood,* 117**,** 6627-37.

DEVLIN, J. R., HANNAN, K. M., HEIN, N., CULLINANE, C., KUSNADI, E., NG, P. Y., GEORGE, A. J., SHORTT, J., BYWATER, M. J., POORTINGA, G., SANIJ, E., KANG, J., DRYGIN, D., O'BRIEN, S., JOHNSTONE, R. W., MCARTHUR, G. A., HANNAN, R. D. & PEARSON, R. B. 2016. Combination Therapy Targeting Ribosome Biogenesis and mRNA Translation Synergistically Extends Survival in MYC-Driven Lymphoma. *Cancer Discov,* 6**,** 59-70.

DEVLIN, J. R., HANNAN, K. M., NG, P. Y., BYWATER, M. J., SHORTT, J., CULLINANE, C., MCARTHUR, G. A., JOHNSTONE, R. W., HANNAN, R. D. & PEARSON, R. B. 2013. AKT signalling is required for ribosomal RNA synthesis and progression of Emu-Myc B-cell lymphoma in vivo. *FEBS J,* 280**,** 5307-16.

DING, Q., HE, X., HSU, J. M., XIA, W., CHEN, C. T., LI, L. Y., LEE, D. F., LIU, J. C., ZHONG, Q., WANG, X. & HUNG, M. C. 2007. Degradation of Mcl-1 by beta-TrCP mediates glycogen synthase kinase 3-induced tumor suppression and chemosensitization. *Mol Cell Biol,* 27**,** 4006-17.

DING, Q., HUO, L., YANG, J. Y., XIA, W., WEI, Y., LIAO, Y., CHANG, C. J., YANG, Y., LAI, C. C., LEE, D. F., YEN, C. J., CHEN, Y. J., HSU, J. M., KUO, H. P., LIN, C. Y., TSAI, F. J., LI, L. Y., TSAI, C. H. & HUNG, M. C. 2008. Down-regulation of myeloid cell leukemia-1 through inhibiting Erk/Pin 1 pathway by sorafenib facilitates chemosensitization in breast cancer. *Cancer Res,* 68**,** 6109-17.

DIPAOLO, J. A., MOORE, G. E. & NIEDBALA, T. F. 1957. Experimental studies with actinomycin D. *Cancer Res,* 17**,** 1127-34.

DOMINGUEZ-SOLA, D., YING, C. Y., GRANDORI, C., RUGGIERO, L., CHEN, B., LI, M., GALLOWAY, D. A., GU, W., GAUTIER, J. & DALLA-FAVERA, R. 2007. Non-transcriptional control of DNA replication by c-Myc. *Nature,* 448**,** 445-51.

DONATI, G., BERTONI, S., BRIGHENTI, E., VICI, M., TRERE, D., VOLAREVIC, S., MONTANARO, L. & DERENZINI, M. 2011. The balance between rRNA and ribosomal protein synthesis up- and downregulates the tumour suppressor p53 in mammalian cells. *Oncogene,* 30**,** 3274-88.

DONATI, G., PEDDIGARI, S., MERCER, C. A. & THOMAS, G. 2013. 5S ribosomal RNA is an essential component of a nascent ribosomal precursor complex that regulates the Hdm2-p53 checkpoint. *Cell Rep,* 4**,** 87-98.

DOTY, R. T., YAN, X., LAUSTED, C., MUNDAY, A. D., YANG, Z., YI, D., JABBARI, N., LIU, L., KEEL, S. B., TIAN, Q. & ABKOWITZ, J. L. 2019. Single-cell analyses demonstrate that a heme-GATA1 feedback loop regulates red cell differentiation. *Blood,* 133**,** 457-469.

DRAPTCHINSKAIA, N., GUSTAVSSON, P., ANDERSSON, B., PETTERSSON, M., WILLIG, T. N., DIANZANI, I., BALL, S., TCHERNIA, G., KLAR, J., MATSSON, H., TENTLER, D., MOHANDAS, N., CARLSSON, B. & DAHL, N. 1999. The gene encoding ribosomal protein S19 is mutated in Diamond-Blackfan anaemia. *Nat Genet,* 21**,** 169-75.

DRYGIN, D., LIN, A., BLIESATH, J., HO, C. B., O'BRIEN, S. E., PROFFITT, C., OMORI, M., HADDACH, M., SCHWAEBE, M. K., SIDDIQUI-JAIN, A., STREINER, N., QUIN, J. E., SANIJ, E., BYWATER, M. J., HANNAN, R. D., RYCKMAN, D., ANDERES, K. & RICE, W. G. 2011. Targeting RNA polymerase I with an oral small molecule CX-5461 inhibits ribosomal RNA synthesis and solid tumor growth. *Cancer Res,* 71**,** 1418-30.

DRYGIN, D., SIDDIQUI-JAIN, A., O'BRIEN, S., SCHWAEBE, M., LIN, A., BLIESATH, J., HO, C. B., PROFFITT, C., TRENT, K., WHITTEN, J. P., LIM, J. K., VON HOFF, D., ANDERES, K. & RICE, W. G. 2009. Anticancer activity of CX-3543: a direct inhibitor of rRNA biogenesis. *Cancer Res,* 69**,** 7653-61.

DUQUETTE, M. L., HANDA, P., VINCENT, J. A., TAYLOR, A. F. & MAIZELS, N. 2004. Intracellular transcription of G-rich DNAs induces formation of G-loops, novel structures containing G4 DNA. *Genes Dev,* 18**,** 1618-29.

DUTT, S., NARLA, A., LIN, K., MULLALLY, A., ABAYASEKARA, N., MEGERDICHIAN, C., WILSON, F. H., CURRIE, T., KHANNA-GUPTA, A., BERLINER, N., KUTOK, J. L. & EBERT, B. L. 2011. Haploinsufficiency for ribosomal protein genes causes selective activation of p53 in human erythroid progenitor cells. *Blood,* 117**,** 2567-76.

DZHAGALOV, I., ST JOHN, A. & HE, Y. W. 2007. The antiapoptotic protein Mcl-1 is essential for the survival of neutrophils but not macrophages. *Blood,* 109**,** 1620-6.

EBERT, B. L., PRETZ, J., BOSCO, J., CHANG, C. Y., TAMAYO, P., GALILI, N., RAZA, A., ROOT, D. E., ATTAR, E., ELLIS, S. R. & GOLUB, T. R. 2008. Identification of RPS14 as a 5q- syndrome gene by RNA interference screen. *Nature,* 451**,** 335-9.

EGLE, A., HARRIS, A. W., BOUILLET, P. & CORY, S. 2004. Bim is a suppressor of Myc-induced mouse B cell leukemia. *Proc Natl Acad Sci U S A,* 101**,** 6164-9.

EILERS, M. & EISENMAN, R. N. 2008. Myc's broad reach. *Genes Dev,* 22**,** 2755-66.

EISCHEN, C. M., ROUSSEL, M. F., KORSMEYER, S. J. & CLEVELAND, J. L. 2001a. Bax loss impairs Myc-induced apoptosis and circumvents the selection of p53 mutations during Myc-mediated lymphomagenesis. *Mol Cell Biol,* 21**,** 7653-62.

EISCHEN, C. M., WEBER, J. D., ROUSSEL, M. F., SHERR, C. J. & CLEVELAND, J. L. 1999. Disruption of the ARF-Mdm2-p53 tumor suppressor pathway in Myc-induced lymphomagenesis. *Genes Dev,* 13**,** 2658-69.

EISCHEN, C. M., WOO, D., ROUSSEL, M. F. & CLEVELAND, J. L. 2001b. Apoptosis triggered by Myc-induced suppression of Bcl-X(L) or Bcl-2 is bypassed during lymphomagenesis. *Mol Cell Biol,* 21**,** 5063-70.

ELGHETANY, M. T. & ALTER, B. P. 2002. p53 protein overexpression in bone marrow biopsies of patients with Shwachman-Diamond syndrome has a prevalence similar to that of patients with refractory anemia. *Arch Pathol Lab Med,* 126**,** 452-5.

EPSTEIN, M. A., ACHONG, B. G. & BARR, Y. M. 1964. Virus Particles in Cultured Lymphoblasts from Burkitt's Lymphoma. *Lancet,* 1**,** 702-3.

ERTEL, F., NGUYEN, M., ROULSTON, A. & SHORE, G. C. 2013. Programming cancer cells for high expression levels of Mcl1. *EMBO Rep,* 14**,** 328-36.

EVAN, G. I., WYLLIE, A. H., GILBERT, C. S., LITTLEWOOD, T. D., LAND, H., BROOKS, M., WATERS, C. M., PENN, L. Z. & HANCOCK, D. C. 1992. Induction of apoptosis in fibroblasts by c-myc protein. *Cell,* 69**,** 119-28.

FALINI, B., BRUNETTI, L. & MARTELLI, M. P. 2015. Dactinomycin in NPM1-Mutated Acute Myeloid Leukemia. *N Engl J Med,* 373**,** 1180-2.

FANCELLO, L., KAMPEN, K. R., HOFMAN, I. J., VERBEECK, J. & DE KEERSMAECKER, K. 2017. The ribosomal protein gene RPL5 is a haploinsufficient tumor suppressor in multiple cancer types. *Oncotarget,* 8**,** 14462-14478.

FARRELL, A. S. & SEARS, R. C. 2014. MYC degradation. *Cold Spring Harb Perspect Med,* 4.

FEDORIW, A. M., STARMER, J., YEE, D. & MAGNUSON, T. 2012. Nucleolar association and transcriptional inhibition through 5S rDNA in mammals. *PLoS Genet,* 8**,** e1002468.

FELSHER, D. W., ZETTERBERG, A., ZHU, J., TLSTY, T. & BISHOP, J. M. 2000. Overexpression of MYC causes p53-dependent G2 arrest of normal fibroblasts. *Proc Natl Acad Sci U S A,* 97**,** 10544-8.

FENG, C., YANG, F. & WANG, J. 2017. FBXO4 inhibits lung cancer cell survival by targeting Mcl-1 for degradation. *Cancer Gene Ther,* 24**,** 342-347.

FERNANDEZ, P. C., FRANK, S. R., WANG, L., SCHROEDER, M., LIU, S., GREENE, J., COCITO, A. & AMATI, B. 2003. Genomic targets of the human c-Myc protein. *Genes Dev,* 17**,** 1115-29.

FERRY, J. A. 2006. Burkitt's lymphoma: clinicopathologic features and differential diagnosis. *Oncologist,* 11**,** 375-83.

FETHERSTON, J., WERNER, E. & PATTERSON, R. 1984. Processing of the external transcribed spacer of murine rRNA and site of action of actinomycin D. *Nucleic Acids Res,* 12**,** 7187-98.

FISCHER, N. W., PRODEUS, A., MALKIN, D. & GARIEPY, J. 2016. p53 oligomerization status modulates cell fate decisions between growth, arrest and apoptosis. *Cell Cycle,* 15**,** 3210-3219.

FREIREICH, E. J., GEHAN, E. A., RALL, D. P., SCHMIDT, L. H. & SKIPPER, H. E. 1966. Quantitative comparison of toxicity of anticancer agents in mouse, rat, hamster, dog, monkey, and man. *Cancer Chemother Rep,* 50**,** 219-44.

FRENZEL, A., LABI, V., CHMELEWSKIJ, W., PLONER, C., GELEY, S., FIEGL, H., TZANKOV, A. & VILLUNGER, A. 2010. Suppression of B-cell lymphomagenesis by the BH3-only proteins Bmf and Bad. *Blood,* 115**,** 995-1005.

FU, P., DU, F., LIU, Y., YAO, M., ZHANG, S., ZHENG, X. & ZHENG, S. 2017. WP1130 increases cisplatin sensitivity through inhibition of usp9x in estrogen receptor-negative breast cancer cells. *Am J Transl Res,* 9**,** 1783-1791.

FULDA, S. & DEBATIN, K. M. 2006. Extrinsic versus intrinsic apoptosis pathways in anticancer chemotherapy. *Oncogene,* 25**,** 4798-811.

FUMAGALLI, S., DI CARA, A., NEB-GULATI, A., NATT, F., SCHWEMBERGER, S., HALL, J., BABCOCK, G. F., BERNARDI, R., PANDOLFI, P. P. & THOMAS, G. 2009. Absence of nucleolar disruption after impairment of 40S ribosome biogenesis reveals an rpL11-translation-dependent mechanism of p53 induction. *Nat Cell Biol,* 11**,** 501-8.

FUMAGALLI, S., IVANENKOV, V. V., TENG, T. & THOMAS, G. 2012. Suprainduction of p53 by disruption of 40S and 60S ribosome biogenesis leads to the activation of a novel G2/M checkpoint. *Genes Dev,* 26**,** 1028-40.

FUMAGALLI, S. & THOMAS, G. 2011. The role of p53 in ribosomopathies. *Semin Hematol,* 48**,** 97-105.

GABAY, M., LI, Y. & FELSHER, D. W. 2014. MYC activation is a hallmark of cancer initiation and maintenance. *Cold Spring Harb Perspect Med,* 4.

GAGLIA, G., GUAN, Y., SHAH, J. V. & LAHAV, G. 2013. Activation and control of p53 tetramerization in individual living cells. *Proc Natl Acad Sci U S A,* 110**,** 15497-501.

GALTIER, N., PIGANEAU, G., MOUCHIROUD, D. & DURET, L. 2001. GC-content evolution in mammalian genomes: the biased gene conversion hypothesis. *Genetics,* 159**,** 907-11.

GARCIA-GUTIERREZ, L., DELGADO, M. D. & LEON, J. 2019. MYC Oncogene Contributions to Release of Cell Cycle Brakes. *Genes (Basel),* 10.

GARRISON, S. P., JEFFERS, J. R., YANG, C., NILSSON, J. A., HALL, M. A., REHG, J. E., YUE, W., YU, J., ZHANG, L., ONCIU, M., SAMPLE, J. T., CLEVELAND, J. L. & ZAMBETTI, G. P. 2008. Selection against PUMA gene expression in Myc-driven B-cell lymphomagenesis. *Mol Cell Biol,* 28**,** 5391-402.

GARZON, R., HEAPHY, C. E., HAVELANGE, V., FABBRI, M., VOLINIA, S., TSAO, T., ZANESI, N., KORNBLAU, S. M., MARCUCCI, G., CALIN, G. A., ANDREEFF, M. & CROCE, C. M. 2009. MicroRNA 29b functions in acute myeloid leukemia. *Blood,* 114**,** 5331-41.

GAZDA, H. T., KHO, A. T., SANOUDOU, D., ZAUCHA, J. M., KOHANE, I. S., SIEFF, C. A. & BEGGS, A. H. 2006. Defective ribosomal protein gene expression alters transcription, translation, apoptosis, and oncogenic pathways in Diamond-Blackfan anemia. *Stem Cells,* 24**,** 2034-44.

GAZDA, H. T., SHEEN, M. R., VLACHOS, A., CHOESMEL, V., O'DONOHUE, M. F., SCHNEIDER, H., DARRAS, N., HASMAN, C., SIEFF, C. A., NEWBURGER, P. E., BALL, S. E., NIEWIADOMSKA, E., MATYSIAK, M., ZAUCHA, J. M., GLADER, B., NIEMEYER, C., MEERPOHL, J. J., ATSIDAFTOS, E., LIPTON, J. M., GLEIZES, P. E. & BEGGS, A. H. 2008. Ribosomal protein L5 and L11 mutations are associated with cleft palate and abnormal thumbs in Diamond-Blackfan anemia patients. *Am J Hum Genet,* 83**,** 769-80.

GENTILELLA, A. & KHALILI, K. 2011. BAG3 expression in glioblastoma cells promotes accumulation of ubiquitinated clients in an Hsp70-dependent manner. *J Biol Chem,* 286**,** 9205-15.

GENTILELLA, A., KOZMA, S. C. & THOMAS, G. 2015. A liaison between mTOR signaling, ribosome biogenesis and cancer. *Biochim Biophys Acta,* 1849**,** 812-20.

GENTILELLA, A., MORON-DURAN, F. D., FUENTES, P., ZWEIG-ROCHA, G., RIANO-CANALIAS, F., PELLETIER, J., RUIZ, M., TURON, G., CASTANO, J., TAULER, A., BUENO, C., MENENDEZ, P., KOZMA, S. C. & THOMAS, G. 2017. Autogenous Control of 5'TOP mRNA Stability by 40S Ribosomes. *Mol Cell,* 67**,** 55-70 e4.

GENTILELLA, A. & THOMAS, G. 2012. Cancer biology: The director's cut. *Nature,* 485**,** 50-1.

GENUTH, N. R. & BARNA, M. 2018. The Discovery of Ribosome Heterogeneity and Its Implications for Gene Regulation and Organismal Life. *Mol Cell,* 71**,** 364-374.

GERSTBERGER, S., HAFNER, M. & TUSCHL, T. 2014. A census of human RNA-binding proteins. *Nat Rev Genet,* 15**,** 829-45.

GERSTBERGER, S., MEYER, C., BENJAMIN-HONG, S., RODRIGUEZ, J., BRISKIN, D., BOGNANNI, C., BOGARDUS, K., STELLER, H. & TUSCHL, T. 2017. The Conserved RNA Exonuclease Rexo5 Is Required for 3' End Maturation of 28S rRNA, 5S rRNA, and snoRNAs. *Cell Rep,* 21**,** 758-772.

GIAM, M., HUANG, D. C. & BOUILLET, P. 2008. BH3-only proteins and their roles in programmed cell death. *Oncogene,* 27 Suppl 1**,** S128-36.

GIBBONS, J. G., BRANCO, A. T., GODINHO, S. A., YU, S. & LEMOS, B. 2015. Concerted copy number variation balances ribosomal DNA dosage in human and mouse genomes. *Proc Natl Acad Sci U S A,* 112**,** 2485-90.

GIBBONS, J. G., BRANCO, A. T., YU, S. & LEMOS, B. 2014. Ribosomal DNA copy number is coupled with gene expression variation and mitochondrial abundance in humans. *Nat Commun,* 5**,** 4850.

GIL, J. & PETERS, G. 2006. Regulation of the INK4b-ARF-INK4a tumour suppressor locus: all for one or one for all. *Nat Rev Mol Cell Biol,* 7**,** 667-77.

GINISTY, H., AMALRIC, F. & BOUVET, P. 1998. Nucleolin functions in the first step of ribosomal RNA processing. *EMBO J,* 17**,** 1476-86.

GIRI, B., GUPTA, V. K., YAFFE, B., MODI, S., ROY, P., SETHI, V., LAVANIA, S. P., VICKERS, S. M., DUDEJA, V., BANERJEE, S., WATTS, J. & SALUJA, A. 2019. Pre-clinical evaluation of Minnelide as a therapy for acute myeloid leukemia. *J Transl Med,* 17**,** 163.

GLASER, S. P., LEE, E. F., TROUNSON, E., BOUILLET, P., WEI, A., FAIRLIE, W. D., IZON, D. J., ZUBER, J., RAPPAPORT, A. R., HEROLD, M. J., ALEXANDER, W. S., LOWE, S. W., ROBB, L. & STRASSER, A. 2012. Anti-apoptotic Mcl-1 is essential for the development and sustained growth of acute myeloid leukemia. *Genes Dev,* 26**,** 120-5.

GOJO, I., ZHANG, B. & FENTON, R. G. 2002. The cyclin-dependent kinase inhibitor flavopiridol induces apoptosis in multiple myeloma cells through transcriptional repression and down-regulation of Mcl-1. *Clin Cancer Res,* 8**,** 3527-38.

GOLDSTEIN, D. P. & BERKOWITZ, R. S. 2012. Current management of gestational trophoblastic neoplasia. *Hematol Oncol Clin North Am,* 26**,** 111-31.

GOLOMB, L., BUBLIK, D. R., WILDER, S., NEVO, R., KISS, V., GRABUSIC, K., VOLAREVIC, S. & OREN, M. 2012. Importin 7 and exportin 1 link c-Myc and p53 to regulation of ribosomal biogenesis. *Mol Cell,* 45**,** 222-32.

GOMEZ-BOUGIE, P., MENORET, E., JUIN, P., DOUSSET, C., PELLAT-DECEUNYNCK, C. & AMIOT, M. 2011. Noxa controls Mule-dependent Mcl-1 ubiquitination through the regulation of the Mcl-1/USP9X interaction. *Biochem Biophys Res Commun,* 413**,** 460-4.

GOMEZ-ROMAN, N., GRANDORI, C., EISENMAN, R. N. & WHITE, R. J. 2003. Direct activation of RNA polymerase III transcription by c-Myc. *Nature,* 421**,** 290-4.

GONG, J., ZHANG, J. P., LI, B., ZENG, C., YOU, K., CHEN, M. X., YUAN, Y. & ZHUANG, S. M. 2013. MicroRNA-125b promotes apoptosis by regulating the expression of Mcl-1, Bcl-w and IL-6R. *Oncogene,* 32**,** 3071-9.

GRABOW, S., DELBRIDGE, A. R., AUBREY, B. J., VANDENBERG, C. J. & STRASSER, A. 2016. Loss of a Single Mcl-1 Allele Inhibits MYC-Driven Lymphomagenesis by Sensitizing Pro-B Cells to Apoptosis. *Cell Rep,* 14**,** 2337-47.

GRABOW, S., DELBRIDGE, A. R., VALENTE, L. J. & STRASSER, A. 2014. MCL-1 but not BCL-XL is critical for the development and sustained expansion of thymic lymphoma in p53-deficient mice. *Blood,* 124**,** 3939-46.

GRANDORI, C., COWLEY, S. M., JAMES, L. P. & EISENMAN, R. N. 2000. The Myc/Max/Mad network and the transcriptional control of cell behavior. *Annu Rev Cell Dev Biol,* 16**,** 653-99.

GRANDORI, C., GOMEZ-ROMAN, N., FELTON-EDKINS, Z. A., NGOUENET, C., GALLOWAY, D. A., EISENMAN, R. N. & WHITE, R. J. 2005. c-Myc binds to human ribosomal DNA and stimulates transcription of rRNA genes by RNA polymerase I. *Nat Cell Biol,* 7**,** 311-8.

GRANDORI, C., WU, K. J., FERNANDEZ, P., NGOUENET, C., GRIM, J., CLURMAN, B. E., MOSER, M. J., OSHIMA, J., RUSSELL, D. W., SWISSHELM, K., FRANK, S., AMATI, B., DALLA-FAVERA, R. & MONNAT, R. J., JR. 2003. Werner syndrome protein limits MYC-induced cellular senescence. *Genes Dev,* 17**,** 1569-74.

GRANNEMAN, S. & TOLLERVEY, D. 2007. Building ribosomes: even more expensive than expected? *Curr Biol,* 17**,** R415-7.

GREEN, D. R. & KROEMER, G. 2009. Cytoplasmic functions of the tumour suppressor p53. *Nature,* 458**,** 1127-30.

GREGORY, G. P., HOGG, S. J., KATS, L. M., VIDACS, E., BAKER, A. J., GILAN, O., LEFEBURE, M., MARTIN, B. P., DAWSON, M. A., JOHNSTONE, R. W. & SHORTT, J. 2015. CDK9 inhibition by dinaciclib potently suppresses Mcl-1 to induce durable apoptotic responses in aggressive MYC-driven B-cell lymphoma in vivo. *Leukemia,* 29**,** 1437-41.

GREGORY, M. A. & HANN, S. R. 2000. c-Myc proteolysis by the ubiquitin-proteasome pathway: stabilization of c-Myc in Burkitt's lymphoma cells. *Mol Cell Biol,* 20**,** 2423-35.

GROSSMAN, S. R. 2001. p300/CBP/p53 interaction and regulation of the p53 response. *Eur J Biochem,* 268**,** 2773-8.

GU, B. W., BESSLER, M. & MASON, P. J. 2008. A pathogenic dyskerin mutation impairs proliferation and activates a DNA damage response independent of telomere length in mice. *Proc Natl Acad Sci U S A,* 105**,** 10173-8.

HAAF, T., HAYMAN, D. L. & SCHMID, M. 1991. Quantitative determination of rDNA transcription units in vertebrate cells. *Exp Cell Res,* 193**,** 78-86.

HAFNER, A., BULYK, M. L., JAMBHEKAR, A. & LAHAV, G. 2019. The multiple mechanisms that regulate p53 activity and cell fate. *Nat Rev Mol Cell Biol,* 20**,** 199-210.

HALD, O. H., OLSEN, L., GALLO-OLLER, G., ELFMAN, L. H. M., LOKKE, C., KOGNER, P., SVEINBJORNSSON, B., FLAEGSTAD, T., JOHNSEN, J. I. & EINVIK, C. 2019. Inhibitors of ribosome biogenesis repress the growth of MYCN-amplified neuroblastoma. *Oncogene,* 38**,** 2800-2813.

HAN, J., GOLDSTEIN, L. A., GASTMAN, B. R., FROELICH, C. J., YIN, X. M. & RABINOWICH, H. 2004. Degradation of Mcl-1 by granzyme B: implications for Bim-mediated mitochondrial apoptotic events. *J Biol Chem,* 279**,** 22020-9.

HANAHAN, D. & WEINBERG, R. A. 2011. Hallmarks of cancer: the next generation. *Cell,* 144**,** 646-74.

HANN, S. R. & EISENMAN, R. N. 1984. Proteins encoded by the human c-myc oncogene: differential expression in neoplastic cells. *Mol Cell Biol,* 4**,** 2486-97.

HANNAN, K. M., BRANDENBURGER, Y., JENKINS, A., SHARKEY, K., CAVANAUGH, A., ROTHBLUM, L., MOSS, T., POORTINGA, G., MCARTHUR, G. A., PEARSON, R. B. & HANNAN, R. D. 2003. mTOR-dependent regulation of ribosomal gene transcription requires S6K1 and is mediated by phosphorylation of the carboxy-terminal activation domain of the nucleolar transcription factor UBF. *Mol Cell Biol,* 23**,** 8862-77.

HANNAN, K. M., SANIJ, E., ROTHBLUM, L. I., HANNAN, R. D. & PEARSON, R. B. 2013. Dysregulation of RNA polymerase I transcription during disease. *Biochim Biophys Acta,* 1829**,** 342-60.

HAO, Z., DUNCAN, G. S., SU, Y. W., LI, W. Y., SILVESTER, J., HONG, C., YOU, H., BRENNER, D., GORRINI, C., HAIGHT, J., WAKEHAM, A., YOU-TEN, A., MCCRACKEN, S., ELIA, A., LI, Q., DETMAR, J., JURISICOVA, A., HOBEIKA, E., RETH, M., SHENG, Y., LANG, P. A., OHASHI, P. S., ZHONG, Q., WANG, X. & MAK, T. W. 2012. The E3 ubiquitin ligase Mule acts through the ATM-p53 axis to maintain B lymphocyte homeostasis. *J Exp Med,* 209**,** 173-86.

HAPPO, L., PHIPSON, B., SMYTH, G. K., STRASSER, A. & SCOTT, C. L. 2012a. Neither loss of Bik alone, nor combined loss of Bik and Noxa, accelerate murine lymphoma development or render lymphoma cells resistant to DNA damaging drugs. *Cell Death Dis,* 3**,** e306.

HAPPO, L., STRASSER, A. & CORY, S. 2012b. BH3-only proteins in apoptosis at a glance. *J Cell Sci,* 125**,** 1081-7.

HARDING, S. M., BOIARSKY, J. A. & GREENBERG, R. A. 2015. ATM Dependent Silencing Links Nucleolar Chromatin Reorganization to DNA Damage Recognition. *Cell Rep,* 13**,** 251-9.

HARLEY, M. E., ALLAN, L. A., SANDERSON, H. S. & CLARKE, P. R. 2010. Phosphorylation of Mcl-1 by CDK1-cyclin B1 initiates its Cdc20-dependent destruction during mitotic arrest. *EMBO J,* 29**,** 2407-20.

HARRIS, A. W., PINKERT, C. A., CRAWFORD, M., LANGDON, W. Y., BRINSTER, R. L. & ADAMS, J. M. 1988. The E mu-myc transgenic mouse. A model for high-incidence spontaneous lymphoma and leukemia of early B cells. *J Exp Med,* 167**,** 353-71.

HARRISON, S. J., KHOT, A., BRAJANOVSKI, N., CAMERON, D., HEIN, N., MCARTHUR, G. A., LIM, J. K., O'BRIEN, S., RYCKMAN, D. M. & YU, G. I. 2015. A phase 1, open-label, dose escalation, safety, PK and PD study of a first in class Pol1 inhibitor (CX-5461) in patients with advanced hematologic malignancies (HM). American Society of Clinical Oncology.

HE, X., LI, Y., DAI, M. S. & SUN, X. X. 2016. Ribosomal protein L4 is a novel regulator of the MDM2-p53 loop. *Oncotarget,* 7**,** 16217-26.

HECHT, J. L. & ASTER, J. C. 2000. Molecular biology of Burkitt's lymphoma. *J Clin Oncol,* 18**,** 3707-21.

HEIN, N., HANNAN, K. M., GEORGE, A. J., SANIJ, E. & HANNAN, R. D. 2013. The nucleolus: an emerging target for cancer therapy. *Trends Mol Med,* 19**,** 643-54.

HEISS, N. S., KNIGHT, S. W., VULLIAMY, T. J., KLAUCK, S. M., WIEMANN, S., MASON, P. J., POUSTKA, A. & DOKAL, I. 1998. X-linked dyskeratosis congenita is caused by mutations in a highly conserved gene with putative nucleolar functions. *Nat Genet,* 19**,** 32-8.

HELTON, E. S. & CHEN, X. 2007. p53 modulation of the DNA damage response. *J Cell Biochem,* 100**,** 883-96.

HEMANN, M. T., BRIC, A., TERUYA-FELDSTEIN, J., HERBST, A., NILSSON, J. A., CORDON-CARDO, C., CLEVELAND, J. L., TANSEY, W. P. & LOWE, S. W. 2005. Evasion of the p53 tumour surveillance network by tumour-derived MYC mutants. *Nature,* 436**,** 807-11.

HENRAS, A. K., PLISSON-CHASTANG, C., O'DONOHUE, M. F., CHAKRABORTY, A. & GLEIZES, P. E. 2015. An overview of pre-ribosomal RNA processing in eukaryotes. *Wiley Interdiscip Rev RNA,* 6**,** 225-42.

HENRAS, A. K., SOUDET, J., GERUS, M., LEBARON, S., CAIZERGUES-FERRER, M., MOUGIN, A. & HENRY, Y. 2008. The post-transcriptional steps of eukaryotic ribosome biogenesis. *Cell Mol Life Sci,* 65**,** 2334-59.

HERKERT, B. & EILERS, M. 2010. Transcriptional repression: the dark side of myc. *Genes Cancer,* 1**,** 580-6.

HERRANT, M., JACQUEL, A., MARCHETTI, S., BELHACENE, N., COLOSETTI, P., LUCIANO, F. & AUBERGER, P. 2004. Cleavage of Mcl-1 by caspases impaired its ability to counteract Bim-induced apoptosis. *Oncogene,* 23**,** 7863-73.

HERTER, E. K., STAUCH, M., GALLANT, M., WOLF, E., RAABE, T. & GALLANT, P. 2015. snoRNAs are a novel class of biologically relevant Myc targets. *BMC Biol,* 13**,** 25.

HERTZ, M. I., LANDRY, D. M., WILLIS, A. E., LUO, G. & THOMPSON, S. R. 2013. Ribosomal protein S25 dependency reveals a common mechanism for diverse internal ribosome entry sites and ribosome shunting. *Mol Cell Biol,* 33**,** 1016-26.

HILL, C. R., COLE, M., ERRINGTON, J., MALIK, G., BODDY, A. V. & VEAL, G. J. 2014. Characterisation of the clinical pharmacokinetics of actinomycin D and the influence of ABCB1 pharmacogenetic variation on actinomycin D disposition in children with cancer. *Clin Pharmacokinet,* 53**,** 741-51.

HINNEBUSCH, A. G., IVANOV, I. P. & SONENBERG, N. 2016. Translational control by 5'-untranslated regions of eukaryotic mRNAs. *Science,* 352**,** 1413-6.

HIRD, A. W. & TRON, A. E. 2019. Recent advances in the development of Mcl-1 inhibitors for cancer therapy. *Pharmacol Ther,* 198**,** 59-67.

HOFFMAN, B. & LIEBERMANN, D. A. 2008. Apoptotic signaling by c-MYC. *Oncogene,* 27**,** 6462-72.

HOLLSTEIN, U. J. C. R. 1974. Actinomycin. Chemistry and mechanism of action. 74**,** 625-652.

HOLZER, P., MASUYA, K., FURET, P., KALLEN, J., VALAT-STACHYRA, T., FERRETTI, S., BERGHAUSEN, J., BOUISSET-LEONARD, M., BUSCHMANN, N., PISSOT-SOLDERMANN, C., RYNN, C., RUETZ, S., STUTZ, S., CHENE, P., JEAY, S. & GESSIER, F. 2015. Discovery of a Dihydroisoquinolinone Derivative (NVP-CGM097): A Highly Potent and Selective MDM2 Inhibitor Undergoing Phase 1 Clinical Trials in p53wt Tumors. *J Med Chem,* 58**,** 6348-58.

HOROS, R., IJSPEERT, H., POSPISILOVA, D., SENDTNER, R., ANDRIEU-SOLER, C., TASKESEN, E., NIERADKA, A., CMEJLA, R., SENDTNER, M., TOUW, I. P. & VON LINDERN, M. 2012. Ribosomal deficiencies in Diamond-Blackfan anemia impair translation of transcripts essential for differentiation of murine and human erythroblasts. *Blood,* 119**,** 262-72.

HORTOBAGYI, G. N. 1997. Anthracyclines in the treatment of cancer. An overview. *Drugs,* 54 Suppl 4**,** 1-7.

HSIEH, A. C., LIU, Y., EDLIND, M. P., INGOLIA, N. T., JANES, M. R., SHER, A., SHI, E. Y., STUMPF, C. R., CHRISTENSEN, C., BONHAM, M. J., WANG, S., REN, P., MARTIN, M., JESSEN, K., FELDMAN, M. E., WEISSMAN, J. S., SHOKAT, K. M., ROMMEL, C. & RUGGERO, D. 2012. The translational landscape of mTOR signalling steers cancer initiation and metastasis. *Nature,* 485**,** 55-61.

HUANG, C. R. & YANG-YEN, H. F. 2010. The fast-mobility isoform of mouse Mcl-1 is a mitochondrial matrix-localized protein with attenuated anti-apoptotic activity. *FEBS Lett,* 584**,** 3323-30.

HUBER, S., OELSNER, M., DECKER, T., ZUM BUSCHENFELDE, C. M., WAGNER, M., LUTZNY, G., KUHNT, T., SCHMIDT, B., OOSTENDORP, R. A., PESCHEL, C. & RINGSHAUSEN, I. 2011. Sorafenib induces cell death in chronic lymphocytic leukemia by translational downregulation of Mcl-1. *Leukemia,* 25**,** 838-47.

IMAMURA, J., MIYOSHI, I. & KOEFFLER, H. P. 1994. p53 in hematologic malignancies. *Blood,* 84**,** 2412-21.

INGOLIA, N. T., LAREAU, L. F. & WEISSMAN, J. S. 2011. Ribosome profiling of mouse embryonic stem cells reveals the complexity and dynamics of mammalian proteomes. *Cell,* 147**,** 789-802.

INUZUKA, H., SHAIK, S., ONOYAMA, I., GAO, D., TSENG, A., MASER, R. S., ZHAI, B., WAN, L., GUTIERREZ, A., LAU, A. W., XIAO, Y., CHRISTIE, A. L., ASTER, J., SETTLEMAN, J., GYGI, S. P., KUNG, A. L., LOOK, T., NAKAYAMA, K. I., DEPINHO, R. A. & WEI, W. 2011. SCF(FBW7) regulates cellular apoptosis by targeting MCL1 for ubiquitylation and destruction. *Nature,* 471**,** 104-9.

IRITANI, B. M. & EISENMAN, R. N. 1999. c-Myc enhances protein synthesis and cell size during B lymphocyte development. *Proc Natl Acad Sci U S A,* 96**,** 13180-5.

ISOMOTO, H., KOBAYASHI, S., WERNEBURG, N. W., BRONK, S. F., GUICCIARDI, M. E., FRANK, D. A. & GORES, G. J. 2005. Interleukin 6 upregulates myeloid cell leukemia-1 expression through a STAT3 pathway in cholangiocarcinoma cells. *Hepatology,* 42**,** 1329-38.

ITAHANA, K., BHAT, K. P., JIN, A., ITAHANA, Y., HAWKE, D., KOBAYASHI, R. & ZHANG, Y. 2003. Tumor suppressor ARF degrades B23, a nucleolar protein involved in ribosome biogenesis and cell proliferation. *Mol Cell,* 12**,** 1151-64.

JAAKO, P., DEBNATH, S., OLSSON, K., ZHANG, Y., FLYGARE, J., LINDSTROM, M. S., BRYDER, D. & KARLSSON, S. 2015. Disruption of the 5S RNP-Mdm2 interaction significantly improves the erythroid defect in a mouse model for Diamond-Blackfan anemia. *Leukemia,* 29**,** 2221-9.

JAAKO, P., FLYGARE, J., OLSSON, K., QUERE, R., EHINGER, M., HENSON, A., ELLIS, S., SCHAMBACH, A., BAUM, C., RICHTER, J., LARSSON, J., BRYDER, D. & KARLSSON, S. 2011. Mice with ribosomal protein S19 deficiency develop bone marrow failure and symptoms like patients with Diamond-Blackfan anemia. *Blood,* 118**,** 6087-96.

JACK, K., BELLODI, C., LANDRY, D. M., NIEDERER, R. O., MESKAUSKAS, A., MUSALGAONKAR, S., KOPMAR, N., KRASNYKH, O., DEAN, A. M., THOMPSON, S. R., RUGGERO, D. & DINMAN, J. D. 2011. rRNA pseudouridylation defects affect ribosomal ligand binding and translational fidelity from yeast to human cells. *Mol Cell,* 44**,** 660-6.

JACOBSEN, K. A., PRASAD, V. S., SIDMAN, C. L. & OSMOND, D. G. 1994. Apoptosis and macrophage-mediated deletion of precursor B cells in the bone marrow of E mu-myc transgenic mice. *Blood,* 84**,** 2784-94.

JADERSTEN, M., SAFT, L., SMITH, A., KULASEKARARAJ, A., POMPLUN, S., GOHRING, G., HEDLUND, A., HAST, R., SCHLEGELBERGER, B., PORWIT, A., HELLSTROM-LINDBERG, E. & MUFTI, G. J. 2011. TP53 mutations in low-risk myelodysplastic syndromes with del(5q) predict disease progression. *J Clin Oncol,* 29**,** 1971-9.

JAFFE, E. S. 2009. The 2008 WHO classification of lymphomas: implications for clinical practice and translational research. *Hematology Am Soc Hematol Educ Program***,** 523-31.

JAFFE, N., FILLER, R. M., FARBER, S., TRAGGIS, D. G., VAWTER, G. F., TEFFT, M. & MURRAY, J. E. 1973. Rhabdomyosarcoma in children. Improved outlook with a multidisciplinary approach. *Am J Surg,* 125**,** 482-7.

JAFFE, N., PAED, D., TRAGGIS, D., SALIAN, S. & CASSADY, J. R. 1976. Improved outlook for Ewing's sarcoma with combination chemotherapy (vincristine, actinomycin D and cyclophosphamide) and radiation therapy. *Cancer,* 38**,** 1925-30.

JAKEL, S. & GORLICH, D. 1998. Importin beta, transportin, RanBP5 and RanBP7 mediate nuclear import of ribosomal proteins in mammalian cells. *EMBO J,* 17**,** 4491-502.

JARIEL-ENCONTRE, I., BOSSIS, G. & PIECHACZYK, M. 2008. Ubiquitin-independent degradation of proteins by the proteasome. *Biochim Biophys Acta,* 1786**,** 153-77.

JEFFERS, J. R., PARGANAS, E., LEE, Y., YANG, C., WANG, J., BRENNAN, J., MACLEAN, K. H., HAN, J., CHITTENDEN, T., IHLE, J. N., MCKINNON, P. J., CLEVELAND, J. L. & ZAMBETTI, G. P. 2003. Puma is an essential mediator of p53-dependent and -independent apoptotic pathways. *Cancer Cell,* 4**,** 321-8.

JENEY, V., BALLA, J., YACHIE, A., VARGA, Z., VERCELLOTTI, G. M., EATON, J. W. & BALLA, G. 2002. Pro-oxidant and cytotoxic effects of circulating heme. *Blood,* 100**,** 879-87.

JI, H., WU, G., ZHAN, X., NOLAN, A., KOH, C., DE MARZO, A., DOAN, H. M., FAN, J., CHEADLE, C., FALLAHI, M., CLEVELAND, J. L., DANG, C. V. & ZELLER, K. I. 2011. Cell-type independent MYC target genes reveal a primordial signature involved in biomass accumulation. *PLoS One,* 6**,** e26057.

JIN, A., ITAHANA, K., O'KEEFE, K. & ZHANG, Y. 2004. Inhibition of HDM2 and activation of p53 by ribosomal protein L23. *Mol Cell Biol,* 24**,** 7669-80.

JONES, N. C., LYNN, M. L., GAUDENZ, K., SAKAI, D., AOTO, K., REY, J. P., GLYNN, E. F., ELLINGTON, L., DU, C., DIXON, J., DIXON, M. J. & TRAINOR, P. A. 2008. Prevention of the neurocristopathy Treacher Collins syndrome through inhibition of p53 function. *Nat Med,* 14**,** 125-33.

JONES, R. M., BRANDA, J., JOHNSTON, K. A., POLYMENIS, M., GADD, M., RUSTGI, A., CALLANAN, L. & SCHMIDT, E. V. 1996. An essential E box in the promoter of the gene encoding the mRNA cap-binding protein (eukaryotic initiation factor 4E) is a target for activation by c-myc. *Mol Cell Biol,* 16**,** 4754-64.

JUIN, P., HUEBER, A. O., LITTLEWOOD, T. & EVAN, G. 1999. c-Myc-induced sensitization to apoptosis is mediated through cytochrome c release. *Genes Dev,* 13**,** 1367-81.

KADAKIA, S., HELMAN, S. N., BADHEY, A. K., SAMAN, M. & DUCIC, Y. 2014. Treacher Collins Syndrome: the genetics of a craniofacial disease. *Int J Pediatr Otorhinolaryngol,* 78**,** 893-8.

KALE, J., OSTERLUND, E. J. & ANDREWS, D. W. 2018. BCL-2 family proteins: changing partners in the dance towards death. *Cell Death Differ,* 25**,** 65-80.

KAMPEN, K. R., SULIMA, S. O., VERBELEN, B., GIRARDI, T., VEREECKE, S., RINALDI, G., VERBEECK, J., OP DE BEECK, J., UYTTEBROECK, A., MEIJERINK, J. P. P., MOORMAN, A. V., HARRISON, C. J., SPINCEMAILLE, P., COOLS, J., CASSIMAN, D., FENDT, S. M., VERMEERSCH, P. & DE KEERSMAECKER, K. 2019. The ribosomal RPL10 R98S mutation drives IRES-dependent BCL-2 translation in T-ALL. *Leukemia,* 33**,** 319-332.

KAPRALOVA, K., SAXOVA, Z., KRALOVA, B., LANIKOVA, L., POSPISILOVA, D., DIVOKY, V. & HORVATHOVA, M. 2017. Inflammatory signature, oxidative stress, and DNA damage response in DBA pathogenesis. Am Soc Hematology.

KASSAVETIS, G. A., BRAUN, B. R., NGUYEN, L. H. & GEIDUSCHEK, E. P. 1990. S. cerevisiae TFIIIB is the transcription initiation factor proper of RNA polymerase III, while TFIIIA and TFIIIC are assembly factors. *Cell,* 60**,** 235-45.

KAUFMANN, S. H., KARP, J. E., SVINGEN, P. A., KRAJEWSKI, S., BURKE, P. J., GORE, S. D. & REED, J. C. 1998. Elevated expression of the apoptotic regulator Mcl-1 at the time of leukemic relapse. *Blood,* 91**,** 991-1000.

KEEL, S. B., DOTY, R. T., YANG, Z., QUIGLEY, J. G., CHEN, J., KNOBLAUGH, S., KINGSLEY, P. D., DE DOMENICO, I., VAUGHN, M. B., KAPLAN, J., PALIS, J. & ABKOWITZ, J. L. 2008. A heme export protein is required for red blood cell differentiation and iron homeostasis. *Science,* 319**,** 825-8.

KELLY, G. L., GRABOW, S., GLASER, S. P., FITZSIMMONS, L., AUBREY, B. J., OKAMOTO, T., VALENTE, L. J., ROBATI, M., TAI, L., FAIRLIE, W. D., LEE, E. F., LINDSTROM, M. S., WIMAN, K. G., HUANG, D. C., BOUILLET, P., ROWE, M., RICKINSON, A. B., HEROLD, M. J. & STRASSER, A. 2014. Targeting of MCL-1 kills MYC-driven mouse and human lymphomas even when they bear mutations in p53. *Genes Dev,* 28**,** 58-70.

KELLY, P. N., GRABOW, S., DELBRIDGE, A. R., STRASSER, A. & ADAMS, J. M. 2011. Endogenous Bcl-xL is essential for Myc-driven lymphomagenesis in mice. *Blood,* 118**,** 6380-6.

KELLY, P. N., PUTHALAKATH, H., ADAMS, J. M. & STRASSER, A. 2007. Endogenous bcl-2 is not required for the development of Emu-myc-induced B-cell lymphoma. *Blood,* 109**,** 4907-13.

KELLY, P. N. & STRASSER, A. 2011. The role of Bcl-2 and its pro-survival relatives in tumourigenesis and cancer therapy. *Cell Death Differ,* 18**,** 1414-24.

KENNETH, N. S., RAMSBOTTOM, B. A., GOMEZ-ROMAN, N., MARSHALL, L., COLE, P. A. & WHITE, R. J. 2007. TRRAP and GCN5 are used by c-Myc to activate RNA polymerase III transcription. *Proc Natl Acad Sci U S A,* 104**,** 14917-22.

KHAJURIA, R. K., MUNSCHAUER, M., ULIRSCH, J. C., FIORINI, C., LUDWIG, L. S., MCFARLAND, S. K., ABDULHAY, N. J., SPECHT, H., KESHISHIAN, H., MANI, D. R., JOVANOVIC, M., ELLIS, S. R., FULCO, C. P., ENGREITZ, J. M., SCHUTZ, S., LIAN, J., GRIPP, K. W., WEINBERG, O. K., PINKUS, G. S., GEHRKE, L., REGEV, A., LANDER, E. S., GAZDA, H. T., LEE, W. Y., PANSE, V. G., CARR, S. A. & SANKARAN, V. G. 2018. Ribosome Levels Selectively Regulate Translation and Lineage Commitment in Human Hematopoiesis. *Cell,* 173**,** 90-103 e19.

KHATTER, H., MYASNIKOV, A. G., NATCHIAR, S. K. & KLAHOLZ, B. P. 2015. Structure of the human 80S ribosome. *Nature,* 520**,** 640-5.

KHOURY, J. D., MEDEIROS, L. J., RASSIDAKIS, G. Z., MCDONNELL, T. J., ABRUZZO, L. V. & LAI, R. 2003. Expression of Mcl-1 in mantle cell lymphoma is associated with high-grade morphology, a high proliferative state, and p53 overexpression. *J Pathol,* 199**,** 90-7.

KIM, J. H., SIM, S. H., HA, H. J., KO, J. J., LEE, K. & BAE, J. 2009. MCL-1ES, a novel variant of MCL-1, associates with MCL-1L and induces mitochondrial cell death. *FEBS Lett,* 583**,** 2758-64.

KIM, J. W., GAO, P., LIU, Y. C., SEMENZA, G. L. & DANG, C. V. 2007. Hypoxia-inducible factor 1 and dysregulated c-Myc cooperatively induce vascular endothelial growth factor and metabolic switches hexokinase 2 and pyruvate dehydrogenase kinase 1. *Mol Cell Biol,* 27**,** 7381-93.

KIM, S. Y., HERBST, A., TWORKOWSKI, K. A., SALGHETTI, S. E. & TANSEY, W. P. 2003. Skp2 regulates Myc protein stability and activity. *Mol Cell,* 11**,** 1177-88.

KLINGE, S. & WOOLFORD, J. L., JR. 2019. Ribosome assembly coming into focus. *Nat Rev Mol Cell Biol,* 20**,** 116-131.

KNIGHT, S. W., HEISS, N. S., VULLIAMY, T. J., GRESCHNER, S., STAVRIDES, G., PAI, G. S., LESTRINGANT, G., VARMA, N., MASON, P. J., DOKAL, I. & POUSTKA, A. 1999. X-linked dyskeratosis congenita is predominantly caused by missense mutations in the DKC1 gene. *Am J Hum Genet,* 65**,** 50-8.

KNOWLES, D. M. 2003. Etiology and pathogenesis of AIDS-related non-Hodgkin's lymphoma. *Hematol Oncol Clin North Am,* 17**,** 785-820.

KOBAYASHI, S., LEE, S. H., MENG, X. W., MOTT, J. L., BRONK, S. F., WERNEBURG, N. W., CRAIG, R. W., KAUFMANN, S. H. & GORES, G. J. 2007. Serine 64 phosphorylation enhances the antiapoptotic function of Mcl-1. *J Biol Chem,* 282**,** 18407-17.

KOCH, R., CHRISTIE, A. L., CROMBIE, J. L., PALMER, A. C., PLANA, D., SHIGEMORI, K., MORROW, S. N., VAN SCOYK, A., WU, W., BREM, E. A., SECRIST, J. P., DREW, L., SCHULLER, A. G., CIDADO, J., LETAI, A. & WEINSTOCK, D. M. 2019. Biomarker-driven strategy for MCL1 inhibition in T-cell lymphomas. *Blood,* 133**,** 566-575.

KOJIMA, S., HYAKUTAKE, A., KOSHIKAWA, N., NAKAGAWARA, A. & TAKENAGA, K. 2010. MCL-1V, a novel mouse antiapoptotic MCL-1 variant, generated by RNA splicing at a non-canonical splicing pair. *Biochem Biophys Res Commun,* 391**,** 492-7.

KOMAR, A. A. & HATZOGLOU, M. 2011. Cellular IRES-mediated translation: the war of ITAFs in pathophysiological states. *Cell Cycle,* 10**,** 229-40.

KONDRASHOV, N., PUSIC, A., STUMPF, C. R., SHIMIZU, K., HSIEH, A. C., ISHIJIMA, J., SHIROISHI, T. & BARNA, M. 2011. Ribosome-mediated specificity in Hox mRNA translation and vertebrate tissue patterning. *Cell,* 145**,** 383-397.

KONG, J. & LASKO, P. 2012. Translational control in cellular and developmental processes. *Nat Rev Genet,* 13**,** 383-94.

KONIKOVA, E. & KUSENDA, J. 2003. Altered expression of p53 and MDM2 proteins in hematological malignancies. *Neoplasma,* 50**,** 31-40.

KORNPROBST, M., TURK, M., KELLNER, N., CHENG, J., FLEMMING, D., KOS-BRAUN, I., KOS, M., THOMS, M., BERNINGHAUSEN, O., BECKMANN, R. & HURT, E. 2016. Architecture of the 90S Pre-ribosome: A Structural View on the Birth of the Eukaryotic Ribosome. *Cell,* 166**,** 380-393.

KOSS, B., MORRISON, J., PERCIAVALLE, R. M., SINGH, H., REHG, J. E., WILLIAMS, R. T. & OPFERMAN, J. T. 2013. Requirement for antiapoptotic MCL-1 in the survival of BCR-ABL B-lineage acute lymphoblastic leukemia. *Blood,* 122**,** 1587-98.

KOTSCHY, A., SZLAVIK, Z., MURRAY, J., DAVIDSON, J., MARAGNO, A. L., LE TOUMELIN-BRAIZAT, G., CHANRION, M., KELLY, G. L., GONG, J. N., MOUJALLED, D. M., BRUNO, A., CSEKEI, M., PACZAL, A., SZABO, Z. B., SIPOS, S., RADICS, G., PROSZENYAK, A., BALINT, B., ONDI, L., BLASKO, G., ROBERTSON, A., SURGENOR, A., DOKURNO, P., CHEN, I., MATASSOVA, N., SMITH, J., PEDDER, C., GRAHAM, C., STUDENY, A., LYSIAK-AUVITY, G., GIRARD, A. M., GRAVE, F., SEGAL, D., RIFFKIN, C. D., POMILIO, G., GALBRAITH, L. C., AUBREY, B. J., BRENNAN, M. S., HEROLD, M. J., CHANG, C., GUASCONI, G., CAUQUIL, N., MELCHIORE, F., GUIGAL-STEPHAN, N., LOCKHART, B., COLLAND, F., HICKMAN, J. A., ROBERTS, A. W., HUANG, D. C., WEI, A. H., STRASSER, A., LESSENE, G. & GENESTE, O. 2016. The MCL1 inhibitor S63845 is tolerable and effective in diverse cancer models. *Nature,* 538**,** 477-482.

KOZOPAS, K. M., YANG, T., BUCHAN, H. L., ZHOU, P. & CRAIG, R. W. 1993. MCL1, a gene expressed in programmed myeloid cell differentiation, has sequence similarity to BCL2. *Proc Natl Acad Sci U S A,* 90**,** 3516-20.

KRESS, T. R., SABO, A. & AMATI, B. 2015. MYC: connecting selective transcriptional control to global RNA production. *Nat Rev Cancer,* 15**,** 593-607.

KRESSLER, D., BANGE, G., OGAWA, Y., STJEPANOVIC, G., BRADATSCH, B., PRATTE, D., AMLACHER, S., STRAUSS, D., YONEDA, Y., KATAHIRA, J., SINNING, I. & HURT, E. 2012. Synchronizing nuclear import of ribosomal proteins with ribosome assembly. *Science,* 338**,** 666-71.

KRESSLER, D., HURT, E. & BASSLER, J. 2010. Driving ribosome assembly. *Biochim Biophys Acta,* 1803**,** 673-83.

KUANG, E., FU, B., LIANG, Q., MYOUNG, J. & ZHU, F. 2011. Phosphorylation of eukaryotic translation initiation factor 4B (EIF4B) by open reading frame 45/p90 ribosomal S6 kinase (ORF45/RSK) signaling axis facilitates protein translation during Kaposi sarcoma-associated herpesvirus (KSHV) lytic replication. *J Biol Chem,* 286**,** 41171-82.

KURLAND, J. F. & TANSEY, W. P. 2008. Myc-mediated transcriptional repression by recruitment of histone deacetylase. *Cancer Res,* 68**,** 3624-9.

LA STARZA, R., BORGA, C., BARBA, G., PIERINI, V., SCHWAB, C., MATTEUCCI, C., LEMA FERNANDEZ, A. G., LESZL, A., CAZZANIGA, G., CHIARETTI, S., BASSO, G., HARRISON, C. J., TE KRONNIE, G. & MECUCCI, C. 2014. Genetic profile of T-cell acute lymphoblastic leukemias with MYC translocations. *Blood,* 124**,** 3577-82.

LACASCE, A., HOWARD, O., LIB, S., FISHER, D., WENG, A., NEUBERG, D. & SHIPP, M. 2004. Modified magrath regimens for adults with Burkitt and Burkitt-like lymphomas: preserved efficacy with decreased toxicity. *Leuk Lymphoma,* 45**,** 761-7.

LAFONTAINE, D. L. 2015. Noncoding RNAs in eukaryotic ribosome biogenesis and function. *Nat Struct Mol Biol,* 22**,** 11-9.

LAM, Y. W., LAMOND, A. I., MANN, M. & ANDERSEN, J. S. 2007. Analysis of nucleolar protein dynamics reveals the nuclear degradation of ribosomal proteins. *Curr Biol,* 17**,** 749-60.

LANE, D. P. 1992. Cancer. p53, guardian of the genome. *Nature,* 358**,** 15-6.

LANGDON, W. Y., HARRIS, A. W., CORY, S. & ADAMS, J. M. 1986. The c-myc oncogene perturbs B lymphocyte development in E-mu-myc transgenic mice. *Cell,* 47**,** 11-8.

LARSSON, O., MORITA, M., TOPISIROVIC, I., ALAIN, T., BLOUIN, M. J., POLLAK, M. & SONENBERG, N. 2012. Distinct perturbation of the translatome by the antidiabetic drug metformin. *Proc Natl Acad Sci U S A,* 109**,** 8977-82.

LAURENTI, E., WILSON, A. & TRUMPP, A. 2009. Myc's other life: stem cells and beyond. *Curr Opin Cell Biol,* 21**,** 844-54.

LE GOUILL, S., PODAR, K., HAROUSSEAU, J. L. & ANDERSON, K. C. 2004. Mcl-1 regulation and its role in multiple myeloma. *Cell Cycle,* 3**,** 1259-62.

LEE, D. H. & GOLDBERG, A. L. 1998. Proteasome inhibitors: valuable new tools for cell biologists. *Trends Cell Biol,* 8**,** 397-403.

LEE, H. C., WANG, H., BALADANDAYUTHAPANI, V., LIN, H., HE, J., JONES, R. J., KUIATSE, I., GU, D., WANG, Z., MA, W., LIM, J., O'BRIEN, S., KEATS, J., YANG, J., DAVIS, R. E. & ORLOWSKI, R. Z. 2017a. RNA Polymerase I Inhibition with CX-5461 as a Novel Therapeutic Strategy to Target MYC in Multiple Myeloma. *Br J Haematol,* 177**,** 80-94.

LEE, K. M., GILTNANE, J. M., BALKO, J. M., SCHWARZ, L. J., GUERRERO-ZOTANO, A. L., HUTCHINSON, K. E., NIXON, M. J., ESTRADA, M. V., SANCHEZ, V., SANDERS, M. E., LEE, T., GOMEZ, H., LLUCH, A., PEREZ-FIDALGO, J. A., WOLF, M. M., ANDREJEVA, G., RATHMELL, J. C., FESIK, S. W. & ARTEAGA, C. L. 2017b. MYC and MCL1 Cooperatively Promote Chemotherapy-Resistant Breast Cancer Stem Cells via Regulation of Mitochondrial Oxidative Phosphorylation. *Cell Metab,* 26**,** 633-647 e7.

LEE, Y. Y., MOUJALLED, D., DOERFLINGER, M., GANGODA, L., WESTON, R., RAHIMI, A., DE ALBORAN, I., HEROLD, M., BOUILLET, P., XU, Q., GAO, X., DU, X. J. & PUTHALAKATH, H. 2013. CREB-binding protein (CBP) regulates beta-adrenoceptor (beta-AR)-mediated apoptosis. *Cell Death Differ,* 20**,** 941-52.

LEONE, G., DEGREGORI, J., SEARS, R., JAKOI, L. & NEVINS, J. R. 1997. Myc and Ras collaborate in inducing accumulation of active cyclin E/Cdk2 and E2F. *Nature,* 387**,** 422-6.

LEONE, G., SEARS, R., HUANG, E., REMPEL, R., NUCKOLLS, F., PARK, C. H., GIANGRANDE, P., WU, L., SAAVEDRA, H. I., FIELD, S. J., THOMPSON, M. A., YANG, H., FUJIWARA, Y., GREENBERG, M. E.,

ORKIN, S., SMITH, C. & NEVINS, J. R. 2001. Myc requires distinct E2F activities to induce S phase and apoptosis. *Mol Cell,* 8**,** 105-13.

LETAI, A., SORCINELLI, M. D., BEARD, C. & KORSMEYER, S. J. 2004. Antiapoptotic BCL-2 is required for maintenance of a model leukemia. *Cancer Cell,* 6**,** 241-9.

LEVENS, D. 2008. How the c-myc promoter works and why it sometimes does not. *J Natl Cancer Inst Monogr***,** 41-3.

LEVENS, D. 2010. You Don't Muck with MYC. *Genes Cancer,* 1**,** 547-554.

LEVERSON, J. D., ZHANG, H., CHEN, J., TAHIR, S. K., PHILLIPS, D. C., XUE, J., NIMMER, P., JIN, S., SMITH, M., XIAO, Y., KOVAR, P., TANAKA, A., BRUNCKO, M., SHEPPARD, G. S., WANG, L., GIERKE, S., KATEGAYA, L., ANDERSON, D. J., WONG, C., EASTHAM-ANDERSON, J., LUDLAM, M. J., SAMPATH, D., FAIRBROTHER, W. J., WERTZ, I., ROSENBERG, S. H., TSE, C., ELMORE, S. W. & SOUERS, A. J. 2015. Potent and selective small-molecule MCL-1 inhibitors demonstrate on-target cancer cell killing activity as single agents and in combination with ABT-263 (navitoclax). *Cell Death Dis,* 6**,** e1590.

LEVINE, A. J. & OREN, M. 2009. The first 30 years of p53: growing ever more complex. *Nat Rev Cancer,* 9**,** 749-58.

LI, J., VIALLET, J. & HAURA, E. B. 2008. A small molecule pan-Bcl-2 family inhibitor, GX15-070, induces apoptosis and enhances cisplatin-induced apoptosis in non-small cell lung cancer cells. *Cancer Chemother Pharmacol,* 61**,** 525-34.

LI, Z., HE, S. & LOOK, A. T. 2019. The MCL1-specific inhibitor S63845 acts synergistically with venetoclax/ABT-199 to induce apoptosis in T-cell acute lymphoblastic leukemia cells. *Leukemia,* 33**,** 262-266.

LIAO, J. M., ZHOU, X., GATIGNOL, A. & LU, H. 2014. Ribosomal proteins L5 and L11 co-operatively inactivate c-Myc via RNA-induced silencing complex. *Oncogene,* 33**,** 4916-23.

LIN, C. Y., LOVEN, J., RAHL, P. B., PARANAL, R. M., BURGE, C. B., BRADNER, J. E., LEE, T. I. & YOUNG, R. A. 2012. Transcriptional amplification in tumor cells with elevated c-Myc. *Cell,* 151**,** 56-67.

LINDSTROM, M. S., JIN, A., DEISENROTH, C., WHITE WOLF, G. & ZHANG, Y. 2007. Cancer-associated mutations in the MDM2 zinc finger domain disrupt ribosomal protein interaction and attenuate MDM2-induced p53 degradation. *Mol Cell Biol,* 27**,** 1056-68.

LINDSTRÖM, M. S. & LATONEN, L. 2013. The nucleolus as a stress response organelle. *Proteins of the Nucleolus.* Springer.

LIU, H., CHEN, W., LIANG, C., CHEN, B. W., ZHI, X., ZHANG, S., ZHENG, X., BAI, X. & LIANG, T. 2015. WP1130 increases doxorubicin sensitivity in hepatocellular carcinoma cells through usp9x-dependent p53 degradation. *Cancer Lett,* 361**,** 218-25.

LIU, J. & LEVENS, D. 2006. Making myc. *Curr Top Microbiol Immunol,* 302**,** 1-32.

LIU, S., TACKMANN, N. R., YANG, J. & ZHANG, Y. 2017. Disruption of the RP-MDM2-p53 pathway accelerates APC loss-induced colorectal tumorigenesis. *Oncogene,* 36**,** 1374-1383.

LLAMBI, F., MOLDOVEANU, T., TAIT, S. W., BOUCHIER-HAYES, L., TEMIROV, J., MCCORMICK, L. L., DILLON, C. P. & GREEN, D. R. 2011. A unified model of mammalian BCL-2 protein family interactions at the mitochondria. *Mol Cell,* 44**,** 517-31.

LLAMBI, F., WANG, Y. M., VICTOR, B., YANG, M., SCHNEIDER, D. M., GINGRAS, S., PARSONS, M. J., ZHENG, J. H., BROWN, S. A., PELLETIER, S., MOLDOVEANU, T., CHEN, T. & GREEN, D. R. 2016. BOK Is a Non-canonical BCL-2 Family Effector of Apoptosis Regulated by ER-Associated Degradation. *Cell,* 165**,** 421-33.

LODISH, H. F. 1974. Model for the regulation of mRNA translation applied to haemoglobin synthesis. *Nature,* 251**,** 385-8.

LOHRUM, M. A., LUDWIG, R. L., KUBBUTAT, M. H., HANLON, M. & VOUSDEN, K. H. 2003. Regulation of HDM2 activity by the ribosomal protein L11. *Cancer Cell,* 3**,** 577-87.

LOWE, S. W., CEPERO, E. & EVAN, G. 2004. Intrinsic tumour suppression. *Nature,* 432**,** 307-15.

LUCKING, U., SCHOLZ, A., LIENAU, P., SIEMEISTER, G., KOSEMUND, D., BOHLMANN, R., BRIEM, H., TEREBESI, I., MEYER, K., PRELLE, K., DENNER, K., BOMER, U., SCHAFER, M., EIS, K., VALENCIA, R., INCE, S., VON NUSSBAUM, F., MUMBERG, D., ZIEGELBAUER, K., KLEBL, B., CHOIDAS, A.,

NUSSBAUMER, P., BAUMANN, M., SCHULTZ-FADEMRECHT, C., RUHTER, G., EICKHOFF, J. & BRANDS, M. 2017. Identification of Atuveciclib (BAY 1143572), the First Highly Selective, Clinical PTEFb/CDK9 Inhibitor for the Treatment of Cancer. *ChemMedChem,* 12**,** 1776-1793.

LUECKING, U. T., SCHOLZ, A., KOSEMUND, D., BOHLMANN, R., BRIEM, H., LIENAU, P., SIEMEISTER, G., TEREBESI, I., MEYER, K. & PRELLE, K. 2017. Identification of potent and highly selective PTEFb inhibitor BAY 1251152 for the treatment of cancer: from po to iv application via scaffold hops. AACR.

MACCALLUM, D. E., MELVILLE, J., FRAME, S., WATT, K., ANDERSON, S., GIANELLA-BORRADORI, A., LANE, D. P. & GREEN, S. R. 2005. Seliciclib (CYC202, R-Roscovitine) induces cell death in multiple myeloma cells by inhibition of RNA polymerase II-dependent transcription and down-regulation of Mcl-1. *Cancer Res,* 65**,** 5399-407.

MACCARTY, W. C. J. T. A. J. O. C. 1936. The value of the macronucleolus in the cancer problem. 26**,** 529-532.

MACIAS, E., JIN, A., DEISENROTH, C., BHAT, K., MAO, H., LINDSTROM, M. S. & ZHANG, Y. 2010. An ARF-independent c-MYC-activated tumor suppression pathway mediated by ribosomal protein-Mdm2 Interaction. *Cancer Cell,* 18**,** 231-43.

MACINNES, A. W. 2016. The role of the ribosome in the regulation of longevity and lifespan extension. *Wiley Interdiscip Rev RNA,* 7**,** 198-212.

MAGGI, L. B., JR., KUCHENRUETHER, M., DADEY, D. Y., SCHWOPE, R. M., GRISENDI, S., TOWNSEND, R. R., PANDOLFI, P. P. & WEBER, J. D. 2008. Nucleophosmin serves as a rate-limiting nuclear export chaperone for the Mammalian ribosome. *Mol Cell Biol,* 28**,** 7050-65.

MAGIERA, M. M., MORA, S., MOJSA, B., ROBBINS, I., LASSOT, I. & DESAGHER, S. 2013. Trim17-mediated ubiquitination and degradation of Mcl-1 initiate apoptosis in neurons. *Cell Death Differ,* 20**,** 281-92.

MAGRATH, I. 2012. Epidemiology: clues to the pathogenesis of Burkitt lymphoma. *Br J Haematol,* 156**,** 744-56.

MAGRATH, I., ADDE, M., SHAD, A., VENZON, D., SEIBEL, N., GOOTENBERG, J., NEELY, J., ARNDT, C., NIEDER, M., JAFFE, E., WITTES, R. A. & HORAK, I. D. 1996. Adults and children with small non-cleaved-cell lymphoma have a similar excellent outcome when treated with the same chemotherapy regimen. *J Clin Oncol,* 14**,** 925-34.

MALOGOLOWKIN, M., COTTON, C. A., GREEN, D. M., BRESLOW, N. E., PERLMAN, E., MISER, J., RITCHEY, M. L., THOMAS, P. R., GRUNDY, P. E., D'ANGIO, G. J., BECKWITH, J. B., SHAMBERGER, R. C., HAASE, G. M., DONALDSON, M., WEETMAN, R., COPPES, M. J., SHEARER, P., COCCIA, P., KLETZEL, M., MACKLIS, R., TOMLINSON, G., HUFF, V., NEWBURY, R., WEEKS, D. & NATIONAL WILMS TUMOR STUDY, G. 2008. Treatment of Wilms tumor relapsing after initial treatment with vincristine, actinomycin D, and doxorubicin. A report from the National Wilms Tumor Study Group. *Pediatr Blood Cancer,* 50**,** 236-41.

MALUMBRES, R., SAROSIEK, K. A., CUBEDO, E., RUIZ, J. W., JIANG, X., GASCOYNE, R. D., TIBSHIRANI, R. & LOSSOS, I. S. 2009. Differentiation stage-specific expression of microRNAs in B lymphocytes and diffuse large B-cell lymphomas. *Blood,* 113**,** 3754-64.

MANOLOV, G. & MANOLOVA, Y. 1972. Marker band in one chromosome 14 from Burkitt lymphomas. *Nature,* 237**,** 33-4.

MARCHENKO, N. D., WOLFF, S., ERSTER, S., BECKER, K. & MOLL, U. M. 2007. Monoubiquitylation promotes mitochondrial p53 translocation. *EMBO J,* 26**,** 923-34.

MARECHAL, V., ELENBAAS, B., PIETTE, J., NICOLAS, J. C. & LEVINE, A. J. 1994. The ribosomal L5 protein is associated with mdm-2 and mdm-2-p53 complexes. *Mol Cell Biol,* 14**,** 7414-20.

MARTINOU, J. C. & YOULE, R. J. 2011. Mitochondria in apoptosis: Bcl-2 family members and mitochondrial dynamics. *Dev Cell,* 21**,** 92-101.

MAURER, U., CHARVET, C., WAGMAN, A. S., DEJARDIN, E. & GREEN, D. R. 2006. Glycogen synthase kinase-3 regulates mitochondrial outer membrane permeabilization and apoptosis by destabilization of MCL-1. *Mol Cell,* 21**,** 749-60.

MAYER, C., ZHAO, J., YUAN, X. & GRUMMT, I. 2004. mTOR-dependent activation of the transcription factor TIF-IA links rRNA synthesis to nutrient availability. *Genes Dev,* 18**,** 423-34.

MAZZOCCOLI, L., ROBAINA, M. C., APA, A. G., BONAMINO, M., PINTO, L. W., QUEIROGA, E., BACCHI, C. E. & KLUMB, C. E. 2018. MiR-29 silencing modulates the expression of target genes related to proliferation, apoptosis and methylation in Burkitt lymphoma cells. *J Cancer Res Clin Oncol,* 144**,** 483-497.

MBULAITEYE, S. M., BIGGAR, R. J., BHATIA, K., LINET, M. S. & DEVESA, S. S. 2009. Sporadic childhood Burkitt lymphoma incidence in the United States during 1992-2005. *Pediatr Blood Cancer,* 53**,** 366-70.

MCGOWAN, K. A., PANG, W. W., BHARDWAJ, R., PEREZ, M. G., PLUVINAGE, J. V., GLADER, B. E., MALEK, R., MENDRYSA, S. M., WEISSMAN, I. L., PARK, C. Y. & BARSH, G. S. 2011. Reduced ribosomal protein gene dosage and p53 activation in low-risk myelodysplastic syndrome. *Blood,* 118**,** 3622-33.

MCMAHON, S. B. 2014. MYC and the control of apoptosis. *Cold Spring Harb Perspect Med,* 4**,** a014407.

MCSTAY, B. & GRUMMT, I. 2008. The epigenetics of rRNA genes: from molecular to chromosome biology. *Annu Rev Cell Dev Biol,* 24**,** 131-57.

MEAD, G. M., SYDES, M. R., WALEWSKI, J., GRIGG, A., HATTON, C. S., PESCOSTA, N., GUARNACCIA, C., LEWIS, M. S., MCKENDRICK, J., STENNING, S. P., WRIGHT, D. & COLLABORATORS, U. L. 2002. An international evaluation of CODOX-M and CODOX-M alternating with IVAC in adult Burkitt's lymphoma: results of United Kingdom Lymphoma Group LY06 study. *Ann Oncol,* 13**,** 1264-74.

MEEK, D. W. & ANDERSON, C. W. 2009. Posttranslational modification of p53: cooperative integrators of function. *Cold Spring Harb Perspect Biol,* 1**,** a000950.

MEI, Y., DU, W., YANG, Y. & WU, M. 2005. Puma(*)Mcl-1 interaction is not sufficient to prevent rapid degradation of Mcl-1. *Oncogene,* 24**,** 7224-37.

MELNIKOV, S., BEN-SHEM, A., GARREAU DE LOUBRESSE, N., JENNER, L., YUSUPOVA, G. & YUSUPOV, M. 2012. One core, two shells: bacterial and eukaryotic ribosomes. *Nat Struct Mol Biol,* 19**,** 560-7.

MENENDEZ, D., INGA, A. & RESNICK, M. A. 2009. The expanding universe of p53 targets. *Nat Rev Cancer,* 9**,** 724-37.

MENSINK, M., ANSTEE, N. S., ROBATI, M., SCHENK, R. L., HEROLD, M. J., CORY, S. & VANDENBERG, C. J. 2018. Anti-apoptotic A1 is not essential for lymphoma development in Emicro-Myc mice but helps sustain transplanted Emicro-Myc tumour cells. *Cell Death Differ,* 25**,** 795-806.

MERINO, D., WHITTLE, J. R., VAILLANT, F., SERRANO, A., GONG, J. N., GINER, G., MARAGNO, A. L., CHANRION, M., SCHNEIDER, E., PAL, B., LI, X., DEWSON, G., GRASEL, J., LIU, K., LALAOUI, N., SEGAL, D., HEROLD, M. J., HUANG, D. C. S., SMYTH, G. K., GENESTE, O., LESSENE, G., VISVADER, J. E. & LINDEMAN, G. J. 2017. Synergistic action of the MCL-1 inhibitor S63845 with current therapies in preclinical models of triple-negative and HER2-amplified breast cancer. *Sci Transl Med,* 9.

MERKEL, O., WACHT, N., SIFFT, E., MELCHARDT, T., HAMACHER, F., KOCHER, T., DENK, U., HOFBAUER, J. P., EGLE, A., SCHEIDELER, M., SCHLEDERER, M., STEURER, M., KENNER, L. & GREIL, R. 2012. Actinomycin D induces p53-independent cell death and prolongs survival in high-risk chronic lymphocytic leukemia. *Leukemia,* 26**,** 2508-16.

MESTRE-ESCORIHUELA, C., RUBIO-MOSCARDO, F., RICHTER, J. A., SIEBERT, R., CLIMENT, J., FRESQUET, V., BELTRAN, E., AGIRRE, X., MARUGAN, I., MARIN, M., ROSENWALD, A., SUGIMOTO, K. J., WHEAT, L. M., KARRAN, E. L., GARCIA, J. F., SANCHEZ, L., PROSPER, F., STAUDT, L. M., PINKEL, D., DYER, M. J. & MARTINEZ-CLIMENT, J. A. 2007. Homozygous deletions localize novel tumor suppressor genes in B-cell lymphomas. *Blood,* 109**,** 271-80.

MEYER, N., KIM, S. S. & PENN, L. Z. 2006. The Oscar-worthy role of Myc in apoptosis. *Semin Cancer Biol,* 16**,** 275-87.

MEYER, N. & PENN, L. Z. 2008. Reflecting on 25 years with MYC. *Nat Rev Cancer,* 8**,** 976-90.

MICHALAK, E. M., JANSEN, E. S., HAPPO, L., CRAGG, M. S., TAI, L., SMYTH, G. K., STRASSER, A., ADAMS, J. M. & SCOTT, C. L. 2009. Puma and to a lesser extent Noxa are suppressors of Myc-induced lymphomagenesis. *Cell Death Differ,* 16**,** 684-96.

MILLER, D. M., THOMAS, S. D., ISLAM, A., MUENCH, D. & SEDORIS, K. 2012. c-Myc and cancer metabolism. *Clin Cancer Res,* 18**,** 5546-53.

MILLMAN, S. E. & PAGANO, M. 2011. MCL1 meets its end during mitotic arrest. *EMBO Rep,* 12**,** 384-5.

MILLS, E. W. & GREEN, R. 2017. Ribosomopathies: There's strength in numbers. *Science,* 358.

MILLS, J. R., HIPPO, Y., ROBERT, F., CHEN, S. M., MALINA, A., LIN, C. J., TROJAHN, U., WENDEL, H. G., CHAREST, A., BRONSON, R. T., KOGAN, S. C., NADON, R., HOUSMAN, D. E., LOWE, S. W. & PELLETIER, J. 2008. mTORC1 promotes survival through translational control of Mcl-1. *Proc Natl Acad Sci U S A,* 105**,** 10853-8.

MITCHELL, K. O., RICCI, M. S., MIYASHITA, T., DICKER, D. T., JIN, Z., REED, J. C. & EL-DEIRY, W. S. 2000. Bax is a transcriptional target and mediator of c-myc-induced apoptosis. *Cancer Res,* 60**,** 6318-25.

MOJSA, B., LASSOT, I. & DESAGHER, S. 2014. Mcl-1 ubiquitination: unique regulation of an essential survival protein. *Cells,* 3**,** 418-37.

MOLDOVEANU, T., FOLLIS, A. V., KRIWACKI, R. W. & GREEN, D. R. 2014. Many players in BCL-2 family affairs. *Trends Biochem Sci,* 39**,** 101-11.

MOORE, J. P., HANCOCK, D. C., LITTLEWOOD, T. D. & EVAN, G. I. 1987. A sensitive and quantitative enzyme-linked immunosorbence assay for the c-myc and N-myc oncoproteins. *Oncogene Res,* 2**,** 65-80.

MORCELLE, C., MENOYO, S., MORÓN-DURAN, F. D., TAULER, A., KOZMA, S. C., THOMAS, G. & GENTILELLA, A. J. C. R. 2019. Oncogenic MYC Induces the Impaired Ribosome Biogenesis Checkpoint and Stabilizes p53 Independent of Increased Ribosome Content. 79**,** 4348-4359.

MORCIANO, G., GIORGI, C., BALESTRA, D., MARCHI, S., PERRONE, D., PINOTTI, M. & PINTON, P. 2016. Mcl-1 involvement in mitochondrial dynamics is associated with apoptotic cell death. *Mol Biol Cell,* 27**,** 20-34.

MOREL, C., CARLSON, S. M., WHITE, F. M. & DAVIS, R. J. 2009. Mcl-1 integrates the opposing actions of signaling pathways that mediate survival and apoptosis. *Mol Cell Biol,* 29**,** 3845-52.

MORGADO-PALACIN, L., LLANOS, S. & SERRANO, M. 2012. Ribosomal stress induces L11- and p53-dependent apoptosis in mouse pluripotent stem cells. *Cell Cycle,* 11**,** 503-10.

MORGADO-PALACIN, L., LLANOS, S., URBANO-CUADRADO, M., BLANCO-APARICIO, C., MEGIAS, D., PASTOR, J. & SERRANO, M. 2014. Non-genotoxic activation of p53 through the RPL11-dependent ribosomal stress pathway. *Carcinogenesis,* 35**,** 2822-30.

MORGADO-PALACIN, L., VARETTI, G., LLANOS, S., GOMEZ-LOPEZ, G., MARTINEZ, D. & SERRANO, M. 2015. Partial Loss of Rpl11 in Adult Mice Recapitulates Diamond-Blackfan Anemia and Promotes Lymphomagenesis. *Cell Rep,* 13**,** 712-722.

MORRISH, F., GIEDT, C. & HOCKENBERY, D. 2003. c-MYC apoptotic function is mediated by NRF-1 target genes. *Genes Dev,* 17**,** 240-55.

MORTON, L. M., WANG, S. S., DEVESA, S. S., HARTGE, P., WEISENBURGER, D. D. & LINET, M. S. 2006. Lymphoma incidence patterns by WHO subtype in the United States, 1992-2001. *Blood,* 107**,** 265-76.

MOSS, T. & STEFANOVSKY, V. Y. 2002. At the center of eukaryotic life. *Cell,* 109**,** 545-8.

MOSSE, C. & WECK, K. 2010. The Molecular pathology of Burkitt lymphoma. *Molecular Pathology of Hematolymphoid Diseases.* Springer.

MOTT, J. L., KOBAYASHI, S., BRONK, S. F. & GORES, G. J. 2007. mir-29 regulates Mcl-1 protein expression and apoptosis. *Oncogene,* 26**,** 6133-40.

MOUJALLED, D. M., POMILIO, G., GHIURAU, C., IVEY, A., SALMON, J., RIJAL, S., MACRAILD, S., ZHANG, L., TEH, T. C., TIONG, I. S., LAN, P., CHANRION, M., CLAPERON, A., ROCCHETTI, F., ZICHI, A., KRAUS-BERTHIER, L., WANG, Y., HALILOVIC, E., MORRIS, E., COLLAND, F., SEGAL, D., HUANG, D., ROBERTS, A. W., MARAGNO, A. L., LESSENE, G., GENESTE, O. & WEI, A. H. 2019. Combining BH3-mimetics to target both BCL-2 and MCL1 has potent activity in pre-clinical models of acute myeloid leukemia. *Leukemia,* 33**,** 905-917.

MOULDING, D. A., GILES, R. V., SPILLER, D. G., WHITE, M. R., TIDD, D. M. & EDWARDS, S. W. 2000. Apoptosis is rapidly triggered by antisense depletion of MCL-1 in differentiating U937 cells. *Blood,* 96**,** 1756-63.

MUKHTAR, F., BOFFETTA, P., RISCH, H. A., PARK, J. Y., BUBU, O. M., WOMACK, L., TRAN, T. V., ZGIBOR, J. C. & LUU, H. N. 2017. Survival predictors of Burkitt's lymphoma in children, adults and elderly in the United States during 2000-2013. *Int J Cancer,* 140**,** 1494-1502.

MURPHY, D. J., JUNTTILA, M. R., POUYET, L., KARNEZIS, A., SHCHORS, K., BUI, D. A., BROWN-SWIGART, L., JOHNSON, L. & EVAN, G. I. 2008. Distinct thresholds govern Myc's biological output in vivo. *Cancer Cell,* 14**,** 447-57.

NAKAJIMA, W., SHARMA, K., LEE, J. Y., MAXIM, N. T., HICKS, M. A., VU, T. T., LUU, A., YEUDALL, W. A., TANAKA, N. & HARADA, H. 2016. DNA damaging agent-induced apoptosis is regulated by MCL-1 phosphorylation and degradation mediated by the Noxa/MCL-1/CDK2 complex. *Oncotarget,* 7**,** 36353-36365.

NARLA, A. & EBERT, B. L. 2010. Ribosomopathies: human disorders of ribosome dysfunction. *Blood,* 115**,** 3196-205.

NEGI, S. S. & BROWN, P. 2015. rRNA synthesis inhibitor, CX-5461, activates ATM/ATR pathway in acute lymphoblastic leukemia, arrests cells in G2 phase and induces apoptosis. *Oncotarget,* 6**,** 18094-104.

NERI, A., BARRIGA, F., KNOWLES, D. M., MAGRATH, I. T. & DALLA-FAVERA, R. 1988. Different regions of the immunoglobulin heavy-chain locus are involved in chromosomal translocations in distinct pathogenetic forms of Burkitt lymphoma. *Proc Natl Acad Sci U S A,* 85**,** 2748-52.

NESBIT, C. E., TERSAK, J. M. & PROCHOWNIK, E. V. 1999. MYC oncogenes and human neoplastic disease. *Oncogene,* 18**,** 3004-16.

NGUYEN, M., MARCELLUS, R. C., ROULSTON, A., WATSON, M., SERFASS, L., MURTHY MADIRAJU, S. R., GOULET, D., VIALLET, J., BELEC, L., BILLOT, X., ACOCA, S., PURISIMA, E., WIEGMANS, A., CLUSE, L., JOHNSTONE, R. W., BEAUPARLANT, P. & SHORE, G. C. 2007. Small molecule obatoclax (GX15-070) antagonizes MCL-1 and overcomes MCL-1-mediated resistance to apoptosis. *Proc Natl Acad Sci U S A,* 104**,** 19512-7.

NIE, Z., HU, G., WEI, G., CUI, K., YAMANE, A., RESCH, W., WANG, R., GREEN, D. R., TESSAROLLO, L., CASELLAS, R., ZHAO, K. & LEVENS, D. 2012. c-Myc is a universal amplifier of expressed genes in lymphocytes and embryonic stem cells. *Cell,* 151**,** 68-79.

NIFOUSSI, S. K., VRANA, J. A., DOMINA, A. M., DE BIASIO, A., GUI, J., GREGORY, M. A., HANN, S. R. & CRAIG, R. W. 2012. Thr 163 phosphorylation causes Mcl-1 stabilization when degradation is independent of the adjacent GSK3-targeted phosphodegron, promoting drug resistance in cancer. *PLoS One,* 7**,** e47060.

NIJHAWAN, D., FANG, M., TRAER, E., ZHONG, Q., GAO, W., DU, F. & WANG, X. 2003. Elimination of Mcl-1 is required for the initiation of apoptosis following ultraviolet irradiation. *Genes Dev,* 17**,** 1475-86.

NISHIMURA, K., KUMAZAWA, T., KURODA, T., KATAGIRI, N., TSUCHIYA, M., GOTO, N., FURUMAI, R., MURAYAMA, A., YANAGISAWA, J. & KIMURA, K. 2015. Perturbation of ribosome biogenesis drives cells into senescence through 5S RNP-mediated p53 activation. *Cell Rep,* 10**,** 1310-23.

O'BRIEN, S. M., CLAXTON, D. F., CRUMP, M., FADERL, S., KIPPS, T., KEATING, M. J., VIALLET, J. & CHESON, B. D. 2009. Phase I study of obatoclax mesylate (GX15-070), a small molecule pan-Bcl-2 family antagonist, in patients with advanced chronic lymphocytic leukemia. *Blood,* 113**,** 299-305.

OLINER, J. D., PIETENPOL, J. A., THIAGALINGAM, S., GYURIS, J., KINZLER, K. W. & VOGELSTEIN, B. 1993. Oncoprotein MDM2 conceals the activation domain of tumour suppressor p53. *Nature,* 362**,** 857-60.

OLIVER, E. R., SAUNDERS, T. L., TARLE, S. A. & GLASER, T. 2004. Ribosomal protein L24 defect in belly spot and tail (Bst), a mouse Minute. *Development,* 131**,** 3907-20.

OLSON, M. O. 2004. Sensing cellular stress: another new function for the nucleolus? *Sci STKE,* 2004**,** pe10.

OPFERMAN, J. T. 2016. Attacking cancer's Achilles heel: antagonism of anti-apoptotic BCL-2 family members. *FEBS J,* 283**,** 2661-75.

OPFERMAN, J. T., IWASAKI, H., ONG, C. C., SUH, H., MIZUNO, S., AKASHI, K. & KORSMEYER, S. J. 2005. Obligate role of anti-apoptotic MCL-1 in the survival of hematopoietic stem cells. *Science,* 307**,** 1101-4.

OPFERMAN, J. T., LETAI, A., BEARD, C., SORCINELLI, M. D., ONG, C. C. & KORSMEYER, S. J. 2003. Development and maintenance of B and T lymphocytes requires antiapoptotic MCL-1. *Nature,* 426**,** 671-6.

OREM, J., MBIDDE, E. K., LAMBERT, B., DE SANJOSE, S. & WEIDERPASS, E. 2007. Burkitt's lymphoma in Africa, a review of the epidemiology and etiology. *Afr Health Sci,* 7**,** 166-75.

ORSOLIC, I., JURADA, D., PULLEN, N., OREN, M., ELIOPOULOS, A. G. & VOLAREVIC, S. 2016. The relationship between the nucleolus and cancer: Current evidence and emerging paradigms. *Semin Cancer Biol,* 37-38**,** 36-50.

ORTEGA, J. A., DONALDSON, S. S., IVY, S. P., PAPPO, A. & MAURER, H. M. 1997. Venoocclusive disease of the liver after chemotherapy with vincristine, actinomycin D, and cyclophosphamide for the treatment of rhabdomyosarcoma. A report of the Intergroup Rhabdomyosarcoma Study Group. Childrens Cancer Group, the Pediatric Oncology Group, and the Pediatric Intergroup Statistical Center. *Cancer,* 79**,** 2435-9.

OTT, G., ROSENWALD, A. & CAMPO, E. 2013. Understanding MYC-driven aggressive B-cell lymphomas: pathogenesis and classification. *Blood,* 122**,** 3884-91.

PAN, W., ISSAQ, S. & ZHANG, Y. 2011. The in vivo role of the RP-Mdm2-p53 pathway in signaling oncogenic stress induced by pRb inactivation and Ras overexpression. *PLoS One,* 6**,** e21625.

PANG, X., ZHANG, J., LOPEZ, H., WANG, Y., LI, W., O'NEILL, K. L., EVANS, J. J., GEORGE, N. M., LONG, J., CHEN, Y. & LUO, X. 2014. The carboxyl-terminal tail of Noxa protein regulates the stability of Noxa and Mcl-1. *J Biol Chem,* 289**,** 17802-11.

PARK, S. H., LEE, D. H., KIM, J. L., KIM, B. R., NA, Y. J., JO, M. J., JEONG, Y. A., LEE, S. Y., LEE, S. I., LEE, Y. Y. & OH, S. C. 2016. Metformin enhances TRAIL-induced apoptosis by Mcl-1 degradation via Mule in colorectal cancer cells. *Oncotarget,* 7**,** 59503-59518.

PASQUALUCCI, L., KHIABANIAN, H., FANGAZIO, M., VASISHTHA, M., MESSINA, M., HOLMES, A. B., OUILLETTE, P., TRIFONOV, V., ROSSI, D., TABBO, F., PONZONI, M., CHADBURN, A., MURTY, V. V., BHAGAT, G., GAIDANO, G., INGHIRAMI, G., MALEK, S. N., RABADAN, R. & DALLA-FAVERA, R. 2014. Genetics of follicular lymphoma transformation. *Cell Rep,* 6**,** 130-40.

PEARSON, M., CARBONE, R., SEBASTIANI, C., CIOCE, M., FAGIOLI, M., SAITO, S., HIGASHIMOTO, Y., APPELLA, E., MINUCCI, S., PANDOLFI, P. P. & PELICCI, P. G. 2000. PML regulates p53 acetylation and premature senescence induced by oncogenic Ras. *Nature,* 406**,** 207-10.

PELICCI, P. G., KNOWLES, D. M., 2ND, MAGRATH, I. & DALLA-FAVERA, R. 1986. Chromosomal breakpoints and structural alterations of the c-myc locus differ in endemic and sporadic forms of Burkitt lymphoma. *Proc Natl Acad Sci U S A,* 83**,** 2984-8.

PELLAGATTI, A., MARAFIOTI, T., PATERSON, J. C., BARLOW, J. L., DRYNAN, L. F., GIAGOUNIDIS, A., PILERI, S. A., CAZZOLA, M., MCKENZIE, A. N., WAINSCOAT, J. S. & BOULTWOOD, J. 2010. Induction of p53 and up-regulation of the p53 pathway in the human 5q- syndrome. *Blood,* 115**,** 2721-3.

PELLETIER, J., THOMAS, G. & VOLAREVIC, S. 2018. Ribosome biogenesis in cancer: new players and therapeutic avenues. *Nat Rev Cancer,* 18**,** 51-63.

PELTONEN, K., COLIS, L., LIU, H., JAAMAA, S., MOORE, H. M., ENBACK, J., LAAKKONEN, P., VAAHTOKARI, A., JONES, R. J., AF HALLSTROM, T. M. & LAIHO, M. 2010. Identification of novel p53 pathway activating small-molecule compounds reveals unexpected similarities with known therapeutic agents. *PLoS One,* 5**,** e12996.

PELTONEN, K., COLIS, L., LIU, H., TRIVEDI, R., MOUBAREK, M. S., MOORE, H. M., BAI, B., RUDEK, M. A., BIEBERICH, C. J. & LAIHO, M. 2014. A targeting modality for destruction of RNA polymerase I that possesses anticancer activity. *Cancer Cell,* 25**,** 77-90.

PEPERZAK, V., VIKSTROM, I., WALKER, J., GLASER, S. P., LEPAGE, M., COQUERY, C. M., ERICKSON, L. D., FAIRFAX, K., MACKAY, F., STRASSER, A., NUTT, S. L. & TARLINTON, D. M. 2013. Mcl-1 is essential for the survival of plasma cells. *Nat Immunol,* 14**,** 290-7.

PEPPER, C., LIN, T. T., PRATT, G., HEWAMANA, S., BRENNAN, P., HILLER, L., HILLS, R., WARD, R., STARCZYNSKI, J., AUSTEN, B., HOOPER, L., STANKOVIC, T. & FEGAN, C. 2008. Mcl-1 expression has in vitro and in vivo significance in chronic lymphocytic leukemia and is associated with other poor prognostic markers. *Blood,* 112**,** 3807-17.

PERCIAVALLE, R. M. & OPFERMAN, J. T. 2013. Delving deeper: MCL-1's contributions to normal and cancer biology. *Trends Cell Biol,* 23**,** 22-9.

PERCIAVALLE, R. M., STEWART, D. P., KOSS, B., LYNCH, J., MILASTA, S., BATHINA, M., TEMIROV, J., CLELAND, M. M., PELLETIER, S., SCHUETZ, J. D., YOULE, R. J., GREEN, D. R. & OPFERMAN, J. T. 2012. Anti-apoptotic MCL-1 localizes to the mitochondrial matrix and couples mitochondrial fusion to respiration. *Nat Cell Biol,* 14**,** 575-83.

PEREZ-GALAN, P., ROUE, G., VILLAMOR, N., CAMPO, E. & COLOMER, D. 2007. The BH3-mimetic GX15-070 synergizes with bortezomib in mantle cell lymphoma by enhancing Noxa-mediated activation of Bak. *Blood,* 109**,** 4441-9.

PERRY, R. P. & KELLEY, D. E. 1970. Inhibition of RNA synthesis by actinomycin D: characteristic dose-response of different RNA species. *J Cell Physiol,* 76**,** 127-39.

PESTOV, D. G., STREZOSKA, Z. & LAU, L. F. 2001. Evidence of p53-dependent cross-talk between ribosome biogenesis and the cell cycle: effects of nucleolar protein Bop1 on G(1)/S transition. *Mol Cell Biol,* 21**,** 4246-55.

PIANESE, G. 1896. *Beitrag zur Histologie und Aetiologie des Carcinoms: Histologische und experimentelle Untersuchungen*, G. Fischer.

PIERANDREI-AMALDI, P., BECCARI, E., BOZZONI, I. & AMALDI, F. 1985. Ribosomal protein production in normal and anucleolate Xenopus embryos: regulation at the posttranscriptional and translational levels. *Cell,* 42**,** 317-23.

PILLET, B., MITTERER, V., KRESSLER, D. & PERTSCHY, B. 2017. Hold on to your friends: Dedicated chaperones of ribosomal proteins: Dedicated chaperones mediate the safe transfer of ribosomal proteins to their site of pre-ribosome incorporation. *Bioessays,* 39**,** 1-12.

POORTINGA, G., HANNAN, K. M., SNELLING, H., WALKLEY, C. R., JENKINS, A., SHARKEY, K., WALL, M., BRANDENBURGER, Y., PALATSIDES, M., PEARSON, R. B., MCARTHUR, G. A. & HANNAN, R. D. 2004. MAD1 and c-MYC regulate UBF and rDNA transcription during granulocyte differentiation. *EMBO J,* 23**,** 3325-35.

POORTINGA, G., QUINN, L. M. & HANNAN, R. D. 2015. Targeting RNA polymerase I to treat MYC-driven cancer. *Oncogene,* 34**,** 403-12.

POORTINGA, G., WALL, M., SANIJ, E., SIWICKI, K., ELLUL, J., BROWN, D., HOLLOWAY, T. P., HANNAN, R. D. & MCARTHUR, G. A. 2011. c-MYC coordinately regulates ribosomal gene chromatin remodeling and Pol I availability during granulocyte differentiation. *Nucleic Acids Res,* 39**,** 3267-81.

POP, C. & SALVESEN, G. S. 2009. Human caspases: activation, specificity, and regulation. *J Biol Chem,* 284**,** 21777-81.

POPOV, N., SCHULEIN, C., JAENICKE, L. A. & EILERS, M. 2010. Ubiquitylation of the amino terminus of Myc by SCF(beta-TrCP) antagonizes SCF(Fbw7)-mediated turnover. *Nat Cell Biol,* 12**,** 973-81.

POST, S. M., QUINTAS-CARDAMA, A., TERZIAN, T., SMITH, C., EISCHEN, C. M. & LOZANO, G. 2010. p53-dependent senescence delays Emu-myc-induced B-cell lymphomagenesis. *Oncogene,* 29**,** 1260-9.

POURDEHNAD, M., TRUITT, M. L., SIDDIQI, I. N., DUCKER, G. S., SHOKAT, K. M. & RUGGERO, D. 2013. Myc and mTOR converge on a common node in protein synthesis control that confers synthetic lethality in Myc-driven cancers. *Proc Natl Acad Sci U S A,* 110**,** 11988-93.

PUSAPATI, R. V., ROUNBEHLER, R. J., HONG, S., POWERS, J. T., YAN, M., KIGUCHI, K., MCARTHUR, M. J., WONG, P. K. & JOHNSON, D. G. 2006. ATM promotes apoptosis and suppresses tumorigenesis in response to Myc. *Proc Natl Acad Sci U S A,* 103**,** 1446-51.

QUELLE, D. E., ZINDY, F., ASHMUN, R. A. & SHERR, C. J. 1995. Alternative reading frames of the INK4a tumor suppressor gene encode two unrelated proteins capable of inducing cell cycle arrest. *Cell,* 83**,** 993-1000.

QUIN, J., CHAN, K. T., DEVLIN, J. R., CAMERON, D. P., DIESCH, J., CULLINANE, C., AHERN, J., KHOT, A., HEIN, N., GEORGE, A. J., HANNAN, K. M., POORTINGA, G., SHEPPARD, K. E., KHANNA, K. K., JOHNSTONE, R. W., DRYGIN, D., MCARTHUR, G. A., PEARSON, R. B., SANIJ, E. & HANNAN, R. D. 2016. Inhibition of RNA polymerase I transcription initiation by CX-5461 activates non-canonical ATM/ATR signaling. *Oncotarget,* 7**,** 49800-49818.

QUIN, J. E., DEVLIN, J. R., CAMERON, D., HANNAN, K. M., PEARSON, R. B. & HANNAN, R. D. 2014. Targeting the nucleolus for cancer intervention. *Biochim Biophys Acta,* 1842**,** 802-16.

QUINN, B. A., DASH, R., AZAB, B., SARKAR, S., DAS, S. K., KUMAR, S., OYESANYA, R. A., DASGUPTA, S., DENT, P., GRANT, S., RAHMANI, M., CURIEL, D. T., DMITRIEV, I., HEDVAT, M., WEI, J., WU, B., STEBBINS, J. L., REED, J. C., PELLECCHIA, M., SARKAR, D. & FISHER, P. B. 2011. Targeting Mcl-1 for the therapy of cancer. *Expert Opin Investig Drugs,* 20**,** 1397-411.

R, S. S. & EASTMAN, A. 2016. BCL2 Inhibitors as Anticancer Drugs: A Plethora of Misleading BH3 Mimetics. *Mol Cancer Ther,* 15**,** 2011-7.

RAMSEY, H. E., FISCHER, M. A., LEE, T., GORSKA, A. E., ARRATE, M. P., FULLER, L., BOYD, K. L., STRICKLAND, S. A., SENSINTAFFAR, J., HOGDAL, L. J., AYERS, G. D., OLEJNICZAK, E. T., FESIK, S. W. & SAVONA, M. R. 2018. A Novel MCL1 Inhibitor Combined with Venetoclax Rescues Venetoclax-Resistant Acute Myelogenous Leukemia. *Cancer Discov,* 8**,** 1566-1581.

REAGAN-SHAW, S., NIHAL, M. & AHMAD, N. 2008. Dose translation from animal to human studies revisited. *FASEB J,* 22**,** 659-61.

REBELLO, R. J., KUSNADI, E., CAMERON, D. P., PEARSON, H. B., LESMANA, A., DEVLIN, J. R., DRYGIN, D., CLARK, A. K., PORTER, L., PEDERSEN, J., SANDHU, S., RISBRIDGER, G. P., PEARSON, R. B., HANNAN, R. D. & FURIC, L. 2016. The Dual Inhibition of RNA Pol I Transcription and PIM Kinase as a New Therapeutic Approach to Treat Advanced Prostate Cancer. *Clin Cancer Res,* 22**,** 5539-5552.

RECHSTEINER, M. & ROGERS, S. W. 1996. PEST sequences and regulation by proteolysis. *Trends Biochem Sci,* 21**,** 267-71.

REN, H., KOO, J., GUAN, B., YUE, P., DENG, X., CHEN, M., KHURI, F. R. & SUN, S. Y. 2013. The E3 ubiquitin ligases beta-TrCP and FBXW7 cooperatively mediates GSK3-dependent Mcl-1 degradation induced by the Akt inhibitor API-1, resulting in apoptosis. *Mol Cancer,* 12**,** 146.

REYA, T., DUNCAN, A. W., AILLES, L., DOMEN, J., SCHERER, D. C., WILLERT, K., HINTZ, L., NUSSE, R. & WEISSMAN, I. L. 2003. A role for Wnt signalling in self-renewal of haematopoietic stem cells. *Nature,* 423**,** 409-14.

RHODES, D. & LIPPS, H. J. 2015. G-quadruplexes and their regulatory roles in biology. *Nucleic Acids Res,* 43**,** 8627-37.

RICHTER-LARREA, J. A., ROBLES, E. F., FRESQUET, V., BELTRAN, E., RULLAN, A. J., AGIRRE, X., CALASANZ, M. J., PANIZO, C., RICHTER, J. A., HERNANDEZ, J. M., ROMAN-GOMEZ, J., PROSPER, F. & MARTINEZ-CLIMENT, J. A. 2010. Reversion of epigenetically mediated BIM silencing overcomes chemoresistance in Burkitt lymphoma. *Blood,* 116**,** 2531-42.

RILEY, T., SONTAG, E., CHEN, P. & LEVINE, A. 2008. Transcriptional control of human p53-regulated genes. *Nat Rev Mol Cell Biol,* 9**,** 402-12.

RINKENBERGER, J. L., HORNING, S., KLOCKE, B., ROTH, K. & KORSMEYER, S. J. 2000. Mcl-1 deficiency results in peri-implantation embryonic lethality. *Genes Dev,* 14**,** 23-7.

ROBERTS, A. W., DAVIDS, M. S., PAGEL, J. M., KAHL, B. S., PUVVADA, S. D., GERECITANO, J. F., KIPPS, T. J., ANDERSON, M. A., BROWN, J. R., GRESSICK, L., WONG, S., DUNBAR, M., ZHU, M., DESAI, M. B., CERRI, E., HEITNER ENSCHEDE, S., HUMERICKHOUSE, R. A., WIERDA, W. G. & SEYMOUR, J. F. 2016. Targeting BCL2 with Venetoclax in Relapsed Chronic Lymphocytic Leukemia. *N Engl J Med,* 374**,** 311-22.

ROBINSON, H. J. & WAKSMAN, S. A. 1942. Studies on the toxicity of actinomycin. *J Pharmacol Exp Ther* 74**,** 25-32.

RODRIGUEZ, R., MILLER, K. M., FORMENT, J. V., BRADSHAW, C. R., NIKAN, M., BRITTON, S., OELSCHLAEGEL, T., XHEMALCE, B., BALASUBRAMANIAN, S. & JACKSON, S. P. 2012. Small-molecule-induced DNA damage identifies alternative DNA structures in human genes. *Nat Chem Biol,* 8**,** 301-10.

ROLLIG, C., SERVE, H., HUTTMANN, A., NOPPENEY, R., MULLER-TIDOW, C., KRUG, U., BALDUS, C. D., BRANDTS, C. H., KUNZMANN, V., EINSELE, H., KRAMER, A., SCHAFER-ECKART, K., NEUBAUER, A., BURCHERT, A., GIAGOUNIDIS, A., KRAUSE, S. W., MACKENSEN, A., AULITZKY, W., HERBST, R., HANEL, M., KIANI, A., FRICKHOFEN, N., KULLMER, J., KAISER, U., LINK, H., GEER, T., REICHLE, A., JUNGHANSS, C., REPP, R., HEITS, F., DURK, H., HASE, J., KLUT, I. M., ILLMER, T., BORNHAUSER, M., SCHAICH, M., PARMENTIER, S., GORNER, M., THIEDE, C., VON BONIN, M., SCHETELIG, J., KRAMER, M., BERDEL, W. E., EHNINGER, G. & STUDY ALLIANCE, L. 2015. Addition of sorafenib versus placebo to standard therapy in patients aged 60 years or younger with newly diagnosed acute myeloid leukaemia (SORAML): a multicentre, phase 2, randomised controlled trial. *Lancet Oncol,* 16**,** 1691-9.

ROOS, W. P. & KAINA, B. 2006. DNA damage-induced cell death by apoptosis. *Trends Mol Med,* 12**,** 440-50.

ROSENWALD, I. B., RHOADS, D. B., CALLANAN, L. D., ISSELBACHER, K. J. & SCHMIDT, E. V. 1993. Increased expression of eukaryotic translation initiation factors eIF-4E and eIF-2 alpha in response to growth induction by c-myc. *Proc Natl Acad Sci U S A,* 90**,** 6175-8.

ROSS, W. E. & BRADLEY, M. O. 1981. DNA double-stranded breaks in mammalian cells after exposure to intercalating agents. *Biochim Biophys Acta,* 654**,** 129-34.

RUBBI, C. P. & MILNER, J. 2003. Disruption of the nucleolus mediates stabilization of p53 in response to DNA damage and other stresses. *EMBO J,* 22**,** 6068-77.

RUGGERO, D. 2013. Translational control in cancer etiology. *Cold Spring Harb Perspect Biol,* 5.

RUGGERO, D. & PANDOLFI, P. P. 2003. Does the ribosome translate cancer? *Nat Rev Cancer,* 3**,** 179-92.

RUSSELL, J. & ZOMERDIJK, J. C. 2005. RNA-polymerase-I-directed rDNA transcription, life and works. *Trends Biochem Sci,* 30**,** 87-96.

SABO, A., KRESS, T. R., PELIZZOLA, M., DE PRETIS, S., GORSKI, M. M., TESI, A., MORELLI, M. J., BORA, P., DONI, M., VERRECCHIA, A., TONELLI, C., FAGA, G., BIANCHI, V., RONCHI, A., LOW, D., MULLER, H., GUCCIONE, E., CAMPANER, S. & AMATI, B. 2014. Selective transcriptional regulation by Myc in cellular growth control and lymphomagenesis. *Nature,* 511**,** 488-492.

SAFT, L., KARIMI, M., GHADERI, M., MATOLCSY, A., MUFTI, G. J., KULASEKARARAJ, A., GOHRING, G., GIAGOUNIDIS, A., SELLESLAG, D., MUUS, P., SANZ, G., MITTELMAN, M., BOWEN, D., PORWIT, A., FU, T., BACKSTROM, J., FENAUX, P., MACBETH, K. J. & HELLSTROM-LINDBERG, E. 2014. p53 protein expression independently predicts outcome in patients with lower-risk myelodysplastic syndromes with del(5q). *Haematologica,* 99**,** 1041-9.

SALGHETTI, S. E., KIM, S. Y. & TANSEY, W. P. 1999. Destruction of Myc by ubiquitin-mediated proteolysis: cancer-associated and transforming mutations stabilize Myc. *EMBO J,* 18**,** 717-26.

SALOMONI, P. & PANDOLFI, P. P. 2002. The role of PML in tumor suppression. *Cell,* 108**,** 165-70.

SAMPATH, P., PRITCHARD, D. K., PABON, L., REINECKE, H., SCHWARTZ, S. M., MORRIS, D. R. & MURRY, C. E. 2008. A hierarchical network controls protein translation during murine embryonic stem cell self-renewal and differentiation. *Cell Stem Cell,* 2**,** 448-60.

SANCHEZ, C. G., TEIXEIRA, F. K., CZECH, B., PREALL, J. B., ZAMPARINI, A. L., SEIFERT, J. R., MALONE, C. D., HANNON, G. J. & LEHMANN, R. 2016. Regulation of Ribosome Biogenesis and Protein Synthesis Controls Germline Stem Cell Differentiation. *Cell Stem Cell,* 18**,** 276-90.

SANT, M., ALLEMANI, C., TEREANU, C., DE ANGELIS, R., CAPOCACCIA, R., VISSER, O., MARCOS-GRAGERA, R., MAYNADIE, M., SIMONETTI, A., LUTZ, J. M., BERRINO, F. & GROUP, H. W. 2010. Incidence of hematologic malignancies in Europe by morphologic subtype: results of the HAEMACARE project. *Blood,* 116**,** 3724-34.

SASAKI, M., KAWAHARA, K., NISHIO, M., MIMORI, K., KOGO, R., HAMADA, K., ITOH, B., WANG, J., KOMATSU, Y., YANG, Y. R., HIKASA, H., HORIE, Y., YAMASHITA, T., KAMIJO, T., ZHANG, Y., ZHU, Y., PRIVES, C., NAKANO, T., MAK, T. W., SASAKI, T., MAEHAMA, T., MORI, M. & SUZUKI, A. 2011. Regulation of the MDM2-P53 pathway and tumor growth by PICT1 via nucleolar RPL11. *Nat Med,* 17**,** 944-51.

SCANDURRA, M., ROSSI, D., DEAMBROGI, C., RANCOITA, P. M., CHIGRINOVA, E., MIAN, M., CERRI, M., RASI, S., SOZZI, E., FORCONI, F., PONZONI, M., MORENO, S. M., PIRIS, M. A., INGHIRAMI, G., ZUCCA, E., GATTEI, V., RINALDI, A., KWEE, I., GAIDANO, G. & BERTONI, F. 2010. Genomic profiling of Richter's syndrome: recurrent lesions and differences with de novo diffuse large B-cell lymphomas. *Hematol Oncol,* 28**,** 62-7.

SCHAEFER, E., COLLET, C., GENEVIEVE, D., VINCENT, M., LOHMANN, D. R., SANCHEZ, E., BOLENDER, C., ELIOT, M. M., NURNBERG, G., PASSOS-BUENO, M. R., WIECZOREK, D., VAN MALDERGEM, L. & DORAY, B. 2014. Autosomal recessive POLR1D mutation with decrease of TCOF1 mRNA is responsible for Treacher Collins syndrome. *Genet Med,* 16**,** 720-4.

SCHEPERS, K., PIETRAS, E. M., REYNAUD, D., FLACH, J., BINNEWIES, M., GARG, T., WAGERS, A. J., HSIAO, E. C. & PASSEGUE, E. 2013. Myeloproliferative neoplasia remodels the endosteal bone marrow niche into a self-reinforcing leukemic niche. *Cell Stem Cell,* 13**,** 285-99.

SCHIMMER, A. D., O'BRIEN, S., KANTARJIAN, H., BRANDWEIN, J., CHESON, B. D., MINDEN, M. D., YEE, K., RAVANDI, F., GILES, F., SCHUH, A., GUPTA, V., ANDREEFF, M., KOLLER, C., CHANG, H., KAMEL-REID, S., BERGER, M., VIALLET, J. & BORTHAKUR, G. 2008. A phase I study of the pan bcl-2 family inhibitor obatoclax mesylate in patients with advanced hematologic malignancies. *Clin Cancer Res,* 14**,** 8295-301.

SCHIMMER, A. D., RAZA, A., CARTER, T. H., CLAXTON, D., ERBA, H., DEANGELO, D. J., TALLMAN, M. S., GOARD, C. & BORTHAKUR, G. 2014. A multicenter phase I/II study of obatoclax mesylate administered as a 3- or 24-hour infusion in older patients with previously untreated acute myeloid leukemia. *PLoS One,* 9**,** e108694.

SCHLOSSER, I., HOLZEL, M., MURNSEER, M., BURTSCHER, H., WEIDLE, U. H. & EICK, D. 2003. A role for c-Myc in the regulation of ribosomal RNA processing. *Nucleic Acids Res,* 31**,** 6148-56.

SCHLOTT, T., REIMER, S., JAHNS, A., OHLENBUSCH, A., RUSCHENBURG, I., NAGEL, H. & DROESE, M. 1997. Point mutations and nucleotide insertions in the MDM2 zinc finger structure of human tumours. *J Pathol,* 182**,** 54-61.

SCHMIDT, E. V. 1999. The role of c-myc in cellular growth control. *Oncogene,* 18**,** 2988-96.

SCHMIDT, E. V. 2004. The role of c-myc in regulation of translation initiation. *Oncogene,* 23**,** 3217-21.

SCHMIDT, E. V., PATTENGALE, P. K., WEIR, L. & LEDER, P. 1988. Transgenic mice bearing the human c-myc gene activated by an immunoglobulin enhancer: a pre-B-cell lymphoma model. *Proc Natl Acad Sci U S A,* 85**,** 6047-51.

SCHMITZ, R., YOUNG, R. M., CERIBELLI, M., JHAVAR, S., XIAO, W., ZHANG, M., WRIGHT, G., SHAFFER, A. L., HODSON, D. J., BURAS, E., LIU, X., POWELL, J., YANG, Y., XU, W., ZHAO, H., KOHLHAMMER, H., ROSENWALD, A., KLUIN, P., MULLER-HERMELINK, H. K., OTT, G., GASCOYNE, R. D., CONNORS, J. M., RIMSZA, L. M., CAMPO, E., JAFFE, E. S., DELABIE, J., SMELAND, E. B., OGWANG, M. D., REYNOLDS, S. J., FISHER, R. I., BRAZIEL, R. M., TUBBS, R. R., COOK, J. R., WEISENBURGER, D. D., CHAN, W. C., PITTALUGA, S., WILSON, W., WALDMANN, T. A., ROWE, M., MBULAITEYE, S. M., RICKINSON, A. B. & STAUDT, L. M. 2012. Burkitt lymphoma pathogenesis and therapeutic targets from structural and functional genomics. *Nature,* 490**,** 116-20.

SCHNEIDER, R. K., SCHENONE, M., FERREIRA, M. V., KRAMANN, R., JOYCE, C. E., HARTIGAN, C., BEIER, F., BRUMMENDORF, T. H., GERMING, U., PLATZBECKER, U., BUSCHE, G., KNUCHEL, R., CHEN, M. C., WATERS, C. S., CHEN, E., CHU, L. P., NOVINA, C. D., LINDSLEY, R. C., CARR, S. A. & EBERT, B. L. 2016. Rps14 haploinsufficiency causes a block in erythroid differentiation mediated by S100A8 and S100A9. *Nat Med,* 22**,** 288-97.

SCHULER, M. & GREEN, D. R. 2001. Mechanisms of p53-dependent apoptosis. *Biochem Soc Trans,* 29**,** 684-8.

SCHULLER, A. P. & GREEN, R. 2018. Roadblocks and resolutions in eukaryotic translation. *Nat Rev Mol Cell Biol,* 19**,** 526-541.

SCHWICKART, M., HUANG, X., LILL, J. R., LIU, J., FERRANDO, R., FRENCH, D. M., MAECKER, H., O'ROURKE, K., BAZAN, F., EASTHAM-ANDERSON, J., YUE, P., DORNAN, D., HUANG, D. C. & DIXIT, V. M. 2010. Deubiquitinase USP9X stabilizes MCL1 and promotes tumour cell survival. *Nature,* 463**,** 103-7.

SEARS, R., OHTANI, K. & NEVINS, J. R. 1997. Identification of positively and negatively acting elements regulating expression of the E2F2 gene in response to cell growth signals. *Mol Cell Biol,* 17**,** 5227-35.

SEARS, R. C. 2004. The life cycle of C-myc: from synthesis to degradation. *Cell Cycle,* 3**,** 1133-7.

SENICHKIN, V. V., STRELETSKAIA, A. Y., ZHIVOTOVSKY, B. & KOPEINA, G. S. 2019. Molecular Comprehension of Mcl-1: From Gene Structure to Cancer Therapy. *Trends Cell Biol,* 29**,** 549-562.

SEOANE, J., LE, H. V. & MASSAGUE, J. 2002. Myc suppression of the p21(Cip1) Cdk inhibitor influences the outcome of the p53 response to DNA damage. *Nature,* 419**,** 729-34.

SERRANO, M., LIN, A. W., MCCURRACH, M. E., BEACH, D. & LOWE, S. W. 1997. Oncogenic ras provokes premature cell senescence associated with accumulation of p53 and p16INK4a. *Cell,* 88**,** 593-602.

SHAH, P., DING, Y., NIEMCZYK, M., KUDLA, G. & PLOTKIN, J. B. 2013. Rate-limiting steps in yeast protein translation. *Cell,* 153**,** 1589-601.

SHARPLESS, N. E. 2005. INK4a/ARF: a multifunctional tumor suppressor locus. *Mutat Res,* 576**,** 22-38.

SHATSKY, I. N., TERENIN, I. M., SMIRNOVA, V. V. & ANDREEV, D. E. 2018. Cap-Independent Translation: What's in a Name? *Trends Biochem Sci,* 43**,** 882-895.

SHI, Z., FUJII, K., KOVARY, K. M., GENUTH, N. R., ROST, H. L., TERUEL, M. N. & BARNA, M. 2017. Heterogeneous Ribosomes Preferentially Translate Distinct Subpools of mRNAs Genome-wide. *Mol Cell,* 67**,** 71-83 e7.

SHILOH, Y. 2003. ATM and related protein kinases: safeguarding genome integrity. *Nat Rev Cancer,* 3**,** 155-68.

SHIUE, C. N., BERKSON, R. G. & WRIGHT, A. P. 2009. c-Myc induces changes in higher order rDNA structure on stimulation of quiescent cells. *Oncogene,* 28**,** 1833-42.

SIBONI, R. B., NAKAMORI, M., WAGNER, S. D., STRUCK, A. J., COONROD, L. A., HARRIOTT, S. A., CASS, D. M., TANNER, M. K. & BERGLUND, J. A. 2015. Actinomycin D Specifically Reduces Expanded CUG Repeat RNA in Myotonic Dystrophy Models. *Cell Rep,* 13**,** 2386-2394.

SIDDIQUI-JAIN, A., GRAND, C. L., BEARSS, D. J. & HURLEY, L. H. 2002. Direct evidence for a G-quadruplex in a promoter region and its targeting with a small molecule to repress c-MYC transcription. *Proc Natl Acad Sci U S A,* 99**,** 11593-8.

SIDMAN, C. L., DENIAL, T. M., MARSHALL, J. D. & ROTHS, J. B. 1993. Multiple mechanisms of tumorigenesis in E mu-myc transgenic mice. *Cancer Res,* 53**,** 1665-9.

SIEGHART, W., LOSERT, D., STROMMER, S., CEJKA, D., SCHMID, K., RASOUL-ROCKENSCHAUB, S., BODINGBAUER, M., CREVENNA, R., MONIA, B. P., PECK-RADOSAVLJEVIC, M. & WACHECK, V. 2006. Mcl-1 overexpression in hepatocellular carcinoma: a potential target for antisense therapy. *J Hepatol,* 44**,** 151-7.

SIGNER, R. A., MAGEE, J. A., SALIC, A. & MORRISON, S. J. 2014. Haematopoietic stem cells require a highly regulated protein synthesis rate. *Nature,* 509**,** 49-54.

SILVA, S., HOMOLKA, D. & PILLAI, R. S. 2017. Characterization of the mammalian RNA exonuclease 5/NEF-sp as a testis-specific nuclear 3' --> 5' exoribonuclease. *RNA,* 23**,** 1385-1392.

SINGH, S. A., GOLDBERG, T. A., HENSON, A. L., HUSAIN-KRAUTTER, S., NIHRANE, A., BLANC, L., ELLIS, S. R., LIPTON, J. M. & LIU, J. M. 2014. p53-Independent cell cycle and erythroid differentiation defects in murine embryonic stem cells haploinsufficient for Diamond Blackfan anemia-proteins: RPS19 versus RPL5. *PLoS One,* 9**,** e89098.

SLOAN, K. E., BOHNSACK, M. T. & WATKINS, N. J. 2013. The 5S RNP couples p53 homeostasis to ribosome biogenesis and nucleolar stress. *Cell Rep,* 5**,** 237-47.

SLOSS, O., TOPHAM, C., DIEZ, M. & TAYLOR, S. 2016. Mcl-1 dynamics influence mitotic slippage and death in mitosis. *Oncotarget,* 7**,** 5176-92.

SONENBERG, N. 2008. eIF4E, the mRNA cap-binding protein: from basic discovery to translational research. *Biochem Cell Biol,* 86**,** 178-83.

SONENBERG, N. & HINNEBUSCH, A. G. 2009. Regulation of translation initiation in eukaryotes: mechanisms and biological targets. *Cell,* 136**,** 731-45.

SONG, L., COPPOLA, D., LIVINGSTON, S., CRESS, D. & HAURA, E. B. 2005. Mcl-1 regulates survival and sensitivity to diverse apoptotic stimuli in human non-small cell lung cancer cells. *Cancer Biol Ther,* 4**,** 267-76.

SONG, T., WANG, Z., JI, F., FENG, Y., FAN, Y., CHAI, G., LI, X., LI, Z. & ZHANG, Z. 2016. Deactivation of Mcl-1 by Dual-Function Small-Molecule Inhibitors Targeting the Bcl-2 Homology 3 Domain and Facilitating Mcl-1 Ubiquitination. *Angew Chem Int Ed Engl,* 55**,** 14250-14256.

SOROKIN, A. V., KIM, E. R. & OVCHINNIKOV, L. P. 2009. Proteasome system of protein degradation and processing. *Biochemistry (Mosc),* 74**,** 1411-42.

SOUERS, A. J., LEVERSON, J. D., BOGHAERT, E. R., ACKLER, S. L., CATRON, N. D., CHEN, J., DAYTON, B. D., DING, H., ENSCHEDE, S. H., FAIRBROTHER, W. J., HUANG, D. C., HYMOWITZ, S. G., JIN, S., KHAW, S. L., KOVAR, P. J., LAM, L. T., LEE, J., MAECKER, H. L., MARSH, K. C., MASON, K. D., MITTEN, M. J., NIMMER, P. M., OLEKSIJEW, A., PARK, C. H., PARK, C. M., PHILLIPS, D. C., ROBERTS, A. W., SAMPATH, D., SEYMOUR, J. F., SMITH, M. L., SULLIVAN, G. M., TAHIR, S. K., TSE, C., WENDT, M. D., XIAO, Y., XUE, J. C., ZHANG, H., HUMERICKHOUSE, R. A., ROSENBERG, S. H. & ELMORE, S. W. 2013. ABT-199, a potent and selective BCL-2 inhibitor, achieves antitumor activity while sparing platelets. *Nat Med,* 19**,** 202-8.

SPEIDEL, D. 2010. Transcription-independent p53 apoptosis: an alternative route to death. *Trends Cell Biol,* 20**,** 14-24.

SPENCER, A., ROSENBERG, A. S., JAKUBOWIAK, A., RAJE, N., CHATTERJEE, M., TRUDEL, S., BAHLIS, N. J., SIEGEL, D. S., WILOP, S., HARRISON, S. J., NAGAKRISHNA, M., DHURIA, S., HINDOYAN, A., MCIVER, Z., HENARY, H., MORROW, P. K. & ROBERTS, A. 2019. A Phase 1, First-in-Human Study of AMG 176, a Selective MCL-1 Inhibitor, in Patients With Relapsed or Refractory Multiple Myeloma [Abstract]. *17th IMW,* 1**,** 81-83.

SPRIGGS, K. A., STONELEY, M., BUSHELL, M. & WILLIS, A. E. 2008. Re-programming of translation following cell stress allows IRES-mediated translation to predominate. *Biol Cell,* 100**,** 27-38.

SRINIVASAN, S. V., DOMINGUEZ-SOLA, D., WANG, L. C., HYRIEN, O. & GAUTIER, J. 2013. Cdc45 is a critical effector of myc-dependent DNA replication stress. *Cell Rep,* 3**,** 1629-39.

STEFFEN, K. K., MCCORMICK, M. A., PHAM, K. M., MACKAY, V. L., DELANEY, J. R., MURAKAMI, C. J., KAEBERLEIN, M. & KENNEDY, B. K. 2012. Ribosome deficiency protects against ER stress in Saccharomyces cerevisiae. *Genetics,* 191**,** 107-18.

STENGEL, A., KERN, W., HAFERLACH, T., MEGGENDORFER, M., FASAN, A. & HAFERLACH, C. 2017. The impact of TP53 mutations and TP53 deletions on survival varies between AML, ALL, MDS and CLL: an analysis of 3307 cases. *Leukemia,* 31**,** 705-711.

STEWART, D. P., KOSS, B., BATHINA, M., PERCIAVALLE, R. M., BISANZ, K. & OPFERMAN, J. T. 2010. Ubiquitin-independent degradation of antiapoptotic MCL-1. *Mol Cell Biol,* 30**,** 3099-110.

STRASSER, A. 2005. The role of BH3-only proteins in the immune system. *Nat Rev Immunol,* 5**,** 189-200.

STRASSER, A., HARRIS, A. W., BATH, M. L. & CORY, S. 1990. Novel primitive lymphoid tumours induced in transgenic mice by cooperation between myc and bcl-2. *Nature,* 348**,** 331-3.

STRUNK, B. S. & KARBSTEIN, K. 2009. Powering through ribosome assembly. *RNA,* 15**,** 2083-104.

STRUNK, B. S., NOVAK, M. N., YOUNG, C. L. & KARBSTEIN, K. 2012. A translation-like cycle is a quality control checkpoint for maturing 40S ribosome subunits. *Cell,* 150**,** 111-21.

STULTS, D. M., KILLEN, M. W., PIERCE, H. H. & PIERCE, A. J. 2008. Genomic architecture and inheritance of human ribosomal RNA gene clusters. *Genome Res,* 18**,** 13-8.

SUBRAMANIAM, D., NATARAJAN, G., RAMALINGAM, S., RAMACHANDRAN, I., MAY, R., QUEIMADO, L., HOUCHEN, C. W. & ANANT, S. 2008. Translation inhibition during cell cycle arrest and apoptosis: Mcl-1 is a novel target for RNA binding protein CUGBP2. *Am J Physiol Gastrointest Liver Physiol,* 294**,** G1025-32.

SUENAGA, Y., KANEKO, Y., MATSUMOTO, D., HOSSAIN, M. S., OZAKI, T. & NAKAGAWARA, A. 2009. Positive auto-regulation of MYCN in human neuroblastoma. *Biochem Biophys Res Commun,* 390**,** 21-6.

SULIC, S., PANIC, L., BARKIC, M., MERCEP, M., UZELAC, M. & VOLAREVIC, S. 2005. Inactivation of S6 ribosomal protein gene in T lymphocytes activates a p53-dependent checkpoint response. *Genes Dev,* 19**,** 3070-82.

SULIMA, S. O., KAMPEN, K. R. & DE KEERSMAECKER, K. 2019. Cancer Biogenesis in Ribosomopathies. *Cells,* 8.

SULLIVAN, K. D., GALBRAITH, M. D., ANDRYSIK, Z. & ESPINOSA, J. M. 2018. Mechanisms of transcriptional regulation by p53. *Cell Death Differ,* 25**,** 133-143.

SUN, H., KAPURIA, V., PETERSON, L. F., FANG, D., BORNMANN, W. G., BARTHOLOMEUSZ, G., TALPAZ, M. & DONATO, N. J. 2011. Bcr-Abl ubiquitination and Usp9x inhibition block kinase signaling and promote CML cell apoptosis. *Blood,* 117**,** 3151-62.

SUNG, M. K., PORRAS-YAKUSHI, T. R., REITSMA, J. M., HUBER, F. M., SWEREDOSKI, M. J., HOELZ, A., HESS, S. & DESHAIES, R. J. 2016. A conserved quality-control pathway that mediates degradation of unassembled ribosomal proteins. *Elife,* 5.

SWERDLOW, S. H., CAMPO, E., HARRIS, N. L., JAFFE, E., PILERI, S., STEIN, H., THIELE, J. & VARDIMAN, J. 2008. World Health Organization classification of tumours of haematopoietic and lymphoid tissues. Lyon: IARC press.

SZYMANSKI, M., BARCISZEWSKA, M. Z., ERDMANN, V. A. & BARCISZEWSKI, J. 2003. 5 S rRNA: structure and interactions. *Biochem J,* 371**,** 641-51.

TAFFOREAU, L., ZORBAS, C., LANGHENDRIES, J. L., MULLINEUX, S. T., STAMATOPOULOU, V., MULLIER, R., WACHEUL, L. & LAFONTAINE, D. L. 2013. The complexity of human ribosome biogenesis revealed by systematic nucleolar screening of Pre-rRNA processing factors. *Mol Cell,* 51**,** 539-51.

TAGAWA, H., KARNAN, S., SUZUKI, R., MATSUO, K., ZHANG, X., OTA, A., MORISHIMA, Y., NAKAMURA, S. & SETO, M. 2005. Genome-wide array-based CGH for mantle cell lymphoma: identification of homozygous deletions of the proapoptotic gene BIM. *Oncogene,* 24**,** 1348-58.

TAKAHASHI, K., TANABE, K., OHNUKI, M., NARITA, M., ICHISAKA, T., TOMODA, K. & YAMANAKA, S. 2007. Induction of pluripotent stem cells from adult human fibroblasts by defined factors. *Cell,* 131**,** 861-72.

TAKAHASHI, K. & YAMANAKA, S. 2006. Induction of pluripotent stem cells from mouse embryonic and adult fibroblast cultures by defined factors. *Cell,* 126**,** 663-76.

TAUB, R., KIRSCH, I., MORTON, C., LENOIR, G., SWAN, D., TRONICK, S., AARONSON, S. & LEDER, P. 1982. Translocation of the c-myc gene into the immunoglobulin heavy chain locus in human Burkitt lymphoma and murine plasmacytoma cells. *Proc Natl Acad Sci U S A,* 79**,** 7837-41.

TAYLOR, M. M. & STORCK, R. 1964. Uniqueness of Bacterial Ribosomes. *Proc Natl Acad Sci U S A,* 52**,** 958-65.

TENG, T., MERCER, C. A., HEXLEY, P., THOMAS, G. & FUMAGALLI, S. 2013. Loss of tumor suppressor RPL5/RPL11 does not induce cell cycle arrest but impedes proliferation due to reduced ribosome content and translation capacity. *Mol Cell Biol,* 33**,** 4660-71.

THOMAS, D. A., FADERL, S., O'BRIEN, S., BUESO-RAMOS, C., CORTES, J., GARCIA-MANERO, G., GILES, F. J., VERSTOVSEK, S., WIERDA, W. G., PIERCE, S. A., SHAN, J., BRANDT, M., HAGEMEISTER, F. B., KEATING, M. J., CABANILLAS, F. & KANTARJIAN, H. 2006. Chemoimmunotherapy with hyper-CVAD plus rituximab for the treatment of adult Burkitt and Burkitt-type lymphoma or acute lymphoblastic leukemia. *Cancer,* 106**,** 1569-80.

THOMAS, L. W., LAM, C. & EDWARDS, S. W. 2010. Mcl-1; the molecular regulation of protein function. *FEBS Lett,* 584**,** 2981-9.

THOREEN, C. C., CHANTRANUPONG, L., KEYS, H. R., WANG, T., GRAY, N. S. & SABATINI, D. M. 2012. A unifying model for mTORC1-mediated regulation of mRNA translation. *Nature,* 485**,** 109-13.

TISATO, V., VOLTAN, R., GONELLI, A., SECCHIERO, P. & ZAULI, G. 2017. MDM2/X inhibitors under clinical evaluation: perspectives for the management of hematological malignancies and pediatric cancer. *J Hematol Oncol,* 10**,** 133.

TONG, W. G., CHEN, R., PLUNKETT, W., SIEGEL, D., SINHA, R., HARVEY, R. D., BADROS, A. Z., POPPLEWELL, L., COUTRE, S., FOX, J. A., MAHADOCON, K., CHEN, T., KEGLEY, P., HOCH, U. & WIERDA, W. G. 2010. Phase I and pharmacologic study of SNS-032, a potent and selective Cdk2, 7, and 9 inhibitor, in patients with advanced chronic lymphocytic leukemia and multiple myeloma. *J Clin Oncol,* 28**,** 3015-22.

TORIHARA, H., UECHI, T., CHAKRABORTY, A., SHINYA, M., SAKAI, N. & KENMOCHI, N. 2011. Erythropoiesis failure due to RPS19 deficiency is independent of an activated Tp53 response in a zebrafish model of Diamond-Blackfan anaemia. *Br J Haematol,* 152**,** 648-54.

TRAJKOVSKI, M., DA SILVA, M. W. & PLAVEC, J. 2012. Unique structural features of interconverting monomeric and dimeric G-quadruplexes adopted by a sequence from the intron of the N-myc gene. *J Am Chem Soc,* 134**,** 4132-41.

TRON, A. E., BELMONTE, M. A., ADAM, A., AQUILA, B. M., BOISE, L. H., CHIARPARIN, E., CIDADO, J., EMBREY, K. J., GANGL, E., GIBBONS, F. D., GREGORY, G. P., HARGREAVES, D., HENDRICKS, J. A., JOHANNES, J. W., JOHNSTONE, R. W., KAZMIRSKI, S. L., KETTLE, J. G., LAMB, M. L., MATULIS, S. M., NOOKA, A. K., PACKER, M. J., PENG, B., RAWLINS, P. B., ROBBINS, D. W., SCHULLER, A. G., SU, N., YANG, W., YE, Q., ZHENG, X., SECRIST, J. P., CLARK, E. A., WILSON, D. M., FAWELL, S. E. & HIRD, A. W. 2018. Discovery of Mcl-1-specific inhibitor AZD5991 and preclinical activity in multiple myeloma and acute myeloid leukemia. *Nat Commun,* 9**,** 5341.

TRUDEL, S., LI, Z. H., RAUW, J., TIEDEMANN, R. E., WEN, X. Y. & STEWART, A. K. 2007. Preclinical studies of the pan-Bcl inhibitor obatoclax (GX015-070) in multiple myeloma. *Blood,* 109**,** 5430-8.

TRUITT, M. L. & RUGGERO, D. 2016. New frontiers in translational control of the cancer genome. *Nat Rev Cancer,* 16**,** 288-304.

TSE, C., SHOEMAKER, A. R., ADICKES, J., ANDERSON, M. G., CHEN, J., JIN, S., JOHNSON, E. F., MARSH, K. C., MITTEN, M. J., NIMMER, P., ROBERTS, L., TAHIR, S. K., XIAO, Y., YANG, X., ZHANG, H., FESIK, S., ROSENBERG, S. H. & ELMORE, S. W. 2008. ABT-263: a potent and orally bioavailable Bcl-2 family inhibitor. *Cancer Res,* 68**,** 3421-8.

UECHI, T., TANAKA, T. & KENMOCHI, N. 2001. A complete map of the human ribosomal protein genes: assignment of 80 genes to the cytogenetic map and implications for human disorders. *Genomics,* 72**,** 223-30.

VAFA, O., WADE, M., KERN, S., BEECHE, M., PANDITA, T. K., HAMPTON, G. M. & WAHL, G. M. 2002. c-Myc can induce DNA damage, increase reactive oxygen species, and mitigate p53 function: a mechanism for oncogene-induced genetic instability. *Mol Cell,* 9**,** 1031-44.

VAN DE WETERING, M., SANCHO, E., VERWEIJ, C., DE LAU, W., OVING, I., HURLSTONE, A., VAN DER HORN, K., BATLLE, E., COUDREUSE, D., HARAMIS, A. P., TJON-PON-FONG, M., MOERER, P., VAN DEN BORN, M., SOETE, G., PALS, S., EILERS, M., MEDEMA, R. & CLEVERS, H. 2002. The beta-catenin/TCF-4 complex imposes a crypt progenitor phenotype on colorectal cancer cells. *Cell,* 111**,** 241-50.

VAN DELFT, M. F. & HUANG, D. C. 2006. How the Bcl-2 family of proteins interact to regulate apoptosis. *Cell Res,* 16**,** 203-13.

VAN DELFT, M. F., WEI, A. H., MASON, K. D., VANDENBERG, C. J., CHEN, L., CZABOTAR, P. E., WILLIS, S. N., SCOTT, C. L., DAY, C. L., CORY, S., ADAMS, J. M., ROBERTS, A. W. & HUANG, D. C. 2006. The BH3 mimetic ABT-737 targets selective Bcl-2 proteins and efficiently induces apoptosis via Bak/Bax if Mcl-1 is neutralized. *Cancer Cell,* 10**,** 389-99.

VAN RIGGELEN, J., YETIL, A. & FELSHER, D. W. 2010. MYC as a regulator of ribosome biogenesis and protein synthesis. *Nat Rev Cancer,* 10**,** 301-9.

VAN SLUIS, M. & MCSTAY, B. 2015. A localized nucleolar DNA damage response facilitates recruitment of the homology-directed repair machinery independent of cell cycle stage. *Genes Dev,* 29**,** 1151-63.

VASSILEV, L. T., VU, B. T., GRAVES, B., CARVAJAL, D., PODLASKI, F., FILIPOVIC, Z., KONG, N., KAMMLOTT, U., LUKACS, C., KLEIN, C., FOTOUHI, N. & LIU, E. A. 2004. In vivo activation of the p53 pathway by small-molecule antagonists of MDM2. *Science,* 303**,** 844-8.

VERVOORTS, J., LUSCHER-FIRZLAFF, J. & LUSCHER, B. 2006. The ins and outs of MYC regulation by posttranslational mechanisms. *J Biol Chem,* 281**,** 34725-9.

VICK, B., WEBER, A., URBANIK, T., MAASS, T., TEUFEL, A., KRAMMER, P. H., OPFERMAN, J. T., SCHUCHMANN, M., GALLE, P. R. & SCHULZE-BERGKAMEN, H. 2009. Knockout of myeloid cell leukemia-1 induces liver damage and increases apoptosis susceptibility of murine hepatocytes. *Hepatology,* 49**,** 627-36.

VLACHOS, A., ROSENBERG, P. S., ATSIDAFTOS, E., ALTER, B. P. & LIPTON, J. M. 2012. Incidence of neoplasia in Diamond Blackfan anemia: a report from the Diamond Blackfan Anemia Registry. *Blood,* 119**,** 3815-9.

VOLAREVIC, S., STEWART, M. J., LEDERMANN, B., ZILBERMAN, F., TERRACCIANO, L., MONTINI, E., GROMPE, M., KOZMA, S. C. & THOMAS, G. 2000. Proliferation, but not growth, blocked by conditional deletion of 40S ribosomal protein S6. *Science,* 288**,** 2045-7.

VOM BERG, J., VROHLINGS, M., HALLER, S., HAIMOVICI, A., KULIG, P., SLEDZINSKA, A., WELLER, M. & BECHER, B. 2013. Intratumoral IL-12 combined with CTLA-4 blockade elicits T cell-mediated glioma rejection. *J Exp Med,* 210**,** 2803-11.

VON DER LEHR, N., JOHANSSON, S., WU, S., BAHRAM, F., CASTELL, A., CETINKAYA, C., HYDBRING, P., WEIDUNG, I., NAKAYAMA, K., NAKAYAMA, K. I., SODERBERG, O., KERPPOLA, T. K. & LARSSON, L. G. 2003. The F-box protein Skp2 participates in c-Myc proteosomal degradation and acts as a cofactor for c-Myc-regulated transcription. *Mol Cell,* 11**,** 1189-200.

VOUSDEN, K. H. & PRIVES, C. 2009. Blinded by the Light: The Growing Complexity of p53. *Cell,* 137**,** 413-31.

WAKSMAN, S. A. & WOODRUFF, H. B. 1942. Selective Antibiotic Action of Various Substances of Microbial Origin. *J Bacteriol,* 44**,** 373-84.

WALL, M., POORTINGA, G., STANLEY, K. L., LINDEMANN, R. K., BOTS, M., CHAN, C. J., BYWATER, M. J., KINROSS, K. M., ASTLE, M. V., WALDECK, K., HANNAN, K. M., SHORTT, J., SMYTH, M. J., LOWE, S. W., HANNAN, R. D., PEARSON, R. B., JOHNSTONE, R. W. & MCARTHUR, G. A. 2013. The mTORC1 inhibitor everolimus prevents and treats Emu-Myc lymphoma by restoring oncogene-induced senescence. *Cancer Discov,* 3**,** 82-95.

WANG, X., BATHINA, M., LYNCH, J., KOSS, B., CALABRESE, C., FRASE, S., SCHUETZ, J. D., REHG, J. E. & OPFERMAN, J. T. 2013. Deletion of MCL-1 causes lethal cardiac failure and mitochondrial dysfunction. *Genes Dev,* 27**,** 1351-64.

WANG, X. W., ZHAN, Q., COURSEN, J. D., KHAN, M. A., KONTNY, H. U., YU, L., HOLLANDER, M. C., O'CONNOR, P. M., FORNACE, A. J., JR. & HARRIS, C. C. 1999. GADD45 induction of a G2/M cell cycle checkpoint. *Proc Natl Acad Sci U S A,* 96**,** 3706-11.

WARMERDAM, D. O., VAN DEN BERG, J. & MEDEMA, R. H. 2016. Breaks in the 45S rDNA Lead to Recombination-Mediated Loss of Repeats. *Cell Rep,* 14**,** 2519-27.

WARNER, J. R. 1977. In the absence of ribosomal RNA synthesis, the ribosomal proteins of HeLa cells are synthesized normally and degraded rapidly. *J Mol Biol,* 115**,** 315-33.

WARNER, J. R. 1999. The economics of ribosome biosynthesis in yeast. *Trends Biochem Sci,* 24**,** 437-40.

WARNER, J. R. & MCINTOSH, K. B. 2009. How common are extraribosomal functions of ribosomal proteins? *Mol Cell,* 34**,** 3-11.

WARNER, J. R., MITRA, G., SCHWINDINGER, W. F., STUDENY, M. & FRIED, H. M. 1985. Saccharomyces cerevisiae coordinates accumulation of yeast ribosomal proteins by modulating mRNA splicing, translational initiation, and protein turnover. *Mol Cell Biol,* 5**,** 1512-21.

WARR, M. R., ACOCA, S., LIU, Z., GERMAIN, M., WATSON, M., BLANCHETTE, M., WING, S. S. & SHORE, G. C. 2005. BH3-ligand regulates access of MCL-1 to its E3 ligase. *FEBS Lett,* 579**,** 5603-8.

WARR, M. R., MILLS, J. R., NGUYEN, M., LEMAIRE-EWING, S., BAARDSNES, J., SUN, K. L., MALINA, A., YOUNG, J. C., JEYARAJU, D. V., O'CONNOR-MCCOURT, M., PELLEGRINI, L., PELLETIER, J. & SHORE, G. C. 2011. Mitochondrion-dependent N-terminal processing of outer membrane Mcl-1 protein removes an essential Mule/Lasu1 protein-binding site. *J Biol Chem,* 286**,** 25098-107.

WARR, M. R. & SHORE, G. C. 2008. Unique biology of Mcl-1: therapeutic opportunities in cancer. *Curr Mol Med,* 8**,** 138-47.

WARREN, C. F. A., WONG-BROWN, M. W. & BOWDEN, N. A. 2019. BCL-2 family isoforms in apoptosis and cancer. *Cell Death Dis,* 10**,** 177.

WATERS, C. M., LITTLEWOOD, T. D., HANCOCK, D. C., MOORE, J. P. & EVAN, G. I. 1991. c-myc protein expression in untransformed fibroblasts. *Oncogene,* 6**,** 797-805.

WATKINS, N. J. & BOHNSACK, M. T. 2012. The box C/D and H/ACA snoRNPs: key players in the modification, processing and the dynamic folding of ribosomal RNA. *Wiley Interdiscip Rev RNA,* 3**,** 397-414.

WEI, G., MARGOLIN, A. A., HAERY, L., BROWN, E., CUCOLO, L., JULIAN, B., SHEHATA, S., KUNG, A. L., BEROUKHIM, R. & GOLUB, T. R. 2012. Chemical genomics identifies small-molecule MCL1 repressors and BCL-xL as a predictor of MCL1 dependency. *Cancer Cell,* 21**,** 547-62.

WEI, G., TWOMEY, D., LAMB, J., SCHLIS, K., AGARWAL, J., STAM, R. W., OPFERMAN, J. T., SALLAN, S. E., DEN BOER, M. L., PIETERS, R., GOLUB, T. R. & ARMSTRONG, S. A. 2006. Gene expression-based chemical genomics identifies rapamycin as a modulator of MCL1 and glucocorticoid resistance. *Cancer Cell,* 10**,** 331-42.

WEI, T., NAJMI, S. M., LIU, H., PELTONEN, K., KUCEROVA, A., SCHNEIDER, D. A. & LAIHO, M. 2018. Small-Molecule Targeting of RNA Polymerase I Activates a Conserved Transcription Elongation Checkpoint. *Cell Rep,* 23**,** 404-414.

WEILEMANN, A., GRAU, M., ERDMANN, T., MERKEL, O., SOBHIAFSHAR, U., ANAGNOSTOPOULOS, I., HUMMEL, M., SIEGERT, A., HAYFORD, C., MADLE, H., WOLLERT-WULF, B., FICHTNER, I., DORKEN, B., DIRNHOFER, S., MATHAS, S., JANZ, M., EMRE, N. C., ROSENWALD, A., OTT, G., LENZ, P., TZANKOV, A. & LENZ, G. 2015. Essential role of IRF4 and MYC signaling for survival of anaplastic large cell lymphoma. *Blood,* 125**,** 124-32.

WELCKER, M., ORIAN, A., JIN, J., GRIM, J. E., HARPER, J. W., EISENMAN, R. N. & CLURMAN, B. E. 2004. The Fbw7 tumor suppressor regulates glycogen synthase kinase 3 phosphorylation-dependent c-Myc protein degradation. *Proc Natl Acad Sci U S A,* 101**,** 9085-90.

WENG, C., LI, Y., XU, D., SHI, Y. & TANG, H. 2005. Specific cleavage of Mcl-1 by caspase-3 in tumor necrosis factor-related apoptosis-inducing ligand (TRAIL)-induced apoptosis in Jurkat leukemia T cells. *J Biol Chem,* 280**,** 10491-500.

WENZEL, S. S., GRAU, M., MAVIS, C., HAILFINGER, S., WOLF, A., MADLE, H., DEEB, G., DORKEN, B., THOME, M., LENZ, P., DIRNHOFER, S., HERNANDEZ-ILIZALITURRI, F. J., TZANKOV, A. & LENZ, G. 2013. MCL1 is deregulated in subgroups of diffuse large B-cell lymphoma. *Leukemia,* 27**,** 1381-90.

WERTZ, I. E., KUSAM, S., LAM, C., OKAMOTO, T., SANDOVAL, W., ANDERSON, D. J., HELGASON, E., ERNST, J. A., EBY, M., LIU, J., BELMONT, L. D., KAMINKER, J. S., O'ROURKE, K. M., PUJARA, K., KOHLI, P. B., JOHNSON, A. R., CHIU, M. L., LILL, J. R., JACKSON, P. K., FAIRBROTHER, W. J., SESHAGIRI, S., LUDLAM, M. J., LEONG, K. G., DUEBER, E. C., MAECKER, H., HUANG, D. C. & DIXIT, V. M. 2011. Sensitivity to antitubulin chemotherapeutics is regulated by MCL1 and FBW7. *Nature,* 471**,** 110-4.

WHITE, R. J. 2008. RNA polymerases I and III, non-coding RNAs and cancer. *Trends Genet,* 24**,** 622-9.

WIERSTRA, I. & ALVES, J. J. A. I. C. R. 2008. The c-myc promoter: still mysterY and challenge. 99**,** 113-333.

WIGGINS, C. M., TSVETKOV, P., JOHNSON, M., JOYCE, C. L., LAMB, C. A., BRYANT, N. J., KOMANDER, D., SHAUL, Y. & COOK, S. J. 2011. BIM(EL), an intrinsically disordered protein, is degraded by 20S proteasomes in the absence of poly-ubiquitylation. *J Cell Sci,* 124**,** 969-77.

WILLEMS, M., WAGNER, E., LAING, R. & PENMAN, S. 1968. Base composition of ribosomal RNA precursors in the HeLa cell nucleolus: further evidence of non-conservative processing. *J Mol Biol,* 32**,** 211-20.

WILSON, D. N. & DOUDNA CATE, J. H. 2012. The structure and function of the eukaryotic ribosome. *Cold Spring Harb Perspect Biol,* 4.

WITTNER, M., HAMPERL, S., STOCKL, U., SEUFERT, W., TSCHOCHNER, H., MILKEREIT, P. & GRIESENBECK, J. 2011. Establishment and maintenance of alternative chromatin states at a multicopy gene locus. *Cell,* 145**,** 543-54.

WONG, R. P., KHOSRAVI, S., MARTINKA, M. & LI, G. 2008. Myeloid leukemia-1 expression in benign and malignant melanocytic lesions. *Oncol Rep,* 19**,** 933-7.

WU, X., BAYLE, J. H., OLSON, D. & LEVINE, A. J. 1993. The p53-mdm-2 autoregulatory feedback loop. *Genes Dev,* 7**,** 1126-32.

WU, X., LUO, Q., ZHAO, P., CHANG, W., WANG, Y., SHU, T., DING, F., LI, B. & LIU, Z. 2019. MGMT-activated DUB3 stabilizes MCL1 and drives chemoresistance in ovarian cancer. *Proc Natl Acad Sci U S A,* 116**,** 2961-2966.

WUILLEME-TOUMI, S., ROBILLARD, N., GOMEZ, P., MOREAU, P., LE GOUILL, S., AVET-LOISEAU, H., HAROUSSEAU, J. L., AMIOT, M. & BATAILLE, R. 2005. Mcl-1 is overexpressed in multiple myeloma and associated with relapse and shorter survival. *Leukemia,* 19**,** 1248-52.

WUILLEME-TOUMI, S., TRICHET, V., GOMEZ-BOUGIE, P., GRATAS, C., BATAILLE, R. & AMIOT, M. 2007. Reciprocal protection of Mcl-1 and Bim from ubiquitin-proteasome degradation. *Biochem Biophys Res Commun,* 361**,** 865-9.

XIANG, Z., LUO, H., PAYTON, J. E., CAIN, J., LEY, T. J., OPFERMAN, J. T. & TOMASSON, M. H. 2010. Mcl1 haploinsufficiency protects mice from Myc-induced acute myeloid leukemia. *J Clin Invest,* 120**,** 2109-18.

XIONG, X., ZHAO, Y., HE, H. & SUN, Y. 2011. Ribosomal protein S27-like and S27 interplay with p53-MDM2 axis as a target, a substrate and a regulator. *Oncogene,* 30**,** 1798-811.

XU, H., DI ANTONIO, M., MCKINNEY, S., MATHEW, V., HO, B., O'NEIL, N. J., SANTOS, N. D., SILVESTER, J., WEI, V., GARCIA, J., KABEER, F., LAI, D., SORIANO, P., BANATH, J., CHIU, D. S., YAP, D., LE, D. D., YE, F. B., ZHANG, A., THU, K., SOONG, J., LIN, S. C., TSAI, A. H., OSAKO, T., ALGARA, T., SAUNDERS, D. N., WONG, J., XIAN, J., BALLY, M. B., BRENTON, J. D., BROWN, G. W., SHAH, S. P., CESCON, D., MAK, T. W., CALDAS, C., STIRLING, P. C., HIETER, P., BALASUBRAMANIAN, S. & APARICIO, S. 2017. CX-5461 is a DNA G-quadruplex stabilizer with selective lethality in BRCA1/2 deficient tumours. *Nat Commun,* 8**,** 14432.

XUE, S. & BARNA, M. 2012. Specialized ribosomes: a new frontier in gene regulation and organismal biology. *Nat Rev Mol Cell Biol,* 13**,** 355-69.

YADA, M., HATAKEYAMA, S., KAMURA, T., NISHIYAMA, M., TSUNEMATSU, R., IMAKI, H., ISHIDA, N., OKUMURA, F., NAKAYAMA, K. & NAKAYAMA, K. I. 2004. Phosphorylation-dependent degradation of c-Myc is mediated by the F-box protein Fbw7. *EMBO J,* 23**,** 2116-25.

YADAVILLI, S., MAYO, L. D., HIGGINS, M., LAIN, S., HEGDE, V. & DEUTSCH, W. A. 2009. Ribosomal protein S3: A multi-functional protein that interacts with both p53 and MDM2 through its KH domain. *DNA Repair (Amst),* 8**,** 1215-24.

YANG, T., BUCHAN, H. L., TOWNSEND, K. J. & CRAIG, R. W. 1996. MCL-1, a member of the BLC-2 family, is induced rapidly in response to signals for cell differentiation or death, but not to signals for cell proliferation. *J Cell Physiol,* 166**,** 523-36.

YEH, T., O'CONNOR, G., CIDADO, J. & BARRETT, J. C. 2018. Development and Use of Clinical Pharmacodynamic Assays to Demonstrate Target Engagement for AZD4573, a Selective and Potent CDK9 Inhibitor Currently in Phase I Clinical Trials. Am Soc Hematology.

YELICK, P. C. & TRAINOR, P. A. 2015. Ribosomopathies: Global process, tissue specific defects. *Rare Dis,* 3**,** e1025185.

YOON, A., PENG, G., BRANDENBURGER, Y., ZOLLO, O., XU, W., REGO, E. & RUGGERO, D. 2006. Impaired control of IRES-mediated translation in X-linked dyskeratosis congenita. *Science,* 312**,** 902-6.

YOULE, R. J. & STRASSER, A. 2008. The BCL-2 protein family: opposing activities that mediate cell death. *Nat Rev Mol Cell Biol,* 9**,** 47-59.

YUNEVA, M. O., FAN, T. W., ALLEN, T. D., HIGASHI, R. M., FERRARIS, D. V., TSUKAMOTO, T., MATES, J. M., ALONSO, F. J., WANG, C., SEO, Y., CHEN, X. & BISHOP, J. M. 2012. The metabolic profile of tumors depends on both the responsible genetic lesion and tissue type. *Cell Metab,* 15**,** 157-70.

ZECH, L., HAGLUND, U., NILSSON, K. & KLEIN, G. 1976. Characteristic chromosomal abnormalities in biopsies and lymphoid-cell lines from patients with Burkitt and non-Burkitt lymphomas. *Int J Cancer,* 17**,** 47-56.

ZHAI, W. & COMAI, L. 2000. Repression of RNA polymerase I transcription by the tumor suppressor p53. *Mol Cell Biol,* 20**,** 5930-8.

ZHANG, H., GUTTIKONDA, S., ROBERTS, L., UZIEL, T., SEMIZAROV, D., ELMORE, S. W., LEVERSON, J. D. & LAM, L. T. 2011. Mcl-1 is critical for survival in a subgroup of non-small-cell lung cancer cell lines. *Oncogene,* 30**,** 1963-8.

ZHANG, J., HARNPICHARNCHAI, P., JAKOVLJEVIC, J., TANG, L., GUO, Y., OEFFINGER, M., ROUT, M. P., HILEY, S. L., HUGHES, T. & WOOLFORD, J. L., JR. 2007. Assembly factors Rpf2 and Rrs1 recruit 5S rRNA and ribosomal proteins rpL5 and rpL11 into nascent ribosomes. *Genes Dev,* 21**,** 2580-92.

ZHANG, Q., SHALABY, N. A. & BUSZCZAK, M. 2014. Changes in rRNA transcription influence proliferation and cell fate within a stem cell lineage. *Science,* 343**,** 298-301.

ZHANG, S., ZHANG, M., JING, Y., YIN, X., MA, P., ZHANG, Z., WANG, X., DI, W. & ZHUANG, G. 2018. Deubiquitinase USP13 dictates MCL1 stability and sensitivity to BH3 mimetic inhibitors. *Nat Commun,* 9**,** 215.

ZHANG, Y. & LU, H. 2009. Signaling to p53: ribosomal proteins find their way. *Cancer Cell,* 16**,** 369-77.

ZHANG, Y., WANG, J., YUAN, Y., ZHANG, W., GUAN, W., WU, Z., JIN, C., CHEN, H., ZHANG, L., YANG, X. & HE, F. 2010. Negative regulation of HDM2 to attenuate p53 degradation by ribosomal protein L26. *Nucleic Acids Res,* 38**,** 6544-54.

ZHANG, Y., WOLF, G. W., BHAT, K., JIN, A., ALLIO, T., BURKHART, W. A. & XIONG, Y. 2003. Ribosomal protein L11 negatively regulates oncoprotein MDM2 and mediates a p53-dependent ribosomal-stress checkpoint pathway. *Mol Cell Biol,* 23**,** 8902-12.

ZHENG, J., LANG, Y., ZHANG, Q., CUI, D., SUN, H., JIANG, L., CHEN, Z., ZHANG, R., GAO, Y., TIAN, W., WU, W., TANG, J. & CHEN, Z. 2015. Structure of human MDM2 complexed with RPL11 reveals the molecular basis of p53 activation. *Genes Dev,* 29**,** 1524-34.

ZHONG, Q., GAO, W., DU, F. & WANG, X. 2005. Mule/ARF-BP1, a BH3-only E3 ubiquitin ligase, catalyzes the polyubiquitination of Mcl-1 and regulates apoptosis. *Cell,* 121**,** 1085-95.

ZHOU, P., LEVY, N. B., XIE, H., QIAN, L., LEE, C. Y., GASCOYNE, R. D. & CRAIG, R. W. 2001. MCL1 transgenic mice exhibit a high incidence of B-cell lymphoma manifested as a spectrum of histologic subtypes. *Blood,* 97**,** 3902-9.

ZHOU, X., HAO, Q., LIAO, J., ZHANG, Q. & LU, H. 2013. Ribosomal protein S14 unties the MDM2-p53 loop upon ribosomal stress. *Oncogene,* 32**,** 388-96.

ZHOU, X., LIAO, W. J., LIAO, J. M., LIAO, P. & LU, H. 2015. Ribosomal proteins: functions beyond the ribosome. *J Mol Cell Biol,* 7**,** 92-104.

ZHU, Y., POYUROVSKY, M. V., LI, Y., BIDERMAN, L., STAHL, J., JACQ, X. & PRIVES, C. 2009. Ribosomal protein S7 is both a regulator and a substrate of MDM2. *Mol Cell,* 35**,** 316-26.

ZINDY, F., EISCHEN, C. M., RANDLE, D. H., KAMIJO, T., CLEVELAND, J. L., SHERR, C. J. & ROUSSEL, M. F. 1998. Myc signaling via the ARF tumor suppressor regulates p53-dependent apoptosis and immortalization. *Genes Dev,* 12**,** 2424-33.

ZUBER, J., MCJUNKIN, K., FELLMANN, C., DOW, L. E., TAYLOR, M. J., HANNON, G. J. & LOWE, S. W. 2011. Toolkit for evaluating genes required for proliferation and survival using tetracycline-regulated RNAi. *Nat Biotechnol,* 29**,** 79-83.